

CONSTRUCTING ORGANIC-INORGANIC BIMETALLIC HYBRID MATERIALS BASED
ON THE POLYOXOMETALATE BACKBONE

by

KANIKA SHARMA

B.Sc., University of Delhi, 2005
M.Sc., University of Delhi, 2007
M.Phil., University of Delhi, 2008

AN ABSTRACT OF A DISSERTATION

submitted in partial fulfillment of the requirements for the degree

DOCTOR OF PHILOSOPHY

Department of Chemistry
College of Arts and Sciences

KANSAS STATE UNIVERSITY
Manhattan, Kansas

2014

Abstract

The thesis focuses on the design and synthesis of novel organoimido delivery reagents capable of forming bimetallic polyoxometalate (POM) hybrids, and their use in the assembly of bimetallic hexamolybdate derivatives. These delivery reagents have been designed thoughtfully and separate organic moieties have been selected for coordinating to both the POM cluster and the second metal atom.

A series of three ligands [4-aminopiperidine, 4-(4-aminophenyl) piperazine, and 4-(4-aminophenyl) piperidine] were selected and used to synthesize the dithiocarbamate metal-coordinating ligands, which in turn were used for preparing the corresponding metal ($M = \text{Cr}, \text{Mn}, \text{Fe}, \text{Co}, \text{Ni}, \text{Cu}, \text{Zn}, \text{Ag}$) complexes. All the complexes were characterized by infrared spectroscopy (IR). Reported routes were followed for the covalent grafting of these metal complexes onto hexamolybdate. But, the poor solubility of these metal complexes was found to be a major stumbling block in our endeavors to synthesize the dithiocarbamate based polyoxometalate hybrids.

The observed poor solubility of metal dithiocarbamate complexes was overcome by synthesizing [potassium(I) tris(3,5-diphenylpyrazole)borate] and [potassium(I) tris(3,5-dimethylpyrazole)borate] *via* thermal dehydrogenative condensation between tetrahydroborate and the respective pyrazole molecule. A series of corresponding transition metal ($M = \text{Co}, \text{Ni}, \text{Cu}, \text{Mn}$) complexes of tris(3,5-diphenylpyrazole)borate and tris(3,5-dimethylpyrazole)borate were synthesized, and characterized by IR and UV-visible spectroscopy, and single crystal X-ray diffraction. The single crystal structure of [manganese(II) (tris(3,5-dimethylpyrazole)borate)₂] turned out to be an outlier as it displayed the formation of a bis-complex, thus having no substitutable anion for further reaction with dithiocarbamates. Thereafter, a series of metal dithiocarbamate complexes of these [hydrotris(pyrazolyl)borates] ($M = \text{Co}, \text{Ni}, \text{Cu}$) were prepared using [sodium 4-aminopiperidyl dithiocarbamate] and were characterized by IR and UV-visible spectroscopy. A remarkable improvement in the solubility of these metal dithiocarbamates in organic solvents was observed. Furthermore, attempts to covalently graft these complexes onto hexamolybdate cluster were undertaken, and found to be unsuccessful possibly due to the strong oxidizing nature of PPh_3Br_2 and hexamolybdate. Although, we were

able to successfully tailor the solubility of the dithiocarbamate complexes to suit our needs, our efforts to achieve the primary goal of synthesizing dithiocarbamate based polyoxometalate hybrids have so far been unsuccessful.

A series of three pyridyl based ligands i.e., 3,5-di(pyridin-2-yl)-4H-1,2,4-triazol-4-amine, 4-(pyridin-4-ylethynyl)aniline and 4-(pyridin-3-ylethynyl)aniline were synthesized and characterized. Covalent attachment of these ligands to hexamolybdate were attempted following various well-known routes. Although, no evidence of covalent attachment of 3,5-di(pyridin-2-yl)-4H-1,2,4-triazol-4-amine to hexamolybdate was observed, the covalent grafting of 4-(pyridin-4-ylethynyl)aniline and 4-(pyridin-3-ylethynyl)aniline to hexamolybdate cluster was successfully achieved. Characterization of these novel organic-inorganic hybrids was done using IR and NMR spectroscopy as analytical tools. Attempts have been undertaken to obtain single crystals of these hybrids. Also, a novel route involving halogen bonding as a purification and separation technique for pyridyl functionalized hexamolybdate hybrids is also being explored.

The novel acetylacetonate moiety has been explored as an imidodelivery reagent for synthesizing hexamolybdate covalent hybrids, wherein [3-(4-((4-aminophenyl)ethynyl)phenyl)-4-hydroxypent-3-en-2-one] ligand has been successfully synthesized and characterized. Traditional methods along with unconventional methods such as heating at elevated temperatures and microwave reaction conditions, have so far proved to be unsuccessful in the synthesis of the hybrids. A series of the corresponding metal complexes have been synthesized and characterized, where the ligand and its corresponding copper(II) complex have been characterized by single crystal XRD. In the crystal structure of the copper complex, the metal ion sits in a slightly distorted square-planar pocket, where no coordination to the -NH_2 group is observed, which highlights the potential of using it as an imidodelivery reagent.

CONSTRUCTING ORGANIC-INORGANIC BIMETALLIC HYBRID MATERIALS BASED
ON THE POLYOXOMETALATE BACKBONE

by

KANIKA SHARMA

B.Sc., University of Delhi, 2005
M.Sc., University of Delhi, 2007
M.Phil., University of Delhi, 2008

A DISSERTATION

submitted in partial fulfillment of the requirements for the degree

DOCTOR OF PHILOSOPHY

Department of Chemistry
College of Arts and Sciences

KANSAS STATE UNIVERSITY
Manhattan, Kansas

2014

Approved by:

Major Professor
Dr. Eric A. Maatta

Copyright

KANIKA SHARMA

2014

Abstract

The thesis focuses on the design and synthesis of novel organoimido delivery reagents capable of forming bimetallic polyoxometalate (POM) hybrids, and their use in the assembly of bimetallic hexamolybdate derivatives. These delivery reagents have been designed thoughtfully and separate organic moieties have been selected for coordinating to both the POM cluster and the second metal atom.

A series of three ligands [4-aminopiperidine, 4-(4-aminophenyl) piperazine, and 4-(4-aminophenyl) piperidine] were selected and used to synthesize the dithiocarbamate metal-coordinating ligands, which in turn were used for preparing the corresponding metal (M = Cr, Mn, Fe, Co, Ni, Cu, Zn, Ag) complexes. All the complexes were characterized by infrared spectroscopy (IR). Reported routes were followed for the covalent grafting of these metal complexes onto hexamolybdate. But, the poor solubility of these metal complexes was found to be a major stumbling block in our endeavors to synthesize the dithiocarbamate based polyoxometalate hybrids.

The observed poor solubility of metal dithiocarbamate complexes was overcome by synthesizing [potassium(I) tris(3,5-diphenylpyrazole)borate] and [potassium(I) tris(3,5-dimethylpyrazole)borate] *via* thermal dehydrogenative condensation between tetrahydroborate and the respective pyrazole molecule. A series of corresponding transition metal (M = Co, Ni, Cu, Mn) complexes of tris(3,5-diphenylpyrazole)borate and tris(3,5-dimethylpyrazole)borate were synthesized, and characterized by IR and UV-visible spectroscopy, and single crystal X-ray diffraction. The single crystal structure of [manganese(II) (tris(3,5-dimethylpyrazole)borate)₂] turned out to be an outlier as it displayed the formation of a bis-complex, thus having no substitutable anion for further reaction with dithiocarbamates. Thereafter, a series of metal dithiocarbamate complexes of these [hydrotris(pyrazolyl)borates] (M = Co, Ni, Cu) were prepared using [sodium 4-aminopiperidyl dithiocarbamate] and were characterized by IR and UV-visible spectroscopy. A remarkable improvement in the solubility of these metal dithiocarbamates in organic solvents was observed. Furthermore, attempts to covalently graft these complexes onto hexamolybdate cluster were undertaken, and found to be unsuccessful possibly due to the strong oxidizing nature of PPh₃Br₂ and hexamolybdate. Although, we were

able to successfully tailor the solubility of the dithiocarbamate complexes to suit our needs, our efforts to achieve the primary goal of synthesizing dithiocarbamate based polyoxometalate hybrids have so far been unsuccessful.

A series of three pyridyl based ligands i.e., 3,5-di(pyridin-2-yl)-4H-1,2,4-triazol-4-amine, 4-(pyridin-4-ylethynyl)aniline and 4-(pyridin-3-ylethynyl)aniline were synthesized and characterized. Covalent attachment of these ligands to hexamolybdate were attempted following various well-known routes. Although, no evidence of covalent attachment of 3,5-di(pyridin-2-yl)-4H-1,2,4-triazol-4-amine to hexamolybdate was observed, the covalent grafting of 4-(pyridin-4-ylethynyl)aniline and 4-(pyridin-3-ylethynyl)aniline to hexamolybdate cluster was successfully achieved. Characterization of these novel organic-inorganic hybrids was done using IR and NMR spectroscopy as analytical tools. Attempts have been undertaken to obtain single crystals of these hybrids. Also, a novel route involving halogen bonding as a purification and separation technique for pyridyl functionalized hexamolybdate hybrids is also being explored.

The novel acetylacetonate moiety has been explored as an imidodelivery reagent for synthesizing hexamolybdate covalent hybrids, wherein [3-(4-((4-aminophenyl)ethynyl)phenyl)-4-hydroxypent-3-en-2-one] ligand has been successfully synthesized and characterized. Traditional methods along with unconventional methods such as heating at elevated temperatures and microwave reaction conditions, have so far proved to be unsuccessful in the synthesis of the hybrids. A series of the corresponding metal complexes have been synthesized and characterized, where the ligand and its corresponding copper(II) complex have been characterized by single crystal XRD. In the crystal structure of the copper complex, the metal ion sits in a slightly distorted square-planar pocket, where no coordination to the $-NH_2$ group is observed, which highlights the potential of using it as an imidodelivery reagent.

Table of Contents

List of Figures	xv
List of Tables	xix
Acknowledgements	xx
Dedication	xxii
Chapter 1 - Introduction	1
1.1 Polyoxometalates	1
1.1.1 Classification of polyoxometalates	2
1.1.1.1 Isopolyanions	2
1.1.1.2 Heteropolyanions	2
1.1.1.3 Molybdenum blue and molybdenum brown reduced POMs	3
1.1.2 Properties of polyoxometalates	3
1.1.3 Applications of polyoxometalates	4
1.2 Modification of polyoxometalates	6
1.2.1 Transition metal	7
1.2.2 Organometallic derivatives	8
1.2.3 Main group elements	9
1.2.3.1 Halides	10
1.2.3.2 Monodentate alkoxide	10
1.2.3.3 Trisalkoxides	11
1.2.3.4 Organosilyl derivatives	12
1.2.3.5 Organoimido derivatives	13
1.3 Methods of preparing organoimido derivatives of hexamolybdate	16
1.4 Organoimido hexamolybdate bimetallic systems	18
1.5 Goals	21
Chapter 2 - 'Dithiocarbamate' as a remote functionality to form bimetallic polyoxometalate hybrids	25
2.1 Introduction	25
2.2 Experimental	30

2.2.1 Synthesis of Zwitter-ion of 4-aminopiperidine, 1	30
2.2.2 Synthesis of Sodium 4-aminopiperidine dithiocarbamate, 2	30
2.2.3 Reaction of Sodium 4-aminopiperidine dithiocarbamate with chromium(II), 2.Cr	31
2.2.4 Reaction of Sodium 4-aminopiperidine dithiocarbamate with manganese(II), 2.Mn	31
2.2.5 Reaction of Sodium 4-aminopiperidine dithiocarbamate with iron(III), 2.Fe	31
2.2.6 Reaction of Sodium 4-aminopiperidine dithiocarbamate with cobalt(II), 2.Co	31
2.2.7 Reaction of Sodium 4-aminopiperidine dithiocarbamate with nickel(II), 2.Ni	32
2.2.8 Reaction of Sodium 4-aminopiperidine dithiocarbamate with copper(II), 2.Cu	32
2.2.9 Reaction of Sodium 4-aminopiperidine dithiocarbamate with zinc(II), 2.Zn	32
2.2.10 Reaction of Sodium 4-aminopiperidine dithiocarbamate with silver(I), 2.Ag	32
2.2.11 Synthesis of Tetrabutylammonium 4-aminopiperidine dithiocarbamate, 3	33
2.2.12 Synthesis of 4-(4-nitrophenyl) piperazine, 4	33
2.2.13 Synthesis of Tetrabutylammonium 4-(4-nitrophenyl) piperazine dithiocarbamate, 5	33
2.2.14 Synthesis of 4-(4-aminophenyl) piperazine, 6	34
2.2.15 Synthesis of Sodium 4-(4-aminophenyl) piperazine dithiocarbamate, 7	34
2.2.16 Reaction of Sodium 4-(4-aminophenyl) piperazine dithiocarbamate with chromium(II), 7.Cr	35
2.2.17 Reaction of Sodium 4-(4-aminophenyl) piperazine dithiocarbamate with manganese(II), 7.Mn	35
2.2.18 Reaction of Sodium 4-(4-aminophenyl) piperazine dithiocarbamate with iron(III), 7.Fe	35
2.2.19 Reaction of Sodium 4-(4-aminophenyl) piperazine dithiocarbamate with cobalt(II), 7.Co	35
2.2.20 Reaction of Sodium 4-(4-aminophenyl) piperazine dithiocarbamate with nickel(II), 7.Ni	36
2.2.21 Reaction of Sodium 4-(4-aminophenyl) piperazine dithiocarbamate with copper(II), 7.Cu	36
2.2.22 Reaction of Sodium 4-(4-aminophenyl) piperazine dithiocarbamate with zinc(II), 7.Zn	36

2.2.23 Synthesis of Tetrabutylammonium 4-(4-aminophenyl) piperazine dithiocarbamate, 8	36
2.2.24 Synthesis of 4-(4-nitrophenyl) piperidine, 9	37
2.2.25 Synthesis of 4-(4-aminophenyl) piperidine, 10	37
2.2.26 Synthesis of Sodium 4-(4-aminophenyl) piperidine dithiocarbamate, 11	38
2.2.27 Reaction of Sodium 4-(4-aminophenyl) piperidine dithiocarbamate with cobalt(II), 11.Co	38
2.2.28 Reaction of Sodium 4-(4-aminophenyl) piperidine dithiocarbamate with nickel(II), 11.Ni	38
2.2.29 Reaction of Sodium 4-(4-aminophenyl) piperidine dithiocarbamate with copper(II), 11.Cu	39
2.2.30 Reaction of Sodium 4-(4-aminophenyl) piperidine dithiocarbamate with zinc(II), 11.Zn	39
2.3 Results and discussion	39
2.3.1 Studies with 4-aminopiperidine	39
2.3.2 Studies with 4-(piperazin-1-yl)aniline	45
2.3.3 Studies with 4-(piperidin-4-yl)aniline.....	48
2.3.4 Microwave assisted covalent grafting of 11.Zn	50
2.4 Conclusions.....	50
Chapter 3 - Extended dithiocarbamate systems based on poly(pyrazolyl)borates as organoimido delivery reagents	53
3.1 Poly(pyrazolyl)borates.....	53
3.2 Experimental.....	56
3.2.1 Synthesis of 3,5-diphenyl pyrazole, 12	56
3.2.2 Synthesis of Potassium tris(3,5-diphenylpyrazolylborate), 13	57
3.2.3 Synthesis of Potassium tris(3,5-dimethylpyrazolylborate), 14	57
3.2.4 Synthesis of Cobalt chloro tris(3,5-diphenylpyrazolylborate), 15	57
3.2.5 Synthesis of Nickel bromo tris(3,5-diphenylpyrazolylborate), 16	58
3.2.6 Synthesis of Nickel nitrate tris(3,5-diphenylpyrazolylborate), 17	58
3.2.7 Synthesis of Copper nitrate tris(3,5-diphenylpyrazolylborate), 18	58
3.2.8 Synthesis of Manganese chloro tris(3,5-diphenylpyrazolylborate), 19	58

3.2.9 Synthesis of Cobalt chloro tris(3,5-dimethylpyrazolylborate), 20	59
3.2.10 Synthesis of Nickel bromo tris(3,5-dimethylpyrazolylborate), 21	59
3.2.11 Synthesis of Copper nitrate tris(3,5-dimethylpyrazolylborate), 22	59
3.2.12 Synthesis of Manganese chloro tris(3,5-dimethylpyrazolylborate), 23	60
3.2.13 Reaction of Cobalt chloro tris(3,5-diphenylpyrazolylborate) with sodium (4-aminopiperidine) dithiocarbamate, 24	60
3.2.14 Reaction of Nickel bromo tris(3,5-diphenylpyrazolylborate) with sodium (4-aminopiperidine) dithiocarbamate, 25	60
3.2.15 Reaction of Copper nitrate tris(3,5-diphenylpyrazolylborate) with sodium (4-aminopiperidine) dithiocarbamate, 26	60
3.2.16 Reaction of Cobalt chloro tris(3,5-dimethylpyrazolylborate) and sodium (4-aminopiperidine) dithiocarbamate, 27	61
3.2.17 Reaction of Nickel bromo tris(3,5-dimethylpyrazolylborate) and sodium (4-aminopiperidine) dithiocarbamate, 28	61
3.2.18 Reaction of Copper nitrate tris(3,5-dimethylpyrazolylborate) and sodium (4-aminopiperidine) dithiocarbamate, 29	61
3.3 Results and discussion	62
3.3.1 Synthesis of Poly(pyrazolyl)borate ligands	62
3.3.2 Synthesis of metal complexes with 13 and 14	64
3.3.2.1 Infrared analysis of metal complexes with 13 and 14	64
3.3.2.2 Electronic spectroscopy of metal complexes of 13 and 14	65
3.3.2.3 Single crystal X-ray structures of metal complexes of 13 and 14	65
3.3.2.3.1 Crystal structure of CuNO ₃ BH[tris(3,5-diphenylpyrazole)].....	65
3.3.2.3.2 Crystal structure of Mn[BH(3,5-dimethylpyrazole) ₃] ₂	66
3.3.3 Synthesis of metal dithiocarbamate complexes of tris(3,5-diphenylpyrazole)borates and tris(3,5-dimethylpyrazole).....	67
3.3.3.1 Infrared analysis of metal dithiocarbamate complexes of tris(3,5-diphenylpyrazole)borates and tris(3,5-dimethylpyrazole)borates.....	68
3.3.3.2 Electronic spectroscopy of metal dithiocarbamate complexes of tris(3,5-diphenylpyrazole)borates and tris(3,5-dimethylpyrazole).....	68

3.3.4 Attempts to prepare POM hybrids with metal dithiocarbamate complexes of tris(3,5-diphenylpyrazole)borates and tris(3,5-dimethylpyrazole)borates.....	69
3.4 Conclusions.....	69
Chapter 4 - Bimetallic hexamolybdate systems based on the pyridyl group.....	72
4.1 Pyridine.....	72
4.1.1 Self-assembled polyoxometalate hybrids bearing the pyridyl group.....	73
4.1.2 Organoimido hexamolybdate derivatives bearing the pyridyl group.....	75
4.2 Experimental.....	79
4.2.1 Synthesis of 3,5-di(pyridin-2-yl)-4H-1,2,4-triazol-4-amine, 30	80
4.2.2 Synthesis of 4-((trimethylsilyl)ethynyl)aniline, 31	80
4.2.3 Synthesis of 4-ethynylaniline, 32	81
4.2.4 Synthesis of 4-(pyridin-4-ylethynyl)aniline, 33	81
4.2.5 Synthesis of 4-(pyridin-3-ylethynyl)aniline, 34	81
4.2.6 Synthesis of phosphineimine of 3,5-di(pyridin-2-yl)-4H-1,2,4-triazol-4-amine, 35	82
4.2.7 Synthesis of Triphenylphosphinimine of 4-(pyridin-4-ylethynyl)aniline, 36	82
4.2.8 Synthesis of Triphenylphosphinimine of 4-(pyridin-3-ylethynyl)aniline, 37	83
4.2.9 Synthesis of HCl salt of 3,5-di(pyridin-2-yl)-4H-1,2,4-triazol-4-amine, 38	83
4.2.10 Synthesis of 4-(pyridin-4-ylethynyl)aniline hydrochloride, 39	83
4.2.11 Synthesis of 4-(pyridin-3-ylethynyl)aniline hydrochloride, 40	83
4.2.12 Synthesis of (TBA) ₂ [Mo ₅ O ₁₈ (Mo(4-(pyridin-4-ylethynyl)aniline))], 41	84
4.2.13 Synthesis of (TBA) ₂ [Mo ₅ O ₁₈ (Mo(4-(pyridin-3-ylethynyl)aniline))], 42	84
4.3 Results and discussion.....	85
4.3.1 Synthesis of pyridyl based ligands.....	85
4.3.1.1 Synthesis of 3,5-di(pyridin-2-yl)-4H-1,2,4-triazol-4-amine, 30	85
4.3.1.2 Synthesis of 33 and 34 ligands.....	85
4.3.2 Attempts to use phosphineimine derivatives of the pyridyl based ligands as imidodelivery reagent.....	87
4.3.2.1 Phosphineimine derivative (35) of 30 as imidodelivery reagent.....	87
4.3.2.2 Phosphineimine derivatives (36 and 37) of 33 and 34 as imidodelivery reagents.....	89
4.3.3 Attempts to use pyridyl ligands directly as imidodelivery reagent via Peng's route... ..	91
4.3.3.1 30 as imidodelivery reagent.....	91

4.3.3.2 33 and 34 ligands as imidodelivery reagents	91
4.3.3.3 30 as imidodelivery reagent	92
4.3.3.4 33 and 34 as imidodelivery reagents	92
4.3.4 Attempts to purify hexamolybdate derivatives, 41 and 42	96
4.3.4.1 Classical attempt of fractional crystallization	96
4.3.4.2 A novel attempt to purify via halogen-bonding	97
4.3.5 Attempts to coordinate second metal ion	98
4.3.5.1 Copper as second metal ion	98
4.3.5.2 Palladium as second metal ion	98
4.4 Conclusions	99
Chapter 5 - Exploring acetylacetonates as a remote functionality to prepare hexamolybdate imido hybrids	101
5.1 Diketones	101
5.1.1 Acetylacetonates	102
5.1.2 Application of metal acetylacetonates	103
5.2 Experimental	104
5.2.1 Synthesis of 4-iodobenzaldehyde, 43	104
5.2.2 Synthesis of biacetyl-trimethylphosphite adduct, 44	105
5.2.3 Synthesis of 4-hydroxy-3-(4-iodophenyl)pent-3-en-2-one, 45	105
5.2.4 Synthesis of 3-(4-((4-aminophenyl)ethynyl)phenyl)-4-hydroxypent-3-en-2-one, 46	105
5.2.5 Synthesis of Triphenylphosphinimine of 3-(4-((4-aminophenyl)ethynyl)phenyl)-4- hydroxypent-3-en-2-one, 47	106
5.2.6 Reaction of 3-(4-((4-aminophenyl)ethynyl)phenyl)-4-hydroxypent-3-en-2-one with manganese (II), 46.Mn	106
5.2.7 Reaction of 3-(4-((4-aminophenyl)ethynyl)phenyl)-4-hydroxypent-3-en-2-one with cobalt(II), 46.Co	107
5.2.8 Reaction of 3-(4-((4-aminophenyl)ethynyl)phenyl)-4-hydroxypent-3-en-2-one with nickel (II), 46.Ni	107
5.2.9 Reaction of 3-(4-((4-aminophenyl)ethynyl)phenyl)-4-hydroxypent-3-en-2-one with copper (II), 46.Cu	107

5.2.10 Reaction of 3-(4-((4-aminophenyl)ethynyl)phenyl)-4-hydroxypent-3-en-2-one with zinc (II), 46.Zn	107
5.2.11 Reaction of 3-(4-((4-aminophenyl)ethynyl)phenyl)-4-hydroxypent-3-en-2-one with indium (II), 46.In	108
5.2.12 Synthesis of 3-(4-((4-aminophenyl)ethynyl)phenyl)-4-hydroxypent-3-en-2-one hydrochloride, 48	108
5.2.13 Synthesis of Triphenylphosphinimine of 4-ethynylaniline, 49	108
5.3 Results and discussion	109
5.3.1 Synthesis of 3-(4-((4-aminophenyl)ethynyl)phenyl)-4-hydroxypent-3-en-2-one	109
5.3.2 Single crystal structure of 3-(4-((4-aminophenyl)ethynyl)phenyl)-4-hydroxypent-3-en-2-one	111
5.3.3 Phosphineimine derivative (47) of 46 as imidodelivery reagent	112
5.3.4 Synthesis of metal complexes of 3-(4-((4-aminophenyl)ethynyl)phenyl)-4-hydroxypent-3-en-2-one	113
5.3.4.1 Characterization of metal complexes of 46 using infrared spectroscopy	114
5.3.4.2 Single crystal structure of 46.Cu	114
5.3.4.3 ¹ H NMR spectroscopic study of 46.Zn complex.....	115
5.3.5 46.Zn metal complex as imidodelivery reagent.....	115
5.3.5.1 Attempts for covalent grafting of 46.Zn on to hexamolybdate using Peng's route	116
5.3.5.2 Microwave assisted covalent grafting of 46.Zn on hexamolybdate	116
5.3.6 Attempts to use 46 as imidodelivery reagent.....	116
5.3.7 Attempts to use phosphineimine derivative of 4-ethynylaniline as imidodelivery reagent.....	117
5.4 Conclusions.....	117
Appendix A - Supramolecular studies with dithiocarbamates.....	120
A.1 Hydrogen-bonding studies of dithiocarbamates.....	120
A.2 Halogen-bonding studies of dithiocarbamates.....	121
A.3 Conclusion	124
Appendix B - ¹ H, ¹³ C and ³¹ P NMR, IR and UV-Visible spectroscopic data.....	126

List of Figures

Figure 1.1 Lindqvist polyoxometalates.....	2
Figure 1.2 Types of heteropolyanions.	3
Figure 1.3 Molybdenum blue and brown POMs.	3
Figure 1.4 Increase in number of publications on polyoxometalates in recent years.	4
Figure 1.5 Types of organic-inorganic POM hybrids.....	7
Figure 1.6 Transition metal functionalized POM interacting with histidine.	7
Figure 1.7 Self-assembled 1D chains of a dimanganese ($Mn^{II/III}$) functionalized POM.....	8
Figure 1.8 Organo-ruthenium functionalized POM.....	9
Figure 1.9 Windmill-like structure of $[\{ Ru(\eta^6\text{-p-MeC}_6\text{H}_4\text{Pr}^i) \}_4 Mo_4 O_{16}]$	9
Figure 1.10 Structure of the fully oxidized $[W_6 O_{14} Cl_{10}]^{2-}$ anion.	10
Figure 1.11 A cobalt complex stabilized by the monomethylated $[IMo_6 O_{23} (OMe)]^4-$ anion.	11
Figure 1.12 (a) Trisalkoxo functionalization as a route towards bimetallic systems; (b) Metalloporphyrin interacting with a trisalkoxo functionalized POM.....	12
Figure 1.13 Organosilyl functionalization of a POM for further chemical modification.	13
Figure 1.14 Lindqvist POM displaying oxygen atoms in three different environments.	14
Figure 1.15 Mixed disubstituted hexamolybdates.	15
Figure 1.16 An organoimido POM $[(Bu_4N)_2 [Mo_6 O_{18} \text{-N-Ph-(o-CH}_3)_2\text{-p-SCN}]$ used as an anode in lithium ion batteries.	16
Figure 1.17 POM hybrid displaying antitumor activity.....	16
Figure 1.18 Suggested mechanism for oxo substitution by phosphineimines in POMs.....	17
Figure 1.19 Suggested mechanism for oxo substitution by isocyanates in POMs.	17
Figure 1.20 Peng's route for hexamolybdate functionalization using arylamine as an organoimido delivery reagent.	18
Figure 1.21 Wei's route for POM functionalization using arylamine as the organoimido delivery reagent in the presence of its hydrochloride salt.....	18
Figure 1.22 Organoimido-based vanadium (V) derivative complexed with: (a) rhodium; and (b) tungsten, forming bimetallic architectures.....	19

Figure 1.23 POM derivatives with metal-coordinating functional groups: (a) <i>m</i> -pyridyl; (b) <i>p</i> -nitrile; and (c) <i>p</i> -carboxyl.	19
Figure 1.24 Control of electron flow in POM hybrids by breaking the conjugation in the system	20
Figure 1.25 Bimetallic POM hybrid having an extended conjugated system.....	20
Figure 1.26 Synthesizing bimetallic organoimido hexamolybdates capable of diverse applications.	21
Figure 2.1 Synthesis of 1,1-dithiolate anion.	25
Figure 2.2 General synthesis of DTCs complexes.....	27
Figure 2.3 Mesomeric structures of DTCs.....	27
Figure 2.4 Synthesis of transition metal DTCs complexes.....	27
Figure 2.5 Different modes of metal coordination of DTC ligand.	28
Figure 2.6 Possible supramolecular arrays resulting from various coordinating modes in dithiocarbamates.	28
Figure 2.7 Metal-centered electrochemical properties of copper dithiocarbamates, Cu(R ₂ dtc) ₂ .	29
Figure 2.8 Type (I) POM hybrid, [Ru ₂ (S ₂ CNMe ₂) ₃ (μ ₃ -S ₂ CNMe ₂) ₂] ₂ [Mo ₆ O ₁₉]·2CH ₃ COCH ₃	29
Figure 2.9 X-ray crystal structure of zwitterion, 1	40
Figure 2.10 Proposed mechanism for formation of 1	41
Figure 2.11 Synthesis of 2	41
Figure 2.12 X-ray crystal structure for 2.Ni	43
Figure 2.13 Attempted covalent grafting of 2.Co to hexamolybdate.	44
Figure 2.14 Synthesis of 3	44
Figure 2.15 Attempts to covalent graft 3 onto hexamolybdate.....	45
Figure 2.16 Synthetic scheme for metal dithiocarbamates of 7 as imidodelivery reagent.	46
Figure 2.17 Synthetic scheme for metal dithiocarbamates of 11 as imidodelivery reagent.	48
Figure 2.18 ¹ H NMR spectrum of zinc dithiocarbamate of 4-(piperidin-4-yl)aniline, 11.Zn	49
Figure 3.1 General routes of synthesis of poly(pyrazolyl)borate ligands.	53
Figure 3.2 Successive pyrazolyl substitution in molten synthesis.....	53
Figure 3.3 Resemblance of poly(pyrazolyl)borate ligand to the shape of a hunting scorpion.	54
Figure 3.4 Comparison of poly(pyrazolyl)borate ligands with cyclopentadienyl ligands.....	54

Figure 3.5 Reported synthesis of dithiocarbamate complexes based on hydrotris(3,5-diphenyl-1-pyrazolyl)borate anion.	55
Figure 3.6 Synthetic scheme for metal complexes of tris(diphenylpyrazolyl)borate ligands as imidodelivery reagent.	62
Figure 3.7 Possible products under the reaction conditions.	63
Figure 3.8 X-ray crystal structure of 13	64
Figure 3.9 X-ray crystal structure of 18	66
Figure 3.10 X-ray crystal structure of 23	67
Figure 3.11 Reaction of metal pyrazolylborate complexes with 2	67
Figure 4.1 Structure of pyridine.....	72
Figure 4.2 Change in the coordination environment upon modification of the pyridyl ligand	73
Figure 4.3 Self-assembled trimer based on bis(pyridine-trisalkoxo)-hexavanadate and [PdCl ₂ (CH ₃ CN) ₂].....	74
Figure 4.4 A molecular switch based on POM-hybrid.....	74
Figure 4.5 Possible extended supramolecular architectures resulting from bimetallic organoimido hexamolybdates.....	75
Figure 4.6 Synthesis of pyridyl based imido-hexamolybdates.....	76
Figure 4.7 Reason for incompetency of pyridylimido hexamolybdate hybrid for metal coordination.....	76
Figure 4.8 Adding electron donating group for improving the σ -donor ability of pyridylimido hexamolybdate.....	77
Figure 4.9 Synthesis of 3-(pyridin-3-yl)phenylimido hexamolybdate.....	77
Figure 4.10 POM cluster rearrangement observed upon use of 1,10-phenanthroline-5-amine as the organoimido delivery reagent.	78
Figure 4.11 Ferrocenylimido–hexamolybdate metal complex.....	78
Figure 4.12 Synthesis of a coordination polymer based on organoimido hexamolybdate.....	79
Figure 4.13 Potential ligand (30) for organoimido functionalization of hexamolybdate.....	85
Figure 4.14 Synthesis of 30	85
Figure 4.15 Designing of new organoimido delivery reagents, 33 and 34	86
Figure 4.16 Scheme for synthesis of common starting materials for 33 and 34	86
Figure 4.17 Final steps to prepare 33 and 34	87

Figure 4.18 Synthesis of 35	88
Figure 4.19 ³¹ P NMR study of 35	88
Figure 4.20 Attempt to synthesize hexamolybdate hybrid using 35 as organoimido delivery reagent.	89
Figure 4.21 Synthesis of 36 and 37	90
Figure 4.22 Maatta's route to functionalize hexamolybdate with 36 and 37	91
Figure 4.23 Peng's route to synthesize derivative with 30	91
Figure 4.24 Wei's route of functionalization with 30	92
Figure 4.25 Wei's route to functionalize hexamolybdate using 33 and 34 as organoimido delivery reagents.	93
Figure 4.26 Infrared spectrum of hybrid, 41 containing 33 covalently anchored to hexamolybdate.	94
Figure 4.27 ¹ H NMR of hybrid, 41 containing 33 covalently anchored to hexamolybdate.	95
Figure 4.28 ¹ H NMR of hybrid, 42 containing 34 covalently anchored to hexamolybdate.	96
Figure 4.29 Halogen bonding in 4-iodopyridine.....	97
Figure 4.30 Selected halogen bond donors.	97
Figure 4.31 Copper iodide affinity for pyridine.....	98
Figure 4.32 Gouzerh <i>et al.</i> Anderson-Evans POM, MnMo ₆ O ₁₈ {(OCH ₂) ₃ CNHCO-(4-C ₅ H ₄ N)} ₂ PdCl ₂	99
Figure 5.1 General structure of diketones	101
Figure 5.2 Different metal coordination modes of monoanionic diketones	101
Figure 5.3 Synthesis of acetylacetonates	102
Figure 5.4 Resonance structures of acetylacetonates.....	102
Figure 5.5 Designing of the organoimido delivery reagent, 46	109
Figure 5.6 Synthetic scheme for 46	110
Figure 5.7 Synthetic scheme of 45	110
Figure 5.8 ¹ H NMR spectrum of 46	111
Figure 5.9 X-ray crystal structure of 46	112
Figure 5.10 ³¹ P NMR spectrum of 47	113
Figure 5.11 X-ray crystal structure of 46.Cu	114
Figure 5.12 ¹ H NMR spectrum of 46.Zn	115

List of Tables

Table 2.1 Types of 1,1-dithiolates.	26
Table 2.2 Metal complexes with 2	42
Table 2.3 Metal dithiocarbamate complexes with 7	47
Table 2.4 Metal dithiocarbamate complexes with 11	49
Table 3.1 IR spectroscopic studies of metal complexes of 13 and 14	65
Table 3.2 IR spectroscopic studies of metal dithiocarbamate complexes of tris(3,5-diphenylpyrazole)borates and tris(3,5-dimethylpyrazole)borates.....	68
Table 4.1 ³¹ P NMR peaks for possible compounds.	90
Table 4.2 ¹ H NMR shift observed in 33 based hybrid of hexamolybdate, 41	94
Table 4.3 ¹ H NMR shift observed in 34 based hybrid of hexamolybdate, 42	95
Table 5.1 IR shifts observed for metal complexes of 46	114

Acknowledgements

I express my deepest gratitude to my advisor Prof. Eric A. Maatta for his unstinted guidance, invaluable ideas and immense support throughout the course of the past five years. His vast knowledge coupled with the good research ethics such as logical thinking that he instilled in me has provided the foundation stone for the present dissertation. You have always been kind and patient with me, and treated me with utmost respect throughout these years. I have learnt a lot from you and that will play a significant part in where I am in my life in future.

I would like to especially thank Prof. Christer B. Aakeröy for always keeping his office door open for me at all times for both professional and personal discussions. Your invaluable suggestions, encouragement and unwavering support always gave me courage and helped me get through the difficult times as well as focus on my research with a renewed energy. Also, thanks a lot for giving me an honorary membership to the Aakeröy group.

I am grateful to my committee members Prof. Kenneth J. Klabunde, Prof. Om Prakash and Prof. John R. Schlup for being on my committee, and for always accommodating me in your busy schedules, as well as providing me with positive feedback.

I would also like to thank Dr. John Desper for kindly collecting data and solving the single crystal structures included in this dissertation, thus helping me solve the many puzzles encountered during my research. Thank you Dr. Leila Maurmann for all the help with my NMR and mass spectroscopy studies. I would also like to thank Ron Jackson for being my handyman and helping me fix all the technical issues encountered during the course of the past five years. A special thanks to Ron and Leila for keeping an eye on me while I was working alone in the lab, and also for all the fun times I had with the two of you. I would also like to thank Jim Hodgson, Tobe Eggers, chemistry staff members and Michael Hinton for making my life enjoyable and so much easier here at K-State. A sincere thank you to the Department of Chemistry, KSU for providing me with teaching assistantship for all these years.

I am much obliged to the Aakeröy group members, past and present, for being good friends and for their unconditional help and support throughout. Importantly, I would like to

acknowledge the endless love and support of all my friends. Thank you all for always being there.

A sincere thanks to Abhi for just being a wonderful person. You have always been a savior and always helped me sail through my difficult times. Thanks so much for being so patient and comforting all this time. In short, thanks for being you.

Last but not the least, I fall short of words in expressing my profound personal gratitude to my family for their unconditional love and affection, patience and constant encouragement throughout all the endeavors in my life. I wish that I remain fortunate enough to always have this support in future as well. You all were and will always be the pillars of my life and career. I could never have achieved all this without you all.

Dedication

I dedicate this dissertation to my ever-caring and supportive father, and my loving and adorable mother. I really love you both.

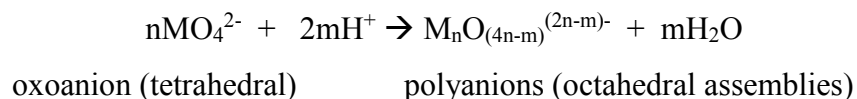
Chapter 1 - Introduction

1.1 Polyoxometalates

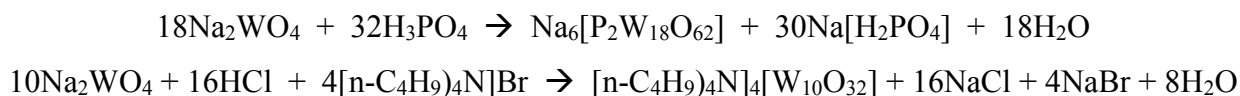
Polyoxometalates (POMs) can be defined as discrete metal-oxygen anionic clusters. The basic connecting unit in these clusters are $\{MO_x\}$ polyhedra, where M are usually early transition metals (V, Nb, Ta, Mo, W) in their highest oxidation states.¹ Although their structures and properties, such as thermal and oxidative stability, are very similar to that of metal-oxides, they are more soluble in water or other solvents. As a result, they are also sometimes referred to as “soluble oxides”.² Another feature that distinguishes POMs from metal-oxides is their ability to incorporate a variety of heteroatoms (P, As, Si, Ge) in the architecture. These are well known for their diverse sizes, nuclearities, and shapes, where these clusters can range from macro (e.g., $Mo_6O_{19}^{2-}$) to nanosized species (e.g., $H_xMo_{368}O_{1032}(H_2O)_{240}(SO_4)_{48}^{48-}$).³

The first polyoxometalate was reported in the early 19th century, when Berzelius synthesized a yellow ammonium salt, $(NH_3)_3PMo_{12}O_{40}$.⁴ But, due to limited analytical techniques, their characterization and a systematic study of their properties did not begin until the early 20th century.⁵ Till date, hundreds of POMs have been reported, of which the most studied structures contain molybdenum (VI) and tungsten (VI), as these metals have empty and accessible *d*-orbitals for metal-oxygen π -bonding which in turn favors the combination of ionic radius and charge.⁶

POMs are typically synthesized in an acidic medium, as shown below, where an oxoanion ion undergoes protonation, and upon polycondensation of the MO_4^{2-} units, nano-sized anionic clusters are formed.³



These anionic assemblies are usually stabilized by the presence of counter cations such as alkali metal ions, ammonium or alkylammonium ions.⁷



1.1.1 Classification of polyoxometalates

Due to the vast diversity in structure types, classification of POMs is a necessity and can be done in several ways. Based on their composition, they can be broadly classified into three major categories.

1.1.1.1 Isopolyanions

The condensation of similar species leads to the formation of an isopolyanion (IPA) with the general formula of $[M_mO_y]^p$.³ The central atom in this category is an oxygen atom around which the metal framework is built. Consequently, these are less stable than other forms of POMs. Nevertheless, they display interesting physical properties, such as high charges and strongly basic oxygen surfaces, which makes them attractive units for use as building blocks.⁸ The most symmetrical structure in this class is the 'Lindqvist Ion', with the general formula $[M_6O_{19}]^x$, where M = Mo, W, V, Nb or Ta and the charge (x) depends upon the number of metal substitutions (Figure 1.1). The structure contains six octahedrons connected through a common vertex, an oxygen atom, which bonds to six metal centers in a μ_6 coordination mode.⁹

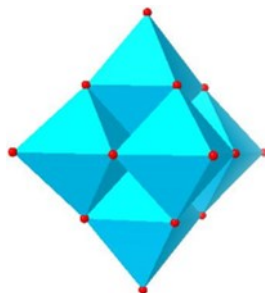


Figure 1.1 Lindqvist polyoxometalates.⁹

1.1.1.2 Heteropolyanions

Several oxoanions condense around a central tetrahedral (e.g., SO_4^{2-} or PO_4^{3-}) or an octahedral template, or around another metal atom, wherein this reaction yields a heteropolyanion (HPA) with the general formula $[X_sM_nO_m]^y$.³ It has been postulated that this reaction is thermodynamically driven.¹⁰ This class of POMs can further be divided into three main categories based on their X/M ratio (where X is heteroatom) (Figure 1.2). These types of anions are much more robust and thus, various tungsten-based Keggin $\{M_{12-n}\}$ and Dawson $\{M_{18-n}\}$ anion based lacunary polyoxometalates have been developed and are still being extensively researched.³

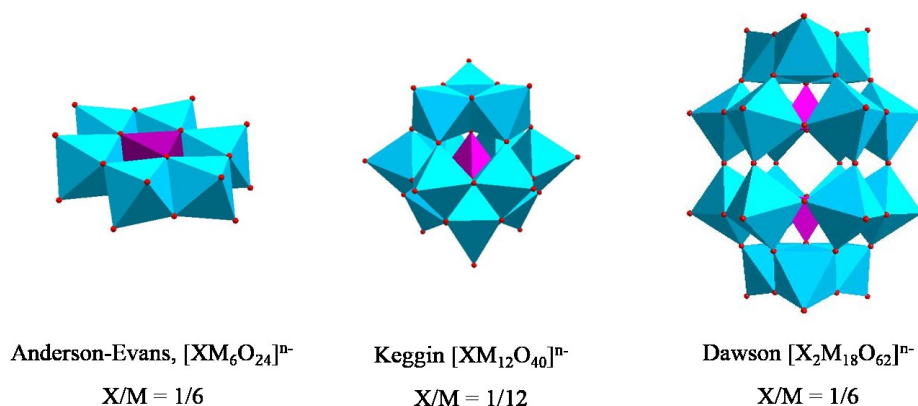


Figure 1.2 Types of heteropolyanions.³

1.1.1.3 Molybdenum blue and molybdenum brown reduced POMs

This is a more recent class of POMs consisting of highly reduced species. Although, molybdenum blue was first reported by Scheele in 1783,¹¹ its actual composition came to light in 1995, when Müller identified it as a high nuclearity cluster $\{Mo_{154}\}$ having a ring topology.¹² Upon altering the pH and amount of reducing agent, these species can transform into molybdenum brown $\{Mo_{132}\}$, which possesses a ball-like spherical structure (Figure 1.3).^{8,12} This class of POMs is attracting increasing attention owing to their photochromic and electrochromic applications.^{3,6,8}

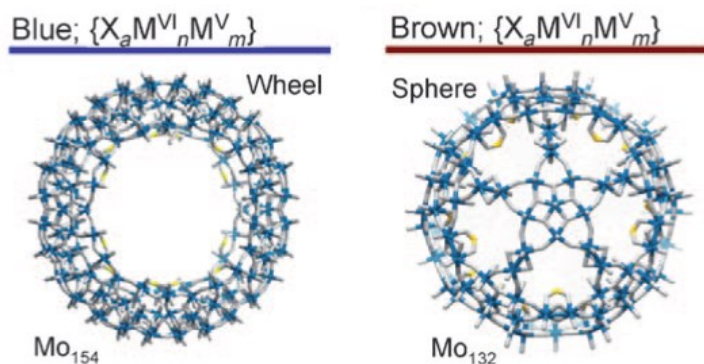
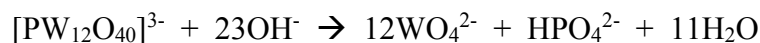


Figure 1.3 Molybdenum blue and brown POMs.⁸

1.1.2 Properties of polyoxometalates

Due to their diverse molecular structure, POMs display remarkable properties which makes them an interesting field of study. The structural similarities with classic metal oxides makes them robust architectures with high thermal and oxidative stability. Moreover, POM clusters exhibit high molecular mass (up to 10,000 amu) and large size (6-25 Å), which in turn

provides them with high surface area.¹³ In aqueous medium, POMs behave as strong acids ($pK_a < 0$) and have gradually replaced use of mineral acids in catalysis.³ POMs decompose under basic conditions in a controlled manner.¹⁴



POMs are highly charged anions (-3 to -14) and modification of the counter cations offers excellent tunable solubility in aqueous as well as in organic solvents, which makes them attractive in both homogeneous and heterogeneous applications.¹⁵ Some POMs are also known for their luminescence¹⁶ and magnetic properties.¹⁷ They are also photoreducible and the oxidized and reduced forms show different visible colors. POMs are also known as electron reservoirs which in turn allows for reversible multi-electron transfers without structure degradation, with remarkable redox properties. For example, some POMs can take up to 32 electrons before the cluster decomposes.¹³

1.1.3 Applications of polyoxometalates

The diverse physical and chemical properties exhibited by POMs (see previous section) renders them as attractive candidates in various fields of research. A wide range of applications of POMs are well documented, and a significant increase in the number of publications and patents based on POMs has been observed in recent years (Figure 1.4).⁶

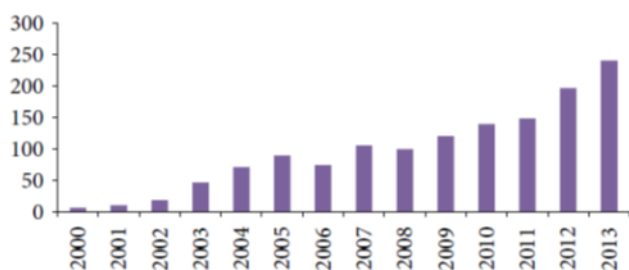


Figure 1.4 Increase in number of publications on polyoxometalates in recent years.^{6,8}

The primary use of POMs is in the field of catalysis, which includes many homogeneous and heterogeneous reactions such as epoxide synthesis, oxidative coupling, esterification, condensation, hydration of olefins, and Friedel-Crafts acylation.¹⁸ Several POM-stabilized multi-electron-metal-based water oxidation catalysts have been developed recently which are more efficient, carbon-free and robust in comparison to previously reported homogeneous or heterogeneous systems.¹⁹ Functionalization of POMs by metal substitution or covalent grafting

of organic groups can considerably alter properties such as polarity, redox potentials, surface charge distribution, shape, and acidity, which makes them attractive in the field of medicine as depending on the target macromolecule, the reactivity of POMs can be altered^{20a} Also, POM based drugs are easier to scale-up in comparison to the counter organic drugs, which makes their use much more economical. POMs are also very popular due to their antiviral and antitumor activities, as well as for their role in enhancing the effectiveness of antibiotics against resistant strains of bacteria.²⁰

Since POMs form stable insoluble salts with large cations and have the ability to accept electrons without major structural changes, these can act as corrosion inhibitors, which reduces toxicity in comparison to traditional inhibitors such as chromates, phosphates or silicates.¹³ Lomakina *et al.* reported corrosion inhibition based on POM alloys, wherein these alloys could be used as construction materials in atomic industries owing to their high radiation stability.²¹ Moreover, the ability of POMs to form stable precipitates with cationic dyes promotes their use as pigments, dyes, and ink in jet printers and photocopier toners.¹³ Combining their acid catalysis property with their photochromic, electrochromic, and ion conductive nature *via* the sol-gel approach yields siloxane-POM acid networks with antireflective and antistatic properties, that can be used as coatings for buildings and automobiles with reliable light control.^{13,22} Mo- and W-based POMs are photosensitive in nature and on combining these with organic reducing agents, photographic materials for the production of images and recording, can be synthesized.²³

POMs can act as a reversible oxidant in wood pulp bleaching process, thus offering a greener alternative to the use of chlorine which forms toxic chlorinated aromatics and dioxins as side products.²⁴ POMs have also been used as process aids for extracting radioactive nuclei (such as Cs-134 and Cs-137) which are usually present in low concentrations in medium active aqueous wastes.²⁵ POM-based membrane devices or sensors such as solid-state electrochromic devices and gas detection apparatuses can be produced, by coupling their high ionic conductivity with their ability to undergo redox processes.²⁶ POMs can also be used as a secondary charge storage system and thus have been utilized for optimizing battery components and capacitors.¹³ Also, POMs are known to self-assemble to form supramolecular gels, which exhibit thermo- and photo-responsive properties.²⁷

1.2 Modification of polyoxometalates

Due to the diverse properties of POMs and their immense potential in several fields of research, there is a growing interest in functionalizing these clusters. Following are some important reasons for the functionalization of POMs:

- a) Metal oxides have been used as catalysts for various organic reactions, but determining the reaction mechanism is difficult in this case. The structural similarities of polyoxometalates to metal oxides coupled with their enhanced solubility, makes them as interesting candidates for use in such reactions and may also provide an understanding of the elementary steps of heterogeneous reactions. Furthermore, new transition metal-based catalysts can be developed, thus generating a new class of oxide-supported catalytic materials.
- b) Functionalization of POMs may improve the stability of otherwise unstable architectures, thus leading to novel building blocks for macroassembly.
- c) Incorporating ligands with remote functionality may provide a means of extending these architectures into interconnected POM networks.
- d) Peripheral oxygen atoms may be activated *via* functionalization of the POM.
- e) Multifunctional oxidation catalysts demonstrating higher selectivity for antiviral chemotherapy may also be prepared by functionalizing POMs.²⁸

Depending on the type of interactions, the POM hybrids can be categorized into two classes. All the systems where the interaction between the organic and inorganic components is non-covalent in nature, such as electrostatic interactions, hydrogen bonds, or van der Waals interactions, are part of class I hybrids (Figure 1.5).²⁹ On the other hand, systems where the two components are interconnected *via* covalent or ionic-covalent bonds comprise of class II hybrids. In class II hybrids, the organic ligand is required to either substitute an oxo group of the POM or bond directly to the metallic center. Since, the terminal oxygen atoms are good nucleophiles, an electrophilic ligand bearing an organic moiety can bond covalently with POMs. Both the chemical nature and the electronic properties of the inorganic moiety needs to be considered before covalent functionalization of POMs. Since, POMs are anionic in nature, neutral or negatively charged organic systems will favor covalent grafting over electrostatic interactions.¹ The work presented in this thesis focuses on class II type hybrids, hence further discussion will focus exclusively on such systems.

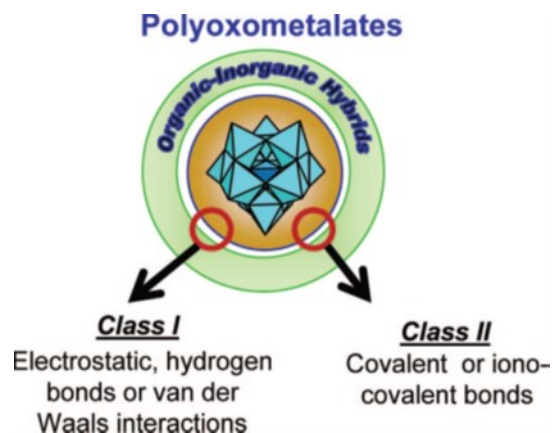


Figure 1.5 Types of organic-inorganic POM hybrids.¹

1.2.1 Transition metal

One of the most common ways of modifying POMs is by incorporating transition metal ions in the framework.^{1,28} Dawson- and Keggin-type POMs under alkaline and other appropriate conditions (*e.g.* pH, temperature, and concentration) lose one or more metal centers in a controlled manner to yield lacunary POM species.^{19d} These lacunary species exhibit isomerism and are known to react with various transition metals (*e.g.*, Fe^{III}, Mn^{II}, Co^{II}, Ni^{II}, Zn^{II}) to form substituted Keggin POMs. These POMs display luminescent and unusual magnetic properties due to the unpaired electrons of transition metals, and hence can be used in nanocomputer storage devices.³

In a recent report, a transition metal-functionalized POM derivative with a well-defined histidine-chelating site, displayed improved A β inhibition and peroxidase-like activity in comparison to the parent POM (Figure 1.6).³⁰

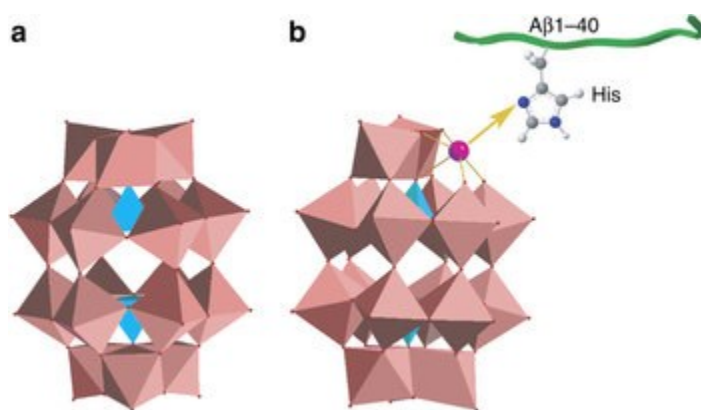


Figure 1.6 Transition metal functionalized POM interacting with histidine.³⁰

A novel dimanganese $Mn^{II/III}$ containing Keggin-type polyoxotungstate $K_6[Mn_2SiW_{10}O_{37}(OH)(H_2O)] \cdot 11H_2O$ self-organizes *via* the divacant $\{SiW_{10}O_{36}\}$ unit to form a 1D POM architecture containing the rarely observed Mn–O–W bridges, wherein the manganese centers display antiferromagnetic behavior (Figure 1.7).³¹

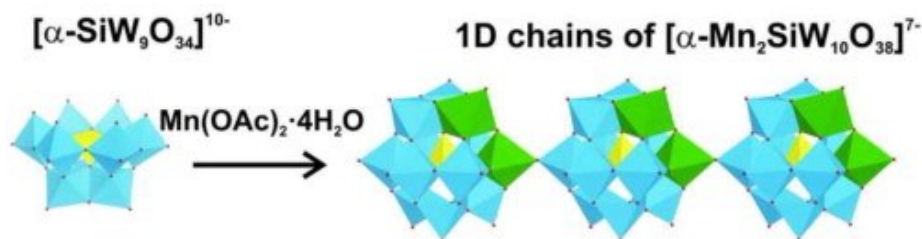


Figure 1.7 Self-assembled 1D chains of a dimanganese ($Mn^{II/III}$) functionalized POM.³¹

1.2.2 Organometallic derivatives

Organometallic compounds are well known for heterogeneous catalysis.³² Many POM derivatives have been prepared by grafting organometallic moieties for investigating any variations in the reactivity and surface dynamics of the organometallic fragment.³³

A series of four organo-ruthenium supported heteropolytungstates were prepared by reacting $[Ru(arene)Cl_2]_2$ (arene = benzene, *p*-cymene) with $[X_2W_{22}O_{74}(OH)_2]^{12-}$ ($X = Sb^{III}, Bi^{III}$) in a buffer medium, wherein these clusters showed a higher catalytic activity for several reactions (Figure 1.8).³⁴ For example, a strong electrocatalytic water oxidation peak which is more positive than its parent $Ru(arene)$ oxidation process was observed. Also, there was an enhancement in the catalytic activity for oxidation reactions of *n*-hexadecane and *p*-xylene (due to the ruthenium substituent on the polyanion).

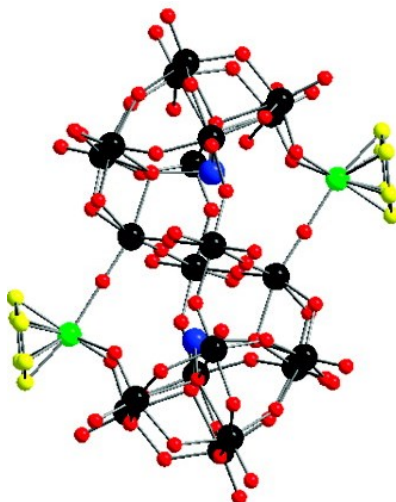


Figure 1.8 Organo-ruthenium functionalized POM.³⁴

An interesting organometallic derivative of POM, $[\{\text{Ru}(\eta^6\text{-p-MeC}_6\text{H}_4\text{Pr}^i)\}_4\text{Mo}_4\text{O}_{16}]$, was observed by Süss-Fink *et al.*, where the $[\text{Ru}_4\text{Mo}_4\text{O}_{12}]$ framework forms a central $[\text{Mo}_4\text{O}_4]$ cube with four folded ORuO flaps resembling the sails of a windmill (Figure 1.9).³⁵

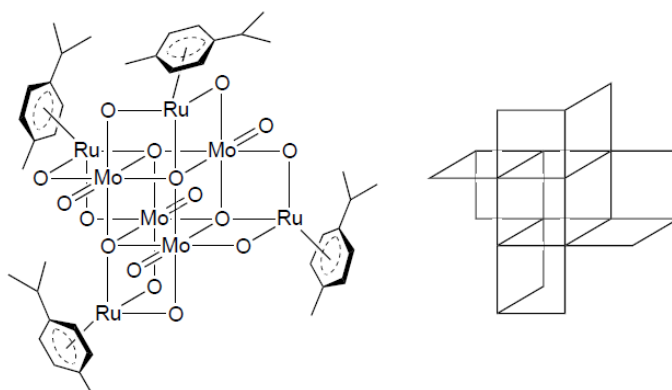


Figure 1.9 Windmill-like structure of $[\{\text{Ru}(\eta^6\text{-p-MeC}_6\text{H}_4\text{Pr}^i)\}_4\text{Mo}_4\text{O}_{16}]$.³⁵

1.2.3 Main group elements

The oxo ligand is isoelectronic to other main group ions such as F^- , HO^- , HN^{2-} , N^{3-} , and HC^{3-} , and thus can be substituted by these ions. Another characteristic of the oxo ligand to be considered, is that they are good π -donors, which might be a key feature for stabilizing the metal atoms in their higher oxidation states. Also, a distinctive feature is their inclination to form multiple bonds.²⁸

1.2.3.1 Halides

Halides, being reactive, are suitable for further modification, and thus have been extensively researched. An ammonium salt of $[\text{CoW}_{11}\text{O}_{38}\text{F}_2\text{H}_4]^{6-}$ having Keggin-like structure was reported by Wasfi *et al.*, wherein the cobalt atom is thought to occupy the octahedral site vacated by the missing tungsten atom.³⁶ The fluorine atoms replace the oxygen atoms that form the central cavity, and are not involved in π -bonding, thus rendering the architecture unavailable for any further chemical modification. This observation highlights the reluctance of fluorine to participate in multiple bonding.

A polyoxochlorotungstate, $[\text{W}_6\text{O}_{14}\text{Cl}_{10}]^{2-}$, was prepared by reacting $(n\text{-Bu}_4\text{N})[\text{W}_2\text{O}_2\text{Cl}_7]$ with *p*-tolyl azide which is an example of a fully oxidized POM (Figure 1.10).³⁷ It consists of two trinuclear $[\text{W}_3\text{O}_3(\mu\text{-O})_3\text{Cl}_4(\mu_3\text{-Cl})]$ fragments joined by two linear W-O-W linkages.

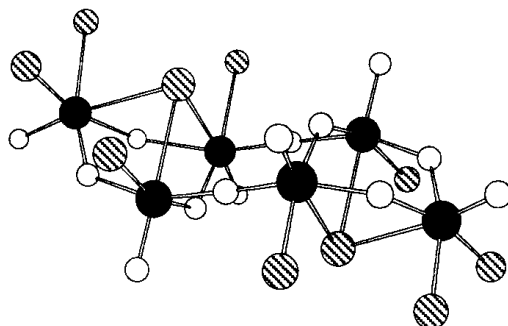


Figure 1.10 Structure of the fully oxidized $[\text{W}_6\text{O}_{14}\text{Cl}_{10}]^{2-}$ anion.³⁷

1.2.3.2 Monodentate alkoxide

Many examples in literature can be found where monodentate alkoxide groups have been incorporated in POMs.^{1,28} For example, monomethylated $[\text{IMo}_6\text{O}_{23}(\text{OMe})]^{4-}$ anions, which adopt an Anderson-type structure stabilized by the steric protection of the supporting ligand in the dinuclear Co complex have been isolated (Figure 1.11).³⁸

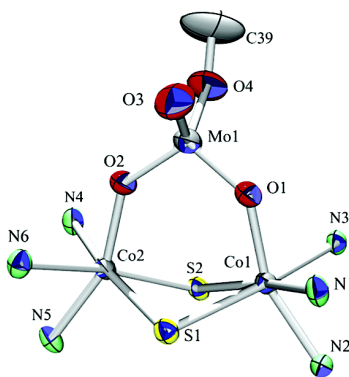


Figure 1.11 A cobalt complex stabilized by the monomethylated $[\text{IMo}_6\text{O}_{23}(\text{OMe})]^{4-}$ anion.³⁸

1.2.3.3 Trisalkoxides

Monodentate alkoxides usually do not form stable Anderson-type clusters. As a result, for stabilizing such systems, a vast number of derivatives have been prepared by using the steric requirements of trisalkoxy moieties. The arms of the trisalkoxy moiety binds three metal atoms in a triangular arrangement forming a bridge, while simultaneously capping the tetrahedral cavities of the POM frameworks. This approach has been explored in developing POM derivatives bearing remote functionalities that can coordinate to a second metal atom (Figure 1.12 (a)).^{33,39,40} For example, POM derivatives where the bridge is a triol moiety bearing a pyridyl functional group has been reported (Figure 1.12 (b)).⁴⁰ These display a δ isomeric-Anderson framework with a trisalkoxo ligand attached on both sides, whereas the pyridyl nitrogen atoms are coordinated to the metalloporphyrins $[\text{ZnTPP}]$ and $[\text{Ru}(\text{CO})\text{TPP}]$. However, cyclic voltammetric studies of these assemblies with $[\text{Ru}(\text{CO})\text{TPP}]$ displayed an irreversible change in the reduction potentials.

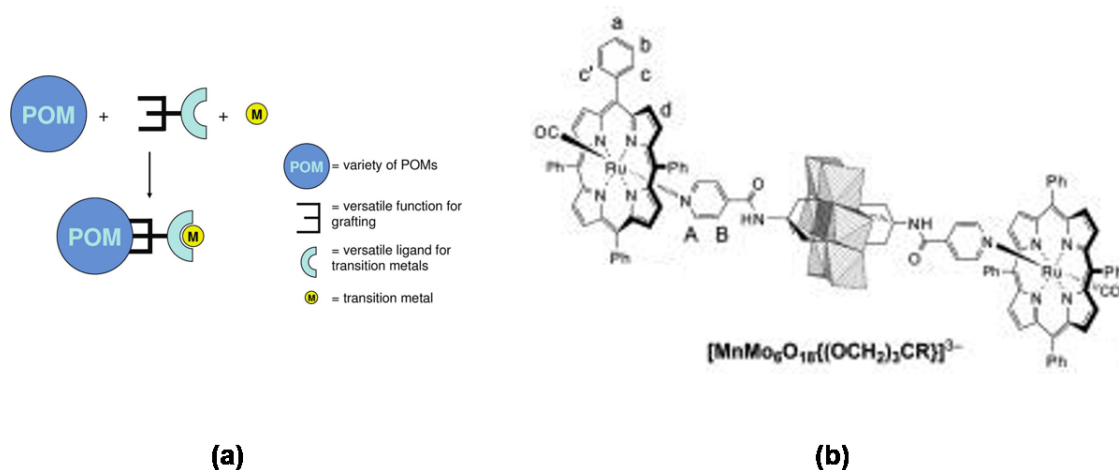


Figure 1.12 (a) Trisalkoxo functionalization as a route towards bimetallic systems²; **(b)** Metalloporphyrin interacting with a trisalkoxo functionalized POM.⁴⁰

1.2.3.4 Organosilyl derivatives

A wide variety of organosilyl POM derivatives with potential for further chemical modifications have been explored.⁴¹ Synthesis of such hybrids usually depends on the nucleophilicity of the oxygen atom of lacunary heteropolyoxometalates (Keggin or Dawson lacunary structures) and the electrophilic nature of organosilanes.¹ In a bid to assemble new hybrids displaying catalytic activity, a phosphine containing alkylsilane was grafted into the defect position of a lacunary $[\text{SiW}_{11}\text{O}_{39}]^{8-}$, which on further treatment with the appropriate rhodium reagent resulted in a POM hybrid, $\{\text{SiW}_{11}\text{O}_{39}[\text{O}(\text{SiCH}_2\text{CH}_2\text{PPh}_2)_2\text{PPh}_3\text{Rh}(\text{I})\text{Cl}]\}^{4-}$, bearing a covalently bonded Wilkinson's type catalyst (Figure 1.13).^{41c} The catalytic activity of the hybrid towards hydrogenation of alkenes showed a marked increase in comparison to the classic Wilkinson's catalyst, $\text{Rh}(\text{I})\text{Cl}(\text{Ph})_3$.

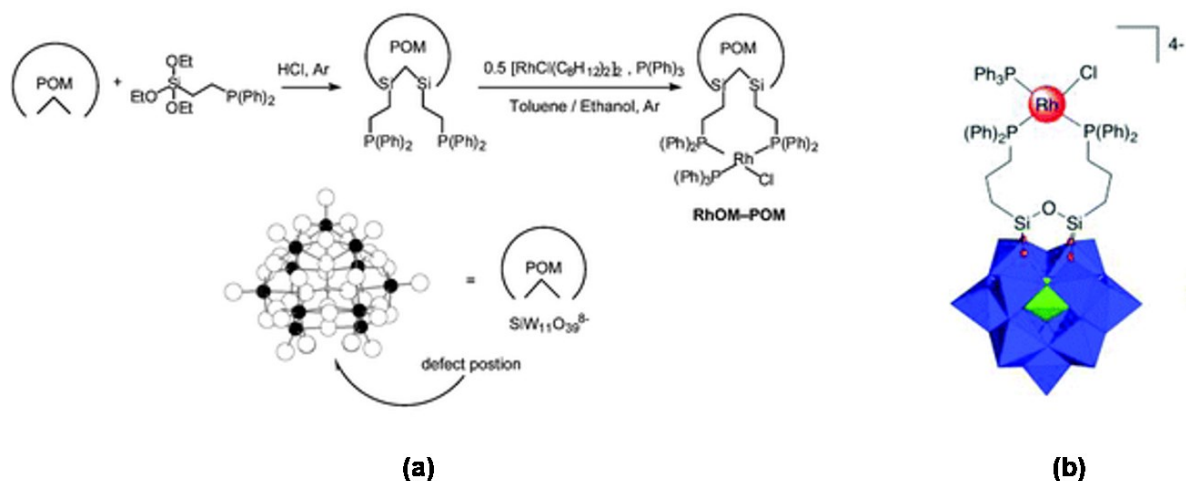


Figure 1.13 Organosilyl functionalization of a POM for further chemical modification.^{41c}

1.2.3.5 Organoimido derivatives

Organoimido ligands are catalytically important for ammoxidation of propylene into acrylonitrile,⁴² olefin aziridination⁴³ and in various nitrogen transfer reactions.⁴⁴ Thus, synthesis of organoimido-POM hybrids are of great interest, as it is expected that the π electrons of an organic group introduced *via* an imido linkage may get extended to the inorganic framework *via* strong d- π interactions, which in turn may modify the electronic structure and redox properties of the resulting hybrid.⁵¹ A common method of introducing an organoimido functionality in a POM framework is by directly substituting the oxo linkage with nitrogenous ligands in a Lindqvist POM.⁴⁵

Lindqvist POMs can be expressed by the general formula, $[M_6O_{19}]^{n-}$, (M = Mo, W, Nb, Ta, V) (see section 1.1.1), wherein the framework contains oxo ligands in three different coordination environments (Figure 1.14).⁹ First, the structure contains a central oxygen atom bound to six metal atoms in a μ_6 coordination mode resulting in an octahedral geometry. Second, each metal atom is further connected to neighboring metal atoms via four oxo ligands in a μ_2 coordination mode, thus forming a bridge. Third, each metal atom is capped by a terminal oxo ligand forming a M=O bond (one σ -bond and two π -bonds).

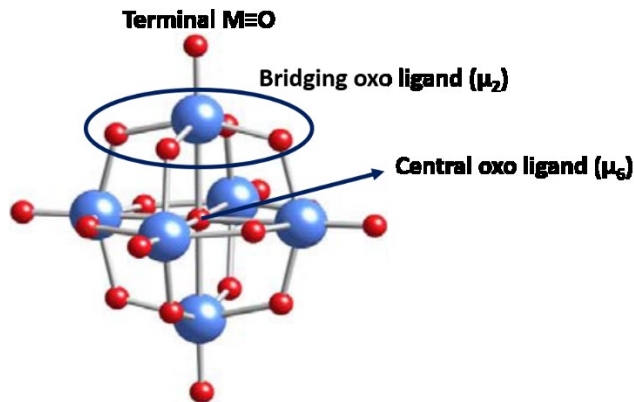


Figure 1.14 Lindqvist POM displaying oxygen atoms in three different environments.⁹

These terminal oxo ligands can potentially be substituted by various isoelectronic nitrogenous ligands such as organoimido,⁴⁶ diazoalkyl,⁴⁷ and diazenido species.⁴⁸ Varying these imido-releasing reagents yields different types of imido-POM derivatives, and can also introduce multi-functionality in the resulting hybrid. The first documented organoimido derivative, $[\text{Mo}_6\text{O}_{18}(\text{NR})]^{2-}$, was synthesized by Zubieta *et al.* in 1988 by reacting $[\text{Mo}(\text{NR})\text{Cl}_4(\text{thf})]$ with $[\text{Mo}_2\text{O}_7]^{2-}$.⁴⁹ The first reported single-crystal X-ray characterization of an organoimido derivative was presented by Maatta *et al.* in 1992, wherein the tolylimido derivative $[\text{Mo}_6\text{O}_{18}(\text{Ntol})]^{2-}$ was prepared by reacting $[\text{Mo}_6\text{O}_{19}]^{2-}$ with $\text{Ph}_3\text{P}=\text{Ntol}$.⁴⁶ This novel study greatly excited the interest in the synthesis and characterization of organoimido POM derivatives.

In the search for assembling multifunctional hybrids, various organic moieties have been incorporated into POM clusters using the imido moiety. Recently, several organic ligands with different functional groups were stepwise grafted onto hexamolybdates to form mixed disubstituted organoimido hexamolybdates, with the aim of synthesizing chiral clusters with reduced symmetry (Figure 1.15).⁵⁰

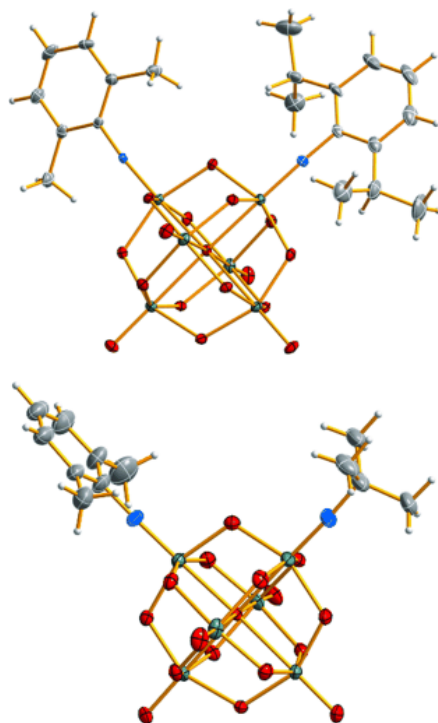


Figure 1.15 Mixed disubstituted hexamolybdates.⁵⁰

The use of POMs is limited in electrochemical applications, owing to their low electronic conductivity. Thus, functionalizing them with organic moieties may improve their electronic conductivity, due to enhanced metal to ligand charge transfer (MLCT) *via* d– π interactions.⁵¹ Moreover, the organic molecules with different donor atoms than oxygen may arrange differently around the binding site, thus providing a handle for adjusting the chemical and geometrical preferences of various other metals. In a recent communication, the authors synthesized an organoimido derivative, $[(\text{Bu}_4\text{N})_2[\text{Mo}_6\text{O}_{18}\text{-N-Ph-(}o\text{-CH}_3)_2\text{-}p\text{-SCN}]$, bearing an electron withdrawing group (–SCN) as a pendant and tested it as an anode for a lithium ion battery (Figure 1.16).⁵² The hybrid showed excellent capacity retention and stable cyclic life for 100 cycles. Also, the cyclic voltammetric studies showed that lithium insertion and extraction by the hybrid is reversible in nature. These properties can be explained by the covalent modification of the POM as it provides high conductivity, faster ion transfer and structure stabilization through d– π interactions.

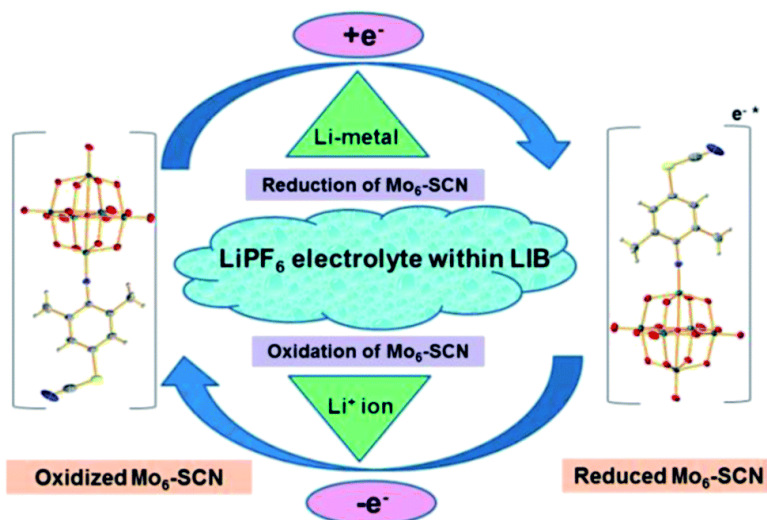


Figure 1.16 An organoimido POM [(Bu₄N)₂[Mo₆O₁₈-N-Ph-(o-CH₃)₂-p-SCN] used as an anode in lithium ion batteries.⁵²

An organoimido derivative of POMs containing an electron-donating ethyl group has been prepared by Yua *et. al*, wherein the single crystal structure of the hybrid displays dimer formation accompanied by π - π stacking between two parallel phenyl rings (Figure 1.17).⁵³ Preliminary studies with the hybrid displayed enhanced antitumor activity on the cellular growth inhibition to K562 cells when compared to the parent hexamolybdate cluster.

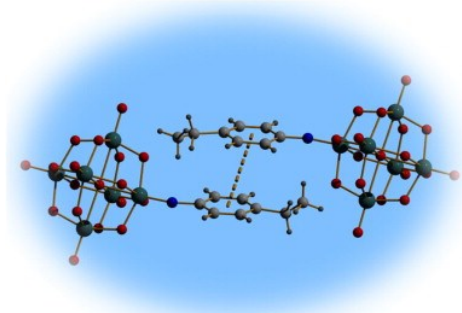


Figure 1.17 POM hybrid displaying antitumor activity.⁵³

1.3 Methods of preparing organoimido derivatives of hexamolybdate

Several methods for preparing organoimido derivatives of hexamolybdates have been documented to date.^{45,69} Maatta group follows the direct reaction of an organoimido delivery reagent and the tetrabutylammonium hexamolybdate, [TBA]₂[Mo₆O₁₉], under an inert atmosphere using mild heating conditions.⁴⁷ The organoimido delivery reagent used is either a phosphineimine (R-N=PPh₃) or an isocyanate (R-NCO). The detailed mechanism for the

functionalization of hexamolymolybdates is still not clear, but with phosphineimines, it has been suggested that the terminal Mo-O bond and the phosphorus-nitrogen double bond are involved in forming a four-membered transition state, similar to that of the Wittig (net) [2 + 2] intermediate, which on rearrangement yields the desired functionalized POM (Figure 1.18).^{46,54,55} The by-product of this reaction is triphenylphosphine oxide which has to be removed.

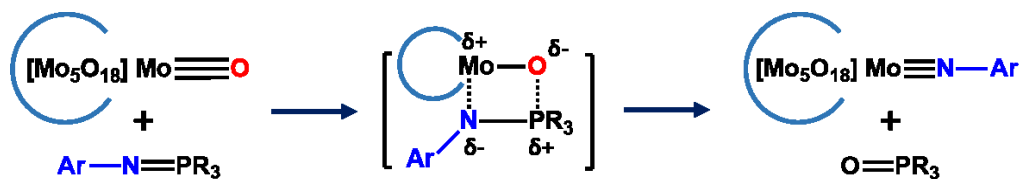


Figure 1.18 Suggested mechanism for oxo substitution by phosphineimines in POMs.⁵⁵

Isocyanates are assumed to react in a similar manner to phosphineimines, *via* a four-membered transition state, but they generally require longer reaction times and the by-product is carbon dioxide which is expelled from the system (Figure 1.19).⁵⁶ This reaction requires minimal workup despite involving longer reaction times, thus making this route more attractive than the phosphineimine route.

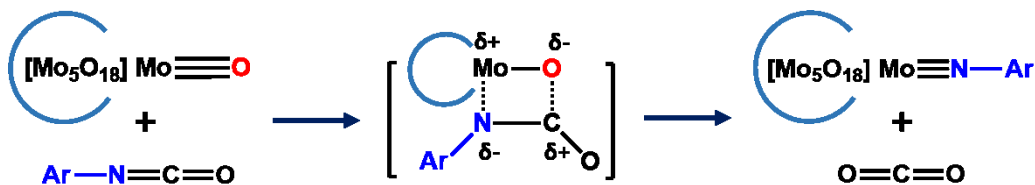


Figure 1.19 Suggested mechanism for oxo substitution by isocyanates in POMs.⁵⁵

New methods for the functionalization of hexamolymolybdates have been developed by Peng and Wei.^{57,58} The organoimido delivery agent in these methods is an arylamine which is used in the presence of N,N'-dicyclohexylcarbodiimide (DCC), and the methods involve refluxing under an inert atmosphere. Peng's route involves direct substitution of the terminal oxygen atom in [TBA]₂[Mo₆O₁₉] with an arylamine, where DCC acts as a dehydrating/activating agent (Figure 1.20). While the mechanism for this method is still unknown, it is suggested that DCC plays two roles: (i) it activates the terminal Mo-O bond of hexamolymolybdate by forming an activated intermediate species, which then interacts with an arylamine (similar to its activating effect on the carboxyl group in the synthesis of amide or peptides); and (ii) as a sacrificial dehydrating reagent. The by-product in this route is N,N'-dicyclohexylurea which needs to be separated, and the overall reported yields are higher in comparison to previous methods.⁵⁷

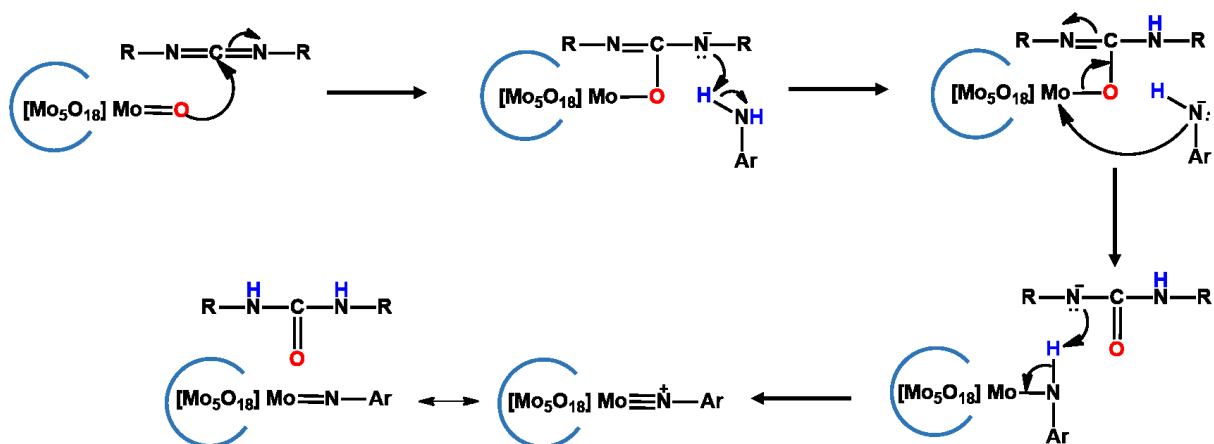


Figure 1.20 Peng's route for hexamolybdate functionalization using arylamine as an organoimido delivery reagent.^{57, 58}

Wei proposed a modified version of Peng's method for the functionalization of POMs, wherein octamolybdate [TBA]₄[Mo₈O₂₆] was utilized in place of hexamolybdate, along with the hydrochloride salt of the corresponding arylamine (Figure 1.21). In this reaction, conversion of octamolybdate to hexamolybdate is a possibility due to the presence of the hydrochloride salt of the arylamine. This synthetic route is reported to be highly efficient with faster reaction rates and higher yields.⁵⁹

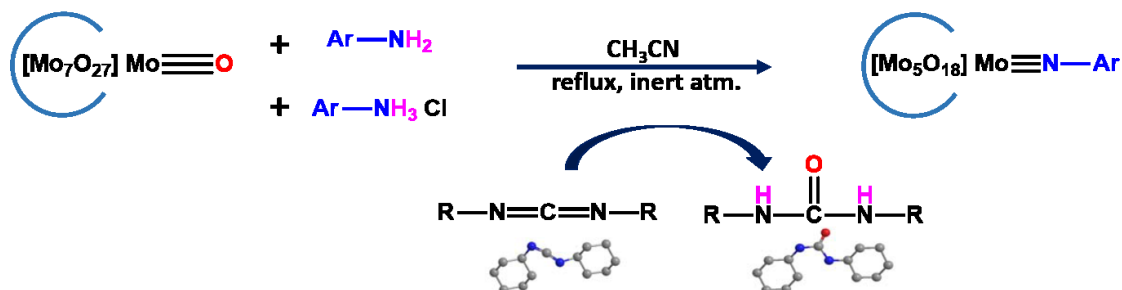


Figure 1.21 Wei's route for POM functionalization using arylamine as the organoimido delivery reagent in the presence of its hydrochloride salt.⁵⁹

1.4 Organoimido hexamolybdate bimetallic systems

Organoimido POM derivatives have been investigated further in a bid to assemble bimetallic systems which find use in the field of electrochemistry⁶² and catalysis.⁶⁰ For example, Maatta and Hill reported a *p*-pyridylimido vanadium (V) complex, wherein the pyridyl nitrogen atom (σ -donor / π -acceptor) was capable of coordinating a second metal center (Figure 1.22).⁶¹ This study attracted a great deal of attention and furthered the work on bimetallic POM architectures.

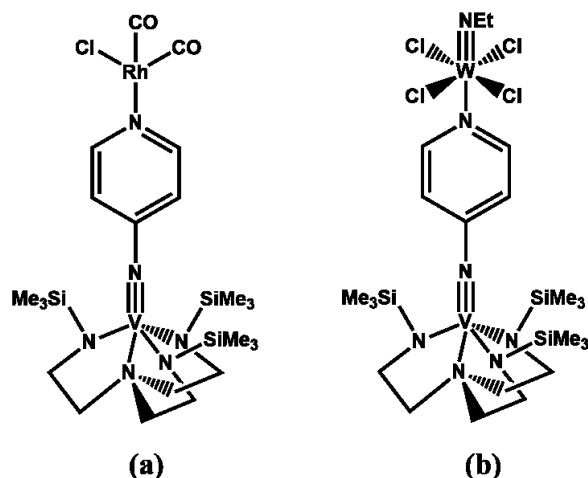


Figure 1.22 Organoimido-based vanadium (V) derivative complexed with: **(a)** rhodium; and **(b)** tungsten, forming bimetallic architectures.⁶¹

The presence of diverse metal-coordinating organic functional groups on the organoimido POM derivatives makes them more active towards coordinating with a second metal atom.⁶² Thus, many organoimido hexamolybdates have been synthesized with metal-coordinating groups such as hydroxyl,⁶³ carboxyl,⁶⁴ pyridyl⁶⁵ and nitrile,⁶⁶ but surprisingly these POM derivatives do not show any coordination with a second metal atom (Figure 1.23).⁴⁵

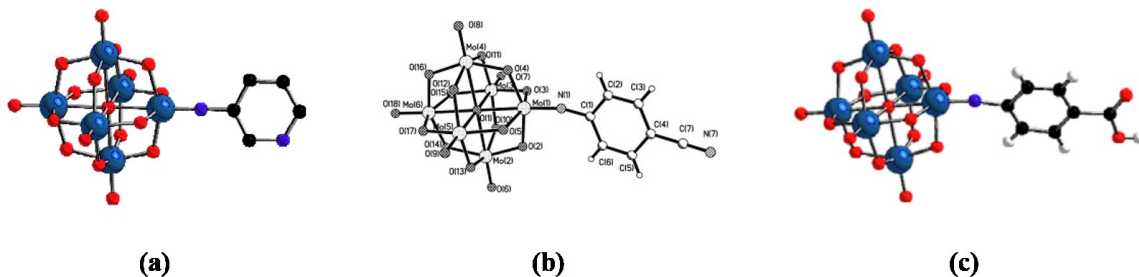


Figure 1.23 POM derivatives with metal-coordinating functional groups: **(a)** *m*-pyridyl;⁶⁵ **(b)** *p*-nitrile,⁶⁶ and **(c)** *p*-carboxyl.⁶⁴

The inability of the above POM derivatives to coordinate with another metal atom can be attributed to the highly electron withdrawing nature of hexamolybdate, which pulls all the electron density into the cluster, thus rendering the donor site non-basic. This problem can be tackled *via* two different routes:

1. By disrupting the conjugation between the cluster and the metal-coordinating functional group. Existing studies have indicated that incorporating non-conjugated systems in the cluster reduces the through-bond flow of electron density into the cluster, thus POM

derivatives having the ability to coordinate different metal atoms can be synthesized (Figure 1.24).⁶⁷

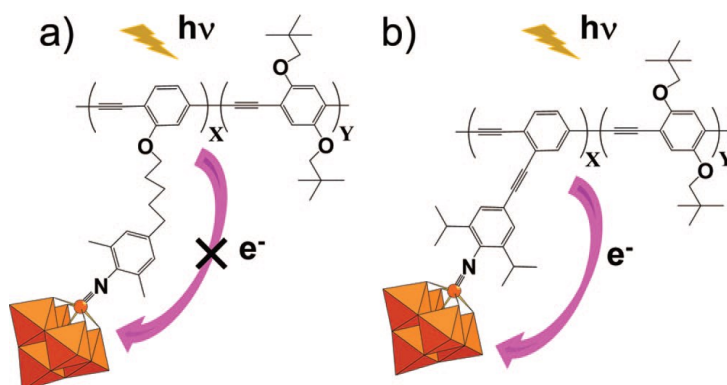


Figure 1.24 Control of electron flow in POM hybrids by breaking the conjugation in the system.⁶⁷

- By adding a conjugated spacer group between the cluster and the metal-coordinating functional group (conjugation is retained in the system). Peng *et. al.* synthesized an imido functionalized hexamolybdate bearing a remote terpyridyl moiety with an extended π -conjugated bridge displaying the capability of coordinating with Zn^{2+} and Ru^{2+} ions (Figure 1.25).⁶⁸

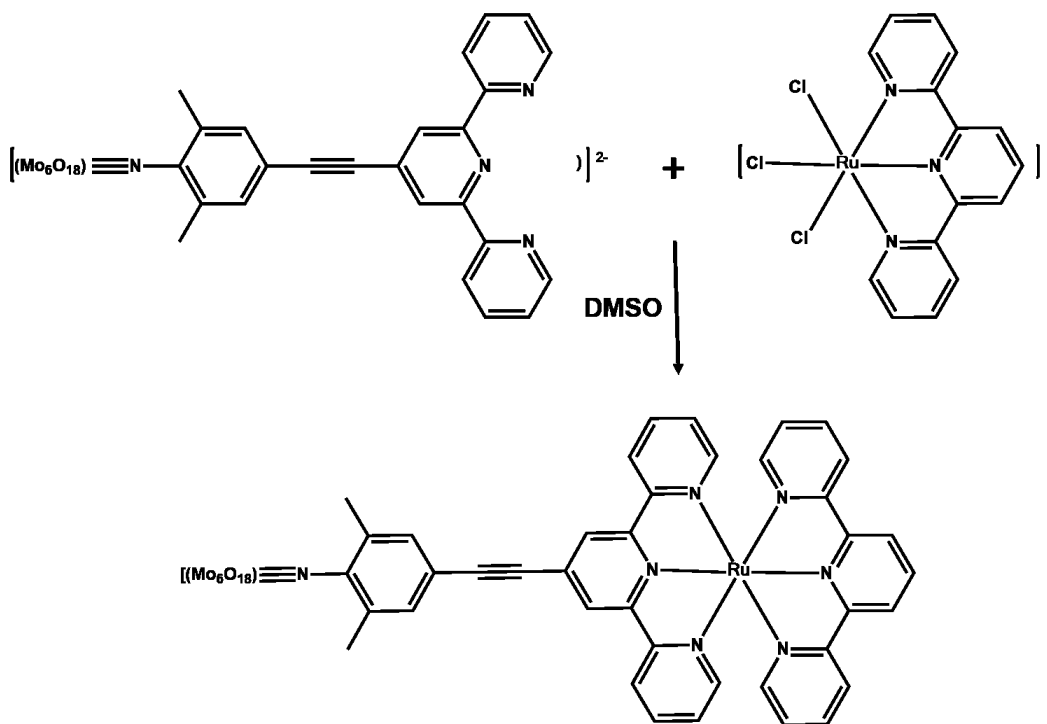


Figure 1.25 Bimetallic POM hybrid having an extended conjugated system.⁶⁸

1.5 Goals

Although, organoimido functionalized POM hybrids have been extensively researched,^{45,69} but studies based on hybrids capable of coordinating another metal atom (bimetallic systems) for use in the fields of catalysis and electrochemistry are still rare. The work in this thesis is focused on the design and synthesis of novel organoimido delivery reagents capable of forming bimetallic POM hybrids, and the use of these ligands towards the synthesis of bimetallic hexamolybdate derivatives. The delivery reagents were designed thoughtfully and separate organic moieties were selected for coordinating to both the cluster and the second metal atom (Figure 1.26).

- (i) -NH_2 group: Are suitable for oxo substitution (isoelectronic to oxo ligands), hence can be used for coordinating to POMs.
- (ii) A functional group having the capability of coordinating with another metal atom.

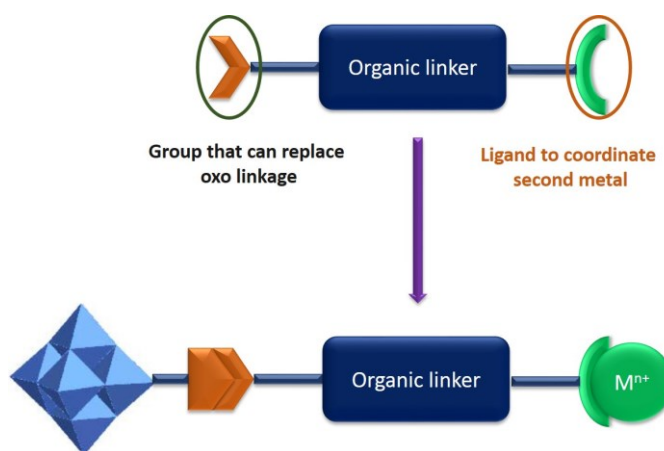


Figure 1.26 Synthesizing bimetallic organoimido hexamolybdates capable of diverse applications.

The selected functional groups having the potential for coordinating to metal atoms are dithiocarbamates (Chapters 2 and 3), extended pyridyl group (Chapter 4), and acetylacetonates (Chapter 5). Detailed synthesis and characterization of these organoimido delivery reagents, and the attempted preparations of the corresponding POM hybrids are outlined in the following chapters. This work was undertaken envisioning organoimido hexamolybdate as the metalloligand, which can coordinate to another metal atom, and exhibit electronic communication between the cluster and the second metal atom, thus leading to the formation of versatile POM hybrids.

References

- ¹ Dolbecq, A.; Dumas, E.; Mayer, C. R.; Mialane, P. *Chem. Rev.* **2010**, *110*, 6009.
- ² Proust, A.; Matt, B.; Villanneau, R.; Guillemot, G.; Gouzerh, P.; Izzet, G. *Chem. Soc. Rev.* **2012**, *41*, 7605.
- ³ Ammam, M. *J. Mater. Chem. A* **2013**, *1*, 6291.
- ⁴ Berzelius, J.; Poggendorfs, J. *Ann. Phys. Chem.* **1826**, *82*, 369.
- ⁵ Rosenheim, A.; Liebknecht, O. *Justus Liebigs Ann. Chem.* **1899**, *308*, 40.
- ⁶ Ivanova, S. *ISRN Chemical Engineering* **2014**, 2014 Article 963792.
- ⁷ Kelmperer, W. G. *Inorganic Syntheses* **1990**, *27*, 71.
- ⁸ Long, D-L.; Tsunashima, R.; Cronin, L. *Angew. Chem. Int. Ed.* **2010**, *49*, 1736.
- ⁹ Jeannin, Y. P. *Chem. Rev.* **1998**, *98*, 51.
- ¹⁰ Hill, C. L. *Chem. Rev.* **1998**, *98*, 1.
- ¹¹ Scheele, C. W. In *Sämtliche Physische und Chemische Werke*, Hermbstädt, D. S. F., Ed.; Martin Sändig oHG: Niederwalluf/ Wiesbaden, **1971**, *1*, 185 (reprint: original 1793).
- ¹² Müller, A.; Krickemeyer, E.; Meyer, J.; Bögge, H.; Peters, F.; Plass, W.; Diemann, E.; Dillinger, S.; Nonnenbruch, F.; Randerath, M.; Menke, C. *Angew. Chem.* **1995**, *107*, 2293.
- ¹³ Katsoulis, D. E. *Chem. Rev.* **1998**, *98*, 359.
- ¹⁴ Pope, M. T. *Heteropoly and Isopoly Oxometalates*, Springer Berlin, 1982.
- ¹⁵ Maayan, G.; Fish, R. H.; Neumann, R. *Org. Lett.* **2003**, *5*, 3547.
- ¹⁶ Ito, T.; Yashiro, H.; Yamase, T. *Langmuir* **2006**, *22*, 2806.
- ¹⁷ (a) Giusti, A.; Charron, G.; Mazerat, S.; Compain, J. D.; Mialane, P.; Dolbecq, A.; Rivière, E.; Wernsdorfer, W.; Biboum, R. N.; Keita, B.; Nadjo, L.; Filoramo, A.; Bourgoïn, J. P.; Mallah, T. *Angew. Chem., Int. Ed.* **2009**, *48*, 4949; (b) Ibrahim, M.; Lan, Y. H.; Bassil, B. S.; Xiang, Y. X.; Suchopar, A.; Powell, A. K.; Kortz, U. *Angew. Chem., Int. Ed.* **2011**, *50*, 4708; (c) Dolbecq, A.; Moll, H. E.; Marrot, J.; Rousseau, G.; Haouas, M.; Taulelle, F.; Rogez, G.; Wernsdorfer, W.; Keita, B.; Mialane, P. *Chem.–Eur. J.* **2012**, *18*, 3845.
- ¹⁸ (a) Mizuno, N.; Yamaguchi, K.; Kamata, K. *Coord. Chem. Rev.* **2005**, *249*, 1944; (b) Hill, C. L. *J. Mol. Catal. A: Chem.* **2007**, *262*, 1; (c) Kozhevnikov, I. V. *Chem. Rev.* **1998**, *98*, 171.
- ¹⁹ (a) Geletii, Y. V.; Botar, B.; Kögerler, P.; Hillesheim, D. A.; Musaev, D. G.; Hill, C. L. *Angew. Chem., Int. Ed.* **2008**, *47*, 3896; (b) Sartorel, A.; Carraro, M.; Scorrano, G.; Zorzi, R. D.; Geremia, S.; McDaniel, N. D.; Bernhard, S.; Bonchio, M. *J. Am. Chem. Soc.* **2008**, *130*, 5006; (c) Zhu, G.; Glass, E. N.; Zhao, C.; Lv, H.; Vickers, J. W.; Geletii, Y. V.; Musaev, D. G.; (d) Song, J.; Hill, C. L. *Dalton Trans.* **2012**, *41*, 13043.
- ²⁰ (a) Rhule, J. T.; Hill, C. L.; Judd, D. A. *Chem. Rev.* **1998**, *98*, 327; (b) Hasenknopf, B. *Front. Biosci.* **2005**, *10*, 275; (c) Pope, M. T.; Muller, A. *Polyoxometalates: from Platonic Solids to Anti-Retroviral Activity*, Kluwer Academic Publishers: Dordrecht, The Netherlands, 1994.
- ²¹ Lomakina, S. V.; Shatova, T. S.; Kazansky, L. P. *Corros. Sci.* **1994**, *36*, 1645.
- ²² Asuka, M.; Myazaki, M.; Nakatani, Y.; Myamoto, K. *Japanese Patent JP 07333401 A2* **1995**; *Chem. Abstr.* **1996**, *124*, 215718.

-
- ²³ Ozawa, T.; Maeda, S.; Kurose, Y. *Japanese Patent JP 62124986A2*, **1987**; *Chem. Abstr.* **1987**, *108*, 46893.
- ²⁴ Gaspar, A. R.; Gamelas, J. A. F.; Evtuguin, D. V.; Neto, C. P. *Green Chem.* **2007**, *9*, 717.
- ²⁵ Blasius, E.; Nilles, K. H. *European Patent EU 73261 A1* **1983**; *Chem. Abstr.* **1983**, *99*, 12575.
- ²⁶ Li, J. *Nanostructured Biomaterials*, Springer Science & Business Media, 2011.
- ²⁷ He, P.; Xu, B.; Liu, H.; He, S.; Saleem F.; Wang, X. *Scientific Reports*, **2013**, *3*, 1833.
- ²⁸ Gouzerh, P.; Proust, A. *Chem. Rev.* **1998**, *98*, 77.
- ²⁹ Sanchez, C.; Ribot, F. *New. J. Chem.* **1994**, *18*, 1007.
- ³⁰ Gao, N.; Sun, H.; Dong, K.; Ren, J.; Duan, T.; Xu, C.; Qu, X. *Nature Communications* **2014**, *5*, 3422.
- ³¹ Cara, P-E.; Spinglera, B.; Weyenethb, S.; Patscheiderc, J.; Patzke, G. R. *Polyhedron* **2013**, *52*, 15.
- ³² Copéret, C.; Chabanas, M.; Saint-Arroman, R. P.; Basset, J.-M. *Angew. Chem. Int. Ed.* **2003**, *42*, 156.
- ³³ Bar-Nahum I.; Cohen H.; Neumann, R. *Inorg. Chem.* **2003**, *42*, 3677.
- ³⁴ Li-Hua B.; Al-Kadamany, G.; Chubarova, E. V.; Dickman, M. H.; Chen, L.; Gopala, D. S.; Richards, R. M.; Keita, B.; Nadjo, L.; Jaensch, H.; Mathys, G.; Kortz, U. *Inorg. Chem.* **2009**, *48*, 10068.
- ³⁵ Suss-Fink, G.; Plasseraud, L.; Ferrand, V.; Stoeckli-Evans, H. *Chem. Commun.* **1997**, 1657.
- ³⁶ Wasfía, S. H.; Johnson III, W. L.; Martin, D. L. *Inorganica Chimica Acta* **1998**, *282*, 136.
- ³⁷ Clegg, W.; Errington, R. J.; Hockless, D. C. R.; Redshaw, C. *Polyhedron* **1989**, *8*, 1788.
- ³⁸ Lozan, V.; Kersting, B. *Inorg. Chem.* **2006**, *45*, 5630.
- ³⁹ (a) Marcoux, P. R.; Hasenknopf, B.; Vaissermann, J.; Gouzerh, P. *Eur. J. Inorg. Chem.* **2003**, *13*, 2406; (b) Santoni, M-P.; Pal, A. K.; Hanan, G. S.; Proust, A.; Hasenknopf, B. *Inorg. Chem.* **2011**, *50*, 6737.
- ⁴⁰ Allain, C.; Favette, S.; Chamoreau, L-M.; Vaissermann, J.; Ruhlmann, L.; Hasenknopf, B. *Eur. J. Inorg. Chem.* **2008**, *22*, 3433.
- ⁴¹ (a) Berardi, S.; Carraro, M.; Iglesias, M.; Sartorel, A.; Scorrano, G.; Albrecht M.; Bonchio, M. *Chem.-Eur. J.* **2010**, *16*, 10662; (b) Bar-Nahum, I.; Neumann, R. *Chem. Commun.* **2003**, 2690.
- ⁴² Graselli, R. K.; Burrington, J. D. *Ind. Eng. Chem. Prod. Res. Dev.* **1984**, *23*, 393.
- ⁴³ Nugent, W. A.; Mayer, J. M. *Metal-Ligand Multiple Bonds*, Wiley, New York, 1988.
- ⁴⁴ Chong, A. O.; Oshima, K.; Sharpless, K. B. *J. Am. Chem. Soc.* **1977**, *99*, 3420.
- ⁴⁵ Zhang, J.; Xiao, F.; Hao, J.; Wei, Y. *Dalton Trans.* **2012**, *41*, 3599.
- ⁴⁶ Du, Y.; Rheingold, A. L.; Maatta, E. A. *J. Am. Chem. Soc.* **1992**, *114*, 345.
- ⁴⁷ Kwen, H.; Young Jr., V. G.; Maatta, E. A. *Angew. Chem., Int. Ed.* **1999**, *38*, 1145.
- ⁴⁸ Hsieh, T. C.; Zubieta, J. A. *Polyhedron* **1986**, *5*, 1655.
- ⁴⁹ Kang, H.; Zubieta, J. *J. Chem. Soc. Chem. Commun.* **1988**, 1192.
- ⁵⁰ Lv, C.; Khan, R. N. N.; Zhang, J.; Hu, J.; Hao, J.; Wei, Y. *Chem.-Eur. J.* **2013**, *19*, 1174.
- ⁵¹ (a) Janjua, M. R. S. A.; Liu, C.-G.; Guan, W.; Zhuang, J.; Muhammad, S.; Yan, L.-K.; Su, Z.-M. *J. Phys. Chem. A* **2009**, *113*, 3576; (b) Lu, M.; Xie, B.; Kang, J.; Chen, F.-C.; Yang, Y.; Peng, Z. *Chem. Mater.* **2005**, *17*, 402; (c) Gao, J.; Liu, X.; Liu, Y.; Yu, L.; Feng, Y.; Chen, H.; Li, Y.; Rakesh, G.; Huan, C. H. A.; Sum, T. C.; Zhao, Y.; Zhang, Q. *Dalton Trans.* **2012**, *41*, 12185.

-
- ⁵² Khan, R. N. N.; Mahmood, N.; Lv, C.; Simaa, G.; Zhanga, J.; Haoa, J.; Hou, Y.; Wei, Y. *RSC Adv.* **2014**, *4*, 7374.
- ⁵³ Yua, H.; Leb, S.; Zenga, X.; Zhanga, J.; Xie, J. *Inorg. Chem. Commun.* **2014**, *39*, 135.
- ⁵⁴ Proust, A.; Thouvenot, R.; Chaussade, M.; Robert, F.; Gouzerh, P. *Inorg. Chim. Acta*, **1994**, *224*, 81.
- ⁵⁵ Stark, J.; Young, V.; Maatta, E. A. *Angew. Chem. Int. Ed.* **1995**, *34*, 2547.
- ⁵⁶ (a) Errington, R. J.; Lax, C.; Richards, D. G.; Clegg, W.; Fraser, K. A. *New Aspects of Non-Aqueous Polyoxometalate Chemistry: 3. Surface Oxide Reactivity*, in *Polyoxometalates: From Platonic Solids to Anti-Retroviral Activity*, Kluwer, Dordrecht, 1994, 112; (b) Strong, J. B.; Ostrander, R.; Rheingold, A. L.; Maatta, E. A. *J. Am. Chem. Soc.* **1994**, *116*, 3601.
- ⁵⁷ Wei, Y.; Xu, B.; Barnes, C. L.; Peng, Z. *J. Am. Chem. Soc.* **2001**, *123*, 4083.
- ⁵⁸ Peng, Z.; Wei, Y.; Xu, B. *US 20020165405 A1*, **2002**.
- ⁵⁹ Ge, N.; Wei, Y.; Wang, Y.; Wang, P.; Guo, H. *Eur. J. Inorg. Chem.* **2004**, 2819.
- ⁶⁰ Araghi, M.; Mirkhani, V.; Moghadam, M.; Tangestaninejad, S.; Mohammdpour-Baltork, I. *Dalton Trans.* **2012**, *41*, 11745.
- ⁶¹ Hill, P. L.; Yap, G. P. A.; Rheingold, A. L.; Maatta, E. A. *J. Chem. Soc., Chem. Commun.* **1995**, 737.
- ⁶² H. S. Nalwa *Handbook of Organic Conductive Molecules and Polymers I–IV*, Wiley, Chichester, 1997.
- ⁶³ Wang, L.; Zhu, L.; Yin, P.; Fu, W.; Chen, J.; Hao, J.; Xiao, F.; Lu, C.; Zhang, J.; Shi, L.; Li, Q.; Wei, Y. *Inorg. Chem.* **2009**, *48*, 9222.
- ⁶⁴ Sima, G.; Li, Q.; Zhu, Y.; Lv, C.; Khan, R. N. N.; Hao, J.; Zhang, J.; Wei, Y. *Inorg. Chem.* **2013**, *52*, 6551.
- ⁶⁵ Moore, A., PhD Thesis, Kansas State University, 1998.
- ⁶⁶ Kwen, H.; Beatty, A. M.; Maatta, E. A. *C. R. Chim.* **2005**, *8*, 1025.
- ⁶⁷ Xu, B.; Lu, M.; Kang, J.; Wang, D.; Brown, J.; Peng, Z. *Chem. Mater.* **2005**, *17*, 2841.
- ⁶⁸ Kang, J.; Xu, B.; Peng, Z.; Zhu, X.; Wei, Y.; Powell, D. R. *Angew. Chem. Int. Ed.* **2005**, *44*, 6902.
- ⁶⁹ Li, Q.; Wang, L.; Yin, P.; Wei, Y.; Hao, J.; Zhu, Y.; Zhu, L.; Yuan, G. *Dalton Trans.* **2009**, 1172.

Chapter 2 - ‘Dithiocarbamate’ as a remote functionality to form bimetallic polyoxometalate hybrids

2.1 Introduction

Polyoxometalates (POMs) are discrete metal-oxygen anionic clusters which are structurally similar to that of metal oxides thus, are sometimes referred as “soluble molecular oxides”.¹ Amongst the many unparalleled properties, POMs are known to undergo multiple electron redox processes which are reversible in nature, which makes them attractive platforms for electron- and/or energy-transfer.² Many POM-based hybrids have been known in literature where these are combined with various organic molecules like N-containing ligands, amino acids, polypeptides, organometallics, tetrathiafulvalene, bis(ethylenedithio)tetrathiafulvalene and perylene, possessing π -electron donor ability.³

The properties that can emerge out of such POM-based hybrids depends vastly on the choice of both the components. In search of synthesizing POM-based bimetallic systems, we chose a very well-studied dithiocarbamate (DTC) functionality. Dithiocarbamate complexes have been known for a very long time and are extensively covered in literature due to their wide range of applications in agricultural and rubber industry materials⁴ and their potential use as chemotherapeutics, pesticides, and fungicides^{5,6} due to their antibacterial,^{7,8} antitumour^{8,9} and antifungal properties.¹⁰ Dithiocarbamates fall under the category of 1,1-dithiolates which are formed when a nucleophile attacks at the neutral carbon disulfide as shown in Figure 2.1.^{10a,11,12}

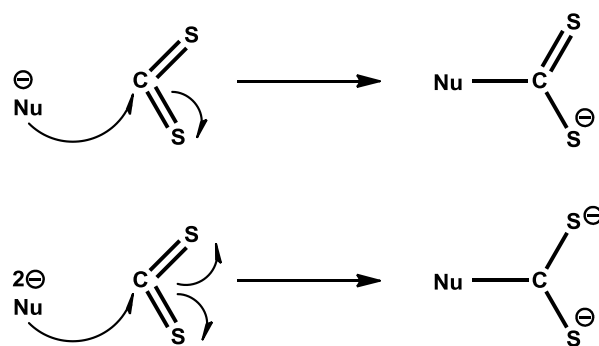
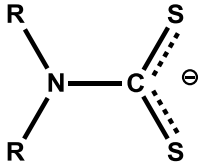
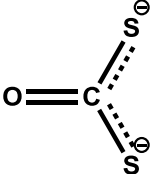
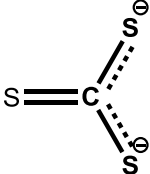
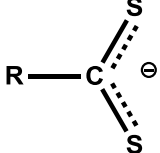
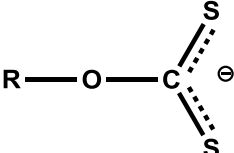
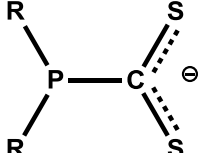
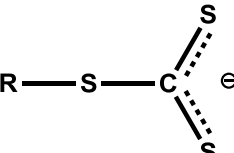
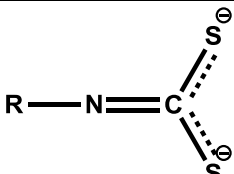


Figure 2.1 Synthesis of 1,1-dithiolate anion.¹³

Some other types of 1,1-dithiolates are summarized in Table 2.1.^{11,12}

Table 2.1 Types of 1,1-dithiolates.^{11,12}

Name	Composition	Structure
Dithiocarbamate	$R_2NCS_2^-$	
Dithiocarbonate	OCS_2^{2-}	
Trithiocarbonate	CS_3^{2-}	
Dithiocarboxylate	RCS_2^-	
Xanthate	$ROCS_2^-$	
Phosphino-dithioformate	$R_2PCS_2^-$	
Thioxanthate	RCS_3^-	
Dithiocarbimate	$RNCS_2^{2-}$	

DTCs are generally prepared by a reaction between primary/secondary amine and carbon disulfide together in an alkaline medium (Figure 2.2).¹³ The reaction is generally exothermic in

nature. Alkali or alkaline earth metal ions usually result in water soluble DTC complexes with limited solubility in organic solvents. To improve the solubility in organic solvents, ammonium complexes have been prepared.⁶

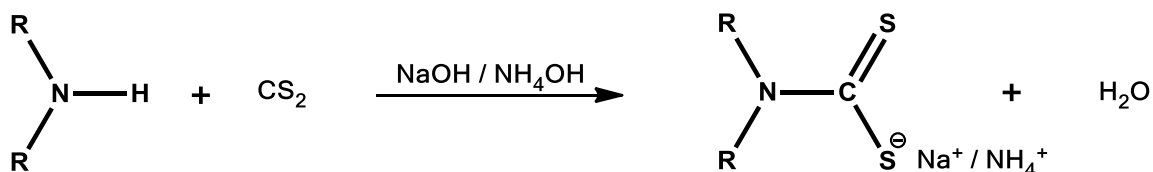


Figure 2.2 General synthesis of DTCs complexes.⁶

The structure of dithiocarbamate anion can be expressed in four resonance structures (Figure 2.3).¹² The strong band found between 1480-1550 cm^{-1} in the infrared spectrum of these complexes is a key diagnostic feature for $\nu_{\text{C-N}}$ stretch having a partial double bond character also known as the thioureide band.^{12,14} The band is intermediate of that of $\nu_{\text{C-N}}$ (1250-1350 cm^{-1}) and $\nu_{\text{C=N}}$ stretch (1640-1690 cm^{-1}) corroborating a significant contribution of the Figure 2.3 (d) resonance structure, thus showing that DTCs are semi-amides of dithiocarbonic acid.

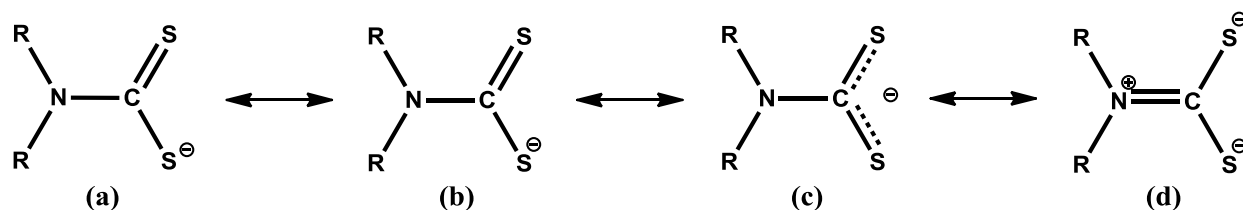


Figure 2.3 Mesomeric structures of DTCs.¹⁵

Dithiocarbamates are the ligands known for their chelation properties with various transition metals and for stabilizing a wide range of oxidation states.¹⁶ Such behavior can be explained due to the presence of sulfur atoms which help in delocalizing the positive charge of the coordinating metal upon complexation.¹⁵ The transition metal complexes can be synthesized by the metathesis of metal salt and alkali/ammonium DTCs complexes (Figure 2.4).

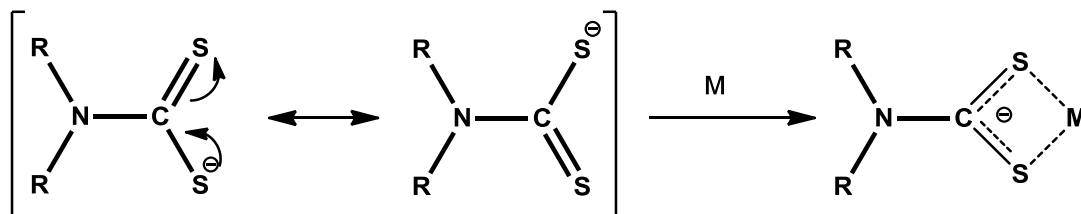


Figure 2.4 Synthesis of transition metal DTCs complexes.¹⁵

From the perspective of inorganic chemistry, the dithiocarbamate functionality is important for two reasons:

- 1) DTCs can adopt various chelation modes in metal complexes providing structural variability in the metal complexes (Figure 2.5).¹⁷

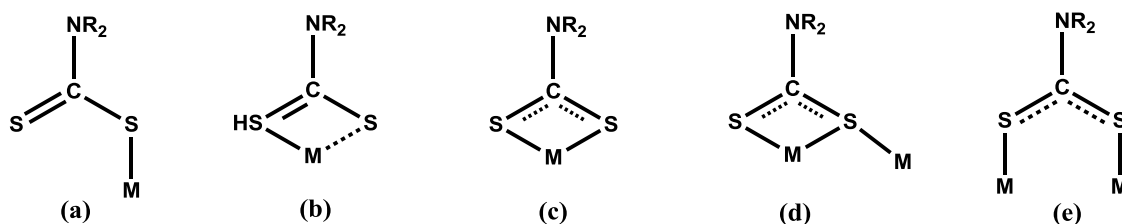


Figure 2.5 Different modes of metal coordination of DTC ligand.¹⁷

The potential of DTCs to form a wide range of coordination complexes results in an array of supramolecular frameworks being formed. Any modification to the structure of the dithiocarbamate ligand results in substantial changes in the structure–behavior of the complexes formed.¹² Choice of appropriate substituents on DTCs and the coordinating metal can lead to coordination architectures capable of cation, anion or neutral guest recognition (Figure 2.6).¹⁵

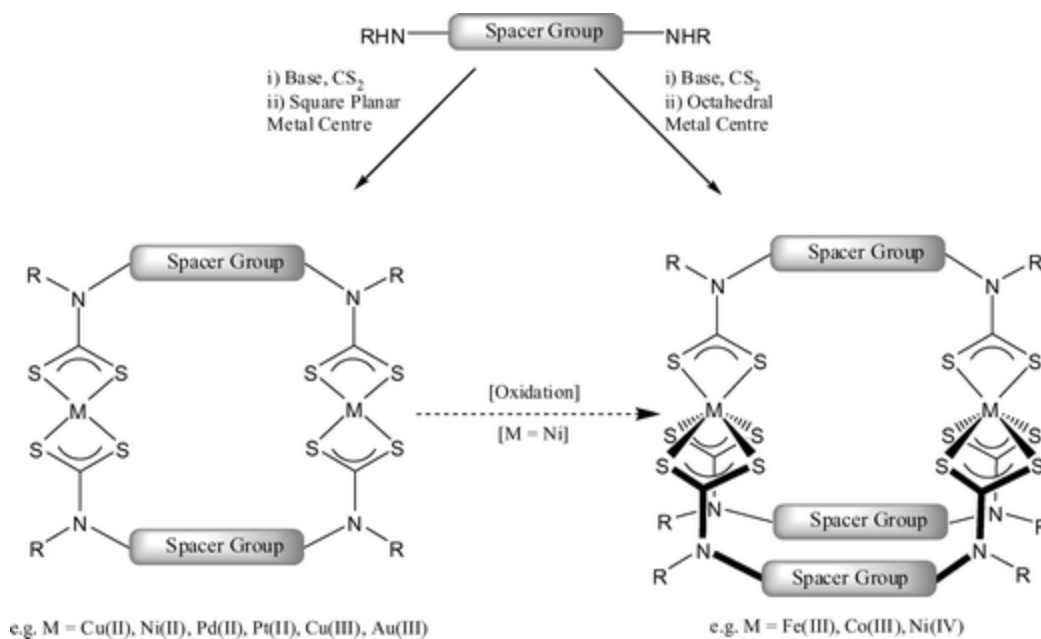


Figure 2.6 Possible supramolecular arrays resulting from various coordinating modes in dithiocarbamates.¹⁵

- 2) Moreover, incorporation of different metal ions in the same molecular framework or modifying the substituents in metal dithiocarbamate complexes provides an opportunity to explore the metal-centered electrochemical properties of the resulting

complexes.¹⁸ For example, Hendrickson *et al.* studied the redox properties using normal pulse, ac, and cyclic voltammetry at a platinum electrode for a series of copper dithiocarbamates, $\text{Cu}(\text{R}_2\text{dtc})_2$, by varying the substituents attached and established two successive and reversible electron transfer series (Figure 2.7).¹⁹

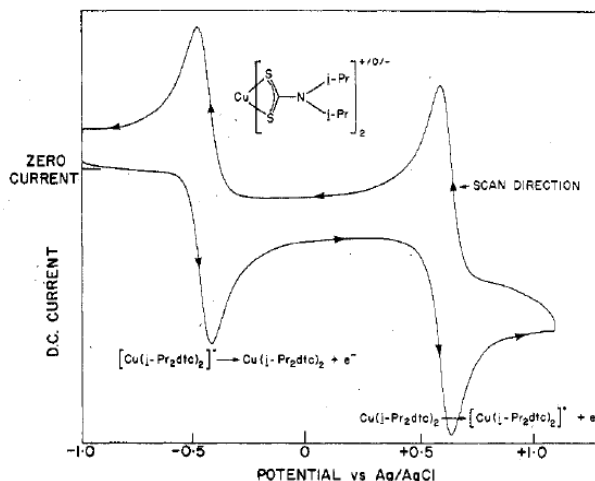
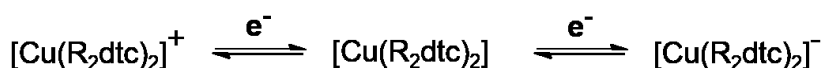


Figure 2.7 Metal-centered electrochemical properties of copper dithiocarbamates, $\text{Cu}(\text{R}_2\text{dtc})_2$.^{18,19}

To date, not many POM hybrids with metal dithiocarbamates have been reported. An example of class (I) POM hybrid, $[\text{Ru}_2(\text{S}_2\text{CNMe}_2)_3(\mu_3\text{-S}_2\text{CNMe}_2)_2]_2[\text{Mo}_6\text{O}_{19}] \cdot 2\text{CH}_3\text{COCH}_3$, was presented by Wu *et al.*²⁰ wherein a dinuclear ruthenium-dithiocarbamate cationic species is electrostatically attached to anionic hexamolybdate and the electrochemical properties of the ruthenium center were examined (Figure 2.8).

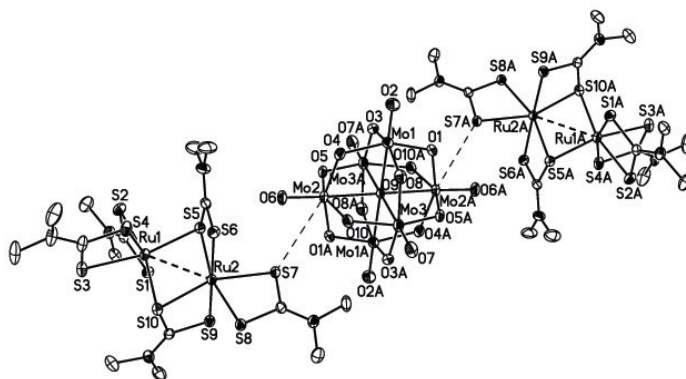


Figure 2.8 Type (I) POM hybrid, $[\text{Ru}_2(\text{S}_2\text{CNMe}_2)_3(\mu_3\text{-S}_2\text{CNMe}_2)_2]_2[\text{Mo}_6\text{O}_{19}] \cdot 2\text{CH}_3\text{COCH}_3$.²⁰

No reports on covalent grafting of dithiocarbamates on polyoxometalate clusters are known. Such an attachment via covalent bonds may exhibit potential electronic communication between two units which may lead to favorable properties. With this goal in mind, we want to investigate covalent grafting of dithiocarbamate onto polyoxometalate.

In this chapter, we have synthesized and characterized a series of novel metal dithiocarbamate complexes and attempted to covalently graft them onto hexamolybdate cluster.

2.2 Experimental

(TBA)₂[Mo₆O₁₈] and (TBA)₄[Mo₈O₂₆] were prepared according to literature methods.²¹ All chemicals were purchased from Aldrich and used without further purification. Acetonitrile (CH₃CN) were dried over CaH₂ and distilled as needed. ¹H, and ¹³C NMR spectra were recorded on a Varian Unity plus 400 MHz spectrometer and were referenced to residual protonated solvent peaks (CDCl₃ = 7.27 ppm, D₂O = 4.75 ppm and DMSO-d⁶ = 2.50 ppm). FT-IR spectra were recorded on a Nicolet 380 instrument. Melting points were determined on a Fisher-Johns melting point apparatus and are uncorrected. Mass spectra were collected using MS system Waters ACQUITY TQD. X-ray data was collected on a Bruker SMART 1000 four-circle CCD diffractometer at 203 K using a fine-focus molybdenum K α tube.

2.2.1 Synthesis of Zwitter-ion of 4-aminopiperidine, 1

4-aminopiperidine (2g, 19.98 mmol) was dissolved in ethanol (30 mL). To this solution, CS₂ (1.2 mL, 19.98 mmol) was added with stirring. The product was obtained as white precipitate instantly which was filtered, washed with ethanol and diethylether and dried in air. The precipitate was dissolved in water heated to 80°C and crystals were obtained using solvent evaporation method. Yield: 2.89g, 82.16%; mp 188-190°C (sublimed); IR (ZnSe): 1492 cm⁻¹ (ν_{C-N}); ¹H (400 MHz, D₂O) δ ppm: 1.54 (d, J=12.50 Hz, 2 H) 1.99 (d, J=12.11 Hz, 2 H) 3.10 (t, J=12.69 Hz, 2 H) 3.44 (d, J=6.64 Hz, 1 H) 5.48 (d, J=12.11 Hz, 2 H); ¹³C NMR (400 MHz, D₂O) δ ppm: 29.88, 48.32, 49.58, 209.22 (N-C=S); m/z (ESI): 177.09 [M+1]⁺, 159.97 [M-NH₂]⁺, 143.89 [M-CS₂]⁺, 126.81 [M-NH₃-S]⁺, 94.91 [M-NH₃-2S]⁺, 83.92 [M-NH₃-CS₂]⁺.

2.2.2 Synthesis of Sodium 4-aminopiperidine dithiocarbamate, 2

4-aminopiperidine (4g, 39.96 mmol) was dissolved in water (30 mL) and CS₂ (2.4 mL, 39.96 mmol) was added with stirring. To this mixture, a solution of NaOH (1.6g, 40.00 mmol) in

16 mL water was added dropwise and it was stirred at room temperature for 2h. The water was removed under vacuum to obtain product as white precipitate. Yield: 6.82g, 86.18%; IR (ZnSe): 1458 cm^{-1} ($\nu_{\text{C-N}}$); ^1H NMR (400 MHz, D_2O) δ ppm: 1.35 (d, $J=12.11$ Hz, 2 H) 1.88 (d, $J=10.54$ Hz, 2 H) 3.03 (br. s., 1 H) 3.24 (t, $J=11.72$ Hz, 2 H) 5.34 (d, $J=12.50$ Hz, 2 H); ^{13}C NMR (400 MHz, D_2O) δ ppm: 33.50, 47.74, 50.56, 207.21 (N-C=S).

2.2.3 Reaction of Sodium 4-aminopiperidine dithiocarbamate with chromium(II), 2.Cr

2 (0.25g, 1.26 mmol) was dissolved in 10 mL water. Chromium nitrate nonahydrate (0.1877g, 0.63 mmol) was dissolved in the minimum amount of water. This solution was added to the reaction mixture dropwise with constant stirring to obtain pale blue precipitate. The reaction mixture was stirred for 2h at room temperature. The product was filtered on a glass filtration frit and dried. Yield: 0.2336g, 64.58%; IR (ZnSe): 1487 cm^{-1} ($\nu_{\text{C-N}}$).

2.2.4 Reaction of Sodium 4-aminopiperidine dithiocarbamate with manganese(II), 2.Mn

2 (0.25g, 1.26 mmol) was dissolved in 10 mL water. Manganese chloride tetrahydrate (0.1247g, 0.63 mmol) was dissolved in the minimum amount of water. This solution was added to the reaction mixture dropwise with constant stirring to obtain light brown precipitate. The reaction mixture was stirred for 2h at room temperature. The product was filtered on a glass filtration frit and dried. Yield: 0.1482g, 58.07%; IR (ZnSe): 1470 cm^{-1} ($\nu_{\text{C-N}}$).

2.2.5 Reaction of Sodium 4-aminopiperidine dithiocarbamate with iron(III), 2.Fe

2 (0.25g, 1.26 mmol) was dissolved in 10 mL water. Ferric nitrate nonahydrate (0.1697g, 0.42 mmol) was dissolved in the minimum amount of water. This solution was added to the reaction mixture dropwise with constant stirring to obtain dark brown precipitate. The reaction mixture was stirred for 2h at room temperature. The product was filtered on a glass filtration frit and dried. Yield: 0.1284g, 52.88%; IR (ZnSe): 1483 cm^{-1} ($\nu_{\text{C-N}}$).

2.2.6 Reaction of Sodium 4-aminopiperidine dithiocarbamate with cobalt(II), 2.Co

2 (0.375g, 1.8 mmol) was dissolved in 15 mL water. Cobalt nitrate hexahydrate (0.1741g, 0.6 mmol) was dissolved in the minimum amount of water. This solution was added to the reaction mixture dropwise with constant stirring to obtain green precipitate. The reaction mixture was stirred for 2h at room temperature. The product was filtered on a glass filtration frit and dried. Yield: 0.2743g, 78.69%; IR (ZnSe): 1478 cm^{-1} ($\nu_{\text{C-N}}$); ^1H NMR (400 MHz, CD_2Cl_2) δ

ppm: 1.35 (br. s., 2 H) 1.88 (d, J=12.89 Hz, 2 H) 3.01 (br. s., 1 H) 3.08 - 3.26 (m, 2 H) 4.42 - 4.58 (m, 2 H); m/z (ESI): 408.99 [M]⁺.

2.2.7 Reaction of Sodium 4-aminopiperidine dithiocarbamate with nickel(II), 2.Ni

2 (0.3175g, 1.6 mmol) was dissolved in 10 mL water. Nickel nitrate hexahydrate (0.2324g, 0.8 mmol) was dissolved in the minimum amount of water. This solution was added to the reaction mixture dropwise with constant stirring to obtain green precipitate. The reaction mixture was stirred for 2h at room temperature. The product was filtered on a glass filtration frit and dried. Yield: 0.1952g, 59.80%; IR (ZnSe): 1442 cm⁻¹ (ν_{C-N}); ¹H NMR (400 MHz, CD₂Cl₂) δ ppm: 1.34 (d, J=10.74 Hz, 2 H) 1.87 (d, J=17.09 Hz, 2 H) 3.05 (br. s., 1 H) 3.18 (t, J=13.67 Hz, 2 H) 4.31 (d, J=13.67 Hz, 2 H).

2.2.8 Reaction of Sodium 4-aminopiperidine dithiocarbamate with copper(II), 2.Cu

2 (0.25g, 1.26 mmol) was dissolved in 10 mL water. Copper nitrate hemipentahydrate (0.1465g, 0.63 mmol) was dissolved in the minimum amount of water. This solution was added to the reaction mixture dropwise with constant stirring to obtain dark brown precipitate. The reaction mixture was stirred for 2h at room temperature. The product was filtered on a glass filtration frit and dried. Yield: 0.1371g, 52.63%; IR (ZnSe): 1485 cm⁻¹ (ν_{C-N}).

2.2.9 Reaction of Sodium 4-aminopiperidine dithiocarbamate with zinc(II), 2.Zn

2 (0.25g, 1.26 mmol) was dissolved in 10 mL water. Zinc nitrate hemipentahydrate (0.1877g, 0.63 mmol) was dissolved in the minimum amount of water. This solution was added to the reaction mixture dropwise with constant stirring to obtain white precipitate. The reaction mixture was stirred for 2h at room temperature. The product was filtered on a glass filtration frit and dried. Yield: 0.1173g, 44.98%; IR (ZnSe): 1477 cm⁻¹ (ν_{C-N}).

2.2.10 Reaction of Sodium 4-aminopiperidine dithiocarbamate with silver(I), 2.Ag

2 (0.25g, 1.26 mmol) was dissolved in 10 mL water. Silver nitrate (0.2142g, 1.26 mmol) was dissolved in the minimum amount of water. This solution was added to the reaction mixture dropwise with constant stirring to obtain brown precipitate. The reaction mixture was stirred for 2h at room temperature. The product was filtered on a glass filtration frit and dried. Yield: 0.1085g, 30.55%; IR (ZnSe): 1477 cm⁻¹ (ν_{C-N}).

2.2.11 Synthesis of Tetrabutylammonium 4-aminopiperidine dithiocarbamate, 3

4-aminopiperidine (1g, 9.99 mmol) was dissolved in water (15 mL) and CS₂ (0.6 mL, 9.99 mmol) was added with stirring. To this mixture, a 40% aqueous solution of TBAOH (6.5 mL, 10.00 mmol) was added dropwise and it was stirred for 2h at room temperature. The solvent was removed under vacuum to obtain product as pale yellow oil which was dried overnight under vacuum at 60°C. Yield: 3.62g, 88.73%; IR (ZnSe): 1460 cm⁻¹ (ν_{C-N}); ¹H NMR (CDCl₃, 400MHz, ppm): 1.00 (12H), 1.38 (2H), 1.45 (8H), 1.71 (8H), 1.80 (2H), 2.88 (1H), 3.16 (2H), 3.44 (8H), 5.82 (2H); ¹³C NMR (CDCl₃, 400MHz, ppm): 13.48, 19.54, 23.96, 35.44, 48.66, 48.97, 58.79, 212.77 (N-C=S).

2.2.12 Synthesis of 4-(4-nitrophenyl) piperazine, 4²²

In a 250 mL round bottom flask with a stir bar, a solution of anhydrous piperazine (16.27g, 188.88 mmol) was prepared in 50 mL n-butanol under nitrogen atmosphere. The solution was brought to reflux during which a solution of 4-chloronitrobenzene (10g, 63.47 mmol) in 50 mL n-butanol was added dropwise with stirring using a syringe in a course of an hour. The reaction mixture was left to reflux overnight at about 130-140°C. The color of the solution turned orange which on cooling resulted in yellow precipitate. The precipitate was collected to which 6N HCl (89 mL) was added. The resulting solution was extracted with ethyl acetate (3x100 mL). All organic layers were combined and neutralized with cold 6N NaOH solution to attain pH=10. The organic layer was separated and was washed twice with bine solution and was dried over Na₂SO₄. The solution was then filtered off and solvent was removed under vacuum to yield bright yellow compound as product. Yield: 28.87g, 73.76%; mp 127-128°C (lit.²³ 129-130°C); ¹H NMR (400 MHz, CDCl₃) δ ppm: 3.04 (dt, J=6.64, 3.32 Hz, 4 H) 3.30 - 3.51 (m, 5 H) 6.83 (dd, J=9.37, 2.73 Hz, 2 H) 8.13 (dd, J=9.57, 2.93 Hz, 2 H); ¹³C NMR (400 MHz, CDCl₃) δ ppm: 46.01, 48.40, 112.87, 126.23.

2.2.13 Synthesis of Tetrabutylammonium 4-(4-nitrophenyl) piperazine dithiocarbamate, 5

In a 50 mL round bottom flask, **4** (0.3g, 1.4477 mmol) was taken in 10 mL methanol to which carbon disulfide (0.087 mL, 1.448 mmol) was added with constant stirring, which resulted in yellow precipitate. To this, a 40% wt. methanol solution of tetrabutylammonium hydroxide (0.968 mL, 1.448 mmol) was added dropwise to obtain yellow solution. The resulting mixture was stirring for 2h at room temperature after which the solvent was removed under vacuum to

obtain yellow precipitate as the product. Yield: 0.6842g, 90.01%; IR (ZnSe): 1486 cm^{-1} ($\nu_{\text{C-N}}$); ^1H NMR (400 MHz, CDCl_3) δ ppm 1.01 (t, $J=7.32$ Hz, 12 H) 1.48 (dd, $J=15.14, 7.32$ Hz, 8 H) 1.73 (dt, $J=7.94, 4.09$ Hz, 8 H) 3.44 - 3.50 (m, 8 H) 3.51 - 3.57 (m, 4 H) 4.64 - 4.74 (m, 4 H) 6.76 (d, $J=9.28$ Hz, 2 H) 8.13 (d, $J=9.28$ Hz, 2 H); ^{13}C NMR (400 MHz, CDCl_3) δ ppm: 13.87, 19.77, 24.17, 48.24, 48.93, 59.05, 111.61, 125.99, 137.88, 154.46, 214.68 (N-C=S).

2.2.14 Synthesis of 4-(4-aminophenyl) piperazine, 6²⁴

In a 500 mL round bottom flask fitted with a stir bar, a solution of **4** (7.14g, 34.45 mmol) was prepared in ethanol (300 mL). To this solution, conc. HCl (69 mL) was added with stirring and the reaction mixture was heated to 70°C. $\text{SnCl}_2 \cdot 2\text{H}_2\text{O}$ (25.54g, 113.22 mmol) was added and the reaction mixture was left to reflux for 24h during which the bright yellow color of the reaction mixture disappeared. The reaction mixture on cooling was neutralized with NaHCO_3 to pH=7-8. A large amounts of white precipitate was observed which was filtered off over Bruckner funnel. The resulting filtrate was diluted with dichloromethane and the organic layer was extracted (3 x 100 mL). All the organic layers were combined and washed with twice with brine solution and was dried over Na_2SO_4 . The solution was filtered off and the solvent was removed under vacuum to yield a purple-brown compound as product. Yield: 4.11g, 67.23%; mp 130-131°C (lit.²⁵ 126°C); ^1H NMR (400 MHz, CDCl_3) δ ppm: 3.00 (d, $J=4.37$ Hz, 8 H) 6.65 (m, $J=8.75$ Hz, 2 H) 6.81 (m, $J=8.75$ Hz, 2 H); ^1H NMR (400 MHz, CD_3OD) δ ppm: 3.02 (s, 8 H) 6.71 (d, $J=8.59$ Hz, 2 H) 6.84 (d, $J=8.59$ Hz, 2 H); ^{13}C NMR (400 MHz, CD_3OD) δ ppm: 46.45, 52.72, 117.97, 120.44.

2.2.15 Synthesis of Sodium 4-(4-aminophenyl) piperazine dithiocarbamate, 7

In a 25 mL round bottom flask, **6** (0.15g, 0.7273 mmol) was taken in 10mL methanol to which carbon disulfide (0.044 mL, 0.7273 mmol) was added with constant stirring on which greyish precipitate was obtained. To this, sodium hydroxide (0.0408g, 0.7273 mmol) in 1 mL was added dropwise during which precipitate redissolved to give pale red solution. The resulting mixture was stirred for 2h at room temperature after which the solvent was removed under vacuum to obtain an off-white precipitate as the product. Yield: 0.12g, 51.36%; IR (ZnSe): 1454 cm^{-1} ($\nu_{\text{C-N}}$); ^1H NMR (400 MHz, D_2O) δ ppm: 1.62 - 1.71 (m, 2 H) 1.86 (d, $J=14.45$ Hz, 2 H) 2.85 (s, 1 H) 3.14 - 3.21 (m, 2 H) 5.60 (br. s., 2 H) 6.80 (m, $J=8.59$ Hz, 2 H) 7.15 (m, $J=8.59$ Hz, 2 H); ^1H NMR (400 MHz, CD_3OD) δ ppm: 2.94 - 3.11 (m, 4 H) 4.47 - 4.65 (m, 4 H) 6.71 (m,

J=8.59 Hz, 2 H) 6.86 (m, J=8.98 Hz, 2 H); ^{13}C NMR (400 MHz, CD_3OD) δ ppm: 51.77, 52.58, 118.02, 120.38, 142.83, 145.47, 213.50 (N-C=S).

2.2.16 Reaction of Sodium 4-(4-aminophenyl) piperazine dithiocarbamate with chromium(II), 7.Cr

7 (0.01g, 0.0364 mmol) was dissolved in 5 mL methanol. Chromium nitrate nonahydrate (0.0073g, 0.0182 mmol) was dissolved in the minimum amount of methanol. This solution was added to the reaction mixture dropwise with constant stirring to obtain pale green precipitate. The reaction mixture was stirred for 2h at room temperature. The product was filtered on a glass filtration frit and dried. Yield: 0.0099g, 67.35%; IR (ZnSe): 1507 cm^{-1} ($\nu_{\text{C-N}}$).

2.2.17 Reaction of Sodium 4-(4-aminophenyl) piperazine dithiocarbamate with manganese(II), 7.Mn

7 (0.01g, 0.0364 mmol) was dissolved in 5 mL methanol. Manganese nitrate (0.0033g, 0.0182 mmol) was dissolved in the minimum amount of methanol. This solution was added to the reaction mixture dropwise with constant stirring to obtain purple-brown precipitate. The reaction mixture was stirred for 2h at room temperature. The product was filtered on a glass filtration frit and dried. Yield: 0.0045g, 44.12%; IR (ZnSe): 1510 cm^{-1} ($\nu_{\text{C-N}}$).

2.2.18 Reaction of Sodium 4-(4-aminophenyl) piperazine dithiocarbamate with iron(III), 7.Fe

7 (0.01g, 0.0364 mmol) was dissolved in 5 mL methanol. Ferric nitrate nonahydrate (0.0049g, 0.0121 mmol) was dissolved in the minimum amount of methanol. This solution was added to the reaction mixture dropwise with constant stirring to obtain grey-brown precipitate. The reaction mixture was stirred for 2h at room temperature. The product was filtered on a glass filtration frit and dried. Yield: 0.0048g, 48.45%; IR (ZnSe): 1511 cm^{-1} ($\nu_{\text{C-N}}$).

2.2.19 Reaction of Sodium 4-(4-aminophenyl) piperazine dithiocarbamate with cobalt(II), 7.Co

7 (0.01g, 0.0364 mmol) was dissolved in 5 mL methanol. Cobalt nitrate hexahydrate (0.0053g, 0.0121 mmol) was dissolved in the minimum amount of methanol. This solution was added to the reaction mixture dropwise with constant stirring to obtain brown precipitate. The reaction mixture was stirred for 2h at room temperature. The product was filtered on a glass filtration frit and dried. Yield: 0.0053g, 53.54%; IR (ZnSe): 1507 cm^{-1} ($\nu_{\text{C-N}}$).

2.2.20 Reaction of Sodium 4-(4-aminophenyl) piperazine dithiocarbamate with nickel(II),

7.Ni

7 (0.01g, 0.0364 mmol) was dissolved in 5 mL methanol. Nickel nitrate hexahydrate (0.0053g, 0.0182 mmol) was dissolved in the minimum amount of methanol. This solution was added to the reaction mixture dropwise with constant stirring to obtain yellow-green precipitate. The reaction mixture was stirred for 2h at room temperature. The product was filtered on a glass filtration frit and dried. Yield: 0.0064g, 62.14%; IR (ZnSe): 1505 cm^{-1} ($\nu_{\text{C-N}}$).

2.2.21 Reaction of Sodium 4-(4-aminophenyl) piperazine dithiocarbamate with copper(II),

7.Cu

7 (0.01g, 0.0364 mmol) was dissolved in 5 mL methanol. Copper nitrate hemipentahydrate (0.0041g, 0.0182 mmol) was dissolved in the minimum amount of methanol. This solution was added to the reaction mixture dropwise with constant stirring to obtain dark brown precipitate. The reaction mixture was stirred for 2h at room temperature. The product was filtered on a glass filtration frit and dried. Yield: 0.0048g, 46.60%; IR (ZnSe): 1507 cm^{-1} ($\nu_{\text{C-N}}$).

2.2.22 Reaction of Sodium 4-(4-aminophenyl) piperazine dithiocarbamate with zinc(II), 7.Zn

7 (0.01g, 0.0364 mmol) was dissolved in 5 mL methanol. Zinc nitrate hexahydrate (0.0054g, 0.0182 mmol) was dissolved in the minimum amount of methanol. This solution was added to the reaction mixture dropwise with constant stirring to obtain white precipitate. The reaction mixture was stirred for 2h at room temperature. The product was filtered on a glass filtration frit and dried. Yield: 0.0055g, 52.88%; IR (ZnSe): 1512 cm^{-1} ($\nu_{\text{C-N}}$).

2.2.23 Synthesis of Tetrabutylammonium 4-(4-aminophenyl) piperazine dithiocarbamate, 8

In a 25 mL round bottom flask, 6 (0.10g, 0.5645 mmol) was taken in 7 mL methanol to which carbon disulfide (0.0341 mL, 0.5645 mmol) was added with constant stirring which resulted in greyish precipitate. To this, a 40% wt. methanol solution of tetrabutylammonium hydroxide (0.4027 mL, 0.5645 mmol) was added dropwise on which the precipitate dissolved to give a red solution. The resulting mixture was stirring for 2h at room temperature after which the solvent was removed under vacuum to obtain red oil as the product. Yield: 0.2216g, 79.27%; IR (ZnSe): 1511 cm^{-1} ($\nu_{\text{C-N}}$); $^1\text{H NMR}$ (400 MHz, CDCl_3) δ ppm: 0.85 (t, $J=7.29$ Hz, 24 H) 1.30 (dq, $J=14.94, 7.33$ Hz, 8 H) 1.47 - 1.57 (m, 8 H) 2.84 - 2.89 (m, 4 H) 3.16 - 3.25 (m, 8 H) 4.46 - 4.54

(m, 4 H) 6.51 (m, J=8.75 Hz, 2 H) 6.65 (m, J=8.75 Hz, 2 H); ¹³C NMR (400 MHz, CDCl₃) δ ppm: 13.34, 19.32, 23.63, 49.54, 50.62, 58.36, 115.72, 118.25, 140.06, 143.75, 213.37 (N-C=S).

2.2.24 Synthesis of 4-(4-nitrophenyl) piperidine, 9²⁶

In a 50 mL round bottom flask with a stir bar, 4-phenylpiperidine (0.5g, 3.06 mmol) was dissolved in acetic acid (2.5 mL). To this, was added a solution of conc. H₂SO₄ (0.165 mL) in 2.5 mL acetic acid keeping the temperature below 25°C. The reaction mixture was then brought below 20°C while adding a solution of conc. HNO₃ (0.13 mL) in 1.25 mL of acetic acid. To the resulting mixture, 2.5 mL of conc. H₂SO₄ was further added without cooling during which the temperature of the solution increased. When the reaction mixture cooled down to 25°C, it was added to 6.25g of ice/water. It was neutralized with a total of 9.375g of NaHCO₃ while heating at 40°C. 5M NaOH solution was further added to the reaction mixture to adjust the pH of the solution to 14. The reaction mixture was separated using dichloromethane (3x 10 mL) and all the organic layers were combined and dried over Na₂SO₄. After filtration, the solvent from the solution was removed under vacuum to yield an oil which was further recrystallized using methanol to give an off-white precipitate as the product. Yield: 0.5g (78.18%); mp 85-87°C (lit.²⁶ 90-92°C); ¹H NMR (400 MHz, CD₃Cl) δ ppm: 1.66 (dd, J=12.45, 3.66 Hz, 4 H) 1.85 (d, J=12.70 Hz, 3 H) 2.69 - 2.84 (m, 4 H) 3.22 (d, J=12.21 Hz, 3 H) 7.38 (d, J=8.79 Hz, 2 H) 8.17 (d, J=8.79 Hz, 2 H); ¹³C NMR (400 MHz, CD₃Cl) δ ppm: 34.01, 43.11, 46.84, 123.77, 127.64.

2.2.25 Synthesis of 4-(4-aminophenyl) piperidine, 10²⁷

In a 500 mL two-necked round bottom flask fitted with a stir bar, sodium borohydride (2.32g, 61.250 mmol) was taken and sealed with a balloon on one side. A solution of **9** (1.26g, 6.125 mmol) and nickel chloride hexahydrate (1.46g, 6.125 mmol) was prepared in 100 mL methanol, which was then injected into the flask. Instantly, blacking of the solution could be observed due to formation of nickel boride along with effervescence due to hydrogen gas evolution which inflated the balloon. The reaction mixture was left to stir at room temperature till all the hydrogen gas produced is used up. On completion, the reaction mixture was filtered off through celite column and the solvent was evaporated under vacuum. The greyish white solid so obtained was extracted with chloroform (3 x 10 mL) and was washed with water and brine solution. All the organic layers were dried over sodium sulfate, filtered and the solvent was removed under vacuum to yield off-white precipitate as the product. Yield: 0.8257g, 76.49%; mp

80-81 °C (lit.²⁶ 85-87 °C); IR (ZnSe): 1473 cm⁻¹ (ν_{C-N}); ¹H NMR (400 MHz, CDCl₃) δ ppm: 1.60 (td, J=12.40, 4.10 Hz, 2 H) 1.78 (d, J=12.50 Hz, 2 H) 2.51 (br. s., 1 H) 2.72 (t, J=12.30 Hz, 2 H) 3.56 (br. s., 2 H) 6.64 (d, J=7.81 Hz, 2 H) 7.01 (d, J=7.81 Hz, 2 H); ¹³C NMR (400 MHz, CD₃OD) δ ppm: 33.77, 42.11, 46.92, 117.09, 128.39.

2.2.26 Synthesis of Sodium 4-(4-aminophenyl) piperidine dithiocarbamate, 11

In a 25 mL round bottom flask, **10** (0.40g, 2.2696 mmol) was taken in 15mL methanol to which carbon disulfide (0.14 mL, 2.2696 mmol) was added with constant stirring on which some precipitation occurred. To this, 0.31mL of 3.275M NaOH solution (2.2696 mmol) in methanol was added dropwise with stirring on which the precipitate dissolved. The reaction mixture was stir for an hour and solvent was then removed under vacuum to obtain off-white precipitate as the product. Yield: 0.5764g, 92.56%; IR (ZnSe): 1460 cm⁻¹ (ν_{C-N}); ¹H NMR (400 MHz, CD₃OD) δ ppm: 1.70 (d, J=12.89 Hz, 2 H) 1.78 (d, J=12.11 Hz, 2 H) 2.72 (br. s., 1 H) 3.01 - 3.15 (m, 2 H) 5.94 (d, J=12.50 Hz, 2 H) 6.68 (d, J=8.20 Hz, 2 H) 6.99 (d, J=8.20 Hz, 2 H); ¹H NMR (400 MHz, CD₃OD) δ ppm: 1.70 (d, J=12.89 Hz, 2 H) 1.78 (d, J=12.11 Hz, 2 H) 2.72 (br. s., 1 H) 3.01 - 3.15 (m, 2 H) 5.94 (d, J=12.50 Hz, 2 H) 6.68 (d, J=8.20 Hz, 2 H) 6.99 (d, J=8.20 Hz, 2 H); ¹³C NMR (400 MHz, CD₃OD) δ ppm: 35.00, 43.40, 53.01, 117.14, 128.51, 137.34, 146.66, 211.75 (N-C=S).

2.2.27 Reaction of Sodium 4-(4-aminophenyl) piperidine dithiocarbamate with cobalt(II),

11.Co

11 (0.04g, 0.1459 mmol) was dissolved in 5 mL methanol. Cobalt nitrate hexahydrate (0.0142g, 0.0488 mmol) was dissolved in the minimum amount of methanol. This solution was added to the reaction mixture dropwise with constant stirring to obtain dark green precipitate. The reaction mixture was stirred for 2h at room temperature. The product was filtered on a glass filtration frit and dried. Yield: 0.0172g, 43.54%; IR (ZnSe): 1491 cm⁻¹ (ν_{C-N}).

2.2.28 Reaction of Sodium 4-(4-aminophenyl) piperidine dithiocarbamate with nickel(II),

11.Ni

11 (0.04g, 0.1459 mmol) was dissolved in 5 mL methanol. Nickel nitrate hexahydrate (0.0212g, 0.0729 mmol) was dissolved in the minimum amount of methanol. This solution was added to the reaction mixture dropwise with constant stirring to obtain green precipitate. The

reaction mixture was stirred for 2h at room temperature. The product was filtered on a glass filtration frit and dried. Yield: 0.0198g, 48.41%; IR (ZnSe): 1506 cm^{-1} ($\nu_{\text{C-N}}$).

2.2.29 Reaction of Sodium 4-(4-aminophenyl) piperidine dithiocarbamate with copper(II),

11.Cu

11 (0.04g, 0.1459 mmol) was dissolved in 5 mL methanol. Copper nitrate hemipentahydrate (0.0165g, 0.0729 mmol) was dissolved in the minimum amount of methanol. This solution was added to the reaction mixture dropwise with constant stirring to obtain dark brown precipitate. The reaction mixture was stirred for 2h at room temperature. The product was filtered on a glass filtration frit and dried. Yield: 0.0142g, 34.47%; IR (ZnSe): 1494 cm^{-1} ($\nu_{\text{C-N}}$).

2.2.30 Reaction of Sodium 4-(4-aminophenyl) piperidine dithiocarbamate with zinc(II), 11.Zn

11 (0.04g, 0.1459 mmol) was dissolved in 5 mL methanol. Zinc nitrate hemipentahydrate (0.0217g, 0.0729 mmol) was dissolved in the minimum amount of methanol. This solution was added to the reaction mixture dropwise with constant stirring to obtain white precipitate. The reaction mixture was stirred for 2h at room temperature. The product was filtered on a glass filtration frit and dried. Yield: 0.0173g, 41.79%. IR (ZnSe): 1490 cm^{-1} ($\nu_{\text{C-N}}$); ^1H NMR (400 MHz, DMSO- d_6) δ ppm: 1.54 (d, $J=9.37$ Hz, 2 H) 1.83 (d, $J=12.50$ Hz, 2 H) 2.66 (br. s., 2 H) 4.87 (br. s., 1 H) 5.01 (d, $J=12.89$ Hz, 2 H) 6.50 (d, $J=7.81$ Hz, 2 H) 6.89 (d, $J=8.20$ Hz, 2 H).

2.3 Results and discussion

2.3.1 Studies with 4-aminopiperidine

Keeping the concept of dual functionality in the ligand, 4-aminopiperidine was selected as this possessed an $-\text{NH}_2$ group which can form imido derivative with polyoxometalate cluster. On the other side it contains a secondary amine, piperidine $-\text{NH}$ group, which is a precursor for forming dithiocarbamate functionality which is known to form complexes with various transition metals. Two different approaches could be employed for the synthesis of the POM clusters:

- a) The ligand could be coordinated first to form imido derivative of ligand and the prepared derivative could be converted to dithiocarbamate to coordinate to transition metals.

- b) Or, the ligand could be converted to dithiocarbamate, of which various transition metal complexes could be prepared, which could further be coordinated to the cluster.

Since, metal coordination involves use of basic medium, which may result in polyoxometalate cluster decomposition, transition metal coordination (step-b) was chosen to be the first step.

Following the known procedure to synthesize dithiocarbamates, 4-aminopiperidine was taken in ethanol to which CS₂ and equivalent amount of NaOH was added which resulted in the formation of a white precipitate. The product was analyzed by infrared spectroscopy where C-N stretch was observed at 1492 cm⁻¹. ¹H NMR also showed changes suggesting the formation of a new compound. To further confirm the formation of desired product, crystals of the product were obtained from water in 2 days. To our surprise, the X-ray crystal structure showed the formation of a hydrated zwitterion (**1**) instead of sodium dithiocarbamate.

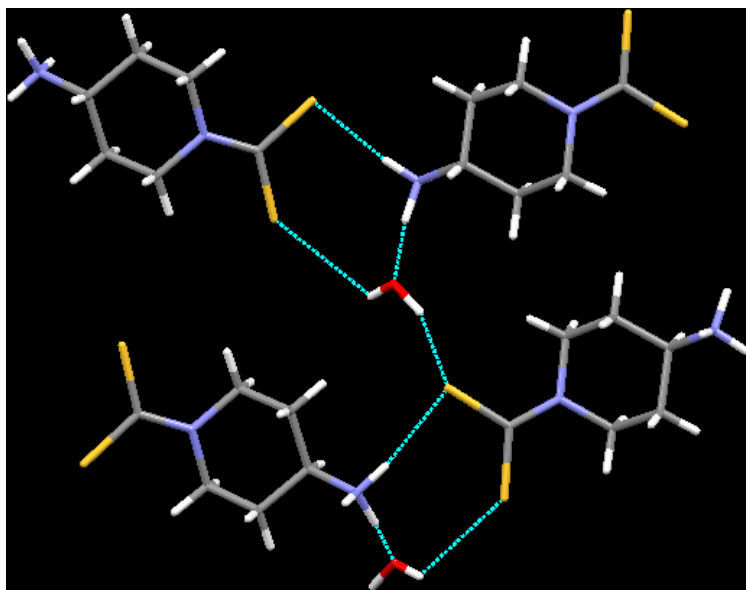


Figure 2.9 X-ray crystal structure of zwitterion, **1**.

1 displays the formation of $R_3^3(8)$ hydrogen-bonded supramolecular motif involving dithiocarbamate moiety, NH₃⁺ and a water molecule (Figure 2.9). The other hydrogen atom of the water molecule is hydrogen-bonded to the CS₂ moiety, and thus is responsible for interlinking two adjacent $R_3^3(8)$ motifs.

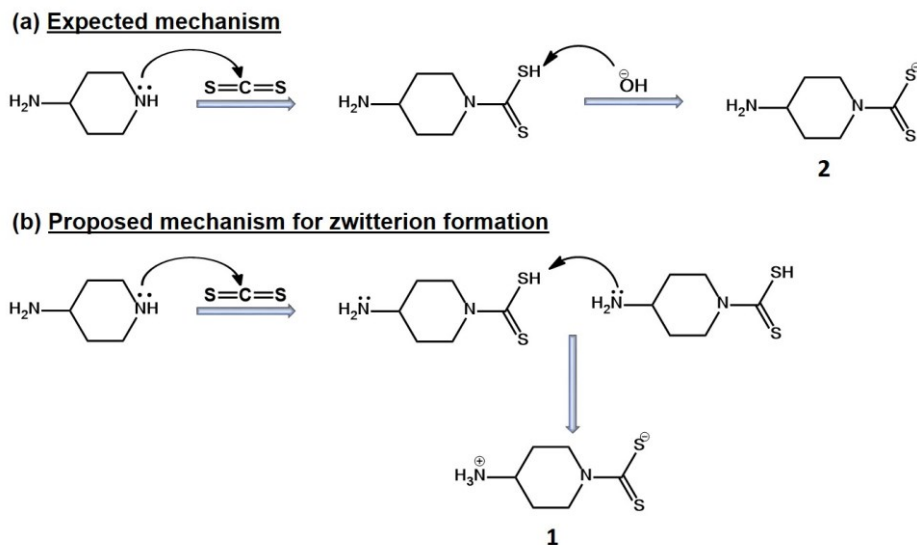


Figure 2.10 Proposed mechanism for formation of **1**.

Usually, in the synthesis of dithiocarbamate complexes, the lone pair of electron on secondary nitrogen atom attacks the nucleophilic carbon atom of CS_2 , which undergoes addition resulting in the formation of carbamic acid intermediates, which are generally unstable in basic medium (Figure 2.10(a)). Thus, further addition of a base abstracts the acidic proton of sulfur generating a dithiocarbamate compound. With 4-aminopiperidine, first step of CS_2 addition occurs in the same manner but contrary to the expected attack from a base, since NH_2 -group was present in the molecule possessing a lone pair of electrons available which attacks instead resulting in the formation of **1** (Figure 2.10(b)).

The next step was attempted in water since **1** was soluble only in water. The formation of sodium dithiocarbamate (**2**) of 4-aminopiperidine was then achieved by dissolving 4-aminopiperidine in water to which equivalent amounts of CS_2 and NaOH (Figure 2.11). The solvent from the reaction mixture was removed under vacuum to yield a white precipitate as product. The IR showed C-N stretch at 1458 cm^{-1} . ^1H and ^{13}C NMR also showed spectra different than zwitterion suggesting the formation of **2**. All the attempts for growing X-ray quality crystals failed.

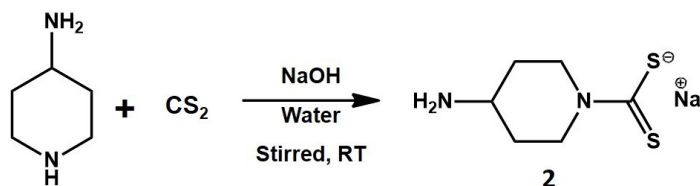
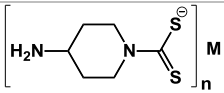


Figure 2.11 Synthesis of **2**.

The transition metal complexes were easily obtained by mixing aqueous solution of **2** with aqueous solution of the desired metal nitrate. The different transition metals used were chosen to adopt different coordination environments. The metal complexes were found to be insoluble in water and thus were collected by filtration, dried in air and were analyzed by infrared spectroscopy (Table 2.2).

Table 2.2 Metal complexes with **2**.

	$\nu_{C-N} / \text{cm}^{-1}$
2.Cr	1487
2.Mn	1470
2.Fe	1483
2.Co	1478
2.Ni	1442
2.Cu	1485
2.Zn	1477
2.Ag	1477

Although **2.Ni** exhibited slight solubility in acetonitrile, Karcher was able to get the single crystal structure of this nickel complex. The nickel atom sits in an octahedral pocket, where it is bonded to two 4-aminopiperidyl dithiocarbamate molecules through four sulfur atoms of $-NCS_2$ units. Unexpectedly, the other two sites were occupied by two $-NH_2$ groups of neighboring piperidine molecules, which rendered the metal complex incapable of use as an imidodelivery reagent. To avoid this unexpected coordination, it was thought to add some other coordinating ligand in the system which has a better donating ability than $-NH_2$ group. For this, pyridine was selected and multiple trials were done wherein along with **2**, few drops of pyridine was also added, but in all the cases results were same as before. Hence, no further studies with this complex could be done.

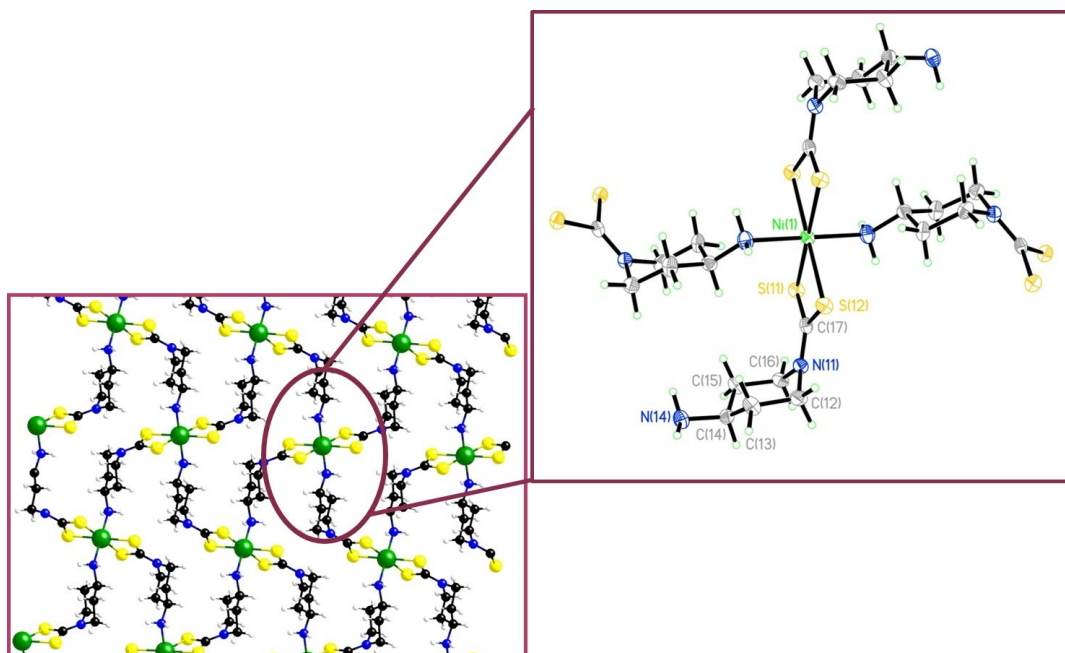


Figure 2.12 X-ray crystal structure for **2.Ni**.²⁸

Cobalt ion commonly forms a tris-complex with an octahedral arrangement, which was expected in the prepared **2.Co**. It also exhibited slight solubility in acetonitrile, dichloromethane and dichloroethane. ¹H NMR spectrum of **2.Co** revealed resolved peaks which corresponds to the Co(III) diamagnetic state showing tris-complexation in the metal complex. To further shed light on the composition of the complex, mass spectroscopy was done wherein a [M⁺] peak for 408.99 was observed which corresponds to a bis-complex. This observation is not new as some air stable bis-complexes cobalt(II) have been reported previously.²⁹ To further examine the actual composition of **2.Co**, multiple trials for obtaining the single crystals were done, but so far no single crystals have been obtained.

Assuming **2.Co** to be a tris-complex, furthermore its coordination to hexamolybdate clusters following Peng's method³⁰ were attempted, but no success in coordination were observed (Figure 2.13), which can be attributed to either non-availability of NH₂- group as previously observed in **2.Ni** or the poor solubility of these metal complexes in common organic solvents of use.

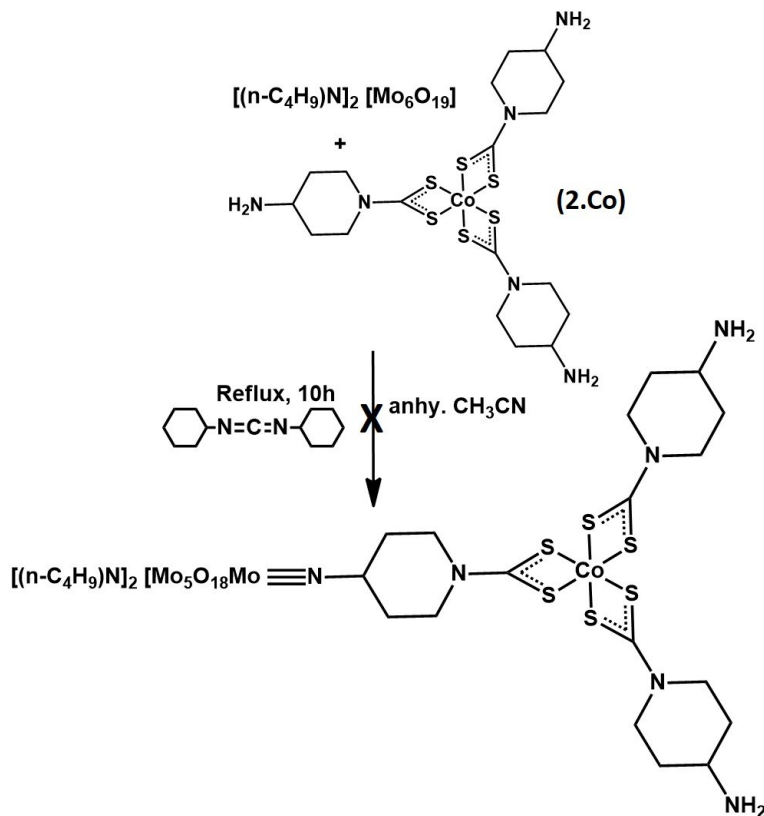


Figure 2.13 Attempted covalent grafting of **2.Co** to hexamolybdate.

All other metal complexes were found to be insoluble in any of the common organic solvents, thus could not be used in any further coordination studies. Since, the poor solubility of the metal complexes restricted their covalent grafting to the POM cluster, we thought of synthesizing tetrabutylammonium (TBA) dithiocarbamate of the ligand (**3**) so as to gain solubility in organic solvents. **3** was also prepared in a similar manner in water as solvent and solvent was removed in vacuum to obtain an oil (Figure 2.14). The IR spectrum of the product showed a C-N stretch at 1460 cm^{-1} . The product formation was also confirmed by ^1H which displayed similar chemical shifts as observed in **2** with an additional four new peaks arising from TBA^+ ion. ^{13}C NMR is also a strong tool in identifying these dithiocarbamates, where a characteristic peak at 212.77 ppm corresponding to CS_2 group was observed.

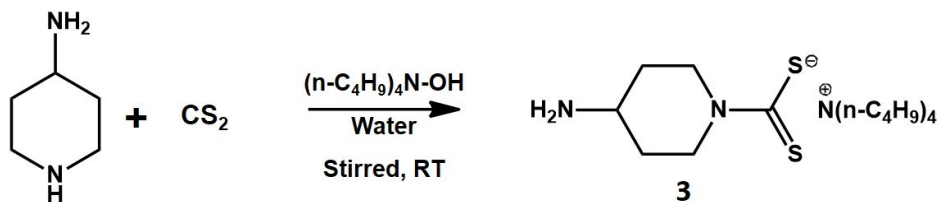


Figure 2.14 Synthesis of **3**.

All attempts to get a solid as the pure product failed, thus the oil so obtained was used as such to prepare phosphineimine derivative of **3** (Figure 2.15). ^1H and ^{31}P NMR suggested no formation of the product. Further, Peng's method³⁰ was adopted to coordinate to hexamolybdate, which proved to be unsuccessful as well. Since both these reactions demand extremely anhydrous conditions, the failure of the reactions suggest a possibility of existence of water, which might be there due to incomplete drying of **3**.

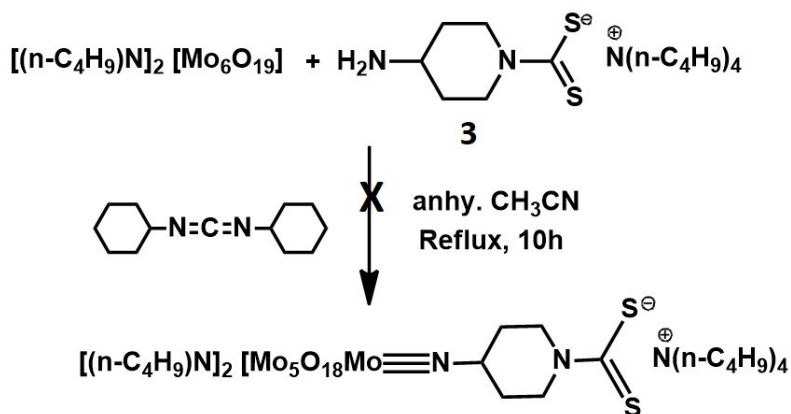


Figure 2.15 Attempts to covalent graft **3** onto hexamolybdate.

2.3.2 Studies with 4-(piperazin-1-yl)aniline

Since aliphatic imido hexmolybdate derivatives are prone to hydrolysis, a modification in the ligand structure was envisaged, so as to have an aromatic $-\text{NH}_2$ group, in a bid to achieve better stability upon coordination to the POM cluster. To achieve this, the ligand was chosen to be 4-(piperazin-1-yl)aniline (**6**) wherein, the molecule bears an aromatic $-\text{NH}_2$ moiety which may provide better coordination to cluster, while the other end bears $-\text{NH}$ group which is available to form the dithiocarbamate functionality.

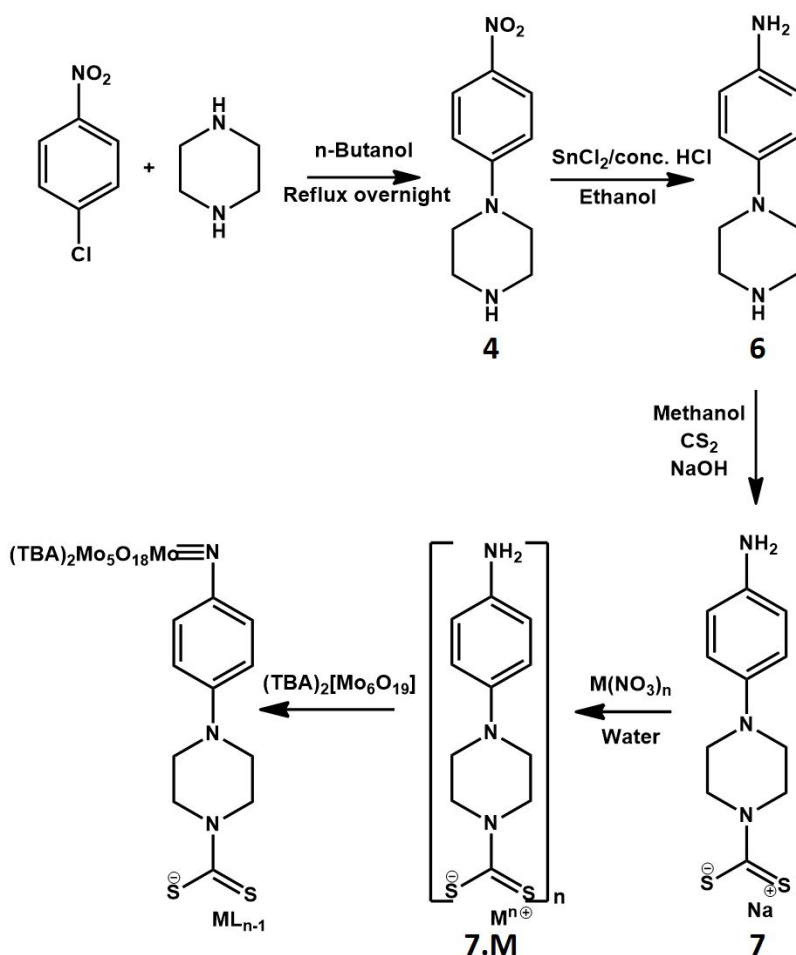
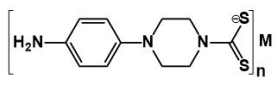


Figure 2.16 Synthetic scheme for metal dithiocarbamates of **7** as imidodelivery reagent.

Synthesis of this ligand was accomplished in three steps (Figure 2.16). First, coupling of p-chloronitrobenzene with piperazine was achieved in butanol under refluxing conditions and 1-(4-nitrophenyl)piperazine (**4**) was obtained as a bright yellow precipitate,²² which was analyzed *via* ^1H and ^{13}C NMR. Tetrabutylammonium dithiocarbamate derivative of 1-(4-nitrophenyl)piperazine (**5**) was prepared as a mimic of the POM hybrid, where NO_2 -group being electron-withdrawing resembles the electron sponge nature of the hexamolybdate cluster. The supramolecular studies of **5** will be discussed in a later section (Appendix A). The nitro dithiocarbamate can help understand the behavior of hybrids with other transition metal ions. To synthesize **5**, equivalent amounts of CS_2 and aqueous TBA-OH were added to **4** in methanol as solvent and the product was extracted on solvent removal. IR spectrum of the product shows a characteristic $\nu_{\text{C-N}}$ stretch at 1486 cm^{-1} . NMR studies also confirmed the formation of the product wherein in ^{13}C NMR a peak at 214.19 ppm showed up corresponding to CS_2 -group.

The reduction of **4** was further achieved with tin(II) chloride in conc. HCl and ethanolic solution²⁴ to prepare the desired ligand (**6**), which was confirmed by ¹H and ¹³C NMR spectroscopy. Sodium dithiocarbamate derivative of 4-(piperazin-1-yl)aniline (**7**) was prepared by dissolving the ligand in methanol to which CS₂ and NaOH in methanol was added. The IR spectrum of **7** showed a C-N stretch at 1454 cm⁻¹. Analyzing the product with ¹H NMR revealed that the peak at 3.02 ppm corresponding to the 8 aliphatic protons of piperazyl ring splits and appears as two multiplets at 3.02 ppm and 4.56 ppm each integrating to 4 protons. This suggests that the formation of dithiocarbamate derivative results in forbidden piperazyl ring rotation thus breaking the symmetry of the molecule. Further, the product formation was confirmed by ¹³C NMR spectroscopy wherein the peak corresponding to N-C=S showed up at 213.50 ppm. Following the synthesis of **7**, metal complexes were prepared and analyzed by infrared spectroscopy (Table 2.3).

Table 2.3 Metal dithiocarbamate complexes with **7**.

	$\nu_{\text{C-N}} / \text{cm}^{-1}$
7.Cr	1507
7.Mn	1510
7.Fe	1511
7.Co	1507
7.Ni	1505
7.Cu	1507
7.Zn	1512

The corresponding TBA dithiocarbamate derivative (**8**) was also prepared with **6** in methanol which appeared as a sticky oil. The IR spectrum of **8** showed a C-N stretch at 1511.33 cm⁻¹. ¹H NMR was found to be similar as the sodium dithiocarbamate derivative with additional four peaks in the aliphatic region corresponding to TBA molecule. ¹³C NMR revealed a peak at 213.37 ppm confirming the synthesis of **8**. Even though the compound showed solubility in organic medium, it could not be used as imidodelivery reagent to coordinate to hexamolybdate since complete drying of the compound could not be achieved even under vacuum.

2.3.3 Studies with 4-(piperidin-4-yl)aniline

In search of ligands providing better stability and solubility, another ligand which was thought of as a suitable candidate as imidodelivery reagent was chosen to be 4-(piperidin-4-yl)aniline (**10**). The molecule bears an aromatic -NH_2 which might provide better coordination to cluster while the other end bears -NH group available which is a precursor for dithiocarbamate functionality. Since the ligand was not readily available, following synthetic scheme was developed to achieve the goal.

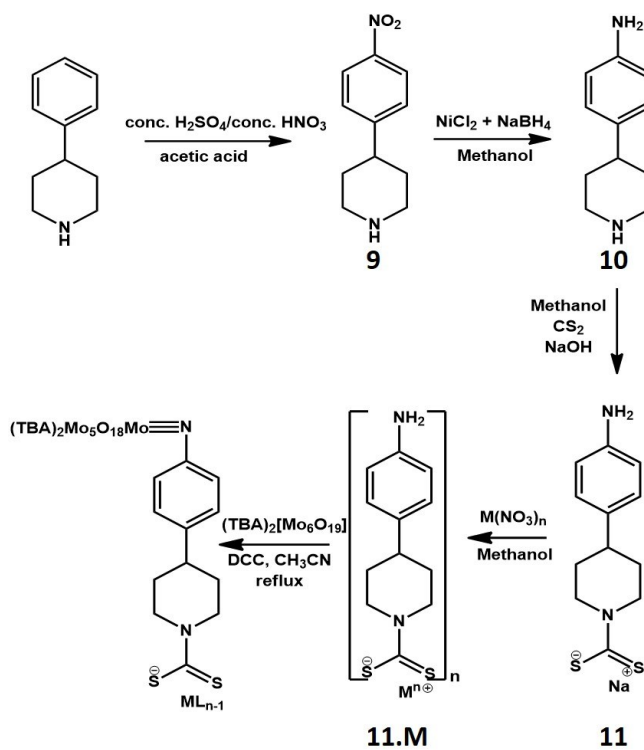
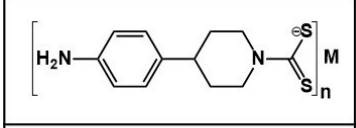


Figure 2.17 Synthetic scheme for metal dithiocarbamates of **11** as imidodelivery reagent.

At first, the nitration of 4-phenylpiperidine was achieved using nitrating mixture $\text{conc. H}_2\text{SO}_4/\text{HNO}_3$ in acetic acid medium²⁶ and the product was analyzed by ^1H and ^{13}C NMR. Further, reduction of 4-nitrophenylpiperidine (**9**) was achieved by reacting it with sodium borohydride and nickel chloride as catalyst.²⁷ The synthesis of the product (**10**) was confirmed by ^1H and ^{13}C NMR. After confirming the synthesis of the ligand, next was to prepare its sodium dithiocarbamate derivative (**11**) which was achieved with CS_2 and NaOH in methanol. The IR spectrum of the product showed a C-N stretch at 1460 cm^{-1} . **11** was also characterized by ^1H and ^{13}C NMR. A drastic shift in a set of aliphatic protons in ^1H NMR appearing at 5.95 ppm suggests deshielding of protons due to the addition of dithiocarbamate unit onto neighboring nitrogen of

piperidine unit. Moreover, a confirmation of the product was provided by ^{13}C NMR spectrum wherein a peak appears at 211.75 ppm corresponding to N-C=S unit. Further metal complexes from **11** were prepared and analyzed by infrared spectroscopy (Table 2.4).

Table 2.4 Metal dithiocarbamate complexes with **11**.

	$\nu_{\text{C-N}} / \text{cm}^{-1}$
11.Co	1491
11.Ni	1506
11.Cu	1494
11.Zn	1490

All of these synthesized metal complexes were generally insoluble, although **11.Zn** was found to be soluble in DMSO. ^1H NMR shows slight shifts in the aromatic peaks (Figure 2.18). Since the zinc coordination occurs at dithiocarbamate moiety, drastic upfield shift is observed with the peak at 6.01 ppm to 5.03 ppm which is assigned to protons on the α -carbons of NCS_2^- group. Shifts in other protons on the aliphatic ring were also observed, which confirms the formation of **11.Zn**.

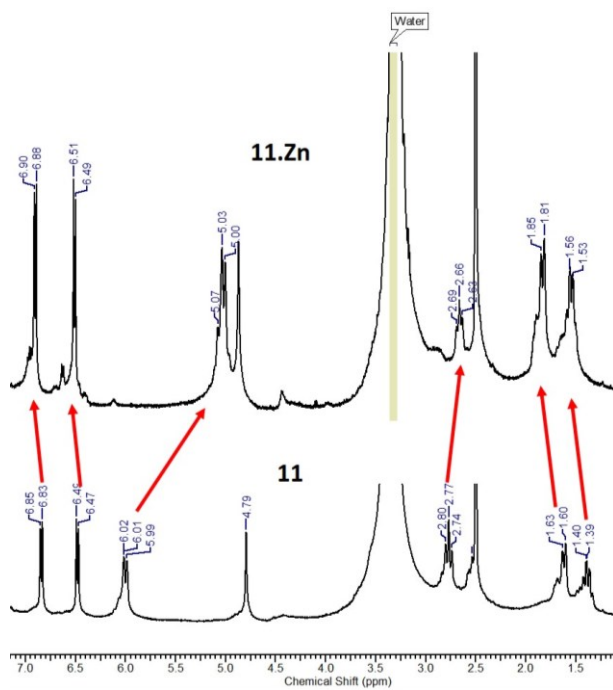


Figure 2.18 ^1H NMR spectrum of zinc dithiocarbamate of 4-(piperidin-4-yl)aniline, **11.Zn**.

Considering the slight solubility of **11.Zn** and the solubility of the complex to increase at refluxing temperatures, further coordination to hexamolybdate was attempted following Peng's route³⁰ but no color changes could be observed. Further IR and NMR analysis also confirmed the lack of reactivity. This may be attributed to quite low solubility in the solvent.

2.3.4 Microwave assisted covalent grafting of 11.Zn

Since the late 1970s, microwave technology has been applied in the field of inorganic chemistry. Microwave irradiation leads to dielectric heating which remotely introduces microwave energy into the chemical reactor which passes through the walls of the vessel without heating it and heats only the reactants and solvent.³¹ The energy transfer is so fast (10^{-9} s) that the molecules are never completely relaxed, which creates a non-equilibrium state resulting in a high instantaneous temperature of the molecules. The uniform temperature increase throughout the sample leads to less by-products and/or decomposition products.³² Such superheating effect results in temperatures much higher than expected under reflux conditions and can sometimes give rise to different results.³¹ Thus, we postulated that reacting **11.Zn** with hexamolybdate under microwave conditions may lead to different results (due to altered solubility of the metal complex). To test this hypothesis, an attempt was made to covalently graft **11.Zn** onto hexamolybdate under microwave conditions. The reaction was conducted for an hour after which the color of the solution was observed to turn brown, which was promising. Unfortunately on further analysis, no evidence of coordination could be observed.

2.4 Conclusions

We wanted to synthesize dithiocarbamate hybrids of hexamolybdate in order to prepare bimetallic systems. Thus, a series of dithiocarbamates and their corresponding metal complexes were prepared and characterized. Attempts to covalently graft them onto hexamolybdate were done using them as imido-delivery reagents following known routes. The poor solubility of these metal complexes proved to be a major stumbling block in our endeavors to synthesize the dithiocarbamate based polyoxometalate hybrids. Thus, it is important to investigate methods to improve the solubility of these metal complexes in future studies.

References

- ¹ Proust, A.; Matt, B.; Villanneau, R.; Guillemot, G.; Gouzerha, P.; Izzeta, G. *Chem. Soc. Rev.* **2012**, *41*, 7605.
- ² Kim, Y.; Shanmugam, S. *ACS Appl. Mater. Interfaces* **2013**, *5*, 12197.
- ³ Han, Z.; Zhao, Y.; Peng, J.; Tian, A.; Feng, Y.; Liu, Q. *J. of Solid St. Chem* **2005**, *178*, 1386.
- ⁴ Amdio, E.; Cavinato, A.; Domella, A.; Ronchini, L.; Toniolo, L.; Vavason, A. *J. Mol. Catal. A: Chem.* **2009**, *298*, 103.
- ⁵ (a) Mohammad, A.; Varshney, C.; Nami, S. A. A. *Spectrochim. Acta Part A* **2009**, *73*, 20; (b) Ozkirimli, S.; Apak, T. I.; Kiraz, M.; Yegenolgu, Y. *Arch. Pharmacol Res.* **2005**, *11*, 1213; (c) Siddiqi, K. S.; Khan, S.; Nami, S. A. A.; El-ajaily, M. M. *Spectrochim. Acta Part A* **2007**, *67*, 995.
- ⁶ Kanchi, S.; Singh, P.; Bisetty, K. *Arabian Journal of Chemistry* **2014**, *7*, 11.
- ⁷ Victorian, L. I. *Polyhedron* **2000**, *19*, 2269; Sahhen, F.; Badshah, A.; Gielen, M.; Dusek, M.; Fejfarova, K.; de Vos, D.; Mirza, B. *J. Organomet. Chem.* **2007**, *692*, 3019.
- ⁸ Khan, S.; Nami, S. A. A.; Siddiqi, K. S. *J. Organomet. Chem.* **2008**, *693*, 1049.
- ⁹ (a) Giovagnini, L.; Sitran, S.; Montopoli, M.; Caparrotta, L.; Corsini, M.; Rosani, C.; Zanello, P.; Dou, Q. P.; Fregona, D. *Inorg. Chem.* **2008**, *47*, 6336; (b) Li, H.; Lai, C. S.; Wu, J.; Ho, P. C.; de Vos, D.; Tiekink, E. R. T. *J. Inorg. Biochem.* **2007**, *101*, 809; (c) Hadjikakou, S. K.; Hadjiliadis, N. *Coord. Chem. Rev.* **2009**, *253*, 254.
- ¹⁰ (a) Rathore, H. S.; Varshney, G.; Majumdar, S. C.; Saleh, M. T. *J. Therm. Anal. Calor.* **2007**, *90*, 681; (b) Singh, R.; Kaushik, N. K. *Spectrochim. Part A* **2008**, *71*, 669.
- ¹¹ Cotton, F. A.; Wilkinson, G.; Murillo, C. A.; Bochmann, M. *Advanced Inorganic Chemistry*, 6th Ed., John Wiley and Sons, Inc, New York, 1996.
- ¹² Karlin, K. D. *Prog. Inorg. Chem.* **2005**, *53*, 71.
- ¹³ Debus, H. *Ann. Chem.*, **1850**, *73*, 26.
- ¹⁴ (a) Coucouvanis, D.; Fackler, Jr., J. P. *Inorg. Chem.* **1967**, *6*, 2047; (b) Kaul, B. B.; Pandeya, A. B. *Transition Met. Chem.* **1979**, *4*, 112; (c) Sarwar, M.; Ahmad, S.; Ali, S.; Awan, S. A. *Transition Met. Chem.* **2007**, *32*, 199; Golcu, A.; Yavuz, P. *Russ. J. Coord. Chem.* **2008**, *34*, 106.
- ¹⁵ Cooksona, J.; Beer, P. D. *Dalton Trans.* **2007**, 1459.
- ¹⁶ Hogarth, G. *Prog. Inorg. Chem.* **2005**, *53*, 71.
- ¹⁷ McCleverty, J. A.; Meyer, T. J. *Comprehensive Coordination Chemistry II From biology to nanotechnology*, Volume 1: Fundamentals: Ligands, Complexes, Synthesis, Purification, and Structure, Elsevier Pergamon, 2003.
- ¹⁸ Bond, A. M.; Martin, R. L. *Coord. Chem. Rev.* **1984**, *54*, 23
- ¹⁹ Hendrickson, A. R.; Martin, R. L.; Rohde, N. M. *Inorg. Chem.* **1976**, *15*, 2115.
- ²⁰ Wu, F.-H.; Liu, Y.-L.; Duanb, T.; Lua, L.; Zhangb, Q.-F.; Leungc, W.-H. *Z. Naturforsch.* **2009**, *64b*, 800.
- ²¹ Klemperer, W. G.; Ginsberg, A. P. *Introduction to Early Transition Metal Polyoxoanions*, Inorganic Syntheses, Volume 27, John Wiley & Sons, Inc., 2007.
- ²² Payne, L. J.; Downham, R.; Sibley, G. E. M.; Edwards, P.; Davies, G. M. WO 2008145963 A1, 2008.

-
- ²³ Bent, R. L.; Dessloch, J. C.; Duennebier, F. C.; Fassett, D. W.; Glass, D. B.; James, T. H.; Julian, D. B.; Ruby, W. R.; Snell, J. M.; Sterner, J. H.; Thirtle, J. R.; Vittum, P. W.; Weissberger, A. *J. Am. Chem. Soc.* **1951**, *73*, 3100.
- ²⁴ Bellamy, F. D.; Ou, K. *Tetrahedron Lett.* **1984**, *25*, 839.
- ²⁵ Prelog, V.; Blazek, Z. *Collection of Czechoslovak Chem. Commun.* **1934**, *6*, 211.
- ²⁶ Bold, G.; Furet, P.; Guagnano, V. WO 2007071752 A2, 2007.
- ²⁷ Osby, J. O.; Ganem, B. *Tet. Lett.* **1985**, *26*, 6413.
- ²⁸ Karcher, J., *PhD Thesis, Kansas State University*, **2007**.
- ²⁹ Marcotrigiano, G.; Pellacani, G. C.; Preti, C. *J. Inorg. Nucl. Chem.* **1974**, *36*, 3709.
- ³⁰ Wei, Y.; Xu, B.; Barnes, C. L.; Peng, Z. *J. Am. Chem. Soc.* **2001**, *123*, 4083.
- ³¹ Lidström, P.; Tierney, J.; Wathey, B.; Westman, J. *Tetrahedron* **2001**, *57*, 922.
- ³² Brittany L. Hayes, *Aldrichchimica Acta*, 2004, *37*, 66.

Chapter 3 - Extended dithiocarbamate systems based on poly(pyrazolyl)borates as organoimido delivery reagents

3.1 Poly(pyrazolyl)borates

Poly(pyrazolyl)borates were introduced in 1966 by Trofimenko¹ after which these became quite popular due to their unusual chemistry and versatile coordination modes. Their ease of synthesis and tuning of their steric and electronic properties by altering the substituents on the pyrazole rings² made them widely applicable in the fields ranging from analytical chemistry and organic synthesis, to catalysis and material science.³

In spite of their complicated looking structures, poly(pyrazolyl)borate ligands can easily be synthesized either by condensation of 1,3-diketone with hydrazine hydrate or via thermal dehydrogenative condensation between tetrahydroborate in molten (Figure 3.1).⁴

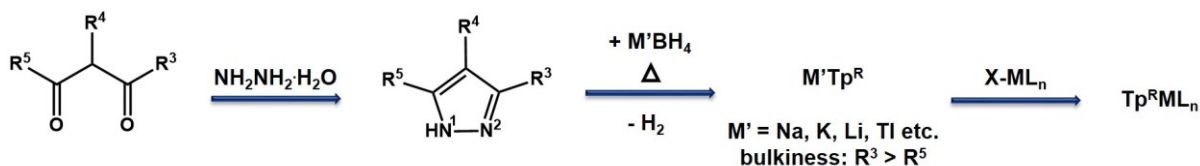


Figure 3.1 General routes of synthesis of poly(pyrazolyl)borate ligands.⁴

Controlling the temperature, the reaction can be stopped to yield bis-, tris-, and in the case of 5-unsubstituted pyrazoles, tetrakis(pyrazolyl)borates (Figure 3.2).³

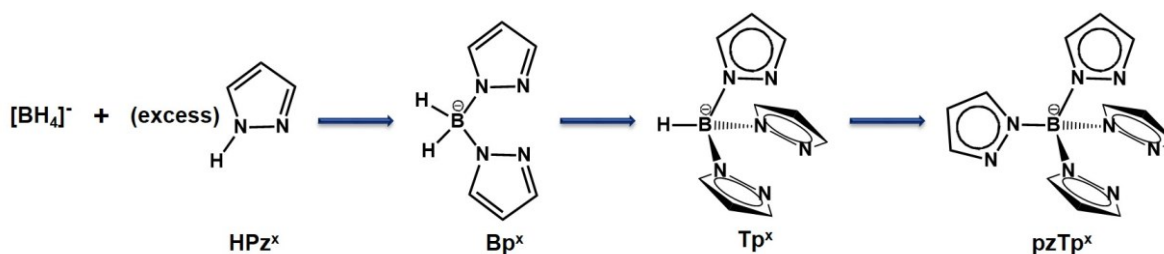


Figure 3.2 Successive pyrazolyl substitution in molten synthesis.³

However, poly(pyrazolyl)borate ligands are known to exhibit metal coordination κ^3 - to κ^0 - fashion,⁵ these more commonly act as tridentate ligands showing a $\kappa^3\text{N,N',N''}$ coordination environment resulting in effective steric shielding of the metal center.^{6,7} Since the κ^3 -binding mode bear a resemblance to the shape of a hunting scorpion (with the two claws and the tail), these have been nicknamed as “scorpionate” (Figure 3.3).^{6b}

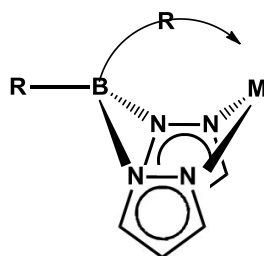


Figure 3.3 Resemblance of poly(pyrazolyl)borate ligand to the shape of a hunting scorpion.^{6b}

The modification in the coordination behavior of the poly(pyrazolyl)borate ligand can be achieved systematically by introduction of appropriate substituents (R^{3-5}) onto the pyrazolyl rings. The 3-substituents (R^3) being in close proximity to the metal center, usually during metal coordination, the bulkier substituent of the R^3 and R^5 groups prefers the R^3 position to relieve the steric repulsion around the metal center.² In contrast, by introducing an electron-donating or -withdrawing groups at the 4- and/or 5-positions ($R^{4,5}$), the electronic environment at the metal center can be tuned. Pertaining to their analogy to charge, facial coordination, and their potential to act as six-electron donors, poly(pyrazolyl)borate ligands have often been compared to the cyclopentadienyl ligands (Figure 3.4).⁶

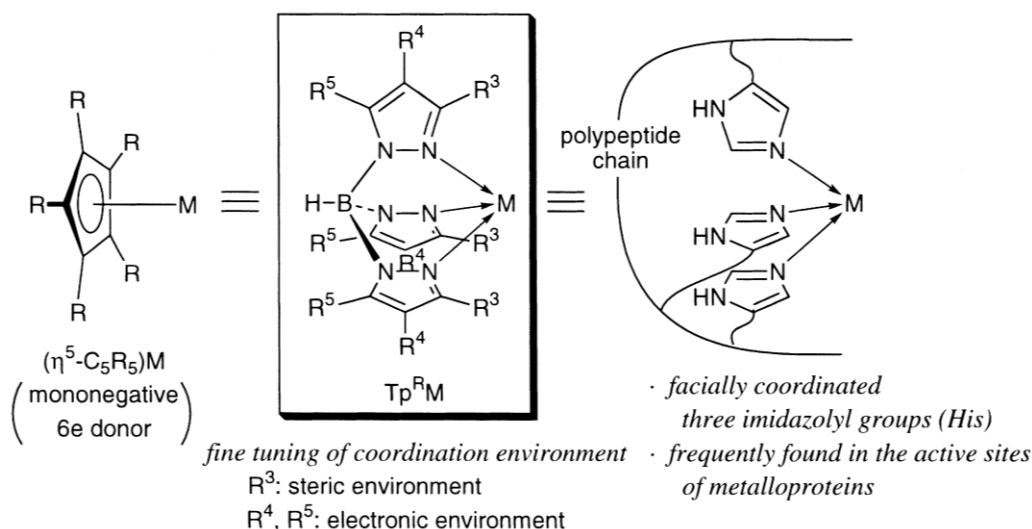


Figure 3.4 Comparison of poly(pyrazolyl)borate ligands with cyclopentadienyl ligands.⁴

These are also sometimes referred as Trofimenko ligands and are commonly used complexing ligands.⁸ These are known to coordinate with many main group elements as well as several transition metals,⁹ lanthanides, and actinides.¹⁰ A variety of bridged polynuclear complexes of Mo were reported by McCleverty and Ward in 1998.^{9b} Further, the coordination and supramolecular chemistry with these TpPy-based ligands were studied in 2001.¹¹

Poly(pyrazolyl)borates gained much attention when these were incorporated as structural and functional models for the active site of metallo-enzymes, for instance, zinc pyrazolylborate chemistry were recently reported to be related to zinc enzymes.¹² Many peroxocopper(II) complexes,¹³ alkylperoxocopper(II) complexes,¹⁴ and thiolatocopper(II) complexes¹⁵ based on $[\text{HB}(3,5\text{-Pr}^i_2\text{pz})_3]^-$ (=hydrotris(3,5-diisopropyl-1-pyrazolyl)borate(1-)) were prepared and used as models for oxy-hemocyanin, copper containing monooxygenases, and blue copper proteins, respectively. Moreover, coordination chemistry of rhodium- and iridium-tris(pyrazolyl)borate complexes and their further use for C-H activation were introduced by Slugovc and Carmona in 2001.¹⁶ A number of organometallic species $[\text{TpRCoR}]$ (R = allyl, alkyl, aryl or alkynyl) were reported by Akita *et al.* to provide an understanding for catalytic transformations or for use as polymerization catalysts.¹⁷

One of their remarkable features which makes poly(pyrazolyl)borate ligands extremely popular is their reliability and role as spectator ligands. This implies that in metal complexes, these ligands do not interfere with the reactions occurring at the metal centers.³ Several such examples have been reported so far amongst which few complexes exhibit metal coordination to dithiocarbamate moieties. In 2009, Ma *et al.* reported ligation of nickel hydrotris(3,5-dimethyl-1-pyrazolyl)borate with dithiocarbamate as nickel superoxide dismutase (NiSOD) mimics.¹⁸ Recently, Harding *et al.* also reported cobalt and nickel dithiocarbamate complexes based on Trofimenko's hydrotris(3,5-diphenyl-1-pyrazolyl)borate anion.¹⁹

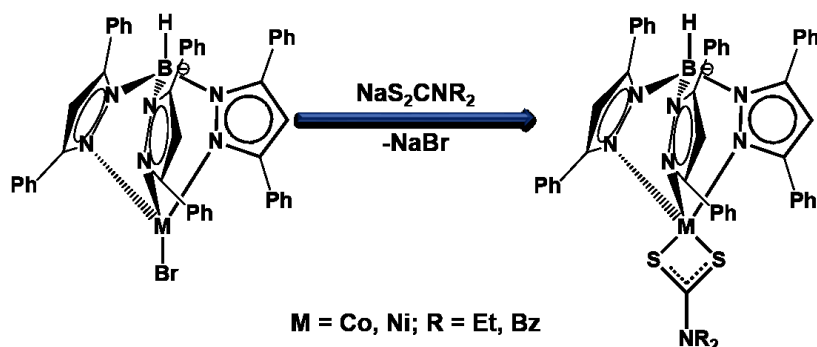


Figure 3.5 Reported synthesis of dithiocarbamate complexes based on hydrotris(3,5-diphenyl-1-pyrazolyl)borate anion.¹⁹

In aforementioned studies, since the metal dithiocarbamate complexes bear tris(pyrazolyl)borate fragments around the metal center, these complexes have been reported to show good solubility in organic solvents in both the studies. As mentioned in the previous chapter, the metal complexes of the selected dithiocarbamate complexes exhibited poor solubility

in organic solvents which resulted in reluctance of preparation of organoimido derivatives of hexamolybdates.

Following the above mentioned studies, in this chapter we plan to prepare a series of metal complexes with diphenyl and dimethyl pyrazolyl borate anions and subsequently co-ligating them with sodium 4-aminopiperidine dithiocarbamate. Furthermore, these metal dithiocarbamate complexes will be exploited as organoimido delivery reagents to prepare hexamolybdate derivatives.

3.2 Experimental

(TBA)₂[Mo₆O₁₈] and (TBA)₄[Mo₈O₂₆] were prepared according to literature methods.²⁰ All chemicals were purchased from Aldrich and used without further purification. All manipulations were done under an inert atmosphere of argon, unless otherwise stated. Tetrahydrofuran (THF) was distilled over sodium; dichloromethane was dried over P₂O₅ and distilled; and triethylamine and acetonitrile (CH₃CN) were dried over CaH₂ and distilled as needed. ¹H, and ¹³C NMR spectra were recorded on a Varian Unity plus 400 MHz spectrometer and were referenced to residual protonated solvent peaks (CDCl₃ = 7.27 ppm and acetone-d₆ = 2.05 ppm). FT-IR spectra were recorded on a Nicolet 380 instrument. Mass spectra were collected using MS system Waters ACQUITY TQD. X-ray data was collected on a Bruker SMART 1000 four-circle CCD diffractometer at 203 K using a fine-focus molybdenum K α tube.

3.2.1 Synthesis of 3,5-diphenyl pyrazole, **12**²²

A solution of dibenzoylmethane (30 g, 133.77 mmol) was prepared in 60 mL of ethanol. To this, hydrazine monohydrate (7.8 mL, 160.52 mmol) was added dropwise and the reaction mixture was kept at 50°C during which benzoylmethane was dissolved and eventually, white precipitate appeared. The mixture was then refluxed for 30 min. On cooling, the white solid was collected by filtration and washed subsequently with water and ethanol. The air dried product was then recrystallized from acetone to give **12** as a white crystalline solid. Yield: 26.90g, 91.29%; ¹H NMR (400 MHz, acetone-d₆) δ ppm: 7.11 (s, 1 H) 7.33 (s, 2 H) 7.38 - 7.50 (m, 4 H) 7.88 (d, J=7.32 Hz, 4 H) 12.56 (br. s., 1 H); ¹H NMR (400 MHz, CDCl₃) δ ppm: 6.86 (s, 1 H) 7.33 - 7.39 (m, 2 H) 7.40 - 7.48 (m, 4 H) 7.75 (d, J=7.25 Hz, 4 H); ¹H NMR (400 MHz, DMSO-d₆) δ ppm: 7.18 (s, 1 H) 7.36 (s, 1 H) 7.33 (s, 1 H) 7.39 - 7.57 (m, 4 H) 7.70 - 7.98 (m, 4 H) 13.36 (s, 1 H).

3.2.2 Synthesis of Potassium tris(3,5-diphenylpyrazolylborate), **13**^{3,22,23}

KBH₄ (2.20g, 40.71 mmol) and **12** (26.90g, 122.12 mmol) were combined with 70 mL anisole in the glove box and the reaction mixture was heated at 250°C for 10 days. On cooling at room temperature, white precipitate appeared which was filtered off onto a glass frit under inert conditions. The product was washed with toluene and dried under vacuum. Single crystals suitable for X-ray diffraction were obtained from acetone using solvent evaporation method performed in a desiccator. Yield: 74.52g, 86.10%; IR (ZnSe): 2529 cm⁻¹ (ν_{B-H}); ¹H NMR (400 MHz, CDCl₃) δ ppm: 6.59 (s, 3 H) 6.95 (d, J=6.84 Hz, 6 H) 6.98 - 7.10 (m, 9 H) 7.22 (d, J=7.32 Hz, 4 H) 7.26 - 7.35 (m, 6 H) 7.68 (d, J=7.81 Hz, 6 H); ¹H NMR (400 MHz, acetone-d₆) δ ppm: 6.77 (d, J=1.88 Hz, 3 H) 6.89 - 7.11 (m, 15 H) 7.12 - 7.32 (m, 9 H) 7.79 - 8.02 (m, 6 H); ¹³C NMR (400 MHz, acetone-d₆) δ ppm: 103.53, 126.21, 127.22, 127.58, 128.23, 129.21, 129.62, 134.93, 136.39, 151.25, 151.70.

3.2.3 Synthesis of Potassium tris(3,5-dimethylpyrazolylborate), **14**^{3,23}

3,5-dimethylpyrazole (10g, 104.03 mmol) and KBH₄ (1.87g, 34.68 mmol) were combined with 40 mL anisole in the glove box and the reaction mixture was heated at 250°C for 10 days. On cooling at room temperature, white precipitate appeared which was filtered off onto a glass frit under inert conditions. The product was recrystallized from acetone yielding the product as a white precipitate. Yield: 29.55g, 84.57%; IR (ZnSe): 2433 cm⁻¹ (ν_{B-H}); ¹H NMR (400 MHz, acetone-d₆) δ ppm: 2.01 (s, 9 H) 2.17 (s, 9 H) 5.54 (s, 3 H).

3.2.4 Synthesis of Cobalt chloro tris(3,5-diphenylpyrazolylborate), **15**²⁴

A THF solution of **13** (9.89g, 13.95 mmol) was prepared. In a separate beaker, a THF solution of cobalt chloride (2.0g, 15.3488 mmol) was prepared giving a blue color. On mixing the two solution, the color of the reaction mixture changed to deeper blue. The mixture was stirred for 4h. The solution was then filtered off to remove the formed precipitate of KCl and the solvent was removed under vacuum to give the product as blue precipitate. Yield: 8.76g, 82.19 %; IR (ZnSe): 2610 cm⁻¹ (ν_{B-H}); UV-Vis (dichloromethane) [λ_{max}/nm (ε/M⁻¹cm⁻¹): 600 (316.9), 638.2 (473.24), 669.2 (421.13). m/z (ESI): 728.45 [M-Cl]⁺.

3.2.5 Synthesis of Nickel bromo tris(3,5-diphenylpyrazolylborate), 16²⁵

A THF solution of **13** (2.13g, 3.0 mmol) was prepared. In a separate beaker, a THF solution of nickel bromide (0.72g, 3.3 mmol) was prepared giving a pale green color. On mixing the two solution, the color of the reaction mixture changed to purple pink. The mixture was stirred for 4h. The solvent was removed under vacuum and the solid was extracted with dichloromethane. On drying under vacuum, product was obtained as purple precipitate. Yield: 1.9427g, 80.11%; IR (ZnSe): 2613 cm^{-1} ($\nu_{\text{B-H}}$); UV-Vis (dichloromethane) [$\lambda_{\text{max}}/\text{nm}$ ($\epsilon/\text{M}^{-1}\text{cm}^{-1}$): 507 (359.04), 829.2 (62.05), 934.2 (98.19)].

3.2.6 Synthesis of Nickel nitrate tris(3,5-diphenylpyrazolylborate), 17

A THF solution of **13** (0.15g, 0.2116 mmol) was prepared. In a separate beaker, a THF solution of nickel nitrate hexahydrate (0.062g, 0.2116 mmol) was prepared giving a green color. On mixing the two solution, the color of the reaction mixture changed to deep green with white precipitate. The mixture was stirred for 4h. The solvent was removed under vacuum and the solid was extracted with dichloromethane. On drying under vacuum, product was obtained as green precipitate. Yield: 0.1482g, 88.63%; IR (ZnSe): 2606 cm^{-1} ($\nu_{\text{B-H}}$); UV-Vis (dichloromethane) [$\lambda_{\text{max}}/\text{nm}$ ($\epsilon/\text{M}^{-1}\text{cm}^{-1}$): 435.2 (113.64), 685.6 (34.21)].

3.2.7 Synthesis of Copper nitrate tris(3,5-diphenylpyrazolylborate), 18

A solution of **13** (0.3g, 0.4233 mmol) in 5mL THF was prepared. In a separate beaker, a solution of copper nitrate (0.0959g, 0.4233 mmol) in 3mL THF was prepared giving a pale blue color. On mixing the two solution, the color of the reaction mixture changed to green with instant white precipitation. The mixture was stirred for 2h and left for solvent evaporation after which dark green crystals were obtained as the product. Yield: 0.3144g, 93.40%; IR (ZnSe): 2614 cm^{-1} ($\nu_{\text{B-H}}$); UV-Vis (dichloromethane) [$\lambda_{\text{max}}/\text{nm}$ ($\epsilon/\text{M}^{-1}\text{cm}^{-1}$): 300.8 (3327.27), 768.4 (409.09)].

3.2.8 Synthesis of Manganese chloro tris(3,5-diphenylpyrazolylborate), 19

A solution of **13** (0.15g, 0.2116 mmol) in 5mL THF was prepared. In a separate beaker, a solution of manganese chloride hexahydrate (0.042g, 0.2116 mmol) in 3mL THF was prepared giving a colorless solution. On mixing the two solution the color of the solution changed to a pale orange with instant white precipitation. The mixture was stirred for 4h. The solvent was removed under vacuum and the solid was extracted with dichloromethane. On solvent

evaporation, product was obtained as white crystals. Yield: 0.0776g, 48.25%; IR (ZnSe): 2617 cm^{-1} ($\nu_{\text{B-H}}$).

3.2.9 Synthesis of Cobalt chloro tris(3,5-dimethylpyrazolyborate), 20

Similar preparatory method was adopted for **20** as used for **15**. A THF solution of **14** (1.00g, 2.977 mmol) was prepared. In a separate beaker, a THF solution of cobalt chloride (0.4255g, 3.2747 mmol) was prepared giving a blue color. On mixing the two solution, the color of the reaction mixture changed to deeper blue. The mixture was stirred overnight. The solution was then filtered off to remove the formed precipitate of KCl and the solvent was removed under vacuum to give the product as blue precipitate. Yield: 0.6638g, 56.94%; IR (ZnSe): 2501 cm^{-1} ($\nu_{\text{B-H}}$); UV-Vis (dichloromethane) [$\lambda_{\text{max}}/\text{nm}$ ($\epsilon/\text{M}^{-1}\text{cm}^{-1}$)]: 579.6 (98.53), 632 (187.55), 670.8 (80.22).

3.2.10 Synthesis of Nickel bromo tris(3,5-dimethylpyrazolyborate), 21

Similar preparatory method was adopted for **21** as used for **16**. A THF solution of **14** (2.13g, 3.0 mmol) was prepared. In a separate beaker, a THF/MeOH solution of nickel bromide (0.2433g, 1.1134 mmol) was prepared giving a pale green color. On mixing the two solution, the color of the reaction mixture changed to purple pink. The mixture was stirred overnight. The solvent was removed under vacuum and the solid was extracted with dichloromethane. On drying under vacuum, product was obtained as purple precipitate. Yield: 0.8537g, 65.30%; IR (ZnSe): 2519 cm^{-1} ($\nu_{\text{B-H}}$); UV-Vis (dichloromethane) [$\lambda_{\text{max}}/\text{nm}$ ($\epsilon/\text{M}^{-1}\text{cm}^{-1}$)]: 504.8 sh (321.30), 581.2 (61.30), 815 (100), 904.4 (100).

3.2.11 Synthesis of Copper nitrate tris(3,5-dimethylpyrazolyborate), 22²¹

A solution of **14** (0.5g, 1.4485 mmol) in 5mL THF was prepared. In a separate beaker, a solution of copper nitrate hemipentahydrate (0.3710g, 1.6374 mmol) in 3mL THF was prepared giving a pale blue color. On mixing the two solution, the color of the reaction mixture changed to green with instant white precipitation. The mixture was stirred for 4h. The solvent was removed under vacuum and the solid was extracted with dichloromethane. On drying under vacuum, product was obtained as green precipitate. Yield: 0.5408g, 88.32%; IR (ZnSe): 2507 cm^{-1} ($\nu_{\text{B-H}}$); UV-Vis (dichloromethane) [$\lambda_{\text{max}}/\text{nm}$ ($\epsilon/\text{M}^{-1}\text{cm}^{-1}$)]: 292.8 (1917.39), 756.6 (230.43).

3.2.12 Synthesis of Manganese chloro tris(3,5-dimethylpyrazolylborate), 23

A solution of **14** (0.15g, 0.4465 mmol) in 5mL THF was prepared. In a separate beaker, a solution of manganese chloride hexahydrate (0.088g, 0.4465 mmol) in 3mL THF was prepared giving a colorless solution. On mixing the two solution instant white precipitation was observed. The mixture was stirred for 4h. The solvent was removed under vacuum and the solid was extracted with dichloromethane. On solvent evaporation, product was obtained as white crystals. Yield 0.0874g, 30.15%; IR (ZnSe): 2519 cm^{-1} ($\nu_{\text{B-H}}$).

3.2.13 Reaction of Cobalt chloro tris(3,5-diphenylpyrazolylborate) with sodium (4-aminopiperidine) dithiocarbamate, 24

15 (3.8g, 4.97 mmol) was suspended in 150mL THF giving a blue solution. In a separate beaker, **2** (0.9861g, 4.97 mmol) was dissolved in minimum amount of water. On mixing the two solution, the color of the reaction mixture changed to brown. The mixture was stirred overnight. The solvent was removed under vacuum and the solid was extracted with dichloromethane. On drying under vacuum, product was obtained as light brown precipitate. Yield: 3.4082g, 75.87%; IR (ZnSe): 2623 cm^{-1} ($\nu_{\text{B-H}}$); UV-Vis (dichloromethane) [$\lambda_{\text{max}}/\text{nm}$ ($\epsilon/\text{M}^{-1}\text{cm}^{-1}$)]: 406.6 (373.79), 565 (48.28). m/z (ESI): 904.31 [M]⁺.

3.2.14 Reaction of Nickel bromo tris(3,5-diphenylpyrazolylborate) with sodium (4-aminopiperidine) dithiocarbamate, 25

16 (0.1g, 0.124 mmol) was suspended in 5mL THF giving a purple solution. In a separate beaker, **2** (0.025g, 0.124 mmol) was dissolved in minimum amount of water. On mixing the two solution, the color of the reaction mixture changed to light green. The mixture was stirred for 4h. The solvent was removed under vacuum and the solid was extracted with dichloromethane. On drying under vacuum, product was obtained as light green precipitate. Yield: 0.0572g, 51.07%; IR (ZnSe): 2612 cm^{-1} ($\nu_{\text{B-H}}$); UV-Vis (dichloromethane) [$\lambda_{\text{max}}/\text{nm}$ ($\epsilon/\text{M}^{-1}\text{cm}^{-1}$)]: 371.8 sh (565.85), 426.8 (454.27), 656.8 (50.81). m/z (ESI): 903.57 [M]⁺, 727.44 [M-DTC-H]⁺.

3.2.15 Reaction of Copper nitrate tris(3,5-diphenylpyrazolylborate) with sodium (4-aminopiperidine) dithiocarbamate, 26

18 (0.02g, 0.0252 mmol) was dissolved in 5mL dichloromethane giving a green solution. In a separate beaker, **2** (0.005g, 0.0252 mmol) was dissolved in minimum amount of water. On

mixing the two solution, the color of the reaction mixture changed to green-brown. The mixture was stirred overnight. The solvent was removed under vacuum and the solid was extracted with dichloromethane. On drying under vacuum, product was obtained as green-brown precipitate. Yield: 0.0068g, 29.71%; IR (ZnSe): 2597 cm^{-1} ($\nu_{\text{B-H}}$); UV-Vis (dichloromethane) [$\lambda_{\text{max}}/\text{nm}$ ($\epsilon/M^{-1}\text{cm}^{-1}$)]: 419.8 (4427.67), 654 (320.75); m/z (ESI): 908.59 $[\text{M}]^+$, 733.49 $[\text{M-DTC}]^+$.

3.2.16 Reaction of Cobalt chloro tris(3,5-dimethylpyrazolylborate) and sodium (4-aminopiperidine) dithiocarbamate, 27

20 (0.0395g, 0.1008 mmol) was suspended in 15mL THF giving a blue solution. In a separate beaker, **2** (0.020g, 0.1008 mmol) was dissolved in minimum amount of water. On mixing the two solution, the color of the reaction mixture changed to deep green. The mixture was stirred overnight. The solvent was removed under vacuum and the solid was extracted with dichloromethane. On drying under vacuum, product was obtained as dark green precipitate. Yield: 0.0205g, 38.25%; IR (ZnSe): 2501 cm^{-1} ($\nu_{\text{B-H}}$); UV-Vis (dichloromethane) [$\lambda_{\text{max}}/\text{nm}$ ($\epsilon/M^{-1}\text{cm}^{-1}$)]: 484.4 (219), 645 (320.75).

3.2.17 Reaction of Nickel bromo tris(3,5-dimethylpyrazolylborate) and sodium (4-aminopiperidine) dithiocarbamate, 28

21 (0.05g, 0.1151 mmol) was suspended in 5mL THF giving a purple solution. In a separate beaker, **2** (0.023g, 0.1151 mmol) was dissolved in minimum amount of water. On mixing the two solution, the color of the reaction mixture changed to light green. The mixture was stirred for 4h. The solvent was removed under vacuum and the solid was extracted with dichloromethane. On drying under vacuum, product was obtained as light green precipitate. Yield: 0.0332g, 54.34%; IR (ZnSe): 2506 cm^{-1} ($\nu_{\text{B-H}}$); UV-Vis (dichloromethane) [$\lambda_{\text{max}}/\text{nm}$ ($\epsilon/M^{-1}\text{cm}^{-1}$)]: 401.6 (348.94), 421 (379.79), 647.6 (55.32); m/z (ESI): 531.38 $[\text{M}]^+$, 355.29 $[\text{M-DTC-H}]^+$.

3.2.18 Reaction of Copper nitrate tris(3,5-dimethylpyrazolylborate) and sodium (4-aminopiperidine) dithiocarbamate, 29

22 (0.02g, 0.0487 mmol) was dissolved in 5mL THF giving a green solution. In a separate beaker, **2** (0.025g, 0.124 mmol) was dissolved in minimum amount of water. On mixing the two solution, the color of the reaction mixture changed to deep green. The mixture was

stirred overnight. The solvent was removed under vacuum and the solid was extracted with dichloromethane. On drying under vacuum, product was obtained as dark green precipitate. Yield: 0.086g, 32.95%; IR (ZnSe): 2501 cm^{-1} ($\nu_{\text{B-H}}$); UV-Vis (dichloromethane) [$\lambda_{\text{max}}/\text{nm}$ ($\epsilon/M^{-1}\text{cm}^{-1}$): 396 (2794.24), 694 (156.38).

3.3 Results and discussion

3.3.1 Synthesis of Poly(pyrazolyl)borate ligands

To improve solubility of metal dithiocarbamates in organic media, we planned to prepare a series of metal dithiocarbamate complexes of tris(diphenyl)- and tris(dimethyl) pyrazolyl borates. For diphenylpyrazolyl borate series, following synthetic scheme was developed (Figure 3.6). A parallel synthetic scheme was followed for the dimethyl series.

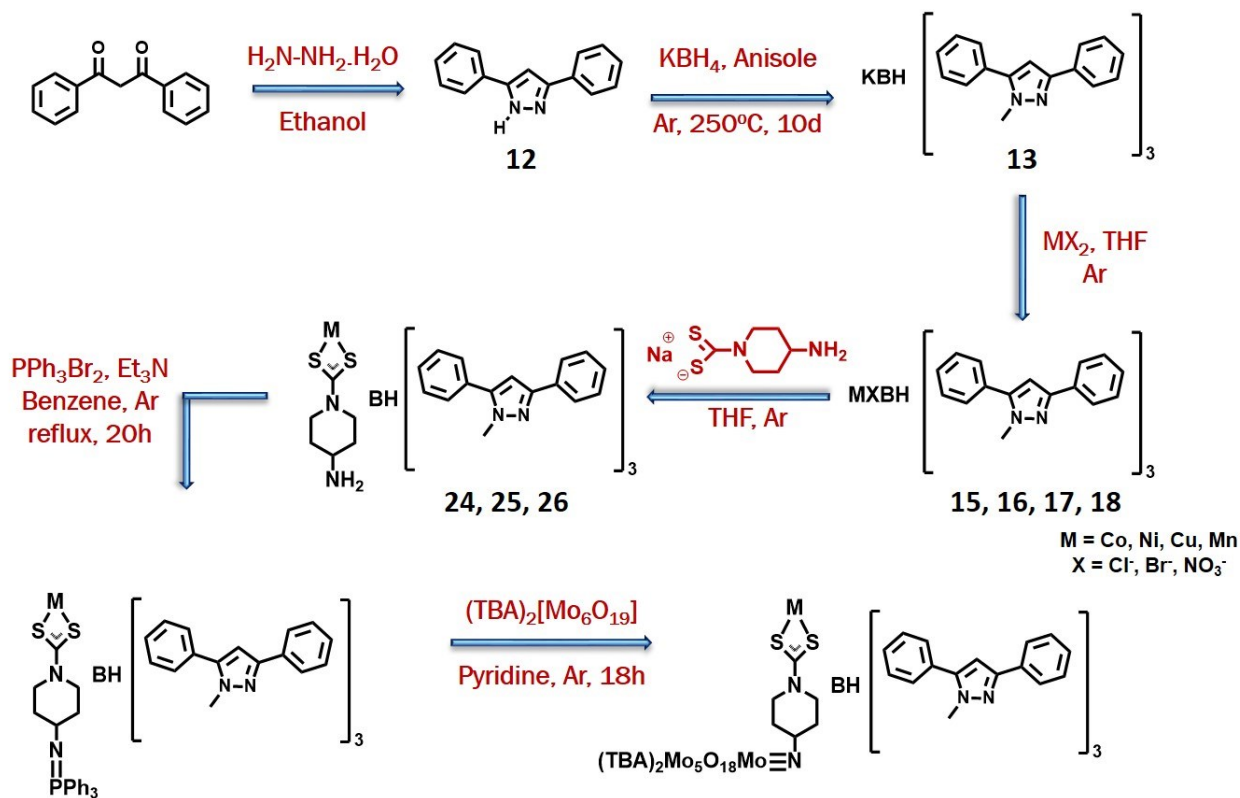


Figure 3.6 Synthetic scheme for metal complexes of tris(diphenylpyrazolyl)borate ligands as imidodelivery reagent.

3,5-dimethylpyrazole was commercially available so was used as such, while 3,5-diphenylpyrazole (**12**) was synthesized. **12** was prepared by a cyclization reaction between dibenzoylmethane and hydrazine hydrate following a literature procedure.²² These pyrazoles

were subsequently refluxed with KBH_4 in anhydrous anisole for 10 days.²³ The products were analyzed by ^1H NMR spectroscopy. With this reaction, there are different possibilities of products wherein all the products will lead to same ^1H NMR spectrum as only the pyrazolyl units will show up (Figure 3.7).

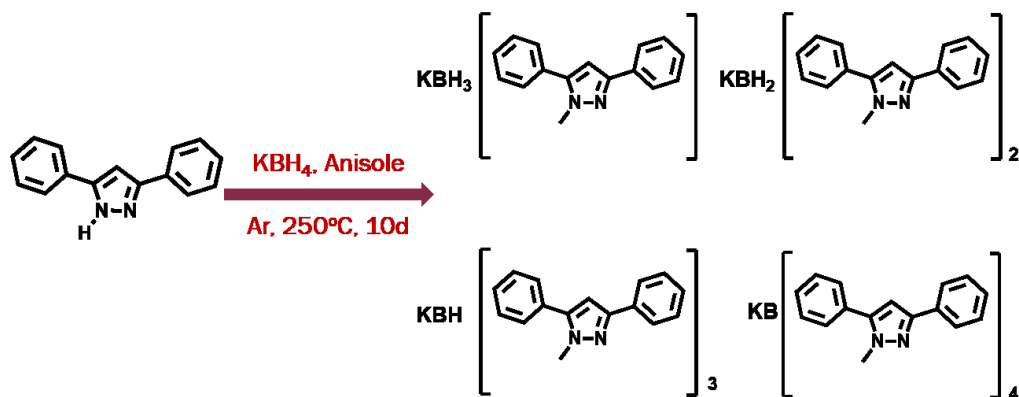


Figure 3.7 Possible products under the reaction conditions.

To gain more details on the structure, we tried to run some ^{11}B NMR experiments but the product showed a very broad peak. This observation can be attributed to the boron atom being attached to the pyrazole rings which results in an increased T_2 relaxation time, thus leading to peak broadening. Since, it was difficult to determine how many hydrogen atoms are attached to the boron atom, the ^{11}B NMR data was deemed to be inconclusive in determining the exact stoichiometry of the molecule. Even on mass analysis of the product, nothing is observed as only starting pyrazole unit was observed in the spectrum which could be due to the instability of the product under these conditions. Thus to provide more insight on the structure of the product, the crystals were grown in a desiccator under vacuum owing to the air sensitive nature of the product.

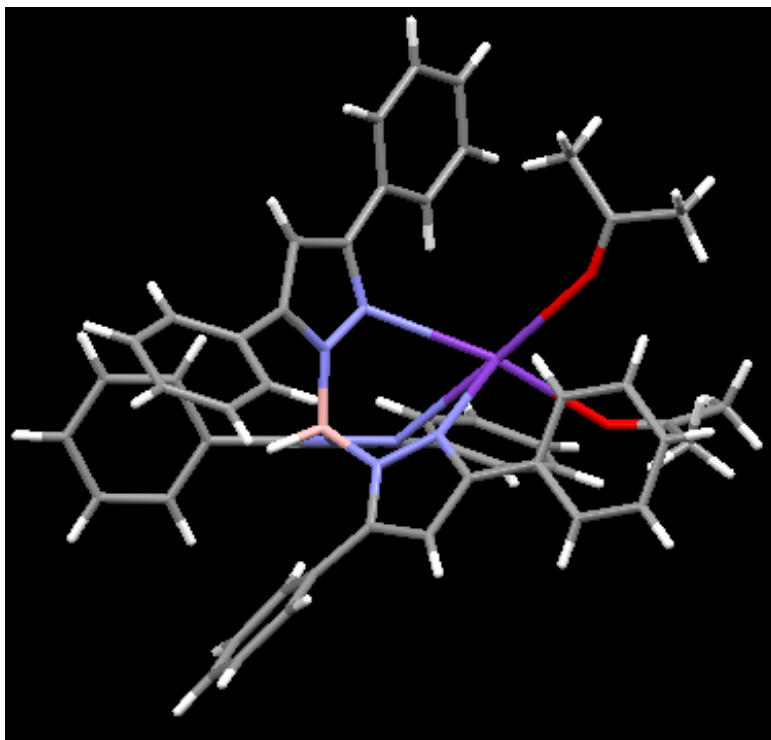


Figure 3.8 X-ray crystal structure of **13**.

The single crystal structure analyses of the metal complex confirmed it as the tris complex, **13**, wherein boron is tetrahedrally coordinated to three nitrogen atoms of three pyrazole moieties and one hydrogen atom (Figure 3.8). Potassium atom exhibits a penta-coordinated state, where it coordinates to the other three nitrogen atoms of the pyrazole units along with two acetone molecules, which was the solvent used to grow the crystals. Upon confirming the structure of the product, metal complexes were prepared subsequently.

3.3.2 Synthesis of metal complexes with 13 and 14

The subsequent metal complexes from **13** and **14** were prepared by reacting them with respective metal salts, MX_n ($\text{X} = \text{Cl}^-$, Br^- or NO_3^-) in anhydrous THF. The resulting metal complexes were analyzed by IR, UV-visible spectroscopy and single crystal X-ray diffraction.

3.3.2.1 Infrared analysis of metal complexes with 13 and 14

IR spectroscopic studies of **13** and **14** reveal a B–H stretch at 2529 and 2433 cm^{-1} indicative of a κ^3 -coordinated TpPh_2 and TpMe_2 ligand, respectively (Table 3.1). On metal coordination, this shifts to higher wave number in the complexes which are typical for other TpPh_2 ^{24,25} and TpMe_2 ²⁶ complexes reported.

Table 3.1 IR spectroscopic studies of metal complexes of **13** and **14**.

SNo.	Diphenyl pyrazole series	IR (ν_{BH}) cm^{-1}	SNo.	Dimethyl pyrazole series	IR (ν_{BH}) cm^{-1}
1	13	2529	1	14	2433
2	15	2610	2	20	2501
3	16	2613	3	21	2529
4	17	2606	4	22	2507
5	18	2614	5	23	2519
6	19	2617			

3.3.2.2 Electronic spectroscopy of metal complexes of **13** and **14**

The electronic spectra of the synthesized metal hydrotris(pyrazolyl)borates were recorded in CH_2Cl_2 . Both **15** and **20** exhibit blue color solutions showing three absorptions at 600, 639.4, 666.4 nm and 579.6, 632, 670.8 nm, respectively, which are typical of tetrahedrally coordinated cobalt.^{24,27} However, **16** and **21** are purple-pink in color and show four absorptions at 507, 584.2(sh), 829.4, 934.2 nm and 504.8, 581.2(sh), 815, 904.4 nm, respectively. These absorptions are assigned to spin-allowed (triplet) transition energies for idealized C_{3v} symmetry²⁸ typical of tetrahedral Ni(II) and compare well with previously reported complexes.²⁹ Additionally, **18** and **22** are green in color. Contrary to previous cases, copper ions in these complexes exist in penta-coordinated state as NO_3^- counter anion exists as nitrate ion, thus acting as a bidentate ligand. Two distinct bands observed in these complexes are at 301.8 (sh), 767.8 nm and 292.8 (sh) and 758.2 nm in respective diphenyl and dimethyl pyrazole copper complexes, which are characteristic of $d-d$ transitions of square-pyramidal or tetragonally elongated octahedral copper(II) complexes.³⁰

3.3.2.3 Single crystal X-ray structures of metal complexes of **13** and **14**

3.3.2.3.1 Crystal structure of $\text{CuNO}_3\text{BH}[\text{tris}(3,5\text{-diphenylpyrazole})]$

Dark green crystals of **18** were obtained in anhydrous THF. Similar to the crystal structure of **13**, the analysis of these crystals shows a tetra-coordinated boron atom coordinated to three pyrazole units and a hydrogen atom (Figure 3.9). The copper atom sits in a distorted penta-coordinated pocket, wherein it coordinates to the other three nitrogen atoms of the

pyrazole units, while the other two sites are occupied by nitrate ligand coordinated through two oxygen atoms. Two THF solvent molecules are also present in the crystal lattice, where one of the THF molecules is disordered. The structure clearly displays the presence of a nitrate ligand, which can readily be displaced by dithiocarbamate ligand in the next step.

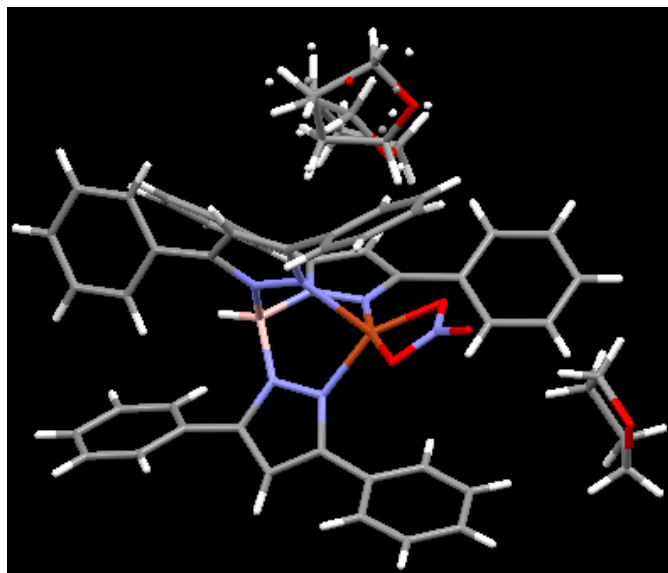


Figure 3.9 X-ray crystal structure of **18**.

3.3.2.3.2 Crystal structure of $Mn[BH(3,5\text{-dimethylpyrazole})_3]_2$

Another crystal structure that was obtained was of the metal complex **23**. Attempts to prepare **23** with equivalent amounts of **14** and manganese(II) chloride resulted in the formation of a bis-complex (Figure 3.10). Transparent crystals were obtained in CH_2Cl_2 upon solvent evaporation. The single crystal structure analysis shows the manganese atom occupying an octahedral pocket, wherein it coordinates to two pyrazole ligands. Within each ligand, the manganese atom is coordinated to three nitrogen atoms of three pyrazole units, thus resulting in a hexa-coordinated arrangement. This suggests that bis-complexation is preferred over $MnClBH[tris(3,5\text{-dimethylpyrazole})]$ synthesis. Since the complex does not have any Cl^- ligands for substitution by dithiocarbamate ligand, it could not be used in further reactions.

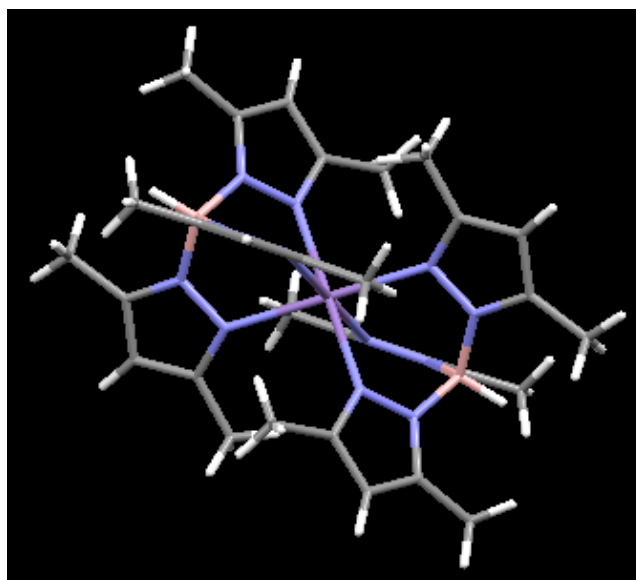


Figure 3.10 X-ray crystal structure of 23.

3.3.3 Synthesis of metal dithiocarbamate complexes of tris(3,5-diphenylpyrazole)borates and tris(3,5-dimethylpyrazole)

After analyzing all the metal complexes, Co, Ni and Cu complexes were further used for ligand substitution reaction by dithiocarbamates. The metal dithiocarbamate complexes based on pyrazole backbone were typically prepared by stirring solutions of respective metal complexes in THF with solution of **2** in minimum amount of water. The resulting pyrazole based metal dithiocarbamate complexes were further analyzed by IR and UV-visible spectroscopy.

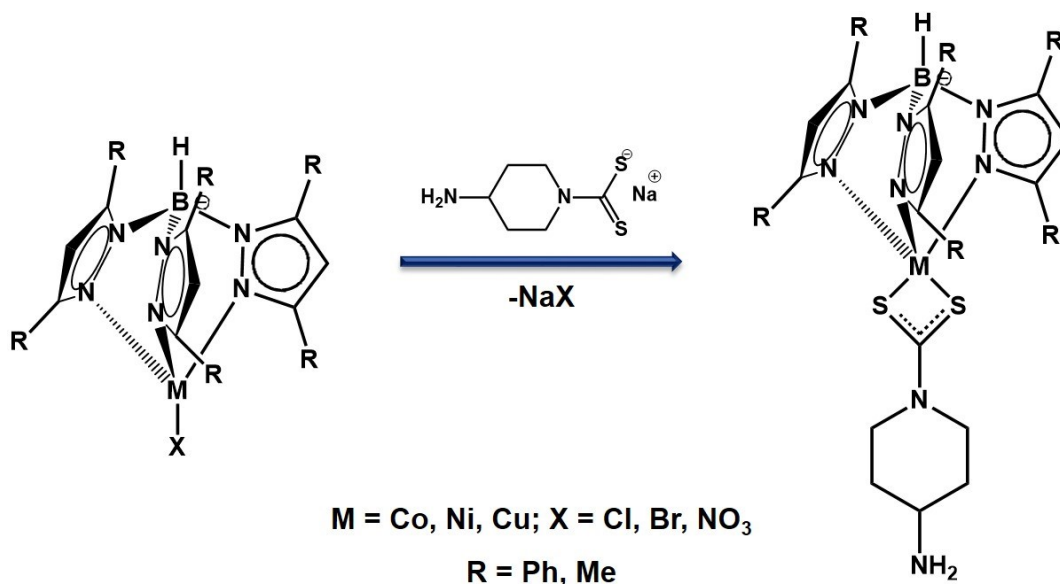


Figure 3.11 Reaction of metal pyrazolylborate complexes with 2.

3.3.3.1 Infrared analysis of metal dithiocarbamate complexes of tris(3,5-diphenylpyrazole)borates and tris(3,5-dimethylpyrazole)borates

IR spectroscopic studies of metal dithiocarbamate complexes of tris(3,5-diphenylpyrazole)borates and tris(3,5-dimethylpyrazole)borates reveal a B–H stretch around 2600 cm⁻¹ and 2500 cm⁻¹ indicative of a κ^3 -coordinated TpPh₂ and TpMe₂ ligand, respectively (Table 3.2).

Table 3.2 IR spectroscopic studies of metal dithiocarbamate complexes of tris(3,5-diphenylpyrazole)borates and tris(3,5-dimethylpyrazole)borates.

SNo.	Diphenylpyrazole DTC complexes	IR (ν_{BH}) cm ⁻¹	SNo.	Dimethylpyrazole DTC complexes	IR (ν_{BH}) cm ⁻¹
1	24	2623	1	27	2501
2	25	2612	2	28	2506
3	26	2597	3	29	2501

3.3.3.2 Electronic spectroscopy of metal dithiocarbamate complexes of tris(3,5-diphenylpyrazole)borates and tris(3,5-dimethylpyrazole)

UV-Vis spectra of these complexes were also recorded in CH₂Cl₂. Both **24** and **27** exhibit two absorptions in the spectra at 406.6, 565 nm and 484.4, 645.2, respectively. The former of these bands with a larger molar extinction coefficient can be assigned to sulfur-to-Co(II) LMCT band,^{19,31} while the other band can be correlated to *d-d* transitions in a five-coordinate complex. The analogous nickel dithiocarbamates, **25** and **28**, feature absorption peaks at 371.8(sh), 426.8, 656.8 nm and 401.6(sh), 421, 647.6 nm, respectively. The shoulders and bands in the UV-vis spectrum between 426 and 429 nm are indicative of sulfur-to-Ni(II) LMCT bands,^{19,32} wherein the shoulder corresponds to a S–Ni $\sigma\text{-}\sigma^*$ transition while other lower energy bands are caused by the S–metal π bond which compares well with the assignments made by Fujisawa et al.³³ Additional bands around 650 nm are present due to *d-d* transitions in metal complexes. Further in **26** and **29**, similar two absorption features were observed in the spectra at 419.8, 654 nm and 396, 694 nm, respectively. The former of the two bands is associated with large extinction coefficients and thus can be assigned to sulfur-to-Cu(II) LMCT bands. On the other hand, bands at 654 and 684, respectively, being lower in energy can be assigned to *d-d* transitions in Cu(II) complexes. Overall, the spectra are consistent with five-coordinate, high spin M(II) complexes.

3.3.4 Attempts to prepare POM hybrids with metal dithiocarbamate complexes of tris(3,5-diphenylpyrazole)borates and tris(3,5-dimethylpyrazole)borates

The solubility of prepared metal dithiocarbamate complexes of hydrotris(pyrazolyl)borates were observed to be greatly enhanced in organic solvents such as tetrahydrofuran, dichloromethane, acetone, acetonitrile and benzene. Thus, first synthesis of phosphineimine derivatives of these complexes were attempted.³⁴ To our surprise, an instant colored precipitation was observed when PPh_3Br_2 was mixed with the solution of these complexes. The reaction mixture was still refluxed with the hope that the resulting precipitate might dissolve at refluxing temperatures and some color changes might occur but no such changes could be observed. This could be attributed to the strong oxidizing nature of PPh_3Br_2 which may lead to some structural changes in these hydrotris(pyrazolyl)borates.

Furthermore, direct coordination with hexamolybdate were also attempted with metal dithiocarbamate complexes of hydrotris(pyrazolyl)borates following Peng's route³⁵ but unfortunately, a similar precipitation on refluxing were observed in these cases as well. The characteristic band in the IR spectra were also not observed. Similar to the above case, hexamolybdate also exhibits a strong oxidizing effect, which might lead to some structural changes in these hydrotris(pyrazolyl)borates.

3.4 Conclusions

To overcome the road block of poor solubility of metal dithiocarbamate complexes (Chapter-2), we synthesized potassium tris(3,5-diphenylpyrazole)borates and tris(3,5-dimethylpyrazole)borates and a series of corresponding metal ($\text{M} = \text{Co}, \text{Ni}, \text{Cu}, \text{Mn}$) complexes of tris(3,5-diphenylpyrazole)borates and tris(3,5-dimethylpyrazole)borates. All these complexes were characterized by infrared, UV-visible spectroscopy and X-ray diffraction. Further, a series of the respective metal dithiocarbamate complexes of these hydrotris(pyrazolyl)borates were prepared using sodium 4-aminopiperidyl dithiocarbamate and were characterized by infrared and UV-visible spectroscopy. All these metal dithiocarbamates exhibited a tremendous improvement in solubility in organic solvents, thus our secondary goal of enhancing the solubility was achieved. Thereafter, we attempted to covalently graft these complexes onto the hexamolybdate cluster. Regretfully, owing to the strong oxidizing nature of PPh_3Br_2 and hexamolybdate, we could not achieve our primary goal of synthesizing the polyoxometalate hybrids.

References

-
- ¹ Trofimenko, S. *J. Am. Chem. Soc.* **1966**, *88*, 1842.
- ² S. Trofimenko, *Scorpionates: The Coordination Chemistry of Polypyrazolylborate Ligands*, Imperial College Press, London, 1999.
- ³ McCleverty, J. A.; Meyer, T. J. *Comprehensive Coordination Chemistry II From biology to nanotechnology*, Volume 1: Fundamentals: Ligands, Complexes, Synthesis, Purification, and Structure, Elsevier Pergamon, 2003.
- ⁴ Akita, M.; Hikichi, S. *Bull. Chem. Soc. Jpn.* **2002**, *75*, 1657.
- ⁵ Malbosc, F.; Kalck, P.; Daran, J.-D.; Etienne, M. *J. Chem. Soc., Dalton Trans.* **1999**, 271; Paneque, M.; Sirol, S.; Trujillo, M.; Gutiérrez-Puebla, E.; Monge, M. A.; Carmona, E. *Angew. Chem., Int. Ed.* **2000**, *39*, 218; Takahashi, Y.; Akita, M.; Hikichi, S.; Moro-oka, Y. *Organometallics* **1998**, *17*, 4884.
- ⁶ (a) Trofimenko, S. *Acc. Chem. Res.* **1971**, *4*, 17; (b) Trofimenko, S. *Chem. Rev.* **1993**, *93*, 943; (c) Parkin, G. *Adv. Inorg. Chem.* **1995**, *42*, 291; (d) Kitajima, N.; Tolman, W. B. *Prog. Inorg. Chem.* **1995**, *43*, 418
- ⁷ (a) Curtis, M. D.; Shiu, K. B.; Butler, W. M. *J. Am. Chem. Soc.* **1986**, *108*, 1550; (b) Curtis, M. D.; Shiu, K. B.; Butler, W. M.; Huffman, J. C. *J. Am. Chem. Soc.* **1986**, *108*, 3335.
- ⁸ Edelmann, F. T. *Angew. Chem. Int. Ed.* **2001**, *40*, 1656.
- ⁹ (a) Byers, P. K.; Canty, A. J.; Honeyman, R. T. *Adv. Organomet. Chem.* **1992**, *34*, 1; (b) McCleverty, J. A.; Ward, M. D. *Acc. Chem. Res.* **1998**, *31*, 842.
- ¹⁰ Santos, S.; Marques, N. *New J. Chem.* **1995**, *19*, 551.
- ¹¹ Ward, M. D.; McCleverty, J. A.; Jeffery, J. C. *Coord. Chem. Rev.* **2001**, *222*, 251.
- ¹² (a) Vahrenkamp, H. *Acc. Chem. Res.* **1999**, *32*, 589; (b) Kremer-Aach, A.; Kläui, W.; Bell, R.; Strerath, A.; Wunderlich H.; Mootz, D. *Inorg. Chem.* **1997**, *36*, 1552; (c) Jacobsen, F. E.; Breece, R. M.; Myers, W. K.; Tierney, D. L.; Cohen, S. M. *Inorg. Chem.* **2006**, *45*, 7306; (d) Han, R.; Looney, A.; McNeill, K.; Parkin, G.; Rheingold, A. L.; Haggerty, B. S. *J. Inorg. Biochem.* **1993**, *49*, 105; (e) Bergquist, C.; Fillebeen, T.; Morlok, M. M.; Parkin, G. *J. Am. Chem. Soc.* **2003**, *125*, 6189.
- ¹³ Kitajima, N.; Fujisawa, K.; Fujimoto, C.; Moro-oka, Y.; Hashimoto, S.; Kitagawa, T.; Toriumi, K.; Tatsumi, K.; Nakamura, A. *J. Am. Chem. Soc.* **1992**, *114*, 1277.
- ¹⁴ Chen, P.; Fujisawa, K.; Solomon, E. I. *J. Am. Chem. Soc.* **2000**, *122*, 10177.
- ¹⁵ Randall, D. W.; George, S. D.; Hedman, B.; Hodgson, K. O.; Fujisawa, K.; Solomon, E. I. *J. Am. Chem. Soc.* **2000**, *122*, 11620.
- ¹⁶ Slugovc, C.; Padilla-Martinez, I.; Sirol, S.; Carmona, E. *Coord. Chem. Rev.* **2001**, *213*, 129.
- ¹⁷ (a) Shirasawa, N.; Nguyet, T. T.; Hikichi, S.; Moro-oka Y.; Akita, M. *Organometallics* **2001**, *20*, 3582; (b) Shirasawa, N.; Akita, M.; Hikichi, S.; Moro-oka, Y. *Chem. Commun.* **1999**, 417; (c) Yoshimitsu, S.; Hikichi, S.; Akita, M. *Organometallics* **2002**, *21*, 3672; (d) Akita, M. *J. Organomet. Chem.* **2004**, *689*, 4540.
- ¹⁸ Ma, H.; Wang, G.; Yee, G. T.; Petersen, J. L.; Jensen, M. P. *Inorg. Chim. Acta* **2009**, *362*, 4563.
- ¹⁹ Harding, D. J.; Harding, P.; Dokmaisrijana, S.; Adams, H. *Dalton Trans.* **2011**, *40*, 1313.

-
- ²⁰ Klemperer, W. G.; Ginsberg, A. P. Introduction to Early Transition Metal Polyoxoanions, *Inorganic Syntheses*, Volume 27, John Wiley & Sons, Inc., 2007.
- ²¹ Fujisawa, K.; Miyashita, Y.; Yamada, Y.; Okamoto, K-I *Bull. Chem. Soc. Jpn.* **2001**, 74, 1065.
- ²² Kitajima, N.; Fujisawa, K.; Fujimoto, C.; Moro-oka, Y.; Hashimoto, S.; Kitagawa, T.; Toriumi, K.; Tatsumi, K.; Nakamura, A. *J. Am. Chem. Soc.* **1992**, 114, 1277.
- ²³ Huang, J.; Lee, L.; Haggerty, B. S.; Rheingold, A. L.; Waiters, M. A. *Inorg. Chem.* **1995**, 34, 4268.
- ²⁴ Harding, D. J.; Harding, P.; Daengngern, R.; Yimklanb, S.; Adams, H. *Dalton Trans.* **2009**, 1314.
- ²⁵ Harding, D. J.; Harding, P.; Adams, H.; Tuntulani, T. *Inorg. Chim. Acta* **2007**, 360, 3335.
- ²⁶ Beheshti, A.; Clegg, W.; Dale, S. H.; Hyvadi, R. *Acta Cryst. Sec. C* **2009**, C65, m314.
- ²⁷ A. B. P. Lever, in *Inorganic Electronic Spectroscopy*, Elsevier, Amsterdam, 2nd edn, 1984, pp. 376.
- ²⁸ Desrochers, P. J.; Telser, J.; Zvyagin, S. A.; Ozarowski, A.; Krzystek, J.; Vivic, D. A. *Inorg. Chem.* **2006**, 45, 8930.
- ²⁹ Desrochers, P. J.; LeLievre, S.; Johnson, R. J.; Lamb, B. T.; Phelps, A. L.; Cordes, A. W.; Gu, W.; Cramer, S. P. *Inorg. Chem.* **2003**, 42, 7945.
- ³⁰ Kumar, U.; Chandra, S. *J. Saudi Chem. Soc.* **2011**, 15, 187; Martens, C. F.; Schenning, A. P. H. J.; Feiters, M. C.; Berens, H. W.; van der Linden, J. G. M.; Admiraal, G.; Beurskens, P. T.; Kooijman, H.; Spek, A. L.; Nolte, R. J. M. *Inorg. Chem.* **1995**, 34, 4735; Bernhardt, P. V.; Hayes, E. *J. Chem. Soc. Dalton Trans* **1998**, 1037.
- ³¹ Jacobsen, F. E.; Breece, R. M.; Myers, W. K.; Tierney, D. L.; Cohen, S. M. *Inorg. Chem.* **2006**, 45, 7306.
- ³² Ma, H.; Chattopadhyay, S.; Petersen, J. L.; Jensen, M. P. *Inorg. Chem.* **2008**, 47, 7966.
- ³³ Fujisawa, K.; Kakizaki, T.; Miyashita, Y.; Okamoto, K. *Inorg. Chim. Acta* **2008**, 361, 1134.
- ³⁴ Bestmann, H. J.; Fritzsche, H. *Chem. Ber.* **1961**, 94, 2477.
- ³⁵ Wei, Y.; Xu, B.; Barnes, C. L.; Peng, Z. *J. Am. Chem. Soc.* **2001**, 123, 4083.

Chapter 4 - Bimetallic hexamolybdate systems based on the pyridyl group

4.1 Pyridine

Coordination chemistry provides both qualitative and quantitative analysis of metals, which in turn plays an important role in the treatment, management and diagnosis of diseases, hence, it is of great significance in the field of medicine. Coordination compounds bearing metal-nitrogen bonds have always been the center of attention, as many of the naturally occurring molecules such as chlorophyll and haemoglobin have similar coordination spheres. Hence, the study of *N*-based metal complexes is of immense use in biochemistry as well as in antioxidants, oil additives, colouring agents for plastics, and pesticides.¹

Amongst the *N*-based ligands, pyridyl based compounds are an important class due to their growing applications in medicinal drugs and in agricultural products such as herbicides, insecticides, fungicides, and plant growth regulators.¹ The structure of pyridine is similar to that of benzene and can be described as a six-membered heterocyclic ring consisting of five carbon atoms and one nitrogen atom. Since the ring nitrogen is more electronegative than the ring carbons, it makes the two-, four-, and six-ring carbons more electropositive which is different, when compared to benzene (Figure 4.1).¹

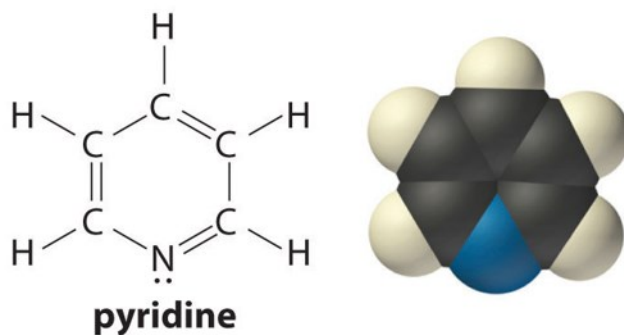


Figure 4.1 Structure of pyridine.

The lone pair electrons on the nitrogen atom are not involved in resonance of the ring π -electron system and thus, are accessible which in turn makes pyridine a weak organic base ($pK_a = 5.22$).¹ As a result, they can undergo typical reactions of a weak base such as protonation, alkylation and acylation. In metal complexation, pyridine can either act as a π or σ ligand, where σ

electron donation predominates. This behavior is attributed to the dipole structure of pyridine, where the electron density is localized on the nitrogen atom, and hence is easily accessible for donation to the central metal atom in the resultant complex.¹ Changing the environment around the pyridyl ligand can alter the coordination sphere around the metal atom in the metal complex (Figure 4.2).²

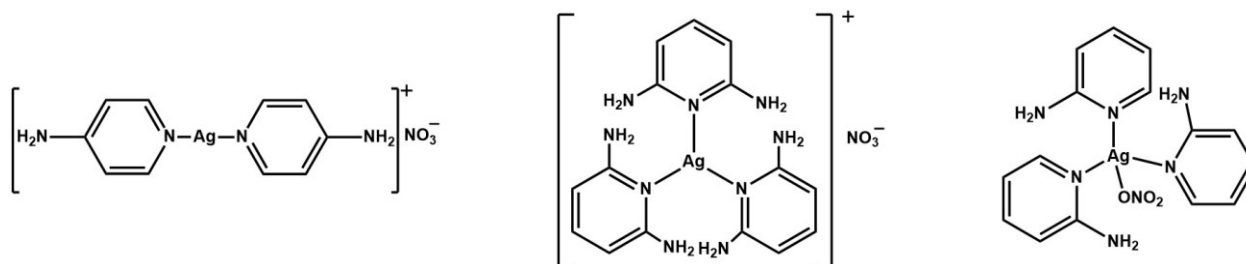


Figure 4.2 Change in the coordination environment upon modification of the pyridyl ligand.²

4.1.1 Self-assembled polyoxometalate hybrids bearing the pyridyl group

Exploiting the concept of reversible transformations in coordination complexes and their versatile coordination environments, has led to the emergence of coordination chemistry as an important tool in designing versatile self-assembled systems. Predictable and rational designing of such systems is applicable in analytical chemistry and material science. As mentioned in the previous chapters, POMs are a class of inorganic compounds possessing interesting properties. The self-assembled POM arrays bearing organic moieties combine the properties of the coordination complexes (optical, redox) with those of the POM cluster, thus offering synergistic effects in these organic-inorganic hybrids.³

Combining the concepts of metallocupramolecular chemistry with organic-inorganic hybrids, Hasenknopf *et al.* recently reported a hybrid based on bis(pyridine-trisalkoxo)-hexavanadate and $[\text{PdCl}_2(\text{CH}_3\text{CN})_2]$, which exhibited a trimeric architecture (Figure 4.3).⁴

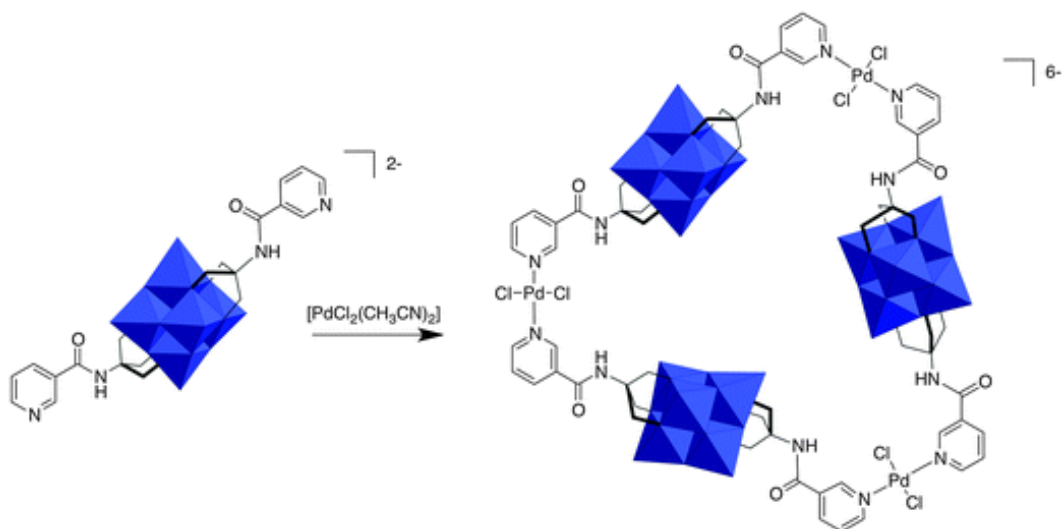


Figure 4.3 Self-assembled trimer based on bis(pyridine-trisalkoxo)-hexavanadate and $[\text{PdCl}_2(\text{CH}_3\text{CN})_2]$.⁴

Molecular switches are capable of switching between two or more states in response to an external stimuli, such as change in pH, light, temperature, redox potential, electric field or the presence/absence of ligands or metal ions. A Dawson-type POM linked by a 2,2'-bipyridine unit is the first reported example of a metal-ion driven molecular switch, $\text{TBA}_{10}\text{H}_2[\{\text{P}_2\text{V}_3\text{W}_{15}\text{O}_{59}(\text{OCH}_2)_3\text{NHCO}\}_2(\text{C}_5\text{H}_3\text{N})_2]$, and demonstrates a fully reversible switching process upon the coordination of Zn^{2+} cations (Figure 4.4).⁵ This switching process is believed to mimic the behavior of metal ion-directed folding and assembly of proteins.

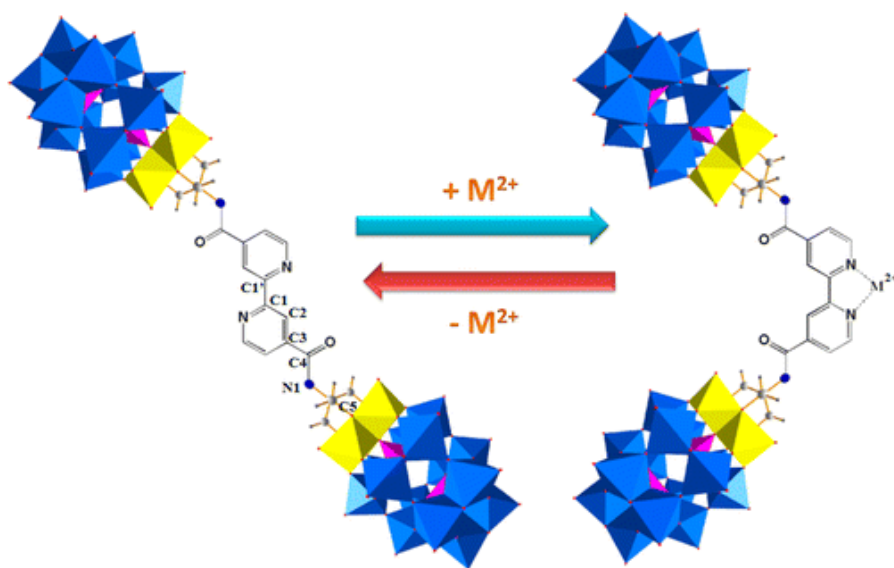


Figure 4.4 A molecular switch based on POM-hybrid.⁵

4.1.2 Organoimido hexamolybdate derivatives bearing the pyridyl group

In theory, the use of highly substituted functionalized hexamolybdates as “building blocks” and metal coordination as a “supramolecular glue” can lead to the design of highly ordered structures exhibiting unique physical, chemical and electronic properties. Thus, it is important to design and synthesize hexamolybdate derivatives bearing one or more of these organoimido ligands with remote functionalities capable of coordinating to metal ions. Furthermore, such hybrid materials can lead to more elaborate supramolecular architectures with favorable properties (Figure 4.5).

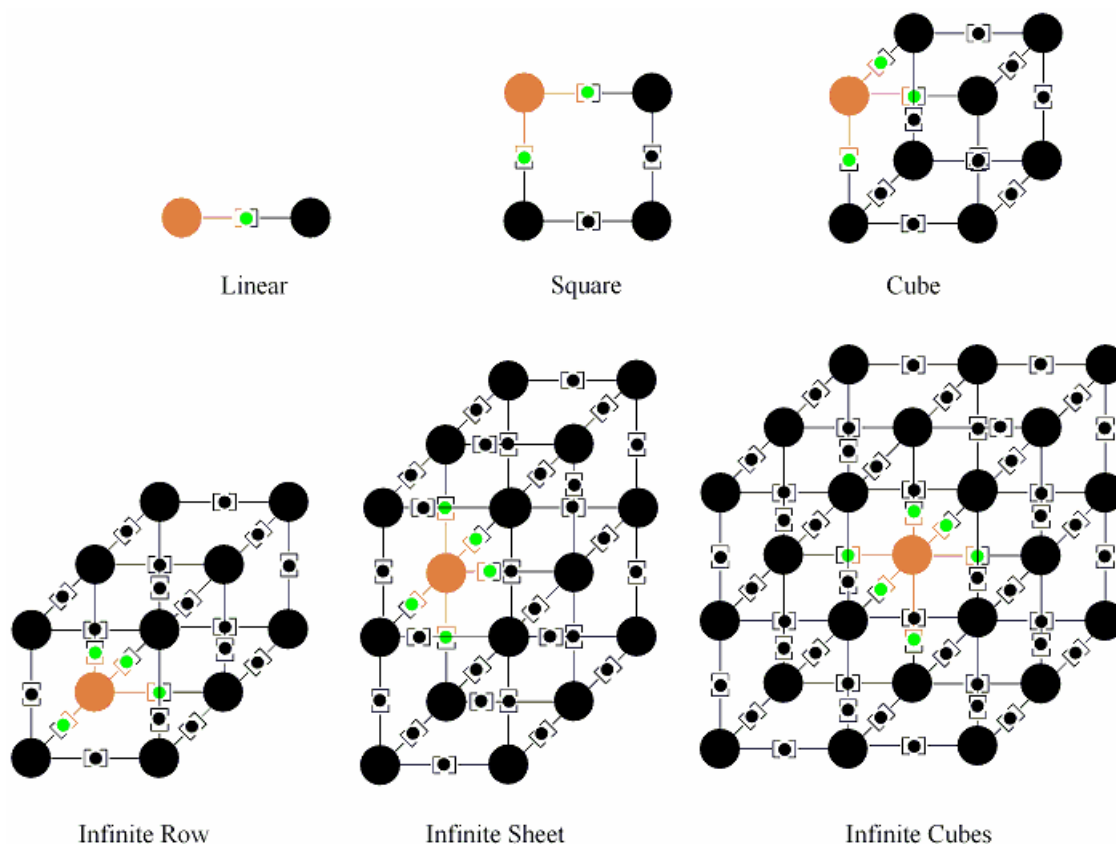


Figure 4.5 Possible extended supramolecular architectures resulting from bimetallic organoimido hexamolybdates.

Several attempts to synthesize hexamolybdate-based organoimido derivatives containing the pyridyl moiety as a pendant have been made (Figure 4.6).⁶

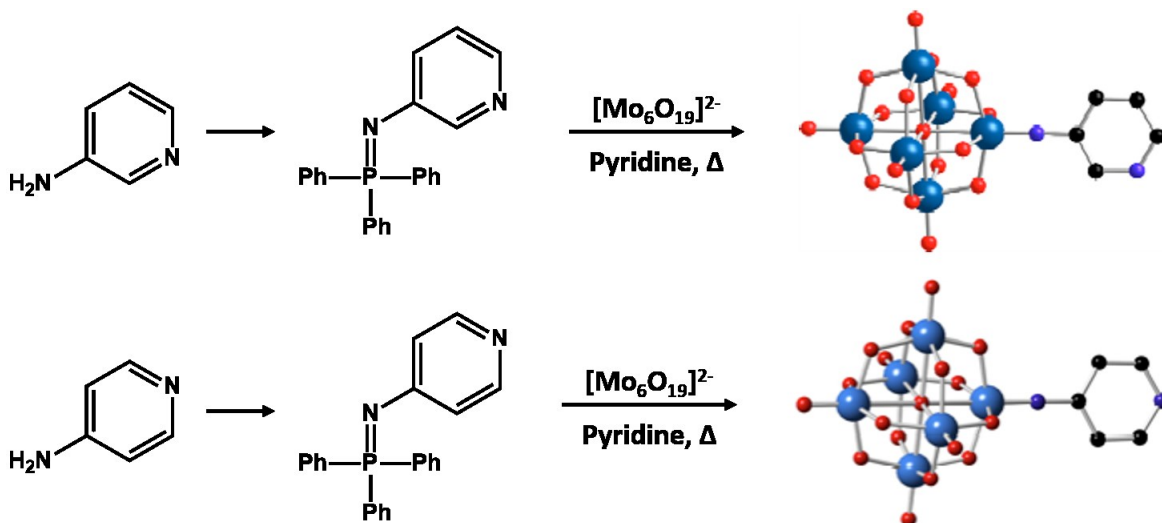


Figure 4.6 Synthesis of pyridyl based imido-hexamolybdates.⁶

These derivatives were readily prepared but metal complexation studies revealed that these systems were incompetent donors as no metal coordination could be observed.⁶ This can be attributed to the electron withdrawing nature of the hexamolybdate cluster owing to the high oxidation state (+6) of the six molybdenum atoms in the cluster, which in turn pulls the electron density away from the conjugated pyridyl ring, thus rendering it less basic and incapable of metal coordination (Figure 4.7).

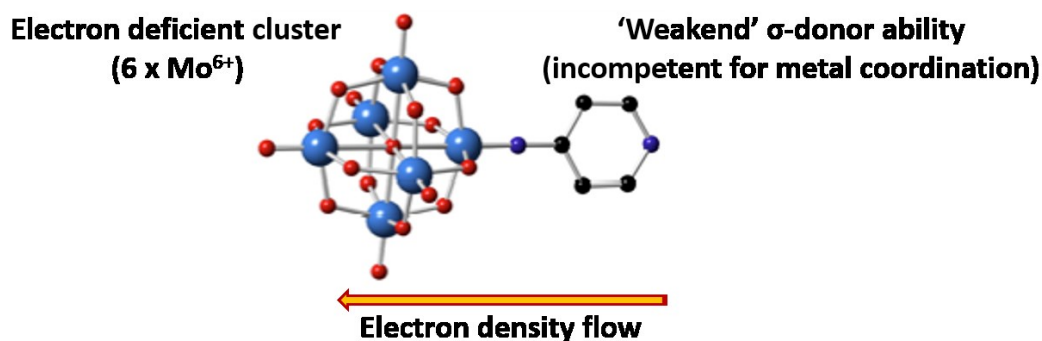


Figure 4.7 Reason for incompetency of pyridylimido hexamolybdate hybrid for metal coordination.⁶

To overcome the “electron-sponge” behavior of hexamolybdate and in turn increase the electron density at the organoimido substituent, placing an electron donating group on the pyridyl ring can be a viable alternative. This concept was explored by C. Moore,⁶ wherein they synthesized *p*-methoxy-*m*-pyridylimido-hexamolybdate (Figure 4.8). The electron donating methoxy group was added to the pyridyl ring for increasing the electron density of the ring.

Moreover, its *para* position on the ring was carefully chosen to create a bidentate pocket for metal coordination. Metal complexation studies revealed no coordination, which suggests that the electron density on the pyridyl ring is not significantly enhanced for metal coordination, upon the addition of a methoxy group.⁶

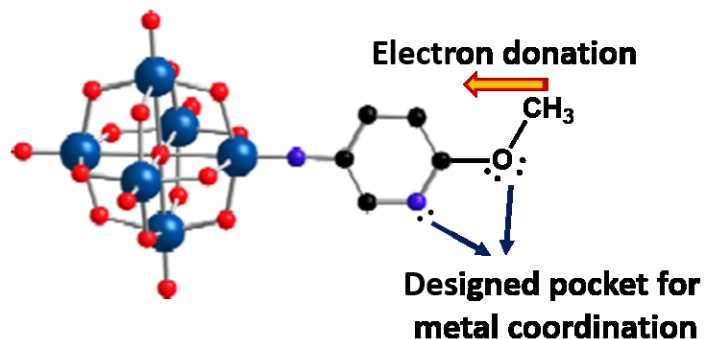


Figure 4.8 Adding electron donating group for improving the σ -donor ability of pyridylimido hexamolybdate.⁶

As mentioned in section 1.4, another method for improving the σ -donor ability is to add a spacer group, while maintaining a conjugated system. This concept was explored by K. Mijares,⁷ where pyrimidylphenyl reagents were attached as organoimido ligands to the hexamolybdate cluster (Figure 4.9). Preliminary results indicated a good σ -donor ability towards ruthenium, but the yields were found to be low.

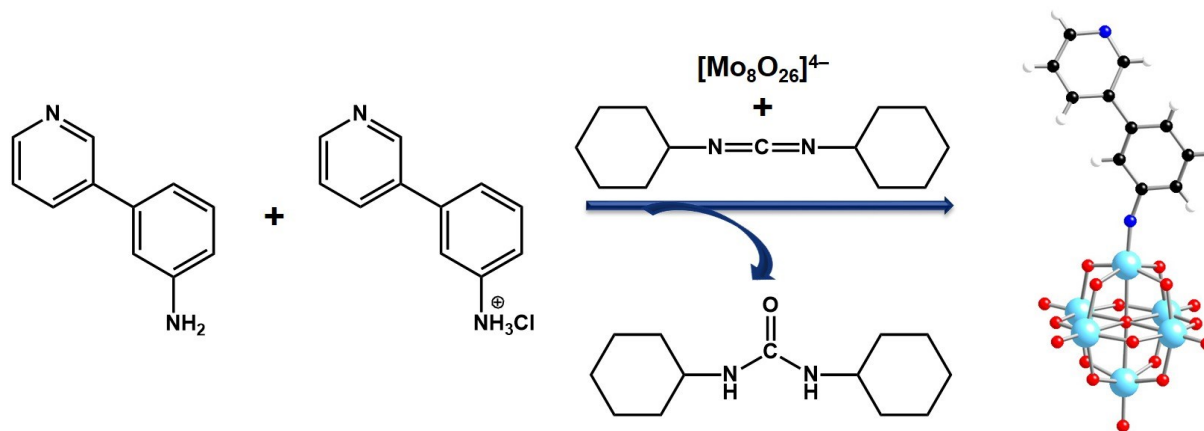


Figure 4.9 Synthesis of 3-(pyridin-3-yl)phenylimido hexamolybdate.⁷

Furthermore, in an attempt to prepare a hexamolybdate derivative with 1,10-phenanthroline-5-amine as the organoimido ligand, cluster rearrangement was observed (Figure 4.10). This indicates that a delicate pH balance exists and careful planning is required when designing the synthesis of novel hexamolybdate derivatives to avoid such rearrangements.

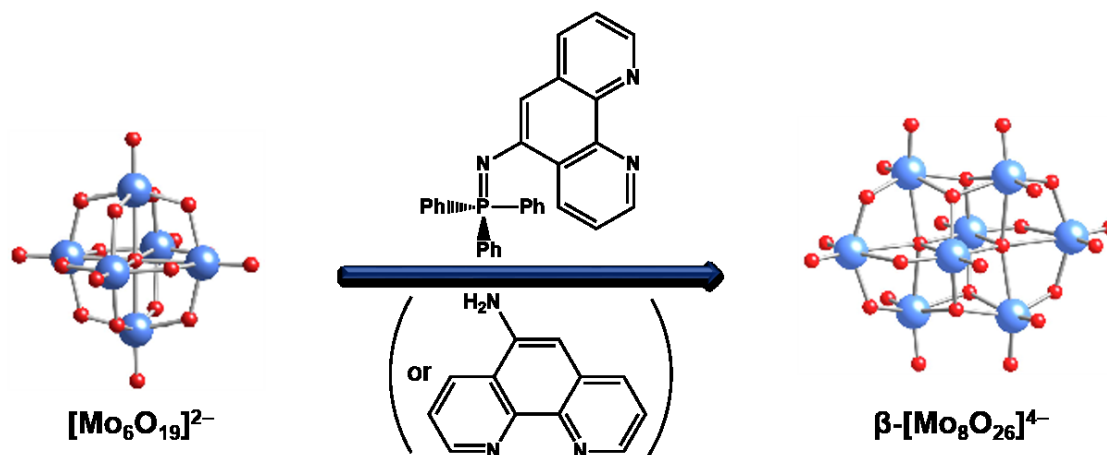


Figure 4.10 POM cluster rearrangement observed upon use of 1,10-phenanthroline-5-amine as the organoimido delivery reagent.

There are a few examples of organoimido functionalized hexamolybdates demonstrating the ability to coordinate to metals *via* a covalently bound remote functionality. One of the earliest POM hybrid was reported by Maatta *et al.*,⁸ wherein iron (II) was coordinated to the hexamolybdate cluster *via* the cyclopentadienylimido ligand, thus resulting in ferrocenylimido-hexamolybdate (Figure 4.11).

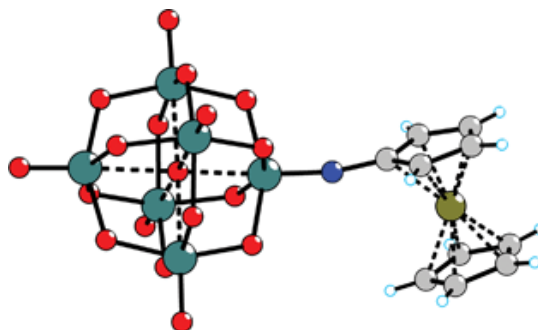


Figure 4.11 Ferrocenylimido-hexamolybdate metal complex.⁸

Another successful organoimido hexamolybdate hybrid was synthesized by Peng and Wei *et al.*,⁹ where the hexamolybdate cluster was difunctionalized with two terpyridyl units linked *via* extended π -conjugated bridges. The POM hybrid complexed with iron (II) ions resulting in the formation of a coordination polymer (Figure 4.12).

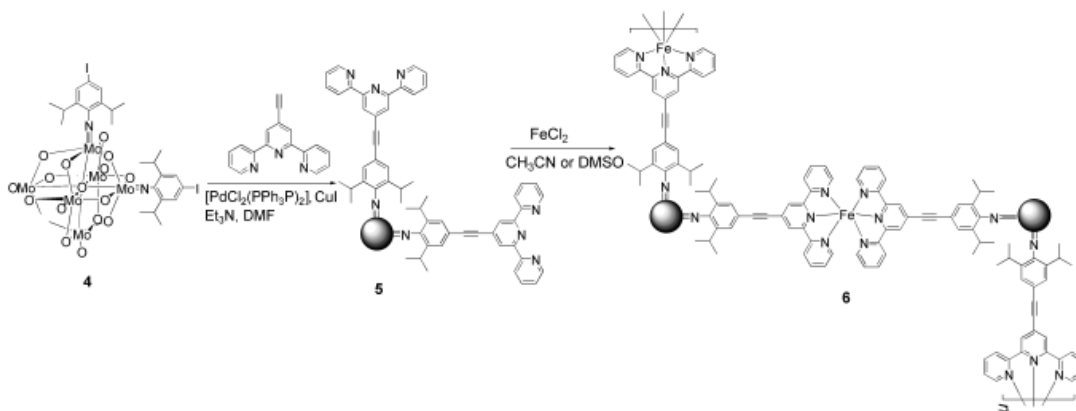


Figure 4.12 Synthesis of a coordination polymer based on organoimido hexamolybdate.⁹

As highlighted above, there are only a handful of existing studies on these organoimido POM hybrids that show successful metal coordination to the POM cluster. Thus, it is important to investigate such systems as they may lead to extended architectures, wherein the pyridyl pendant acts as a donor and the hexamolybdate cluster serves as an electron acceptor site, thus demonstrating the capability for electron- and energy-transfer. In this chapter, we are extending the work on organoimido hexamolybdate derivatives bearing a remote functionality for metal coordination by;

- Designing new pyridyl based organoimido delivery reagents for attaching to the hexamolybdate cluster in a bid to assemble bimetallic organic-inorganic hybrids.
- Synthesizing and characterizing new organoimido delivery reagents *via* two different routes [aryl amine (Ar-NH₂) and phosphineimine (R-N=PPh₃)].
- Attaching the synthesized organoimido delivery reagents to the hexamolybdate cluster.
- Attempting to coordinate the synthesized organic-inorganic POM hybrids to a second metal atom.

4.2 Experimental

(TBA)₂[Mo₆O₁₈] and (TBA)₄[Mo₈O₂₆] were prepared according to literature methods.¹⁰ All other starting materials and Pd(II) catalyst were purchased from Sigma Aldrich, TCI America, Matrix Scientific or Fisher Scientific. Silica gel was purchased from AnalTech (150 Å pore). Solids were dried under vacuum at 40 °C for 24 hours prior to use. All manipulations were done under an inert atmosphere of argon, unless otherwise stated. Tetrahydrofuran (THF) was

distilled over sodium; dichloromethane was dried over P₂O₅ and distilled; and triethylamine, diethylether and acetonitrile (CH₃CN) were dried over CaH₂ and distilled as needed. All glassware was thoroughly dried by flame under reduced pressure. ¹H, ¹³C and ³¹P NMR spectra were recorded on a Varian Unity plus 400 MHz spectrometer and were referenced to residual protonated solvent peaks (CDCl₃ = 7.27 ppm, CD₃CN = 1.94 ppm, D₂O = 4.80 ppm and DMSO-d₆ = 2.50 ppm). FT-IR spectra were recorded on a Nicolet 380 instrument. Melting points were determined on a Fisher-Johns melting point apparatus and are uncorrected.

4.2.1 Synthesis of 3,5-di(pyridin-2-yl)-4H-1,2,4-triazol-4-amine, 30¹³

2-Pyridinecarbonitrile (5g, 48.026 mmol), hydrazine dihydrochloride (5.041g, 48.026 mmol) and hydrazine hydrate (7.002 mL, 144.078 mmol) were taken in 24 mL diethylene glycol, and the resulting mixture was heated at 130 °C for 5 hours. Upon cooling the solution, 50 mL water was added and the resulting white precipitate was filtered off, washed with water, and dried in air. The ligand was recrystallized in ethanol and the product was obtained as a white crystalline solid. Yield: 9.37g (81.97%); mp 184-186°C (lit.¹³ 185-186°C); ¹H NMR (400 MHz, CDCl₃) δ ppm: 7.39 (s, 2 H), 7.89 (d, *J*=1.95 Hz, 2 H), 8.38 - 8.42 (m, 2 H), 8.52 (s, 2 H), 8.66 - 8.70 (m, 2 H).

4.2.2 Synthesis of 4-((trimethylsilyl)ethynyl)aniline, 31¹⁴

In a 500 mL round bottom flask fitted with stir bar, 300 mL of triethylamine was degassed and taken under argon atmosphere. To this, 4-iodoaniline (36 g, 164.36 mmol), copper (I) iodide (0.314 g, 1.644 mmol), dichlorobis(triphenylphosphine)palladium(II) (0.576 g, 0.8218 mmol) were added. The reaction mixture was degassed again and was kept under argon atmosphere again. To this, trimethylsilylacetylene (25 mL, 175.88 mmol) was added and the reaction mixture was stirred at room temperature for 2d. After this, the solvent was removed from the reaction mixture under vacuum. The slurry was redissolved in 200 mL chloroform and was washed with 2M ammonium chloride solution (2x 200 mL) and further with 100 mL 1M sodium chloride solution. The solvent was removed from the organic layer to obtain the product. Yield: 30.37g (97.56%); ¹H NMR (400 MHz, CDCl₃) δ ppm: 0.12 - 0.33 (m, 9 H) 3.79 (br. s., 2 H) 6.58 (d, *J*=8.33 Hz, 2 H) 7.29 (s, 2 H).

4.2.3 Synthesis of 4-ethynylaniline, **32**¹¹

In a 500 mL Erlenmeyer flask, **31** (16 g, 86.25 mmol) was dissolved in 250 mL methanol. To this, potassium carbonate (17.89 g, 129.38 mmol) was added and the reaction mixture was stirred overnight at room temperature. The organics were separated using chloroform (3x 100 mL) and further washed with brine (200 mL) and dried over sodium sulfate. The solvent was then removed under vacuum to yield product. Yield: 9.62g (95.23%); ¹H NMR (400 MHz, CDCl₃) δ ppm: 2.96 (s, 1 H) 3.82 (br. s., 2 H) 6.61 (d, J=8.60 Hz, 2 H) 7.30 (d, J=8.60 Hz, 2 H).

4.2.4 Synthesis of 4-(pyridin-4-ylethynyl)aniline, **33**

The synthesis of **33** was adapted from a literature method.¹² In a 500 mL round bottom flask fitted with stir bar, 250 mL of triethylamine was degassed and was taken under argon atmosphere. To this, 4-iodopyridine (14.72 g, 71.79 mmol), copper (I) iodide (0.1367 g, 0.7179 mmol), dichlorobis(triphenylphosphine)palladium(II) (0.2519 g, 0.3599 mmol) were added. The reaction mixture was degassed again and was kept under argon atmosphere again. To this, **32** (9 g, 76.82 mmol) was added and the reaction mixture was stirred at 40-50°C for 2d. After this, the solvent was removed from the reaction mixture under vacuum. The slurry was diluted with 100 mL chloroform was washed with 2M ammonium chloride solution (2x 50 mL) and further with 30 mL 1M sodium chloride solution. The solvent was removed from the organic layer to obtain the product and was purified by column chromatography (Hexane : Ethylacetate, 60:40). The product was further dried under vacuum for 24h. Yield: 8.28g (59.48%); mp 191-193°C (Decomp.); ¹H NMR (400 MHz, CDCl₃) δ ppm: 3.91 (br. s., 2 H) 6.60 - 6.71 (m, 2 H) 7.28 - 7.43 (m, 4 H) 8.56 (br. s., 2 H); ¹H NMR (400 MHz, CD₃CN) δ ppm: 4.59 (br. s., 2 H) 6.66 (d, J=8.87 Hz, 2 H) 7.30 (s, 2 H) 7.36 (d, J=1.61 Hz, 2 H) 8.54 (br. s., 2 H); ¹³C NMR (400 MHz, CDCl₃) δ ppm: 85.37, 95.59, 111.54, 114.99, 125.59, 132.48, 133.74, 147.82, 149.96; ¹³C NMR (400 MHz, CD₃CN) δ ppm: 115.47, 126.28, 134.63, 150.97, 151.19.

4.2.5 Synthesis of 4-(pyridin-3-ylethynyl)aniline, **34**

The synthesis of **34** was adapted from a literature method.¹² In a 250 mL round bottom flask fitted with stir bar, 150 mL of triethylamine was degassed and was taken under argon atmosphere. To this, 3-iodopyridine (6.542 g, 31.91 mmol), copper (I) iodide (0.0061g, 0.319 mmol), dichlorobis(triphenylphosphine)palladium(II) (0.12 g, 0.1709 mmol) were added. The reaction mixture was degassed again and was kept under argon atmosphere again. To this, **32**

(4.07 g, 31.14 mmol) was added and the reaction mixture was stirred at 40-50°C for 2d. After this, the solvent was removed from the reaction mixture under vacuum. The slurry was diluted with 200 mL chloroform washed with 2M ammonium chloride solution (2x 100 mL) and further with 100 mL 1M sodium chloride solution. The solvent was removed from the organic layer to obtain the product. The product was further washed with hexane to yield pure product which was dried under vacuum for 24h. Yield: 4.43 g (71.50%); mp 121-123°C; ¹H NMR (400 MHz, CDCl₃) δ ppm: 3.87 (br. s., 2 H) 6.66 (d, J=8.30 Hz, 2 H) 7.30 (br. s., 1 H) 7.36 (d, J=8.30 Hz, 2 H) 7.77 (d, J=7.81 Hz, 1 H) 8.51 (d, J=4.88 Hz, 1 H) 8.74 (s, 1 H); ¹H NMR (400 MHz, CD₃CN) δ ppm: 4.51 (br. s., 2 H) 6.60 - 6.72 (m, 2 H) 7.22 - 7.44 (m, 3 H) 7.74 - 7.91 (m, 1 H) 8.48 (dd, J=4.64, 1.71 Hz, 1 H) 8.66 (d, J=1.47 Hz, 1 H); ¹H NMR (400 MHz, DMSO-d₆) δ ppm: 5.63 (s, 2 H) 6.56 (d, J=7.32 Hz, 2 H) 7.22 (d, J=7.32 Hz, 2 H) 7.36 - 7.45 (m, 1 H) 7.86 (d, J=9.77 Hz, 1 H) 8.50 (d, J=4.88 Hz, 1 H) 8.65 (s, 1 H); ¹³C NMR (400 MHz, CDCl₃) δ ppm: 83.99, 93.54, 111.74, 114.71, 121.12, 122.95, 132.67, 133.10, 133.91, 138.08, 147.11, 147.92, 152.03; ¹³C NMR (400 MHz, CD₃CN) δ ppm: 110.58, 113.85, 114.97, 121.75, 124.14, 131.39, 133.09, 133.72, 134.54, 138.64, 148.90, 149.99, 152.34.

4.2.6 Synthesis of phosphineimine of 3,5-di(pyridin-2-yl)-4H-1,2,4-triazol-4-amine, 35

In a 50 mL round bottom flask, **30** (2.38 g, 10 mmol) and triphenylphosphine dibromide (5.065 g, 12 mmol) were added to 25 mL of anhydrous dichloromethane in a glove box. To this mixture, anhydrous triethylamine (2.79 mL, 20 mmol) was added, and the reaction mixture was stirred under reflux for 16h. Upon cooling, the mixture was filtered and the solvent was removed under vacuum resulting in a dark red residue. Yield: 4.4846 g (90% stoichiometric conversion based on ¹H NMR); ¹H NMR (400 MHz, CDCl₃) δ ppm: 7.15 - 7.20 (m, 2 H), 7.21 - 7.32 (m, 15 H), 7.42 - 7.50 (m, 5 H), 7.60 (s, 2 H), 7.80 (dd, J=7.81, 1.17 Hz, 2 H), 8.44 (d, J=4.69 Hz, 2 H); ³¹P NMR (400 MHz, CDCl₃, ref = H₃PO₄) δ ppm: 26.67.

4.2.7 Synthesis of Triphenylphosphinimine of 4-(pyridin-4-ylethynyl)aniline, 36

In a 50 mL round bottom flask, **33** (0.5g, 2.58 mmol), triphenylphosphine dibromide (1.087 g, 2.58 mmol) were combined with 15 mL of anhydrous benzene in glove box. To this, anhydrous triethylamine (0.72 mL, 5.15 mmol) was added and stirred. The reaction mixture was then refluxed for 16h. On cooling, the mixture was filtered and the solvent from resulting dark

red solution was removed under vacuum. Yield: 0.9539g (81.56%, based on ^1H NMR); ^{31}P NMR (400 MHz, CDCl_3 , ref = H_3PO_4): δ 5.84 ppm.

4.2.8 Synthesis of Triphenylphosphinimine of 4-(pyridin-3-ylethynyl)aniline, 37

In a 50 mL round bottom flask, **34** (0.5g, 2.58 mmol), triphenylphosphine dibromide (1.087 g, 2.58 mmol) were combined with 15 mL of anhydrous benzene in glove box. To this, anhydrous triethylamine (0.72 mL, 5.15 mmol) was added and stirred. The reaction mixture was then refluxed for 16h. On cooling, the mixture was filtered and the solvent from resulting dark red solution was removed under vacuum. Yield: 0.7252g (62%, based on ^1H NMR); ^{31}P NMR (400 MHz, CDCl_3 , ref = H_3PO_4): δ 5.52 ppm.

4.2.9 Synthesis of HCl salt of 3,5-di(pyridin-2-yl)-4H-1,2,4-triazol-4-amine, 38

30 (2 g, 8.40 mmol) was dissolved in 15 mL anhydrous THF and 2N HCl in ether (4.165 mL, 8.40 mmol) was added dropwise, upon which instant white precipitation was observed. The reaction mixture was stirred for 2h at room temperature and the precipitate was filtered off, washed twice with THF, and dried under vacuum for 24h. Yield: 2.12 g (91.94%); ^1H NMR (400 MHz, CDCl_3) δ ppm: 7.40 - 7.50 (m, 2 H), 7.89 - 8.00 (m, 2 H), 8.41 - 8.54 (m, 2 H), 8.70 (br. s., 2 H).

4.2.10 Synthesis of 4-(pyridin-4-ylethynyl)aniline hydrochloride, 39

In a 150 mL beaker, **33** (2g, 10.30 mmol) was dissolved in 50 mL anhydrous THF and 2N HCl in ether (5.152 mL, 10.39 mmol) was added during which instant precipitation was observed. The reaction mixture was stirred for 2h at room temperature and the precipitate was filtered off, washed twice with THF and dried under vacuum for 24h. Yield: 2.06g (86.69 %); ^1H NMR (400 MHz, D_2O) δ ppm: 7.14 (m, J=8.20 Hz, 2 H) 7.65 (m, J=8.59 Hz, 2 H) 8.02 (d, J=7.03 Hz, 2 H) 8.68 (d, J=6.64 Hz, 2 H).

4.2.11 Synthesis of 4-(pyridin-3-ylethynyl)aniline hydrochloride, 40

In a 100 mL beaker, **34** (2g, 10.30 mmol) was dissolved in 50 mL anhydrous THF and 2N HCl in ether (5.152 mL, 10.39 mmol) was added during which instant precipitation was observed. The reaction mixture was stirred for 2h at room temperature and the precipitate was filtered off, washed twice with THF and dried under vacuum for 24h. Yield: 2.19g (92.17 %); ^1H

NMR (400 MHz, D₂O) δ ppm: 7.34 (d, $J=8.30$ Hz, 2 H) 7.71 (d, $J=8.30$ Hz, 2 H) 8.03 (dd, $J=8.30, 5.86$ Hz, 1 H) 8.63 (d, $J=8.30$ Hz, 1 H) 8.72 (d, $J=5.86$ Hz, 1 H) 8.91 (s, 1 H).

4.2.12 Synthesis of (TBA)₂ [Mo₅O₁₈(Mo(4-(pyridin-4-ylethynyl)aniline)], 41

In a 100 mL round bottom flask, octamolybdate (0.7022g, 0.3261 mmol) and DCC (0.2365g, 1.1481 mmol) were combined with 10 mL of anhydrous acetonitrile. In a separate beaker, **33** (0.0865g, 0.4455 mmol) was dissolved in 15 mL of anhydrous acetonitrile and was then added to round bottom flask. The reaction mixture was stirred for 10 min after which **39**(0.1028g, 0.4457 mmol) was added and the sides were washed with 5 mL anhydrous acetonitrile. The resulting mixture was then stirred at 90°C for 15h. On cooling, the mixture was filtered off to remove dicyclohexyl urea and the solvent from resulting dark red solution was removed under vacuum. IR (ZnSe): 974 sh ($\nu_{\text{Mo=N}}$), 946 cm⁻¹ ($\nu_{\text{Mo=O}}$); ¹H NMR (400 MHz, CD₃CN) δ ppm: 0.97 (td, $J=7.25, 2.15$ Hz, 24 H) 1.26 - 1.49 (m, 16 H) 1.51 - 1.75 (m, 16 H) 2.94 - 3.23 (m, 16 H) 7.27 (d, $J=7.25$ Hz, 2 H) 7.44 (br. s., 2 H) 7.55 - 7.67 (m, 2 H) 8.60 (br. s., 2 H); ¹³C NMR (400 MHz, CD₃CN) δ ppm: 14.25, 20.75, 24.79, 59.73, 127.53, 129.70, 133.52, 134.62, 151.19, 151.34.

4.2.13 Synthesis of (TBA)₂ [Mo₅O₁₈(Mo(4-(pyridin-3-ylethynyl)aniline)], 42

In a 100 mL round bottom flask, octamolybdate (0.7022g, 0.3261 mmol) and DCC (0.2365g, 1.1481 mmol) were combined with 5 mL of anhydrous acetonitrile. In a separate beaker, **34** (0.0865g, 0.4455 mmol) was dissolved in 5 mL of anhydrous acetonitrile and was then added to round bottom flask. The reaction mixture was stirred for 10 min after which **40** (0.1028g, 0.4457 mmol) was added and the sides were washed with 2 mL anhydrous acetonitrile. The resulting mixture was then stirred at 90°C for 15h. On cooling, the mixture was filtered off to remove dicyclohexyl urea and the solvent from resulting dark red solution was removed under vacuum. IR (ZnSe): 975 sh ($\nu_{\text{Mo=N}}$), 946 cm⁻¹ ($\nu_{\text{Mo=O}}$); ¹H NMR (400 MHz, CD₃CN) δ ppm: 0.97 (t, $J=7.32$ Hz, 24 H) 1.37 (m, 16 H) 1.62 (m, 16 H) 3.14 - 3.10 (m, 16 H) 7.25 (d, $J=8.30$ Hz, 2 H) 7.39 (s, 1 H) 7.59 (d, $J=8.79$ Hz, 2 H) 7.89 (d, $J=10.25$ Hz, 1 H) 8.55 (s, 1 H). 8.73 (s, 1H); ¹³C NMR (400 MHz, CD₃CN) δ ppm: 14.17, 20.64, 24.68, 59.58, 115.38, 124.67, 126.91, 127.41, 129.57, 133.12, 134.10, 139.03, 139.75, 149.29, 153.07.

4.3 Results and discussion

4.3.1 Synthesis of pyridyl based ligands

4.3.1.1 Synthesis of 3,5-di(pyridin-2-yl)-4H-1,2,4-triazol-4-amine, 30

To prepare organoimido derivatives of hexamolybdate, we first selected **30** as a potential candidate (Figure 4.13). The ligand contains an amino functionality for coordinating with the POM cluster, two bidentate pockets for coordinating with metal atoms, and complete conjugation in the system for maintaining an electronic communication between the two units of the hybrid.

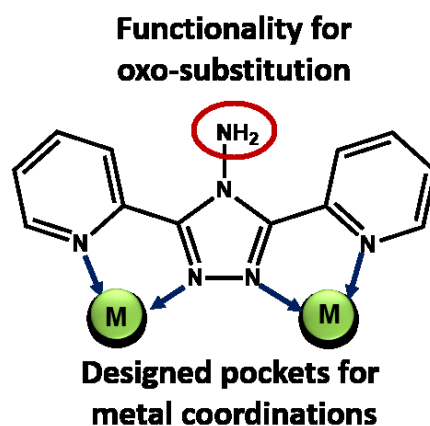


Figure 4.13 Potential ligand (**30**) for organoimido functionalization of hexamolybdate.

30 was synthesized following the literature method which proceeded with ease yielding the product in stoichiometric amounts (Figure 4.14).¹³

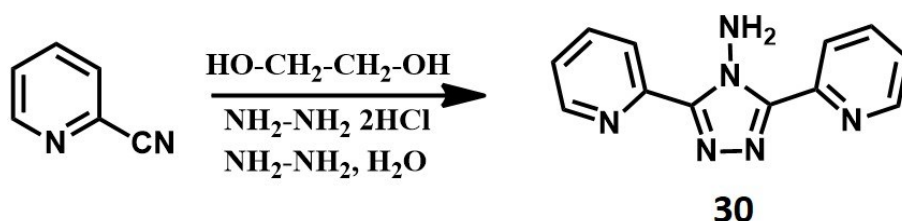


Figure 4.14 Synthesis of **30**.¹³

4.3.1.2 Synthesis of 33 and 34 ligands

Following the results of Mijares, wherein for improving the yields increasing the spacing between the hexamolybdate cluster and the pyridyl functionality was thought to be an alternative. Based on this concept, two new ligands were designed (Figure 4.15).

No further purification was required and the product was deprotected to yield the ethynyl derivative, **32**.¹⁵ Product formation was confirmed by ¹H NMR spectrum showing shifts in peaks with reference to the starting material along with the disappearance of the peak for the TMS-group and appearance of an acetylene proton at 2.96 ppm.

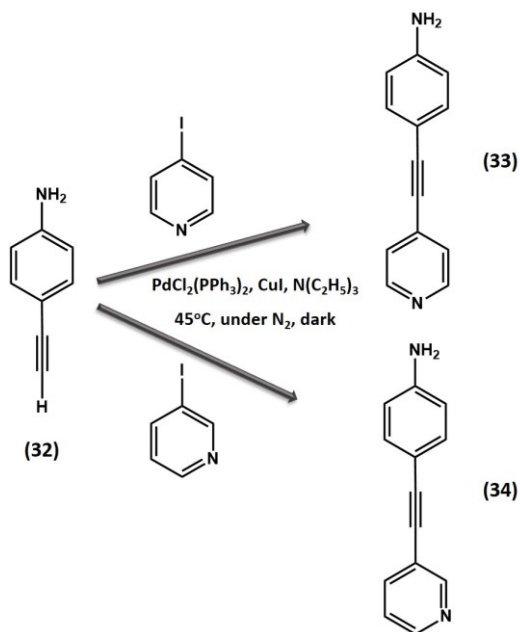


Figure 4.17 Final steps to prepare **33** and **34**.

Furthermore, **32** underwent Sonogashira coupling reaction with 3-iodopyridine and 4-iodopyridine to yield the desired ligands **33** and **34**, respectively (Figure 4.17).¹⁴ The pure products were extracted after column chromatography and were analyzed using ¹H and ¹³C NMR spectroscopy. **33** is a symmetric molecule, thus shows four sets of aromatic peaks and one peak corresponding to NH₂ group. On the other hand, **34** being an asymmetric molecule, shows six set of aromatic peaks along with a peak for NH₂ group.

4.3.2 Attempts to use phosphineimine derivatives of the pyridyl based ligands as imidodelivery reagent

4.3.2.1 Phosphineimine derivative (35) of 30 as imidodelivery reagent

After **30** was synthesized and fully characterized, **35** as the organoimido delivery reagent was prepared. Usually, the ratio between amine and PPh₃Br₂ used is 1:1 for this reaction,¹⁶ but the product conversion was observed to be low (around 50-60%). When the ratio of amine to PPh₃Br₂ was changed to 1:1.2, product formation could be seen in high yields (Figure 4.18).

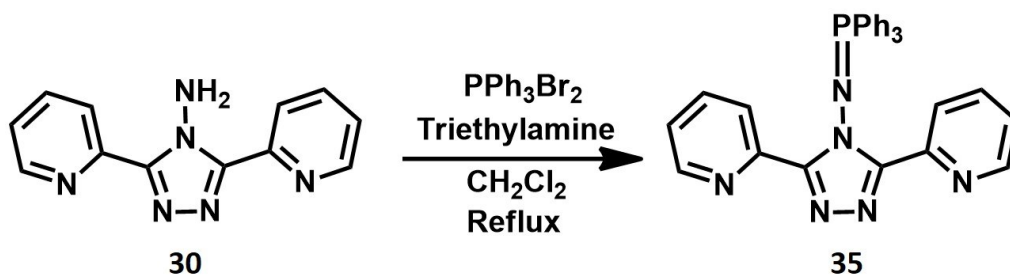


Figure 4.18 Synthesis of **35**.

In ^1H NMR, the peak corresponding to the NH_2 group in the ligand shows up at 8.52 ppm, which disappears in the spectrum of the product suggesting the removal of these protons due to bonding of PPh_3 group. Moreover, the peaks corresponding to the attached pyridyl groups are downfield shifted, which also suggests that the product is formed. The spectrum also shows the presence of triphenylphosphine oxide, a side-product of the reaction which forms due to the hydrolysis of some of PPh_3Br_2 (or hydrolysis of the phosphinimine) by trace amounts water. To avoid any ambiguity in the analysis of the phosphineimine, ^{31}P NMR has been used as a reliable technique as a new peak corresponding to the product should appear. The results showed the presence of two peaks, 30.136 and 26.731 ppm (relative to H_3PO_4) (Figure 4.19). On comparing the peaks to other possible compounds in the reaction, a new peak at 26.731 ppm confirmed the formation of **35**.

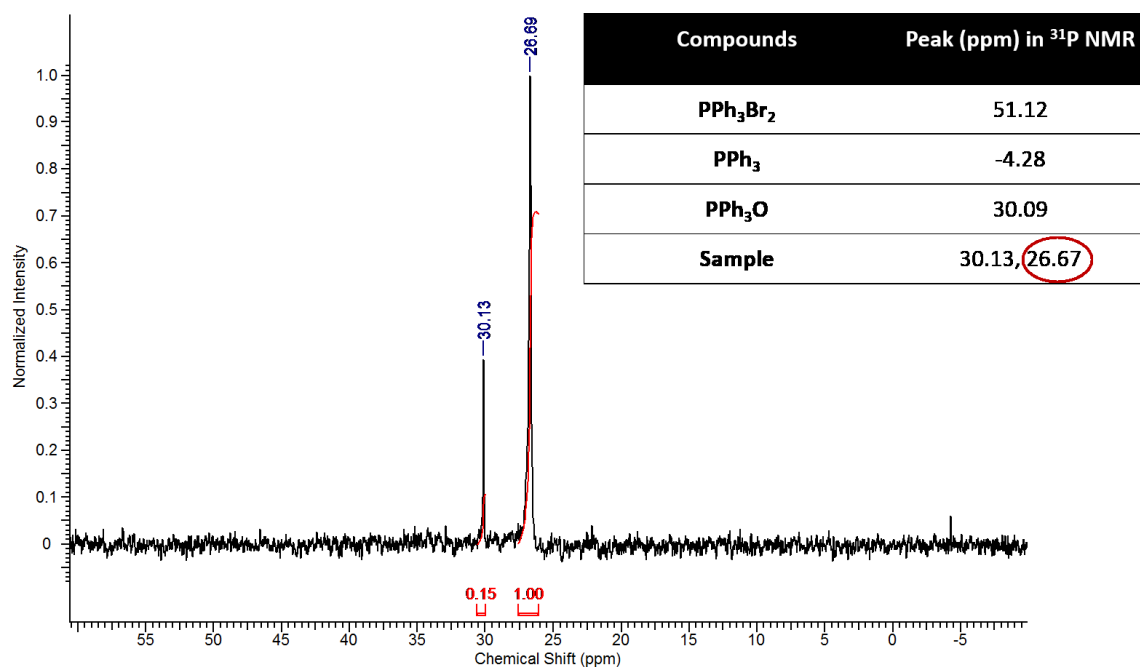


Figure 4.19 ^{31}P NMR study of **35**.

Considering the sensitivity of the product, no further purification could be done and the product was used as such for additional reactions. First, a direct metathetical reaction was performed by reacting **35** with hexamolybdate following the literature method reported by Maatta et. al (Figure 4.20).¹⁷

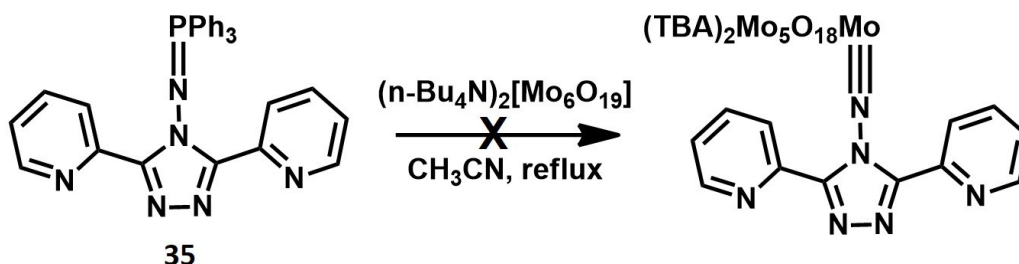


Figure 4.20 Attempt to synthesize hexamolybdate hybrid using **35** as organoimido delivery reagent.

No color change corresponding to the product formation was observed. Also, in the infrared spectrum, a shoulder peak at around 970 cm^{-1} was not observed (characteristic peak for formation of monofunctionalized hexamolybdate derivatives). Furthermore, in ^1H NMR spectrum, the peak corresponding to the NH_2 -group appeared along with the peaks of **30** and TBA peaks from hexamolybdate confirming that the reagents existed as a mixture with no observable derivative formation. Multiple reactions were attempted by modifying the reaction conditions, like varying the reaction times and solvents, but no reaction could be observed. Furthermore, **35** was used to react with dimolybdate ($(\text{TBA})_2[\text{Mo}_2\text{O}_7]$) to prepare hexamolybdate derivative¹⁸ but no product formation could be detected. The failure observed in the functionalization of hexamolybdate was not completely surprising since not all phosphineimines are capable of functionalizing hexamolybdate.^{6,7}

4.3.2.2 Phosphineimine derivatives (**36** and **37**) of **33** and **34** as imido delivery reagents

After confirming the synthesis of the desired **33** and **34** ligands, firstly phosphineimine derivatives¹⁶ of the ligands were prepared using dichloromethane and THF as solvents. In both the cases, some new peaks in ^1H NMR spectrum suggested product formation, but the conversions were found to be lower with reference to starting ligands. On changing the solvent to benzene, the product conversions were observed to increase (Figure 4.21).

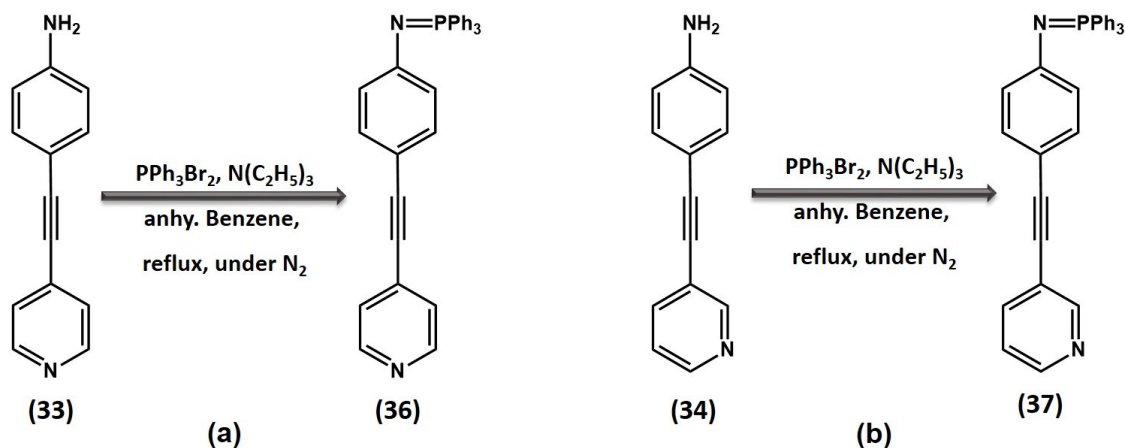


Figure 4.21 Synthesis of **36** and **37**.

The ^1H NMR spectra of the products showed the appearance of some new peaks. Differentiation of the chemical shifts and multiplicities of the desired phosphinimines of the ligands was difficult from the peaks corresponding to triphenylphosphine oxide which is typically formed as a side product. Thus, ^{31}P NMR spectroscopy was used as a confirmatory tool which clearly showed the emergence of new chemical shifts.

Table 4.1 ^{31}P NMR peaks for possible compounds.

Compounds	Peak (ppm) in ^{31}P NMR
PPh_3Br_2	51.12
PPh_3	-4.28
PPh_3O	30.09
36	30.08, 5.84
37	29.93, 5.52

The ^{31}P NMR spectra of **36** and **37** showed new signals at 5.84 and 5.52 ppm (relative to H_3PO_4) which are close in the range of literature values for aryl phosphinimines confirming the successful synthesis of phosphineimines derivatives of the two ligands (Table 4.1).¹⁹

Due to the air and moisture sensitivity of these derivatives, no further purification could be done and they were used as such. Following Maatta's route¹⁷ for the functionalization of hexamolybdates, the phosphineimines of both the ligands were refluxed with hexamolybdate (Figure 4.22). Multiple reactions with various solvents like pyridine, acetonitrile,

dichloromethane and anhy. THF were tried, but the characteristic shoulder peak around 970 cm^{-1} could not be observed.

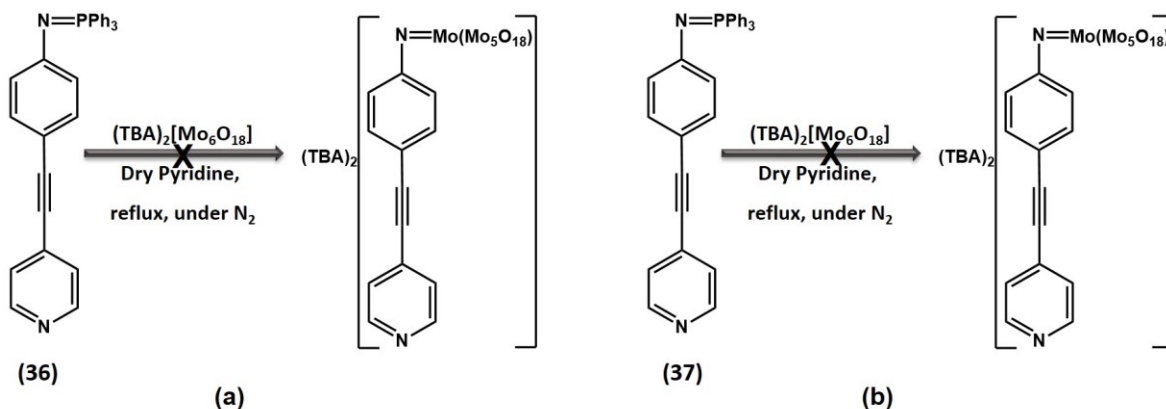


Figure 4.22 Maatta's route to functionalize hexamolybdate with **36** and **37**.

4.3.3 Attempts to use pyridyl ligands directly as imidodelivery reagent via Peng's route

4.3.3.1 **30** as imidodelivery reagent

After these unproductive attempts to functionalize hexamolybdate using phosphineimine, **30** by itself was used as the organoimido delivery reagent following Peng's protocol, but this method was also unsuccessful (Figure 4.23).^{20,21}

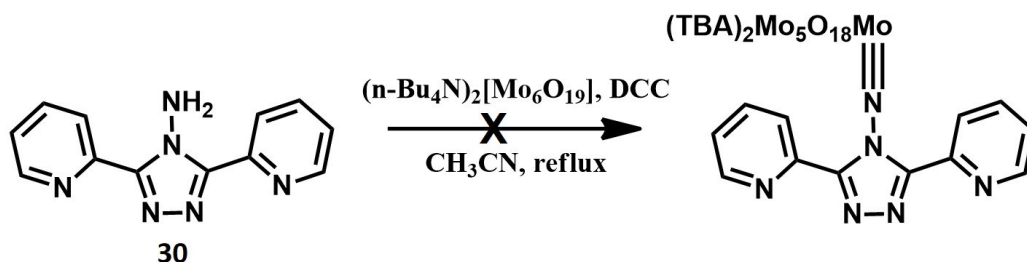


Figure 4.23 Peng's route to synthesize derivative with **30**.

4.3.3.2 **33** and **34** ligands as imidodelivery reagents

Next, Peng's route for hexamolybdate functionalization was adopted with **33** and **34** ligands.²⁰ IR and ^1H NMR spectrum showed some new peaks, but in general the reactions were found to be very low yielding.

4.3.3.3 30 as imidodelivery reagent

Furthermore, functionalization of hexamolybdate with the **30** was attempted using Wei's method which unlike previous methods, utilizes octamolybdate in the presence of the corresponding amine salt.²² Thus, first the hydrochloride salt of the ligand, **38** was prepared with 2N HCl in ether, which was characterized by ¹H NMR spectroscopy, wherein the peak corresponding to NH₂ group disappeared and shifts in all other peaks could be observed. After confirmation of the synthesis of **38**, **30** was employed in Wei's method along with octamolybdate and DCC (Figure 4.24).²²

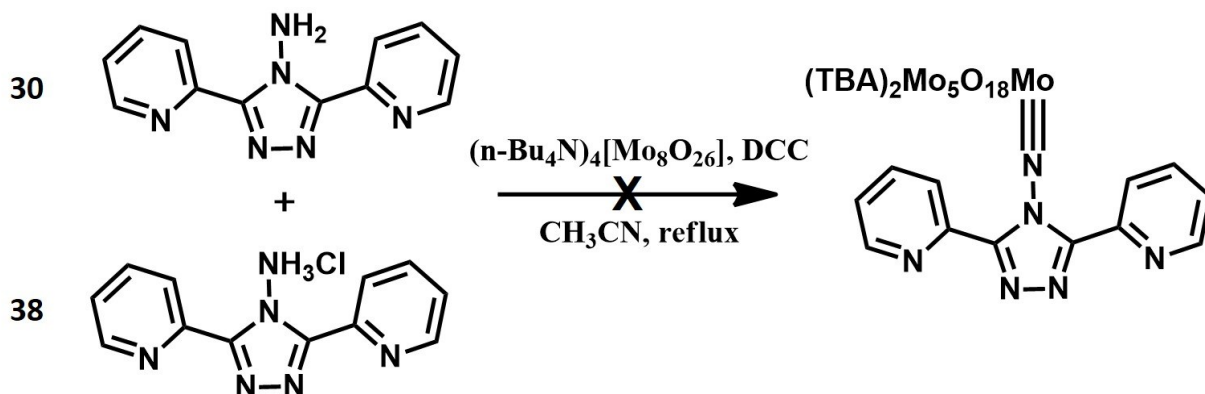


Figure 4.24 Wei's route of functionalization with **30**.

Unfortunately, no product formation could be detected in IR or ¹H NMR spectra. It was suspected that Mo=N-N bonds may not be stable or the hybrid may be too sensitive in these analytical conditions. All the routes for the functionalization of hexamolybdate with **30** were found to be unsuccessful even after multiple attempts with modified reaction conditions, like ratios, temperature and reaction times and thus, no further trials could be done.

4.3.3.4 33 and 34 as imidodelivery reagents

After all previous unfruitful attempts, Wei's method for functionalization of hexamolybdate was explored with **33** and **34** (Figure 4.25).²² At first, hydrochloride salts (**39** and **40**) of both **33** and **34** were prepared in anhydrous THF using 2N HCl solution in ether. **39** and **40** were then characterized by ¹H NMR spectroscopy. Subsequently, **33** and **34** were used as potential organoimido delivery reagents. As outlined, to an acetonitrile solution of an equivalent of tetrabutylammonium octamolybdate and 3.4 equivalents of DCC, 1.34 equivalents of the **33** or **34** and its corresponding hydrochloride salt **39** or **40** were mixed. The resulting dark orange suspension was heated to 90°C under argon with constant stirring for 15 hours. On cooling to

room temperature, the resulting off-white precipitate of urea was filtered off and the red filtrate was concentrated under reduced pressure.

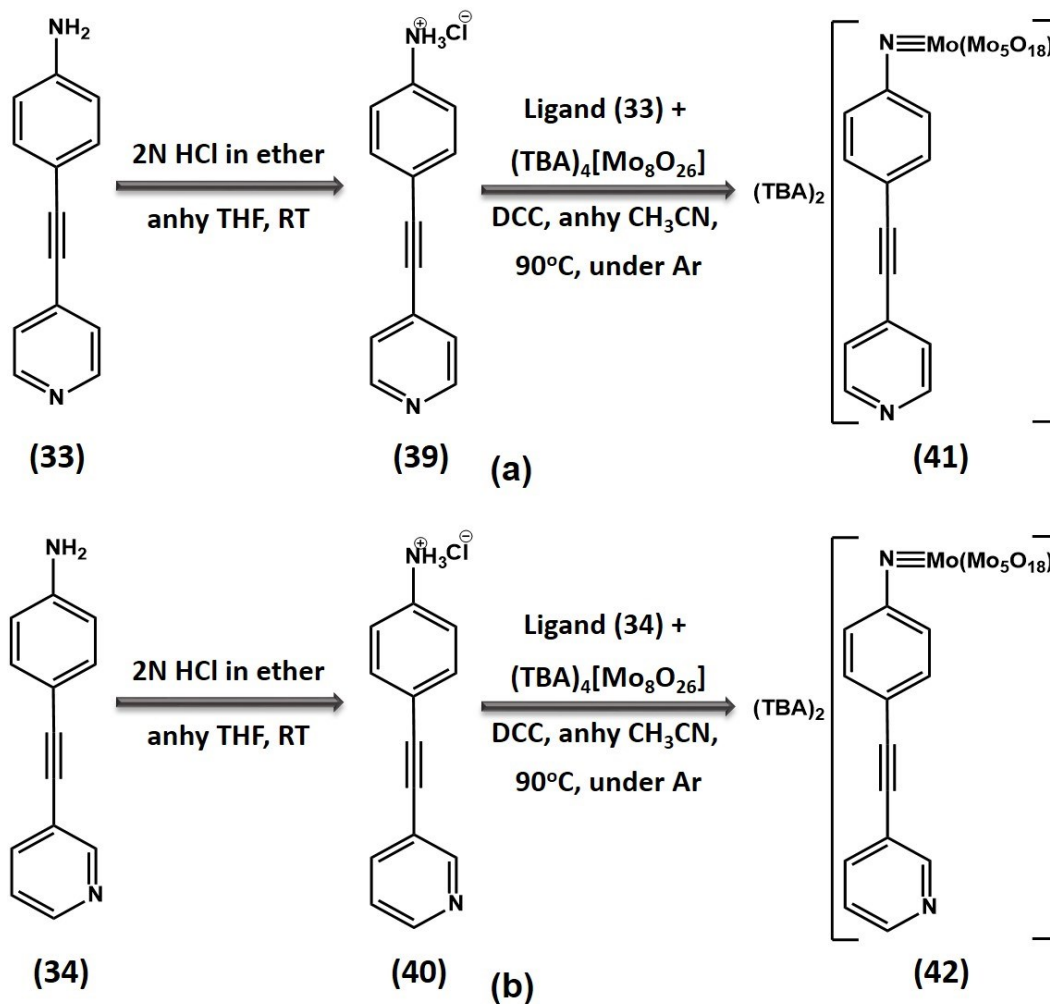


Figure 4.25 Wei's route to functionalize hexamolybdate using **33** and **34** as organoimido delivery reagents.

In infrared spectra of the crude reaction mixtures of **41** and **42**, the characteristic shoulder appeared at 974 cm^{-1} and 975 cm^{-1} , respectively (Figure 4.26). This suggested the successful incorporation of organoimido ligands in hexamolybdate.

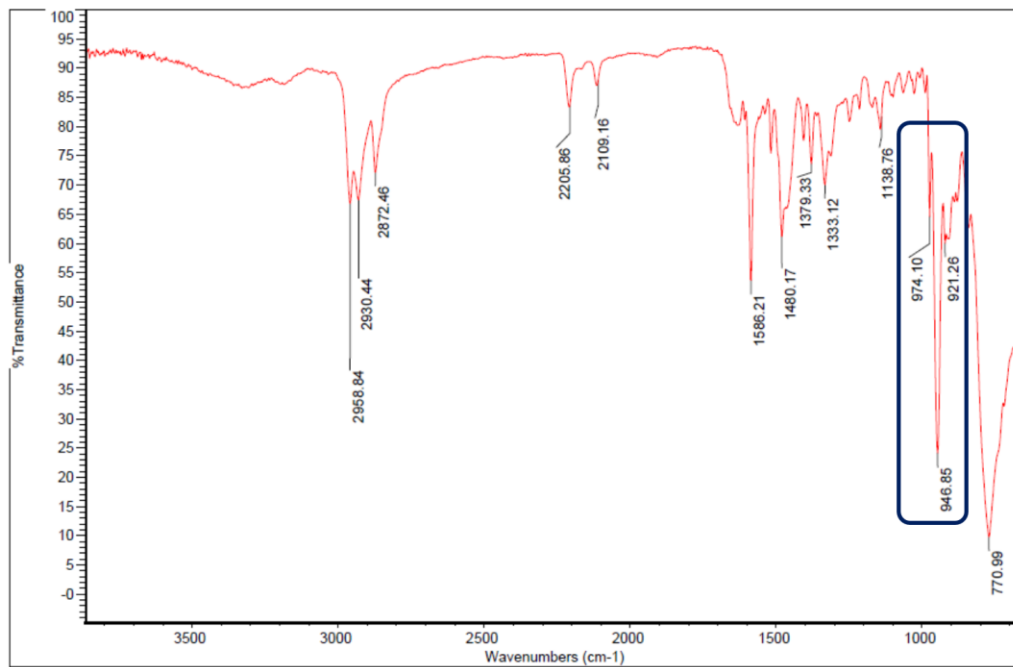


Figure 4.26 Infrared spectrum of hybrid, **41** containing **33** covalently anchored to hexamolybdate.

^1H NMR spectra of the products from both the ligands exhibit chemical shifts in the aromatic region along with peaks in the aliphatic region corresponding to $[\text{TBA}]^+$ ions (Table 4.2, Figure 4.27).

Table 4.2 ^1H NMR shift observed in **33** based hybrid of hexamolybdate, **41**.

33 (ppm)	41 (ppm)
8.53	8.60
7.35	7.61
7.30	7.44
6.66	7.27

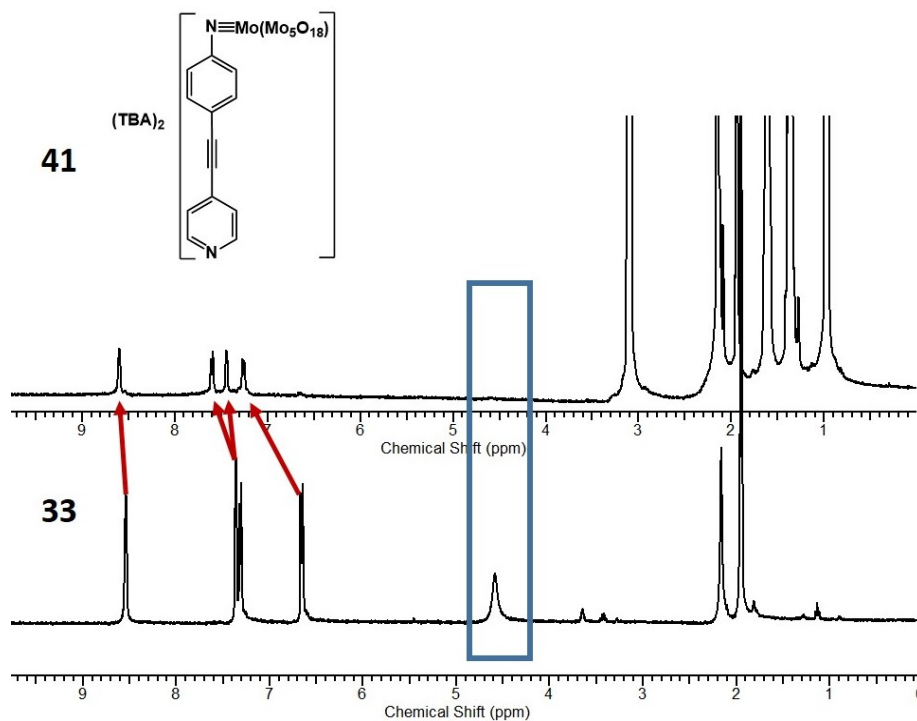


Figure 4.27 ^1H NMR of hybrid, **41** containing **33** covalently anchored to hexamolybdate.

41 showed four set of aromatic peaks deshielded as compared to **33** which is a direct reflection of the electron withdrawing nature of the hexamolybdate, confirming the functionalization.

Table 4.3 ^1H NMR shift observed in **34** based hybrid of hexamolybdate, **42**.

34 (ppm)	42 (ppm)
8.66	8.73
8.48	8.55
7.79	7.89
7.33	7.39
7.27	7.59
6.66	7.25

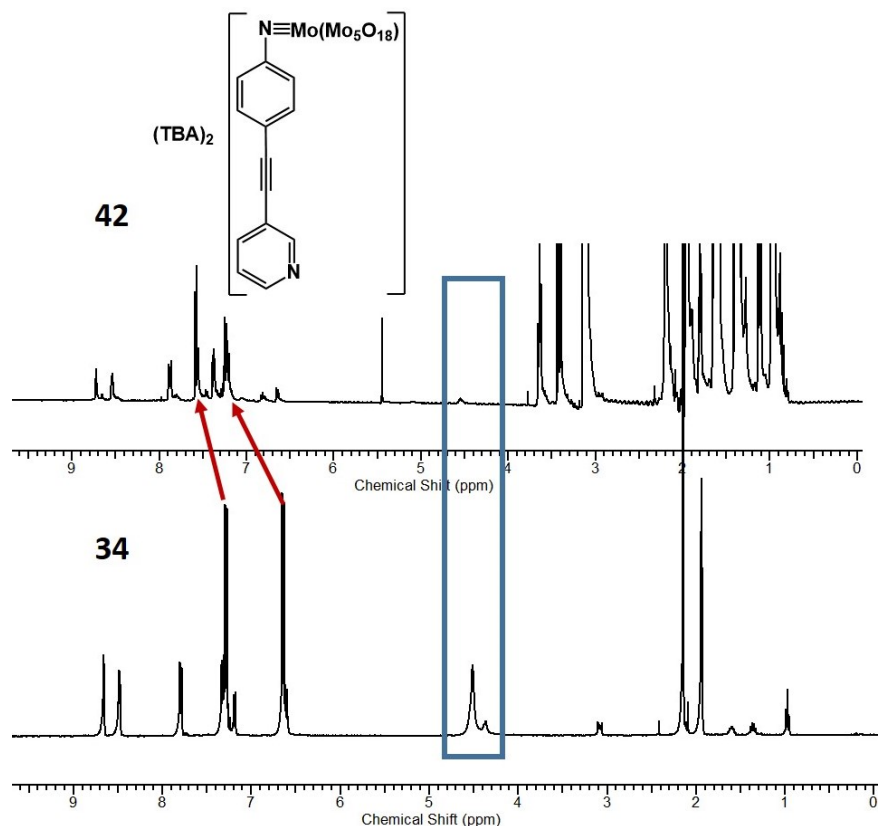


Figure 4.28 ^1H NMR of hybrid, **42** containing **34** covalently anchored to hexamolybdate.

42 also showed couple of sets of aromatic peaks deshielded as compared to **34** which is a direct reflection of the electron withdrawing nature of the hexamolybdate, confirming the functionalization.

4.3.4 Attempts to purify hexamolybdate derivatives, **41** and **42**

4.3.4.1 Classical attempt of fractional crystallization

In both the cases, excess peaks corresponding to $[\text{TBA}^+]$ were observed in ^1H NMR spectrum which suggests the presence of the parent cluster $(\text{TBA})_2[\text{Mo}_6\text{O}_{19}]$ or $(\text{TBA})_4[\text{Mo}_8\text{O}_{26}]$ in the crude reaction mixture, hence further purification was required before it could be used in further reactions. $\text{Mo}=\text{N}$ bond in organoimido derivatives is susceptible to hydrolysis, which results in its decomposition yielding parent amine and hexamolybdate cluster. Thus, known methods like column chromatography and prep-TLC for product purification could not be employed. The physical properties of the derivatives are similar to that of the parent cluster, thus the only possible way of purification is fractional crystallization. For this, several attempts of solvent evaporation and vapor diffusion of ether in acetonitrile solution of the

reaction mixture of **41** and **42** were done. In various instances orange-red crystals were obtained but the X-ray crystal analysis showed either hexamolybdate or octamolybdate cluster. The red color of the crystal shows that the product merely forms a coating over these crystals.

4.3.4.2 A novel attempt to purify via halogen-bonding

Due to unsuccessful attempts to grow the crystals of the hexamolybdate derivatives, we thought of exploiting halogen bonding as a method for the separation and purification of the POM derivatives. Halogen-bonding (XB) is a non-covalent interaction which is electrostatic in nature and is comparable in strength to hydrogen-bonds. Pyridines are well known as halogen-bond acceptors wherein the structure-directing force of interaction is the $N \cdots X$ halogen-bond between the pyridine nitrogen atom and the halogen atom ($X = \text{Br}, \text{I}$), which gives rise to infinite 1-D chains (Figure 4.29).²³

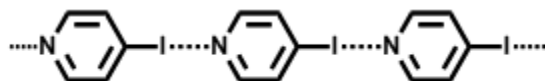


Figure 4.29 Halogen bonding in 4-iodopyridine.

Thus, six iodine donors were selected and were mixed respectively with approximately equivalent amount of **41** and **42** in acetonitrile as solvent (Figure 4.30). The resulting reaction mixtures were left to crystallize *via* solvent evaporation method. Some red crystals were obtained only with **41** and iodopentafluorobenzene, but upon examining its structure with X-ray crystallography, it was found to be just hexamolybdate.

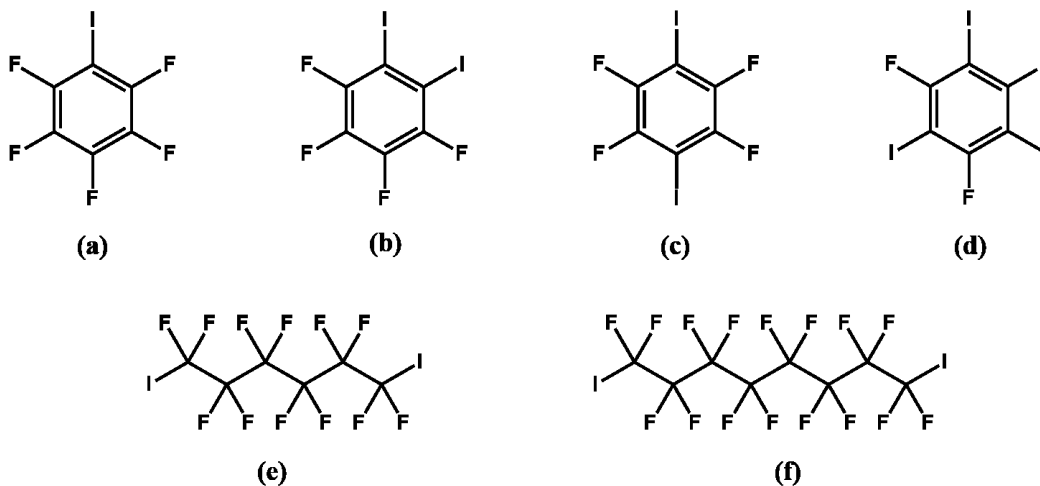


Figure 4.30 Selected halogen bond donors.

4.3.5 Attempts to coordinate second metal ion

4.3.5.1 Copper as second metal ion

Copper iodide is also well known to coordinate with pyridyl functionality (Figure 4.31).²⁴ Thus, **41** was mixed in equimolar ratios with copper iodide solution in acetonitrile and was left for slow evaporation to grow single crystals of the adduct. No crystals have been observed so far.

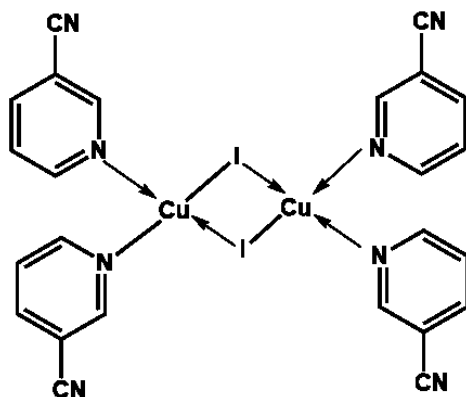


Figure 4.31 Copper iodide affinity for pyridine.²⁴

4.3.5.2 Palladium as second metal ion

Upon successful characterization of **41**, the metal coordination capabilities of this hybrid was prompted. Gouzerh *et al.*²⁵ reported that the benzonitrile molecules of bisbenzonitrile-dichloro palladium (II) can be displaced by the pyridyl substituents in the bis-alkoxy functionalized Anderson-Evans POM resulting in the formation of an adduct, $\text{MnMo}_6\text{O}_{18}\{(\text{OCH}_2)_3\text{CNHCO}-(4\text{-C}_5\text{H}_4\text{N})\}_2\text{PdCl}_2$ (Figure 4.32). The formation of the adduct was confirmed by FT-IR and ¹H NMR spectroscopy but no single crystal structure of the adduct could be obtained. Following their study, two equivalents of **41** were added to a solution of [Pd(II)] in acetonitrile and the reaction mixture was refluxed for 30 min. On cooling, diethyl ether was added to it to precipitate out the product which was then filtered off and washed further with diethyl ether to remove any leftover benzonitrile. On drying, the reaction mixture was analyzed by ¹H NMR. Shifts in some peaks could be observed but Pd coordination with the pyridyl moiety of the derivatives was inconclusive.

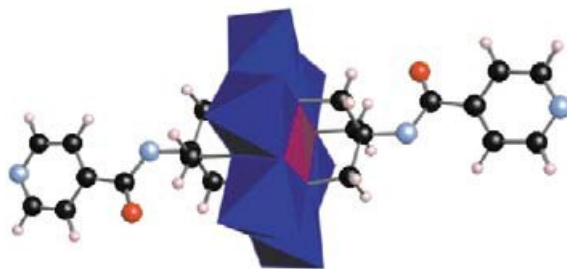


Figure 4.32 Gouzerh *et al.* Anderson-Evans POM, $\text{MnMo}_6\text{O}_{18}\{(\text{OCH}_2)_3\text{CNHCO}-(4\text{-C}_5\text{H}_4\text{N})\}_2\text{PdCl}_2$.²⁵

4.4 Conclusions

Pyridine based ligands were explored as imidodelivery reagents in this chapter. A series of three different ligands were synthesized and characterized. Various attempts to covalently attach these ligands were done following known routes. Although no evidence of covalent attachment of 3,5-di(pyridin-2-yl)-4H-1,2,4-triazol-4-amine to hexamolybdate could be observed, we were able to successfully attach 4-(pyridin-4-ylethynyl)aniline and 4-(pyridin-3-ylethynyl)aniline to the hexamolybdate cluster. We characterized these organic-inorganic hybrids using infrared and NMR spectroscopy as analytical tools. We have been trying to get single crystals of these hybrids. We have also attempted to use a novel method involving halogen bonding as a purification and separation technique for pyridyl functionalized hexamolybdate hybrids.

References

- ¹ Brown, D. J. *The Chemistry of Heterocyclic Compounds, Pyridine Metal Complexes*, John Wiley & Sons, 2009.
- ² (a) Kristiansson, O. *Acta Crystallographica Sec-C* **2000**, *56*, 165; (b) Jebas, S. R.; Balasubramaniana, T.; Slawin, A. M. Z. *Acta Crystallographica Sec-B* **2007**, *63*, 1624.
- ³ (a) Compain, J.-D.; Deniard, P.; Dessapt, R.; Dolbecq, A.; Oms, O.; Secheresse, F.; Marrot, J.; Mialane, P. *Chem. Commun.* **2010**, *46*, 7733; (b) Pradeep, C. P.; Li, F. Y.; Lydon, C.; Miras, H. N.; Long, D. L.; Xu, L.; Cronin, L. *Chem.–Eur. J.* **2011**, *17*, 7472.
- ⁴ Santoni, M. P.; Pal, A. K.; Hanan, G. S.; Tang, M. C.; Venne, K.; Furtos, A.; Menard-Tremblay, P.; Malveau, C.; Hasenknopf, B. *Chem. Commun.* **2012**, *48*, 200.
- ⁵ Yin, P.; Li, T.; Forgan, R. S.; Lydon, C.; Zuo, X.; Zheng, Z. N.; Lee, B.; Long, D.; Cronin, L.; Liu, T. *J. Am. Chem. Soc.* **2013**, *135*, 13425.
- ⁶ Moore, A., *PhD Thesis, Kansas State University*, **1998**.
- ⁷ Kristopher Mijares, *PhD Thesis, Kansas State University*, **2008**.
- ⁸ Stark, J.; Young, V.; Maatta, E. A. *Angew. Chem. Int. Ed. Engl.* **1995**, *34*, 2547.
- ⁹ Kang, J.; Xu, B.; Peng, Z.; Zhu, X.; Wei, Y.; Powell, D. R. *Angew. Chem. Int. Ed.* **2005**, *44*, 6902.
- ¹⁰ Klemperer, W. G.; Ginsberg, A. P. *Introduction to Early Transition Metal Polyoxoanions*, Inorganic Syntheses, Volume 27, John Wiley & Sons, Inc., 2007.
- ¹¹ Liu, M.; Deng, J.; Lai, C.; Chen, O.; Zhao, Q.; Zhang, Y.; Li, H.; Yao, S. *Talanta* **2012**, *100*, 229.
- ¹² Wood, M. R.; Bock, M. G.; Su, D.-S.; Kuduk, S. D.; Han, W.; Dorsey, B. D. WO 2002099388 A2, 2002.
- ¹³ Bentiss, F.; Langrenée, M.; Traisnel, M.; Mernari, B.; Elattari, H. *J. Het. Chem.* **1999**, *36*, 149.
- ¹⁴ Cho, G.-J.; Kim, J.-J.; Choi, E.-J.; Kim, N.-Y.; Park, C.-S. Yang, H.-T. *US 2008/0087887 A1* **2008**.
- ¹⁵ Marqués-González, S.; Yufit, D. S.; Howard, J. A. K.; Martín, S.; Osorio, H. M.; Garcia-Suarez, V. M.; Nichols, R. J.; Higgins, S. J.; Ceac, P.; Low, P. J. *Dalton Trans.* **2013**, *42*, 338.
- ¹⁶ Bestmann, H. J.; Fritzsche, H. *Chem. Ber.* **1961**, *94*, 2477.
- ¹⁷ Kwen, H.; Young Jr., V. G.; Maatta, E. A. *Angew. Chem., Int. Ed.* **1999**, *38*, 1145.
- ¹⁸ Che, T. M.; Day, V. W.; Francesconi, L. C.; Fredrich, M. F.; Kelmperer, W. G.; Shum, W. *Inorg. Chem.* **1985**, *24*, 4055.
- ¹⁹ Krishnamurthy, S. S.; Ramabrahmam, A. R.; Murthy, A. R. V. *Z. Anorg. Allg. Chem.* **1985**, *522*, 226.
- ²⁰ Wei, Y.; Xu, B.; Barnes, C. L.; Peng, Z. *J. Am. Chem. Soc.* **2001**, *123*, 4083.
- ²¹ Peng, Z.; Wei, Y.; Xu, B. *US 20020165405 A1*, **2002**.
- ²² Ge, N.; Wei, Y.; Wang, Y.; Wang, P.; Guo, H. *Eur. J. Inorg. Chem.* **2004**, 2819.
- ²³ Ahrens, B.; Jones, P. G. *Acta Crystallogr., Sect. C.: Cryst. Struct. Commun.* **1999**, *55*, 1308.
- ²⁴ Huang, X.-C.; Ng, S. W. *Acta Cryst. E* **2004**, *60*, 1055.
- ²⁵ Favette, S.; Hasenknopf, B.; Vaissermann, J.; Gouzerha, P.; Rouxb, C. *Chem. Commun.* **2003**, 2664.

Chapter 5 - Exploring acetylacetonates as a remote functionality to prepare hexamolybdate imido hybrids

prepare hexamolybdate imido hybrids

5.1 Diketones

Diketones are the molecules containing two keto groups at 1,3-positions (Figure 5.1). These are one of the oldest class of chelating ligands and play an important role in stabilizing otherwise unstable metallic or organometallic derivatives developing structural and physico-chemical variability.¹ Due to various recent industrial applications of their metal complexes, they have been attracting significant attention.

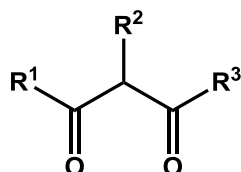


Figure 5.1 General structure of diketones.¹

Metal coordination in diketones can be classified into the neutral, mono- and dianionic forms. Monoanionic diketones with metals presents a vast variety of coordination modes which results in structural variability.¹

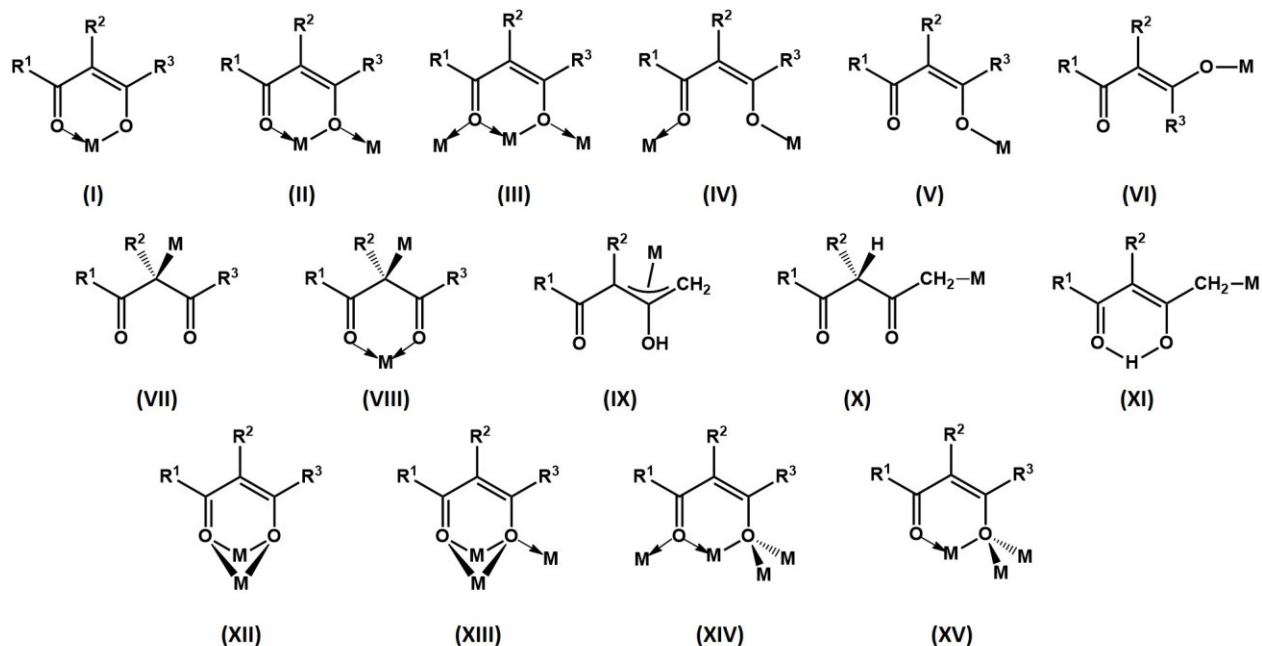


Figure 5.2 Different metal coordination modes of monoanionic diketones.¹

5.1.1 Acetylacetones

Acetylacetones (acacH) or 2,4-pentanedione are the simplest member of β -1,3-diketone family wherein $R^1, R^3 = \text{CH}_3$ and $R^2 = \text{H}$. These are usually prepared either by the reaction of acetone with acetic anhydride catalyzed by Lewis acid (e.g. BF_3) or by the reaction of the enolate of acetone with ethyl acetate.²

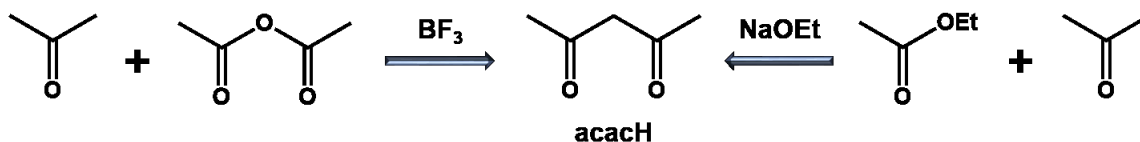


Figure 5.3 Synthesis of acetylacetones.²

The presence of β -carbonyl group along with a proton on intermediate carbon atom (C3) is a key feature for the molecule to exhibit tautomerism, where it exists as an equilibrium mixture of keto and enol forms.²

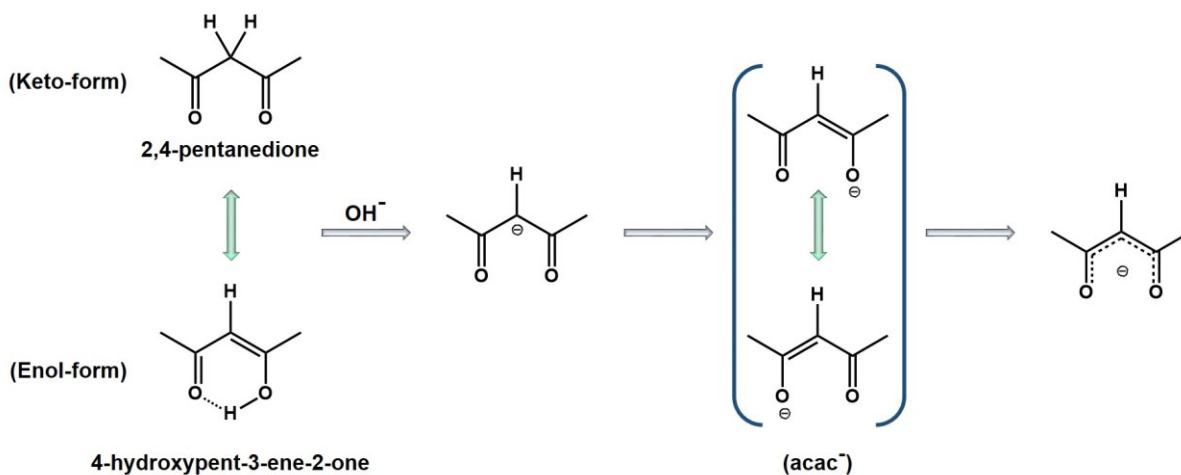


Figure 5.4 Resonance structures of acetylacetones.²

Due to intramolecular H-bonding and restricted conformation in the resulting conjugated system, the enol tautomer exhibits more stability than its corresponding keto tautomer.³ Even though the enol form is predominantly observed under most conditions, the molecule is commonly known as the diketone (2,4-pentanedione). The enol form is a weak acid with a dissociation constant, $K_a = 1.12 \times 10^{-9}$, thus deprotonation of the enolic proton at C3 results in a monoanion (acac^-) being stabilised by the charge delocalisation over both C and O in the molecule.⁴ These are known to coordinate to almost all the metal ions in various oxidation states in the periodic table presenting a vast literature on metal acetylacetonates. In these complexes,

the anion (acac^-) acts as a bidentate ligand giving rise to a six-membered "pseudoaromatic" ring with the metal since the metal atom is not a part of the aromaticity.⁴

5.1.2 Application of metal acetylacetonates

These metal complexes display high thermal stability, volatility and solubility in organic solvents which makes them applicable in various fields.⁵ The solubility of these complexes in organic solvents is a key to incorporate metal ions into important industrial processes like vulcanization of rubber,⁶ as additives and metal plating from organic solvents plastics, gasoline, lubricating oils, paints, and enamels^{6,5} These metal complexes have emerged as versatile catalysts for a range of industrially and academically important organic reactions⁷ like polymerization of unsaturated hydrocarbons⁸ and of silicone monomers,⁹ for oxidation of hydrocarbons,¹⁰ epoxidation of allylic alcohols,¹¹ acetylation of phenols, alcohols, and amines,¹² for Negishi-type coupling,¹³ for acidolysis reactions,¹⁴ hydrosilylation of alkynes, coupling of organic halides¹⁵ and in transesterification.¹⁶ Metal acetylacetonates have also been applied as efficient and cost effective catalysts for the formation of cyclic carbonates by cycloaddition of carbon dioxide with epoxides.¹⁷ The metal acetylacetonates have also been exploited as combustion promoters in jet fuels.¹⁸ Chromic acetylacetonate reduces the tendency of nitromethane to detonate under shock increasing the power output when used in a rocket motor.¹⁹ These complexes have been applied for the extraction and separation of metals.²⁰

Iron (III) acetylacetonate was used as the organometallic precursor to prepare magnetite nanoparticles which is utilized for industrial waste-water treatment.²¹ A ZrAcac as cathode buffer layer shows decreased series resistance and enhanced photocurrent demonstrating high performance polymer solar cells (PSCs).²² These have been explored as semiconductors²³ and antioxidants.²⁴ Their aptitude as NMR probe renders their use as NMR shift reagents.²⁵ Metal chelate anions of beta-ketoenolates have also shown the ability for laser emission under specific conditions.²⁶ The appropriate combination of volatility and thermal stability make these complexes suitable precursors for chemical vapor deposition.²⁷ These metal complexes have been found to be effective against fungal attack on canvas-paint systems.²⁸ $\text{Pd}(\text{acac})_2$ reveals proapoptotic activity by activating endoplasmic reticulum stress, which makes them a promising candidate as a future metal-based anticancer drug development.²⁹ β -Diketone-cobalt complex,

$\text{Co}(\text{acac})_2(\text{H}_2\text{O})_2$, has recently been reported to exhibit potential antitumor activity which demonstrates an ability to form a new family of non-platinum metal based antitumor drugs.³⁰

Thus, acetylacetonates are versatile ligands demonstrating diverse metal coordination and various fields of application. Moreover, polyoxometalates (POMs) as discussed in chapter-1 display various useful properties. So far, coordination of acetylacetonates with POMs has never been explored. Considering our goal of preparing a POM-based bimetallic system, acetylacetonate becomes a potential candidate as a remote functionality with a strong metal coordinating ability. Covalent grafting of the acetylacetonate moiety onto the hexamolybdate cluster may give rise to a novel architecture. Furthermore, maintaining the conjugation between these units in a POM hybrid might lead to functional materials with interesting and favorable properties. In this chapter, we will attempt to use acetylacetonate ligand as an imido delivery reagent to prepare novel POM hybrids with potential for use in the fields of electrochemistry.

5.2 Experimental

$(\text{TBA})_2[\text{Mo}_6\text{O}_{18}]$ and $(\text{TBA})_4[\text{Mo}_8\text{O}_{26}]$ were prepared according to literature methods.³¹ All other starting materials and Pd(II) catalyst were purchased from Sigma Aldrich, TCI America, Matrix Scientific or Fisher Scientific. Silica gel was purchased from AnalTech (150 Å pore). Solids were dried under vacuum at 40°C for 24 hours prior to use. All manipulations were done under an inert atmosphere of argon, unless otherwise stated. Tetrahydrofuran (THF) was distilled over sodium; dichloromethane was dried over P_2O_5 and distilled; and triethylamine, diethylether and acetonitrile (CH_3CN) were dried over CaH_2 and distilled as needed. All glassware was thoroughly dried by flame under reduced pressure. ^1H , ^{13}C and ^{31}P NMR spectra were recorded on a Varian Unity plus 400 MHz spectrometer and were referenced to residual protonated solvent peaks ($\text{CDCl}_3 = 7.27$ ppm, $\text{CD}_3\text{CN} = 1.94$ ppm, $\text{D}_2\text{O} = 4.80$ ppm and $\text{DMSO-d}^6 = 2.50$ ppm). FT-IR spectra were recorded on a Nicolet 380 instrument. Melting points were determined on a Fisher-Johns melting point apparatus and are uncorrected. X-ray data was collected on a Bruker SMART 1000 four-circle CCD diffractometer at 203 K using a fine-focus molybdenum $\text{K}\alpha$ tube.

5.2.1 Synthesis of 4-iodobenzaldehyde, 43³²

4-iodobenzonitrile (12.0g, 52.40 mmol) was dissolved in 150 mL anhydrous dichloromethane in a round bottom flask fitted under argon environment. The flask was then

kept on ice-water bath. To this, 1M solution of DIBAL-H in hexane (64mL, 64mmol) was added slowly in a course of an hour. The reaction mixture was then left to stir for 5h. On completion the reaction mixture was poured on 400g of ice. The mixture was then acidified with 5M HCl (500mL) and was stirred for 2h. The pH of the solution was brought to 7-8 with 6M NaOH solution and the mixture was extracted with dichloromethane (3x 100 mL), washed further with brine (100mL) and dried over Na₂SO₄. The solvent was removed under vacuum to obtain a yellow-colored product. Yield: 11.22g, 92.29%; mp 79-80°C (lit.³² 77-78°C); ¹H NMR (400 MHz, CDCl₃) δ ppm: 7.60 (m, J=7.52 Hz, 2 H) 7.92 (m, J=7.25 Hz, 2 H) 9.97 (s, 1 H).

5.2.2 Synthesis of biacetyl-trimethylphosphite adduct, 44³³

In a flame-dried round bottom flask, trimethyl phosphite (40mL, 339.14 mmol) was taken under argon environment and the flask was kept over ice-water bath. To this, diacetyl (23.50mL, 267.47 mmol) was added dropwise over the course of an hour while observing the yellow color changing to colorless. The reaction mixture was left to stir overnight. The product was obtained as a colorless liquid and was stored under argon.

5.2.3 Synthesis of 4-hydroxy-3-(4-iodophenyl)pent-3-en-2-one, 45³⁴

43 (10g, 43.10 mmol) was taken in a round bottom flask fitted under argon environment. To this, **44** (11.64 mL, 64.66 mmol) was added and the mixture was stirred at room temperature for 24h. Then, 200mL of methanol was added to the mixture and it was refluxed for 4h. On cooling, the solvent from the reaction mixture was reduced to about 50mL under vacuum. It was cooled further over dry ice and the white precipitate formed was collected with filtration. The filtrate was left overnight and white crystals were observed further which were collected and all the product was combined washed with cold methanol solution and dried under air. Yield: 9.6g, 73.72%; mp 121-123°C (lit.³⁴ 120-121°C); ¹H NMR (400 MHz, CDCl₃) δ ppm: 1.86 - 1.93 (m, 6 H) 6.94 (d, J=8.33 Hz, 2 H) 7.74 (d, J=8.33 Hz, 2 H) 16.67 (s, 1 H); ¹H NMR (400 MHz, CD₃CN) δ ppm: 1.84 (s, 7 H) 7.04 (d, J=8.30 Hz, 2 H) 7.78 (d, J=8.30 Hz, 2 H) 16.78 (s, 1 H).

5.2.4 Synthesis of 3-(4-((4-aminophenyl)ethynyl)phenyl)-4-hydroxypent-3-en-2-one, 46

45 (8.522g, 28.22 mmol) was dissolved in 100 mL anhydrous THF. To this, copper(I) iodide (0.163g, 0.96 mmol), triphenylphosphine (0.6844g, 2.61 mmol) and dichlorobis(triphenylphosphine)palladium(II) (0.5876g, 0.83 mmol) were added and stirred

under inert condition. Further on, 150 mL of triethylamine and a solution of **32** (4.00g, 34.14 mmol) in 50 mL anhydrous THF were added. The reaction mixture was heated at 80°C for 3d. On completion, the reaction mixture was diluted with 100 mL ethyl acetate and the organics were extracted. The aqueous layer was further washed with ethyl acetate (2x 50mL). All the organic layers were combined, washed with brine (2x100 mL) and dried over Na₂SO₄. The solvent was then removed under vacuum. The pure product was obtained after column chromatography with Hexane:Ethyl acetate (80:20) as eluent. Yield: 2.4g, 29.21%; IR (ZnSe): 1626 cm⁻¹ (ν_{C=O}), 1595 (ν_{C=C}); mp 138-141°C; ¹H NMR (400 MHz, CDCl₃) δ ppm: 1.91 (s, 6 H) 3.85 (br. s., 2 H) 6.66 (d, J=8.75 Hz, 2 H) 7.15 (m, J=8.26 Hz, 2 H) 7.36 (d, J=8.75 Hz, 2 H) 7.52 (m, J=8.26 Hz, 2 H) 16.68 (s, 1 H); ¹H NMR (400 MHz, CD₃CN) δ ppm: 1.81 - 1.91 (m, 6 H) 4.47 (br. s., 2 H) 6.60 - 6.68 (m, 2 H) 7.18 - 7.35 (m, 4 H) 7.44 - 7.56 (m, 2 H); ¹H NMR (400 MHz, DMSO-d₆) δ ppm: 1.87 (s, 6 H) 5.57 (s, 2 H) 6.56 (d, J=8.30 Hz, 2 H) 7.20 (d, J=8.30 Hz, 2 H) 7.28 (m, J=7.81 Hz, 2 H) 7.48 (m, J=7.81 Hz, 2 H) 16.83 (br. s., 1 H); ¹³C NMR (400 MHz, CDCl₃) δ ppm: 24.16, 86.81, 90.81, 112.41, 114.74, 123.21, 131.08, 131.77, 133.00, 136.30, 146.78, 190.84.

5.2.5 Synthesis of Triphenylphosphinimine of 3-(4-((4-aminophenyl)ethynyl)phenyl)-4-hydroxypent-3-en-2-one, 47

In a 50 mL round bottom flask, **46** (0.25g, 0.8587 mmol), triphenylphosphine dibromide (0.3625g, 0.8587 mmol) were combined with 10 mL of anhydrous benzene in glove box. To this, anhydrous triethylamine (0.48 mL, 3.4348 mmol) was added and stirred. The reaction mixture was then refluxed for 16h. On cooling, the mixture was filtered and the solvent from resulting dark red solution was removed under vacuum. Yield: 0.3111g (65.69%, based on ¹H NMR); ³¹P NMR (400 MHz, CDCl₃, ref = H₃PO₄): 5.59 ppm.

5.2.6 Reaction of 3-(4-((4-aminophenyl)ethynyl)phenyl)-4-hydroxypent-3-en-2-one with manganese (II), 46.Mn

46 (0.015g, 0.0515 mmol) was dissolved in 2mL acetonitrile to which a drop of triethylamine was added. A separate solution of Mn(ClO₄)₂.6H₂O (0.0094g, 0.0258 mmol) was prepared in 1mL acetonitrile and both the solutions were mixed together resulting in brown precipitate which was filtered off and dried in air. Yield: 0.0074g (45.12%); IR (ZnSe): 1597 cm⁻¹ (ν_{C=O}), 1578 (ν_{C=C}).

5.2.7 Reaction of 3-(4-((4-aminophenyl)ethynyl)phenyl)-4-hydroxypent-3-en-2-one with cobalt(II), 46.Co

46 (0.015g, 0.0515 mmol) was dissolved in 2mL acetonitrile to which a drop of triethylamine was added. A separate solution of $\text{Co}(\text{BF}_4)_2 \cdot 6\text{H}_2\text{O}$ (0.0088g, 0.0258 mmol) was prepared in 1mL acetonitrile and both the solutions were mixed together resulting in green-brown precipitate which was filtered off and dried in air. Yield: 0.0082g (51.57%); IR (ZnSe): 1595 cm^{-1} ($\nu_{\text{C=O}}$), 1572 cm^{-1} ($\nu_{\text{C=C}}$).

5.2.8 Reaction of 3-(4-((4-aminophenyl)ethynyl)phenyl)-4-hydroxypent-3-en-2-one with nickel (II), 46.Ni

46 (0.015g, 0.0515 mmol) was dissolved in 2mL acetonitrile to which a drop of triethylamine was added. A separate solution of $\text{Ni}(\text{BF}_4)_2 \cdot 6\text{H}_2\text{O}$ (0.0088g, 0.0258 mmol) was prepared in 1mL acetonitrile and both the solutions were mixed together resulting in lime green precipitate which was filtered off and dried in air. Yield: 0.0086g (52.12%); IR (ZnSe): 1610 cm^{-1} ($\nu_{\text{C=O}}$), 1564 cm^{-1} ($\nu_{\text{C=C}}$).

5.2.9 Reaction of 3-(4-((4-aminophenyl)ethynyl)phenyl)-4-hydroxypent-3-en-2-one with copper (II), 46.Cu

46 (0.06g, 0.1030 mmol) was dissolved in 5mL acetonitrile to which 4 drops of triethylamine was added. A separate solution of $\text{Cu}(\text{BF}_4)_2 \cdot 6\text{H}_2\text{O}$ (0.0489g, 0.0515 mmol) was prepared in 4mL acetonitrile and both the solutions were mixed together resulting in green-brown precipitate. The reaction mixture was left as such for solvent evaporation which yield dark green crystals which were analyzed by X-ray crystallography. Yield: 0.0156g (47.07%); IR (ZnSe): 1600 cm^{-1} ($\nu_{\text{C=O}}$), 1563 cm^{-1} ($\nu_{\text{C=C}}$).

5.2.10 Reaction of 3-(4-((4-aminophenyl)ethynyl)phenyl)-4-hydroxypent-3-en-2-one with zinc (II), 46.Zn

46 (0.30g, 1.0304 mmol) was dissolved in 5mL acetonitrile to which 3 drops of triethylamine was added. A separate solution of $\text{Zn}(\text{HClO}_4)_2 \cdot 6\text{H}_2\text{O}$ (0.1918g, 0.5152 mmol) was prepared in 2mL acetonitrile and both the solutions were mixed together. The instantaneous pale yellow precipitate that formed was filtered off, washed with acetonitrile and dried in air. Yield: 0.2269g (68.24%); IR (ZnSe): 1598 cm^{-1} ($\nu_{\text{C=O}}$), 1581 cm^{-1} ($\nu_{\text{C=C}}$); ^1H NMR (400 MHz, DMSO- d_6) δ

ppm: 1.67 (br. s., 6 H) 5.55 (br. s., 2 H) 6.56 (d, $J=7.81$ Hz, 2 H) 7.20 (br. s., 2 H) 7.45 (d, $J=6.84$ Hz, 2 H).

5.2.11 Reaction of 3-(4-((4-aminophenyl)ethynyl)phenyl)-4-hydroxypent-3-en-2-one with indium (II), 46.In

46 (0.015g, 0.0515 mmol) was dissolved in 5mL acetonitrile to which 2 drops of triethylamine was added. A separate solution of $\text{In}(\text{NO}_3)_2 \cdot x\text{H}_2\text{O}$ (0.0155g, 0.0258 mmol) was prepared in 2mL acetonitrile and both the solutions were mixed together. The instantaneous off-white precipitate that formed was filtered off, washed with acetonitrile and dried in air. Yield: 0.0112g (62.57%); IR (ZnSe): 1601 cm^{-1} ($\nu_{\text{C=O}}$), 1576 cm^{-1} ($\nu_{\text{C=C}}$).

5.2.12 Synthesis of 3-(4-((4-aminophenyl)ethynyl)phenyl)-4-hydroxypent-3-en-2-one hydrochloride, 48

In a 100 mL beaker, **46** (0.5g, 1.72 mmol) was dissolved in 5 mL anhydrous THF and 2N HCl in ether (0.86 mL, 1.72 mmol) was added and instant precipitation was observed. The reaction mixture was stirred for 2h at room temperature and the precipitate was filtered off, washed twice with THF and dried under vacuum for 24h. Yield: 0.52g (92.42 %); ^1H NMR (400 MHz, CDCl_3) δ ppm: 1.91 (s, 6 H) 7.21 (s, 2 H) 7.57 (s, 4 H) 7.62 (s, 2 H) 16.69 (s, 1 H); ^1H NMR (400 MHz, DMSO-d_6) δ ppm: 1.87 (s, 6 H) 7.00 (br. s., 2 H) 7.31 (d, $J=7.81$ Hz, 2 H) 7.44 (m, $J=7.81$ Hz, 2 H) 7.54 (m, $J=7.81$ Hz, 2 H) 16.84 (br. s., 1 H).

5.2.13 Synthesis of Triphenylphosphinimine of 4-ethynylaniline, 49

In a 50 mL round bottom flask, **32** (0.5g, 4.268 mmol), triphenylphosphine dibromide (1.8015g, 4.268 mmol) were combined with 10 mL of anhydrous benzene in glove box. To this, anhydrous triethylamine (1.1906 mL, 3.4348 mmol) was added and stirred. The reaction mixture was then refluxed for 16h. On cooling, the mixture was filtered and the solvent from resulting dark red solution was removed under vacuum. Yield: 1.4004g (87%, based on ^1H NMR); 2.95 (s, 1 H) 6.71 (d, $J=8.18$ Hz, 3 H) 7.16 (d, $J=7.27$ Hz, 3 H); ^{31}P NMR (400 MHz, CDCl_3 , ref = H_3PO_4): 5.81 ppm.

5.3 Results and discussion

5.3.1 Synthesis of 3-(4-((4-aminophenyl)ethynyl)phenyl)-4-hydroxypent-3-en-2-one

Considering the electron withdrawing nature of hexamolybdate, **46** was selected as anchoring ligand (Figure 5.5). It was designed in a way to keep the acetylacetonate functionality at a distance from the cluster to keep the remote functionality active for metal coordination.

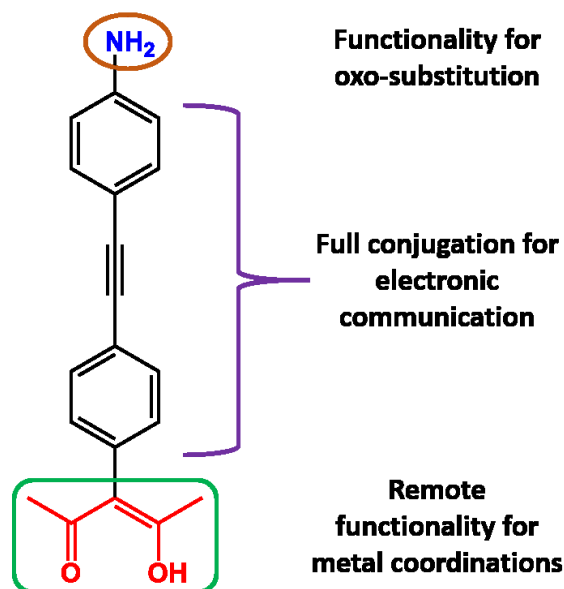


Figure 5.5 Designing of the organoimido delivery reagent, **46**.

One end of the ligand bears NH_2 group which can reliably undergo oxo substitution in hexamolybdate cluster to covalently modify the cluster, while the other side bears the acetylacetonate moiety for coordinating to a second metal atom. The conjugation within the system may give rise to the possibility of electronic communication between the two metal centers.

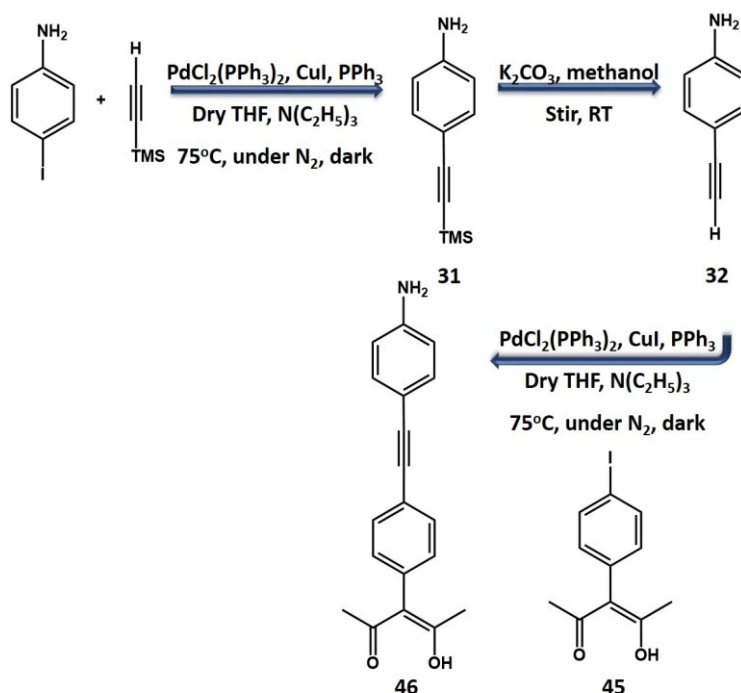


Figure 5.6 Synthetic scheme for **46**.

Once the designing of the ligand was done, the synthetic scheme for **46** was prepared (Figure 5.6). The first two steps of the scheme is common to that used in the synthesis of **33** and **34** ligands in chapter-4, thus have been discussed before. After **32** was synthesized, before the second Sonogashira coupling, **45** is needed for which the literature method was followed (Figure 5.7).^{32,34}

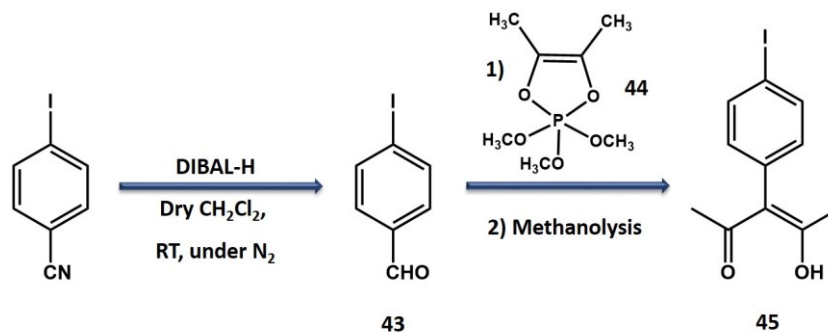


Figure 5.7 Synthetic scheme of **45**.^{32,34}

At first, the reduction of the nitrile group in 4-iodobenzonitrile, **43** was achieved using DIBAL-H as the reducing agent.³² The appearance of a new peak in the ¹H NMR spectrum at 9.97 ppm characteristic of the aldehyde functionality confirmed the conversion of CN group to CHO group. Furthermore, to convert CHO group to the acac functionality, **43** was stirred for 24h with **44** at room temperature and methanolysis of the corresponding reaction mixture was done

for 4h.³⁴ After removing the solvent and cooling the resulting oil to -78°C , product was isolated as a white precipitate. In ^1H NMR spectrum, the disappearance of the peak at 9.97 ppm and the appearance of a new peak at 16.67 ppm corresponding to the enol-proton of the acac moiety was observed which confirmed the complete conversion of CHO group to the acac moiety. An additional peak at 1.90 ppm for two CH_3 protons of the acac moiety further substantiate the synthesis of the desired product, **45**. Once the synthesis of **45** was confirmed, it was subjected to Sonogashira coupling with **32** to obtain the anticipated **46**.

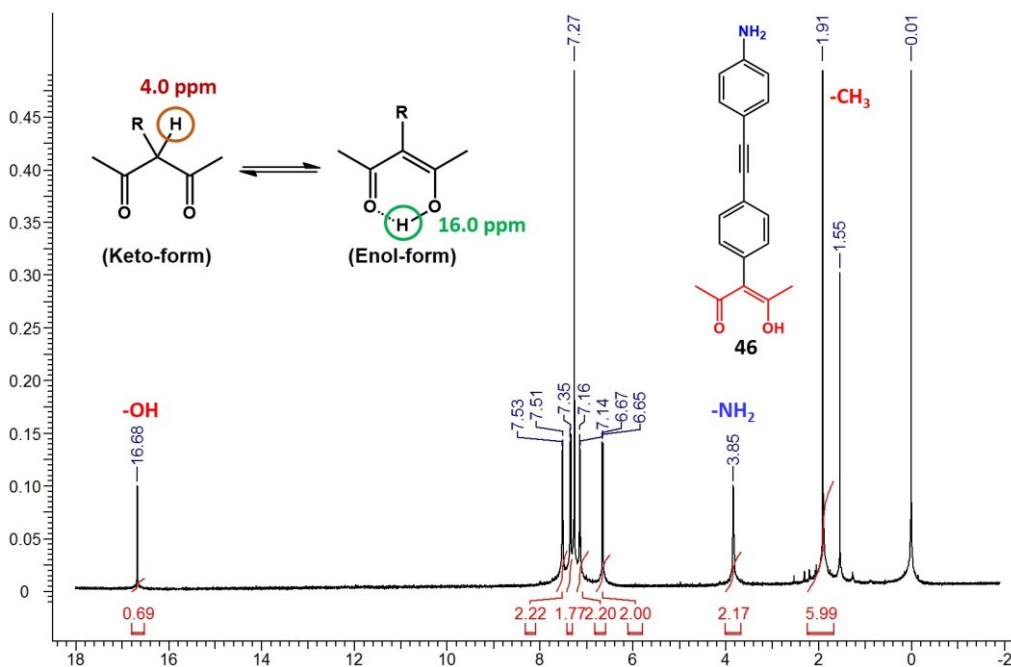


Figure 5.8 ^1H NMR spectrum of **46**.

^1H NMR spectrum of **46** shows a set of four aromatic peaks suggesting the coupling of the two aromatic rings. The peaks at 1.91 and 3.85 ppm show the presence of $-\text{CH}_3$ and $-\text{NH}_2$ groups (Figure 5.8). A peak at 16.68 ppm characteristic of the enol-proton suggests that the ligand exists as the enol tautomer.

5.3.2 Single crystal structure of 3-(4-((4-aminophenyl)ethynyl)phenyl)-4-hydroxypent-3-en-2-one

The single crystal structure determination of **46** shows that the molecule exists as the enol tautomer exhibiting intramolecular $\text{O}-\text{H}\cdots\text{O}$ hydrogen-bonding (Figure 5.9). The two aromatic rings are non-planar and are orthogonal to each other. The NH_2 group further displays H-bonding

with the oxygen atom of the acac moiety of a neighboring molecule, thus extending the network into 1-D chains.

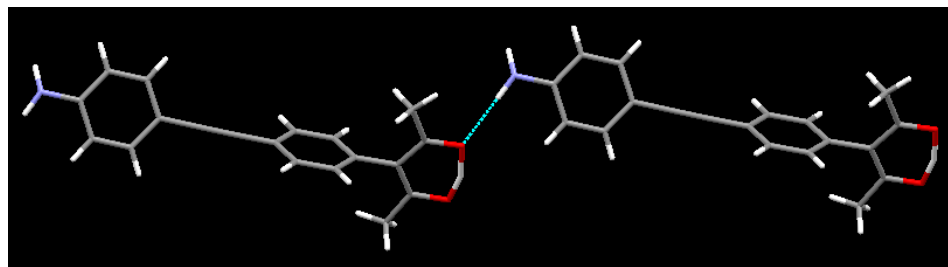


Figure 5.9 X-ray crystal structure of **46**.

5.3.3 Phosphineimine derivative (47) of 46 as imidodelivery reagent

Confirming the synthesis of **46**, phosphineimine derivative, **47** was prepared by refluxing it with PPh_3Br_2 and triethylamine. Usually, triethylamine is taken 2 equivalents to **46** but since **46** bears an acac group, wherein the enolic proton is also susceptible to deprotonation, an excess of triethylamine was used in this case. ^1H NMR of the reaction mixture displayed the emergence of some new peaks but was inconclusive as the region of interest is crowded by the peaks for triphenylphosphine oxide, which is a side product of the reaction. Thus to confirm the synthesis of **47**, ^{31}P NMR was used as a conclusive technique which shows a new peak at 5.59 ppm different from other possible compounds, which also falls close in range to the reported phosphineimines, thus confirming the formation of the derivative (Figure 5.10).

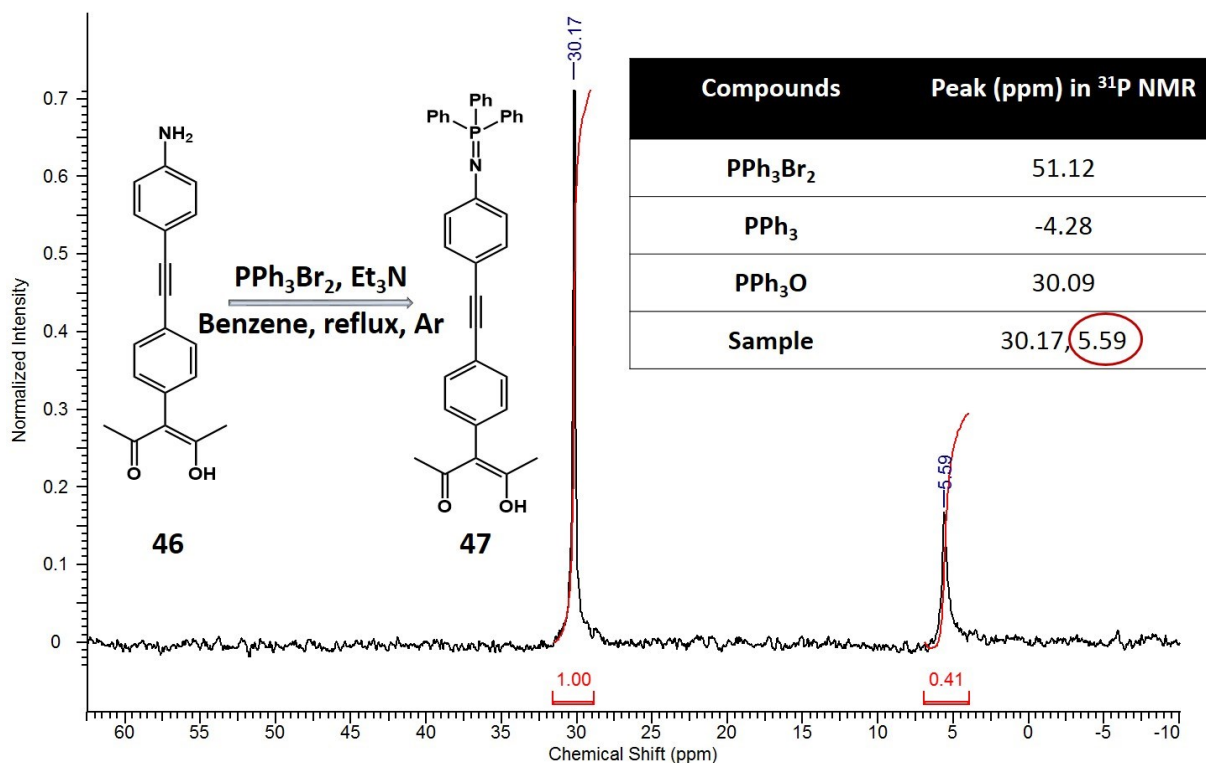


Figure 5.10 ^{31}P NMR spectrum of **47**.

Owing to the sensitivity of **47**, no further purification could be done. It was then incorporated as an organoimido delivery reagent to functionalize hexamolybdate following Maatta *et. al.* synthetic route.³⁵ No color changes were observed, thus suggesting the failure of the reaction, which was further confirmed by ^1H NMR spectroscopy where peaks corresponding to **46** reappeared in the spectrum, thus indicating a decomposition of the phosphineimine compound.

5.3.4 Synthesis of metal complexes of 3-(4-((4-aminophenyl)ethynyl)phenyl)-4-hydroxypent-3-en-2-one

As the acac moiety is prone to deprotonation in the presence of triethylamine in phosphineimine synthesis, we thought of blocking the site first by coordinating it to some metal ions to avoid any kind of interference. Thus, some metal complexes of **46** were prepared and analyzed using infrared spectroscopy since it is a strong tool to characterize the acac ligand and its corresponding metal complexes.

5.3.4.1 Characterization of metal complexes of 46 using infrared spectroscopy

The C=O and C=C bond stretches in acac moiety shows up around 1626.97 and 1595.72, respectively in **46** (Table 5.1). Metal ion coordinates to acac moiety, thus significant shifts in the corresponding bands are indicative of successful metal complexation.

Table 5.1 IR shifts observed for metal complexes of **46**.

Compounds	Observed bands in infrared spectra (cm ⁻¹)	
	46	1626
46.Mn	1597	1578
46.Co	1595	1572
46.Ni	1601	1564
46.Cu	1600	1563
46.Zn	1598	1581
46.In	1601	1576

5.3.4.2 Single crystal structure of 46.Cu

Furthermore, the single crystals of **46.Cu** were successfully obtained and analyzed by single crystal X-ray diffraction, wherein the copper(II) ion is tetra-coordinated displaying a distorted square planar geometry (Figure 5.11). Similar to the structure of the ligand, the two aromatic rings are orthogonal to each other. The H-bonding character is retained in the metal complex, wherein the NH₂ group displays a bifurcated hydrogen-bond to the metal-coordinated acac oxygen atoms of a neighboring molecule.

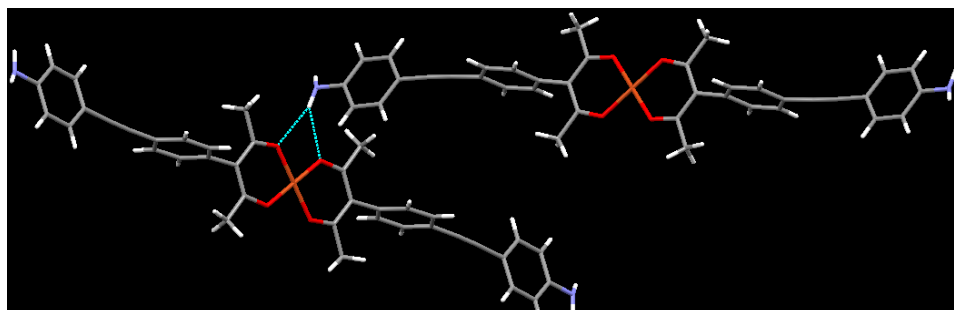


Figure 5.11 X-ray crystal structure of **46.Cu**.

5.3.4.3 ^1H NMR spectroscopic study of **46.Zn** complex

Amongst the synthesized metal complexes, only **46.Zn** is diamagnetic and can be characterized by ^1H NMR spectroscopy (Figure 5.12). The addition of triethylamine abstracts the enol-proton and the activated acac moiety then coordinates to the metal ion. Thus, one indicative feature is the disappearance of the peak corresponding to the enol-proton of the acac moiety. Moreover, due to the metal coordination at the acac moiety, the peak in the aliphatic region corresponding to CH_3 -groups also show a shift of 0.2 ppm. The aromatic region also seems to have been slightly shifted in the spectrum, thus supporting the formation of the metal-complex.

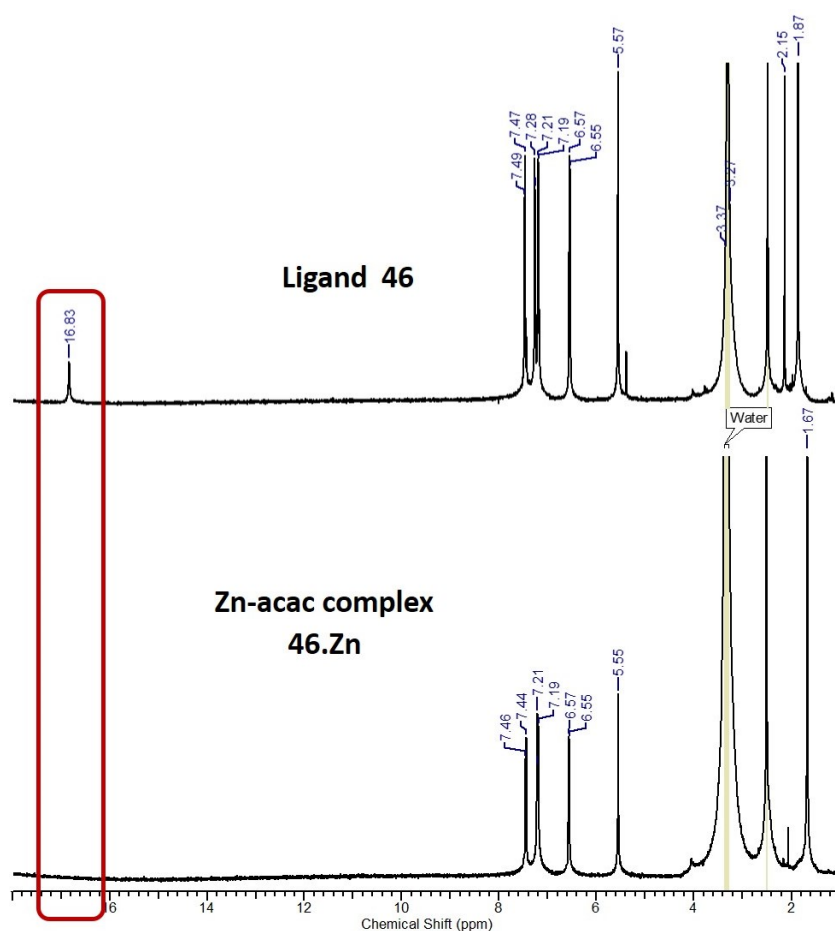


Figure 5.12 ^1H NMR spectrum of **46.Zn**.

5.3.5 **46.Zn** metal complex as imidodelivery reagent

46.Zn metal complex being the only diamagnetic system, was used for the attempted synthesis of the hexamolybdate derivatives. Due to low solubility of the zinc complex, the synthesis of its phosphinimine derivative was not attempted. Wei's method of functionalization

could not be attempted as HCl salt of zinc complex could not be prepared owing to its low solubility.

5.3.5.1 Attempts for covalent grafting of 46.Zn on to hexamolybdate using Peng's route

Following Peng's protocol, **46.Zn** complex was refluxed with hexamolybdate and DCC with excess solvent. The color change from yellow to red-brown was promising, but further analysis did not show the characteristic shoulder peak around 970 cm^{-1} in the infrared spectrum or any peak shifts in NMR spectra as would be expected for the hexamolybdate hybrid.

5.3.5.2 Microwave assisted covalent grafting of 46.Zn on hexamolybdate

As discussed in Chapter-2, microwave irradiation leads to dielectric heating which remotely introduces microwave energy into the chemical reactor, which in turn passes through the walls of the vessel without heating it and heats only the reactants and solvent uniformly, thus leading to less by-products and/or decomposition products.^{36,37} Following the concept, we postulated that the solubility of **46.Zn** complex might be enhanced under microwave conditions. To test this hypothesis, an attempt to covalent graft the **46.Zn** complex onto hexamolybdate under microwave conditions was undertaken. First the reaction was conducted for 10 min and no color change could be observed. After 30 min, a slight color started to develop. Finally, the reaction was conducted for an hour after which the color of the solution was observed to turn red-brown, which seemed promising. Unfortunately on further analysis, no evidence of grafting of the zinc complex on to the POM cluster could be observed.

5.3.6 Attempts to use 46 as imidodelivery reagent

Since no further reactions with the metal complexes could be done owing to their poor solubility, **46** was then used by itself as an organoimido delivery reagent *via* Peng's route of functionalization, but no color change for the reaction mixture was observed and spectroscopic characterization confirmed the reaction to be unsuccessful.

Next, to try Wei's route of functionalization, first the HCl salt of **46**, **48** was prepared and was characterized by NMR spectroscopy. The disappearance of the peak at 5.57 ppm for the NH_2 -group and the shifts in the aromatic peaks confirmed the synthesis of the HCl salt of the ligand. Later on, following Wei's method, **46** and **48** were refluxed with octamolybdate and DCC in acetonitrile. Again, the color change of the reaction mixture was encouraging, but

further analysis showed no shoulder peak at 970 cm^{-1} and the ^1H NMR spectrum showed peaks corresponding to both the ligand and hexamolybdate, thus suggesting that only a mixture of the two components existed.

5.3.7 Attempts to use phosphineimine derivative of 4-ethynylaniline as imidodelivery reagent

Since, all the attempts with **46** failed, we thought of preparing a POM derivative of 4-ethynylaniline, **32** and doing a post-synthetic modification on the obtained POM cluster *via* Sonogashira coupling reactions. Thus, phosphineimine derivative (**49**) of **32** was prepared. In ^1H NMR spectrum, the peak at 3.82 ppm corresponding to NH_2 -group disappeared and two new peaks in the aromatic region showed up at 6.70 and 7.15 ppm which suggested the successful synthesis of **49**. To gain further confirmation on **49**, ^{31}P NMR spectroscopy was used, wherein a new peak corresponding to the product appears at 5.81 ppm. **49** was then incorporated as the organoimido delivery reagent following Maatta's protocol, but the observations and the characterization of the reaction mixture confirmed that no hexamolybdate derivative was formed.

5.4 Conclusions

A novel acetylacetonate moiety was explored as an imidodelivery reagent for synthesizing hexamolybdate covalent hybrids. The acac ligand was prepared *via* a multistep synthetic route. Various attempts with known routes were carried out to covalently graft the ligand on to the hexamolybdate cluster, but without success. The single crystal structures of the ligand and its corresponding copper complex have been determined. An examination of the crystal structure of the copper complex highlights the potential of using it as an imidodelivery reagent since the NH_2 - group is not blocked in any coordination, and thus is available for covalent grafting. Other methods such as heating at elevated temperatures and microwave reactions with the zinc acac complex for synthesizing the hybrids have also proved unsuccessful so far.

References

-
- ¹ McCleverty, J. A.; Meyer, T. J. *Comprehensive Coordination Chemistry II From biology to nanotechnology, Volume 1: Fundamentals: Ligands, Complexes, Synthesis, Purification, and Structure*, Elsevier Pergamon, 2003.
- ² Olivier, J-H.; Harrowfield, J.; Ziessel, R. *Chem. Commun.* **2011**, 47, 11176.
- ³ (a) Kawaguchi, S. *Coord. Chem. Rev.* **1986**, 70, 51; (b) Kawaguchi, S. *Variety in Coordination of Ligands in Metal Complexes: Inorganic Concepts*, Springer Verlag: Berlin, 1988, 11, 75.
- ⁴ Sew, M. *J. Chem. Edu.* **1989**, 66, 779.
- ⁵ (a) Lamprey, H. *Annals of the New York Academy of Sciences* 1960, 88, 519; (b) Bhattacharjee, C. R.; Chaudhuri, M. K. *Proc. Ind. Natn. Sci. Acad.* **1989**, 55, 194.
- ⁶ Taylor, K. *US Patent 3,134,797*, **1964**; *Chem. Abstr.* **1964**, 61, 5233f.
- ⁷ (a) Caille, J. R.; Debuigne, A.; Jérôme, R. *J. Polym. Sci., Part A: Polym. Chem.* **2005**, 43, 2723; (b) Verala, R.; Nasreen, A.; Adapa, S. R. *Can. J. Chem.* **2007**, 85, 148; (c) Struzinski, T. H.; Gohren, L. R.; MacArthur, A. H. R. *Trans. Met. Chem.* **2009**, 34, 637.
- ⁸ (a) Haghihara, N. *J. Chem. Soc. (Japan), Pure Chem. Sect.* **1952**, 73, 323; (b) James D. B. Smith, J. D. B.; Kauffman, R. N. *US 4254351 A*, **1981**.
- ⁹ (a) Nitzsche, S. *US Patent 2645629*, **1953**; (b) Caille, J. R.; Debuigne, A.; Jérôme, R. *J. Polym. Sci., Part A: Polym. Chem.* **2005**, 43, 2723; (c) Haghihara, N. *J. Chem. Soc. (Japan), Pure Chem. Sect.* **1952**, 73, 323.
- ¹⁰ (a) Roebuckd, D. S. P. *US Patent 2644840*, **1953**; (b) Sodhi, R. K.; Paul, S.; Clark, J. H. *Green Chem.* **2012**, 14, 1649; (c) Tsunoji, N.; Ide, Y.; Yagenji, Y.; Sadakane, M.; Sano, T. *ACS Appl. Mater. Interfaces* **2014**, 6, 4616.
- ¹¹ Pereira, C.; Silva, J. F.; Pereira, A. M.; Araújo, J. P.; Blanco, G.; Pintado, J. M.; Freire, C. *Catal. Sci. Technol.* **2011**, 1, 784.
- ¹² Verala, R.; Nasreen, A.; Adapa, S. R. *Can. J. Chem.* **2007**, 85, 148.
- ¹³ Struzinski, T. H.; Gohren, L. R.; MacArthur, A. H. R. *Trans. Met. Chem.* **2009**, 34, 637.
- ¹⁴ Brandstroay, A. *Arkiv. Kem.* **1955**, 7, 65.
- ¹⁵ Jolly, P. W.; Wilke, G. *The chemistry of Nickel*, Academic Press: New York, **1975**.
- ¹⁶ Hofacker, S. *US 20060052572 A1*, **2006**.
- ¹⁷ Kumar, S.; Jain, S.; Sain, B. *Cat. Lett.* **2012**, 142, 615.
- ¹⁸ Maisner, H. *US Patent 2690964*, **1954**; Maisner, H. *US Patent 2712,989*, **1955**.
- ¹⁹ Laurence, E. A.; VonBrecht, F. L. *US Patent 2815270*, **1957**.
- ²⁰ (a) McKavenery, J. P.; Fraiser, H. *Anal. Chem.* **1957**, 29, 288; (b) McKavenery, J. P.; Fraiser, H. *Anal. Chem.* **1958**, 30, 1965; (c) Morrison, G. H.; Frieser, H. *Solvent Extraction in Analytical Chemistry*, Wiley: New York, 1957.
- ²¹ Haryono, A.; Harmami, S. B.; Sondari, D. *Material Science Forum* **2013**, 737, 153.
- ²² Tan, Z.; Li, S.; Wang, F.; Qian, D.; Lin, J.; Hou, J.; Li, Y. *Scientific Reports* **2013**, Article number 4691.
- ²³ Chappe, A. P.; Vargas, J. I. *Phys. Stat. Solid A.* **1972**, 10, 4543.
- ²⁴ Stemmiski, J. R.; Wilson, G. S.; Smith, J. O.; McHugh, K. L. *Trans. Am. Soc. Lub. Engne.* **1964**, 7, 43.

-
- ²⁵ (a) Heinrichs, P. M.; Gross, S. *J. Magn. Reson.* **1975**, *17*, 399; (b) Levy, G. C.; Dechter, J. J. *J. Am. Chem. Soc.* **1978**, *100*, 2308.
- ²⁶ (a) Lempicki, A.; Samelson, H. *Phys. Rev. Lett.* **1963**, *4*, 133; (b) Schimitschek, E. J. *Appl. Phys. Lett.* **1963**, *3*, 117.
- ²⁷ Premkumar, P. A.; Bahlawane, N.; Reiss, G.; Kohse-Höinghaus, K. *Chem. Vap. Deposition* **2007**, *13*, 227.
- ²⁸ Stoner, J. H.; Indictor, N.; Baer, N. S. *J. Am. Inst. for Conserv.* **1973**, *13*, 114.
- ²⁹ Wang, Y.; Hu, J.; Cai, Y.; Xu, S.; Weng, B.; Peng, K.; Wei, X.; Wei, T.; Zhou, H.; Li, X.; Liang, G. *J. Med. Chem.* **2013**, *56*, 9601.
- ³⁰ Zhang, K.; Zhao, X.; Liu, J.; Fang, X.; Wang, X.; Wang, X.; Li, R. *Oncol. Lett.* **2014**, *7*, 881.
- ³¹ Klemperer, W. G.; Ginsberg, A. P. Introduction to Early Transition Metal Polyoxoanions, Inorganic Syntheses, Volume 27, John Wiley & Sons, Inc., 2007.
- ³² Thamyongkit, P.; Muresan, A. Z.; Diers, J. R.; Holten, D.; Bocian, D. F.; Jonathan, S. L. *J. Org. Chem.* **2007**, *72*, 5207.
- ³³ Ramirez, F.; Patwardhan, A. V.; Ramanathan, N.; Desai, N. B.; Greco, C. V.; Heller, S. R. *J. Am. Chem. Soc.* **1965**, *87*, 543.
- ³⁴ Aakeröy, C. B.; Sinha, A. S.; Chopade, P. D.; Desper, J. *Dalton Trans.* **2011**, *40*, 12160.
- ³⁵ Stark, J.; Young, V.; Maatta, E. A. *Angew. Chem. Int. Ed. Engl.* **1995**, *34*, 2547.
- ³⁶ Lidström, P.; Tierney, J.; Wathey, B.; Westman, J. *Tetrahedron* **2001**, *57*, 922.
- ³⁷ Brittany L. Hayes, *Aldrichchimica Acta*, 2004, *37*, 66.

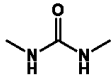
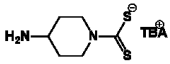
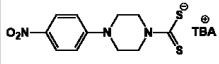
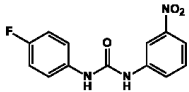
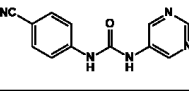
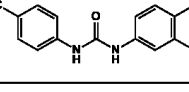
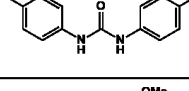
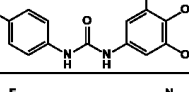
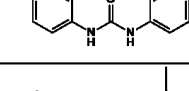
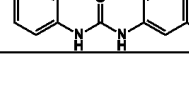
Appendix A - Supramolecular studies with dithiocarbamates

In Chapter 2, dithiocarbamate complexes have been exploited for coordination with the hexamolybdate cluster, wherein the NH_2 - moiety of the molecule is used for oxo-substitution in the cluster, while the dithiocarbamate motif is utilized for coordinating a second metal atom towards the assembly of inorganic-organic hybrids. Supramolecular interactions such as hydrogen- and halogen-bonds have been utilized in a parallel study with these dithiocarbamates as a handle for constructing predictable extended architectures.

A.1 Hydrogen-bonding studies of dithiocarbamates

Dithiocarbamate functionality contains a NCS_2^- moiety where negative charge is evenly distributed between two sulfur atoms, thus creating a pocket which can act as a potential hydrogen bond acceptor site. Considering its geometrical aspects, a series of diphenyl urea molecules were selected, wherein the NH-CO-NH moiety may be used as suitable hydrogen-bond donors. For this, tetrabutylammonium dithiocarbamates were selected so that the NCS_2^- site does not get blocked by the presence of a metal ion, and thus is approachable by the urea motif. A total of 14 grind experiments were done in which equivalent amounts of dithiocarbamate and the urea compounds were ground together in a mortar/pestle using a drop of methanol. Infrared spectroscopy (IR) was used as the analytical tool for identifying the formation of a multicomponent material. Secondary amides usually exhibit characteristic bands in IR for N-H stretch at $3370\text{-}3170\text{ cm}^{-1}$, C=O stretch at $1680\text{-}1630\text{ cm}^{-1}$, N-H in-plane bend at $1570\text{-}1515\text{ cm}^{-1}$, C-N stretch at $1310\text{-}1230\text{ cm}^{-1}$, and N-H out-of-plane bend at $750\text{-}680\text{ cm}^{-1}$.¹ All of these bands except for the carbonyl stretch overlap with the bands observed for the dithiocarbamate molecule. Hence, shifts in the carbonyl stretch has been examined carefully, as any changes would be indicative of the NH-CO-NH moiety being involved in hydrogen bonding with the NCS_2^- moiety of the dithiocarbamates. The results of the grind experiments have been shown in Table A.1.

Table A.1 Results of hydrogen-bond experiments of dithiocarbamates with urea compounds.

Urea	 Original / cm ⁻¹	 Urea mix / cm ⁻¹	Δ (carbonyl L1-urea) cm-1	 Urea mix / cm ⁻¹	Δ (carbonyl L2NO2-urea) cm-1
	1669.38	1706.06	36.68	1703.93	34.55
	1671.15	1692.1	20.95	1699.08	27.93
	1678.13	1702.57	24.44	1702.57	24.44
	1626.45	1692.1	65.65	1699.08	72.63
	1627.36	1695.59	68.23	1692.1	64.74
	1709.55	1702.57	-6.98	1702.42	-7.13
	1625.02	1688.61	63.59	1695.59	70.57

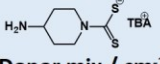
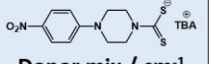
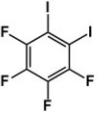
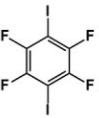
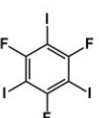
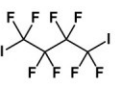
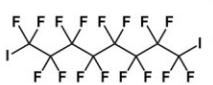
In all the cases, a significant shift in the carbonyl stretch is observed, which suggests possible hydrogen bonding between the two compounds and the formation of multi-component materials. To examine the intermolecular interactions present in the supramolecular architecture, the dithiocarbamates and the urea compounds have been dissolved in equimolar quantities in a solvent of choice and single crystals are being grown *via* slow evaporation technique.

A.2 Halogen-bonding studies of dithiocarbamates

Similar to the hydrogen-bond based study, we also thought of exploring halogen-bond intermolecular interactions as a supramolecular tool for extending the dithiocarbamate architectures. The electron density around the halogen atom nucleus is highly anisotropic which makes them act as Lewis acids, thus giving rise to the possibility of a variety of intermolecular interactions.² Dithiocarbamate functionality bearing NCS₂⁻ moiety results in a negatively charged pocket which can act as a Lewis base, and can potentially result in the formation of multi-component materials held together by bifurcated halogen-bonds. To gain an in-depth knowledge of the postulated interactions, grind experiments were conducted with a series of halogen-bond

donor molecules. A total of 10 grind experiments were done in which equivalent amounts of dithiocarbamate and the halogen-bond donor were ground in a mortar/pestle using a drop of methanol. Infrared spectroscopy (IR) was used as the analytical tool for identifying the possible formation of multicomponent materials. The fundamental C-I bond stretch ($550 - 485 \text{ cm}^{-1}$) falls beyond the detection range of the instrument.³ Hence, to examine the formation of the multicomponent product, the IR spectrum of each reaction mixture was carefully compared with the IR spectra of the individual components, and shifts in the stretches corresponding to C=C, C-F, and C-H bonds were monitored. The resulting shifts from these experiments are depicted in Table A.2.

Table A.2 Results of halogen-bond experiments of dithiocarbamates with halogen-bond donors.

Halogen donors	Original bands / cm^{-1}	 Donor mix / cm^{-1}	Δ (Donor-L1 mix) cm^{-1}	 Donor mix / cm^{-1}	Δ (Donor-L2NO ₂ mix) cm^{-1}
	772.89	756.12	16.77	771.01	1.88
	813.90	807.45	6.45	809.52	4.38
	1023.51	1007.74	15.77	ND	ND
	1438.61	1430.14	8.47	1427.02	11.59
	1489.58	1481.81	7.77	1482.42	7.16
	759.26	749.42	9.84	767.26	-8.00
	940.59	938.38	2.21	925.64	14.95
	947.37	ND	ND	933.60	13.77
	968.99	956.08	12.9	964.09	4.9
	985.40	ND	ND	979.17	6.23
	1214.77	1203.29	11.5	ND	ND
	1356.36	1344.27	12.1	1361.92	-5.56
	1459.45	1453.25	6.2	ND	ND
	704.31	709.28	-5.30	709.14	-4.83
	1049.81	1037.23	12.6	1036.24	13.57
	1325.84	ND	ND	1319.50	6.34
	1403.79	1393.04	10.80	1389.47	14.32
	1562.67	1559.45	3.22	1558.40	4.27
	717.63	ND	ND	723.58	-5.95
	763.61	758.22	5.39	752.51	11.10
	888.43	877.97	10.46	894.59	-6.16
	1040.58	1038.03	2.55	1037.83	2.75
	1133.72	1116.70	17.02	1122.90	10.82
	1192.45	1173.41	19.04	1179.13	13.32
	834.18	-	-	818.19	15.99
	1055.95	1052.47	3.48	1053.82	2.13
	1089.97	-	-	1080.05	9.92
	1112.73	-	-	1105.20	7.5
	1146.86	-	-	1145.32	1.54
	1204.63	1201.00	3.63	1195.55	9.08

Although the magnitude of these shifts are comparatively lower and the direction of the shift (blue/red) is inconsistent, they still indicate the formation of multi-component materials. Similar observations are known to exist as the C=C, C-F, and C-H bonds are not directly involved in the $\text{CS}_2 \cdots \text{X-C}$ halogen bond, and thus are indirectly affected as a result of changes in the neighboring environment in the solid-state.^{4,5}

A.3 Conclusion

We have demonstrated the potential of dithiocarbamate moiety as a supramolecular motif in hydrogen- and halogen-bonding by grinding a series of urea molecules and perfluorinated halogen-bond donors with tetrabutylammonium dithiocarbamates. Infrared spectroscopy has been used as an analytical tool for this study to confirm the formation of multi-component materials. Single crystals of these combinations are being grown for examining the interplay between the different intermolecular interactions present in the crystal lattice and their role in the assembly of extended architectures.

References

- ¹ Infrared Spectral Interpretation: A Systematic Approach. By Brian C. Smith, 1999, CRC Press LLC.
- ² Clark, T.; Hennemann, M.; Murray, J. S.; Politzer, P. *J. Mol. Model.* **2007**, *13*, 291.
- ³ Applications of Infrared, Raman, and Resonance Raman Spectroscopy in Biochemistry. By Frank S. Parker, 1983, Springer Science & Business Media.
- ⁴ Aakeröy, C. B.; Baldrighi, M.; Desper, J.; Metrangolo, P.; Resnati, G. *Chem. Eur. J.* **2013**, *19*, 16240.
- ⁵ Sinha, A. S. *PhD Thesis*, Kansas State University, 2013.

Appendix B - ^1H , ^{13}C and ^{31}P NMR, IR and UV-Visible spectroscopic data

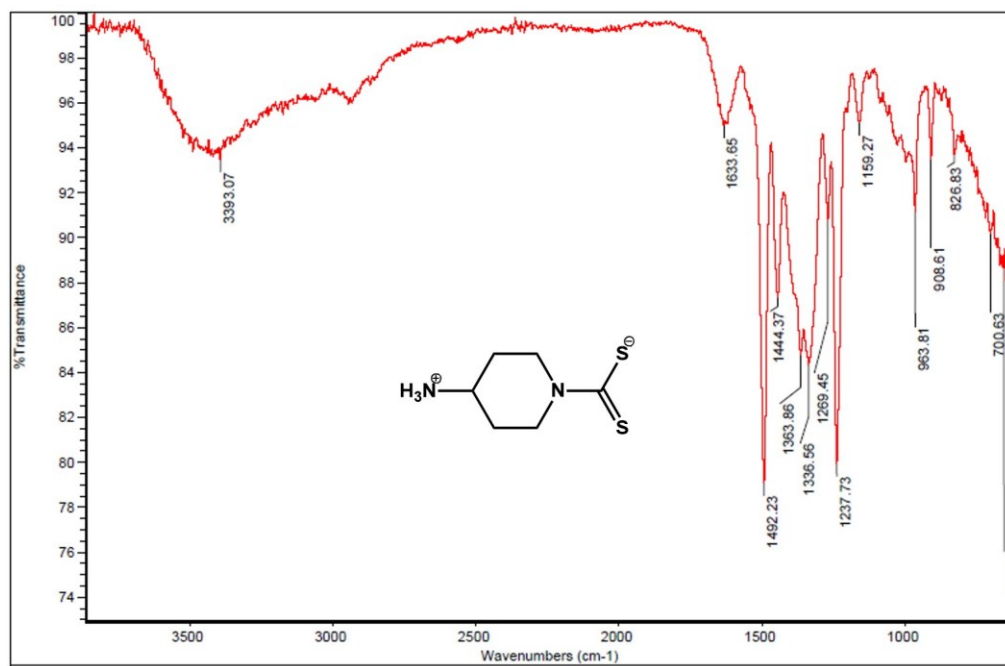


Figure B.1 IR spectrum of 1.

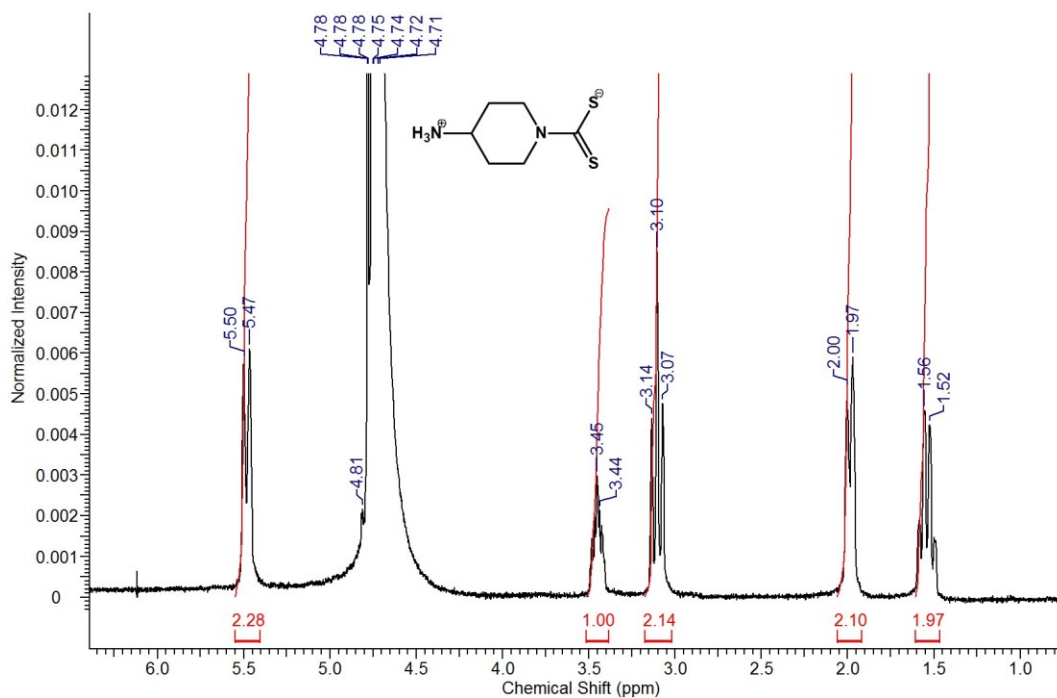


Figure B.2 ^1H NMR spectrum of 1.

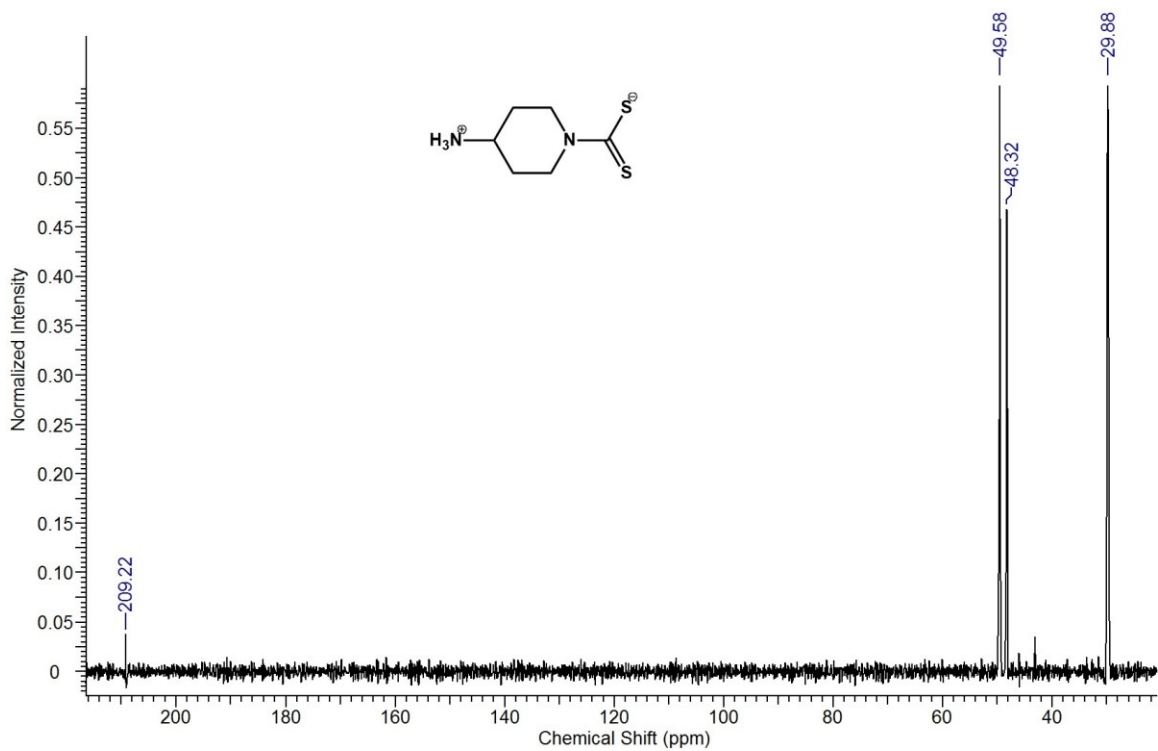


Figure B.3 ^{13}C NMR spectrum of 1.

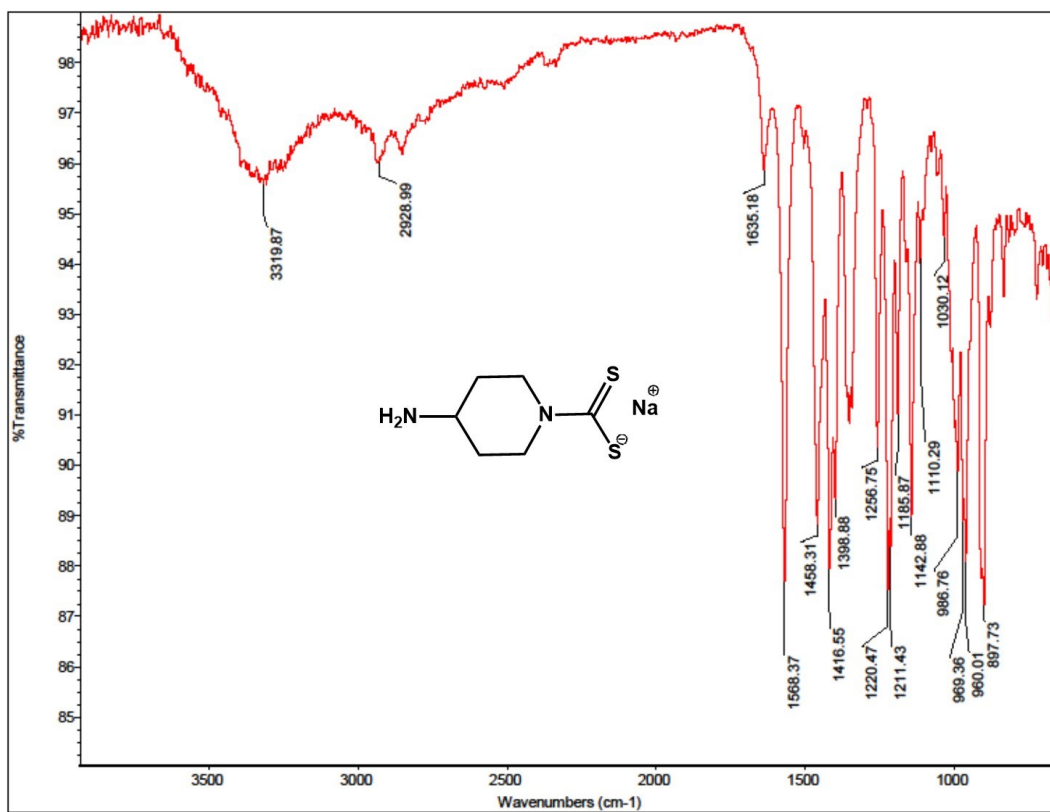


Figure B.4 IR spectrum of 2.

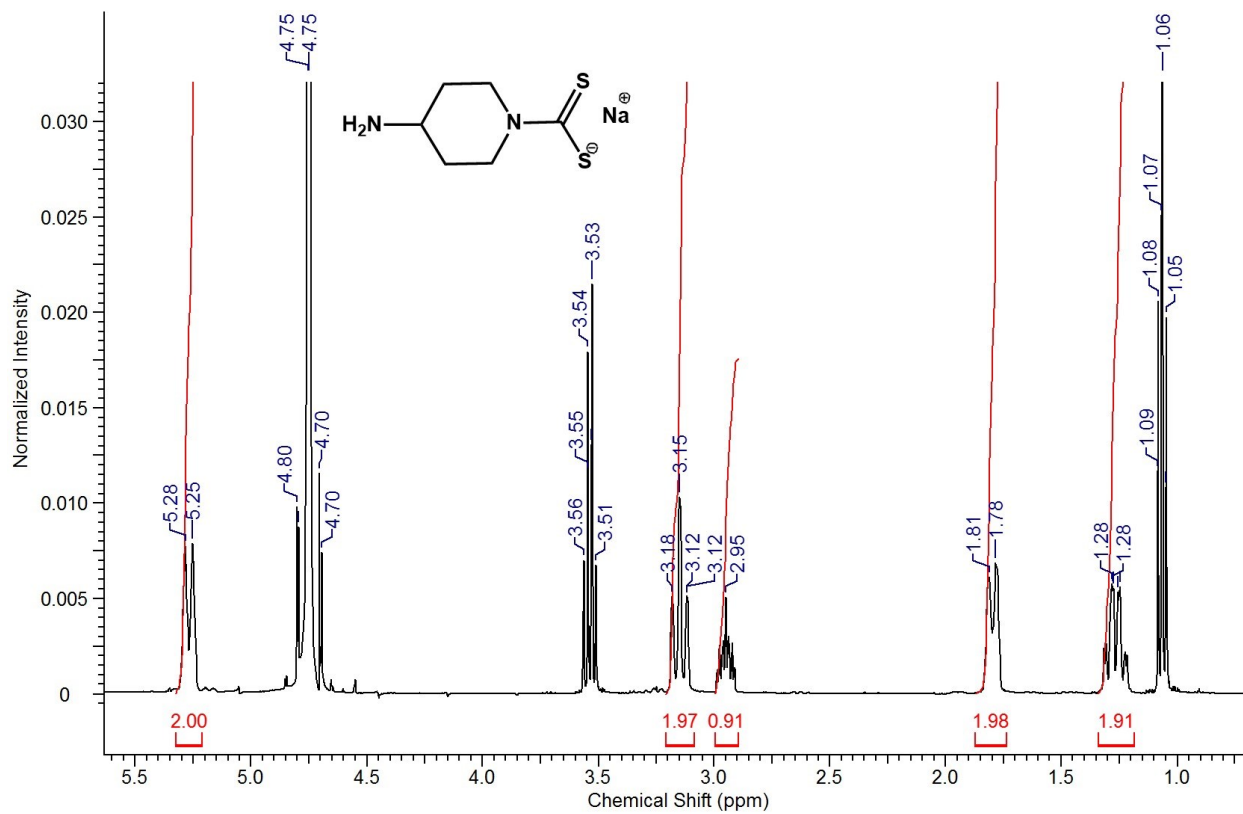


Figure B.5 ^1H NMR spectrum of 2.

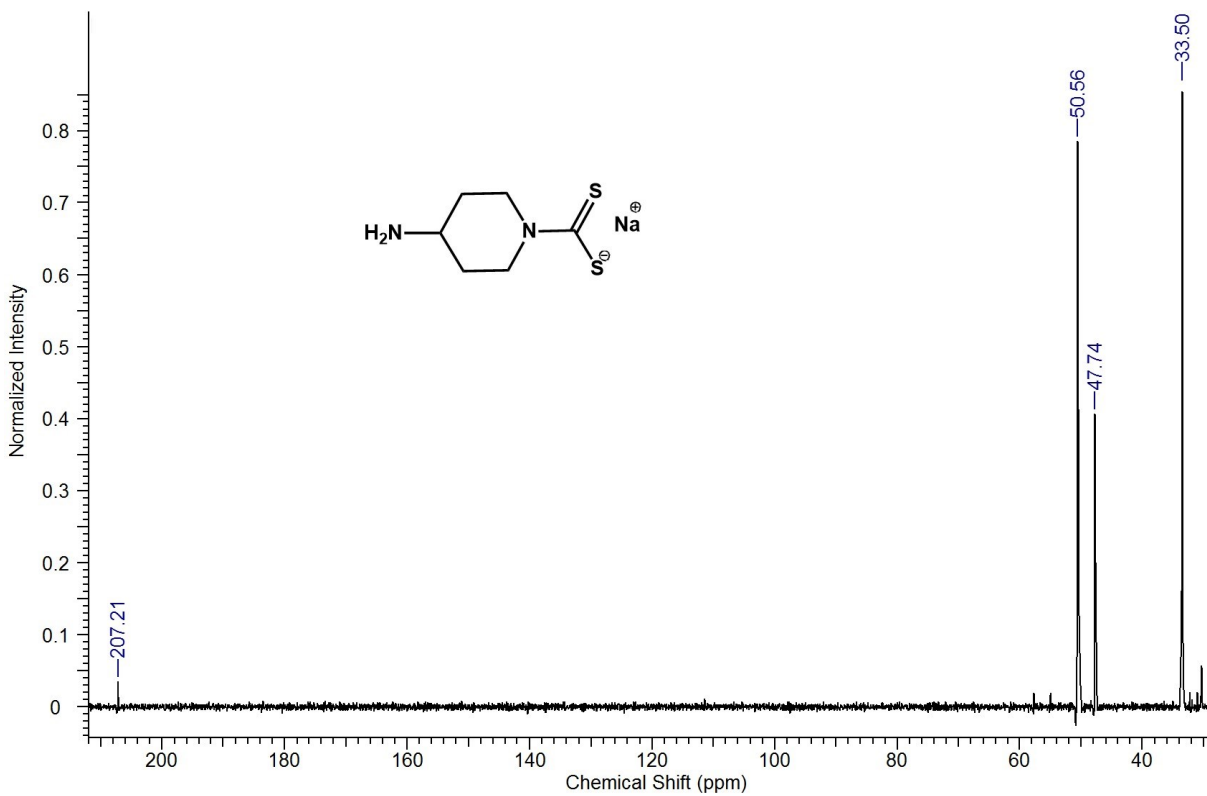


Figure B.6 ^{13}C NMR spectrum of 2.

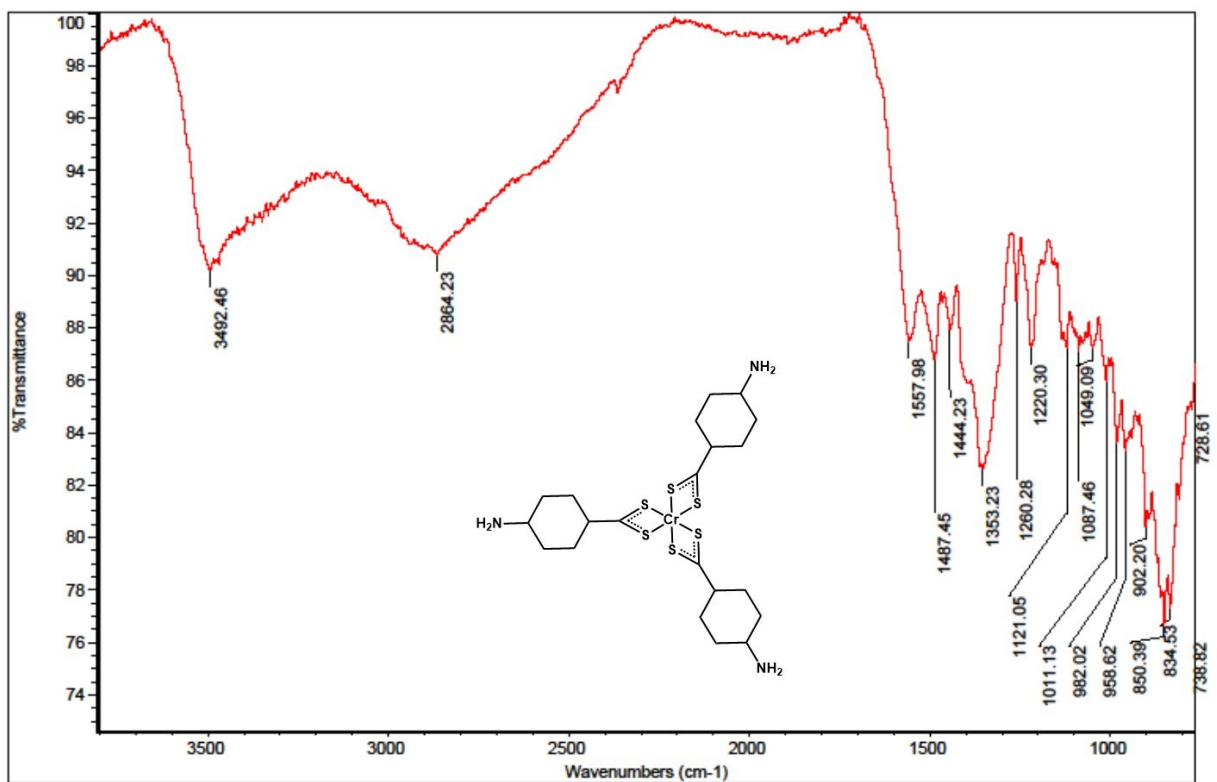


Figure B.7 IR spectrum of 2.Cr.

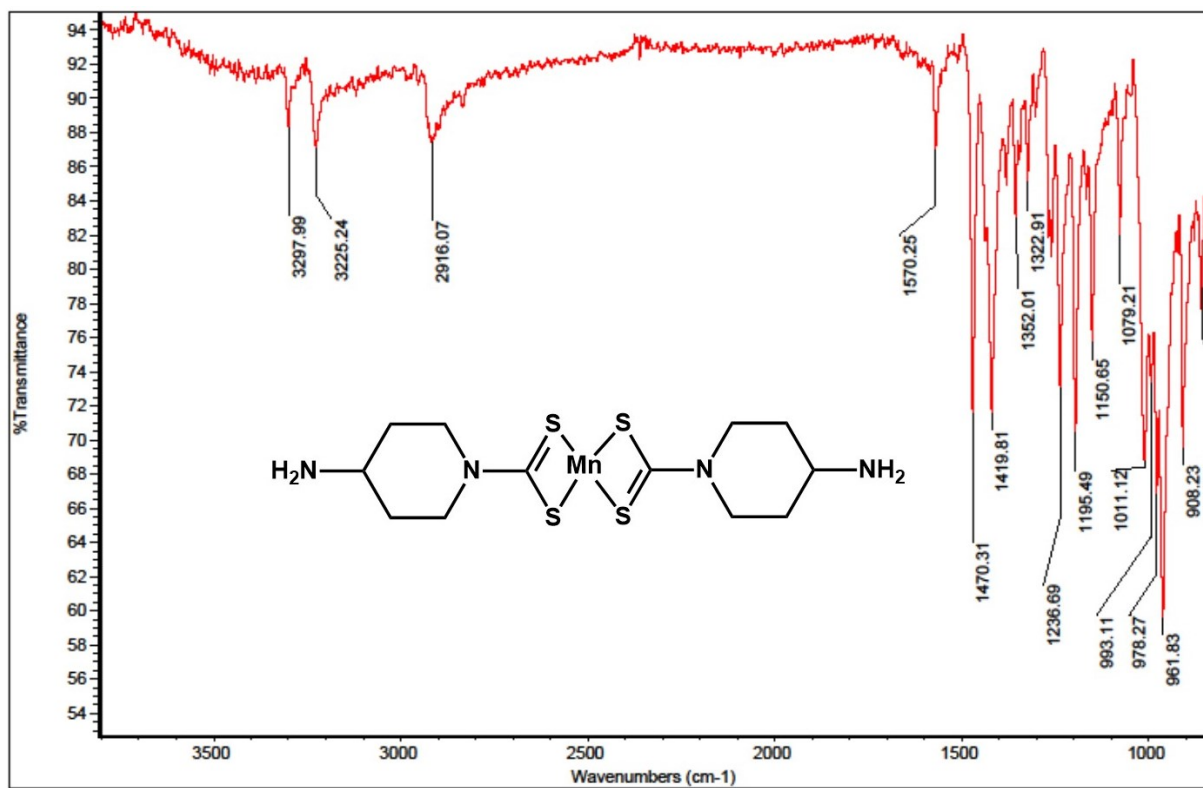


Figure B.8 IR spectrum of 2.Mn.

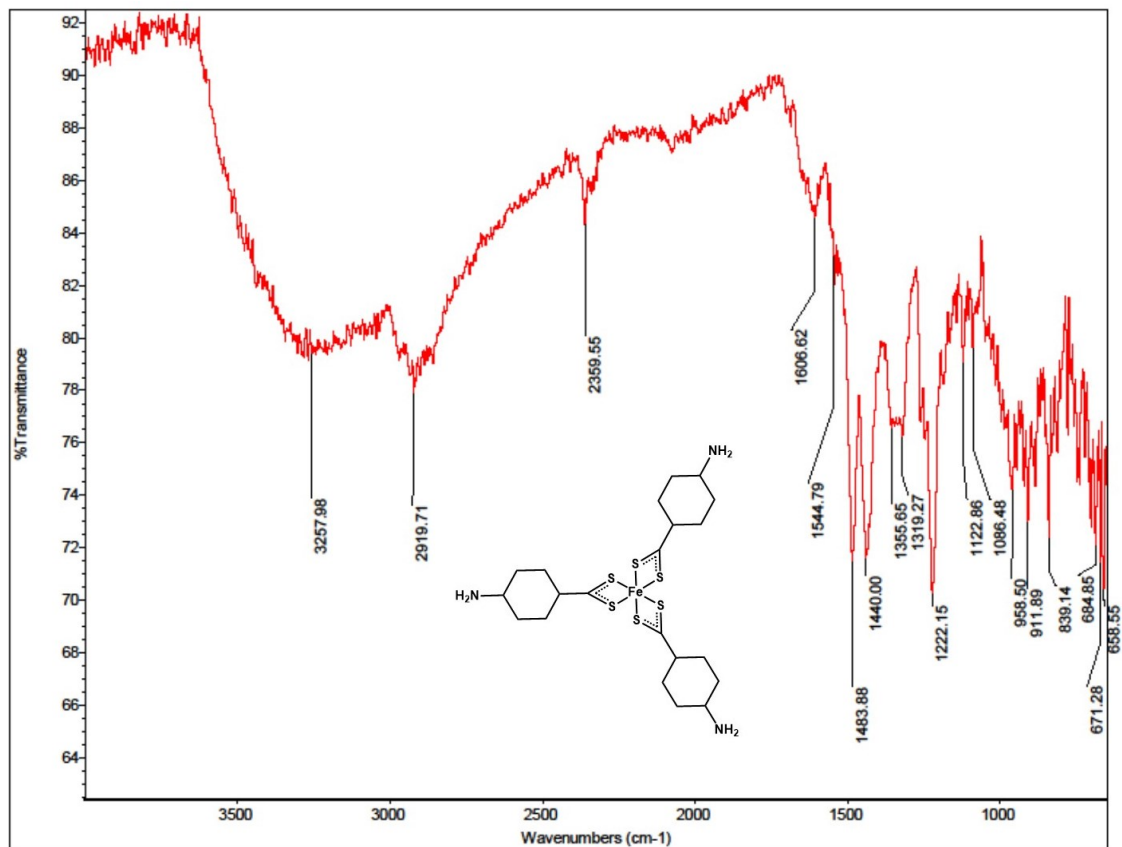


Figure B.9 IR spectrum of 2.Fe.

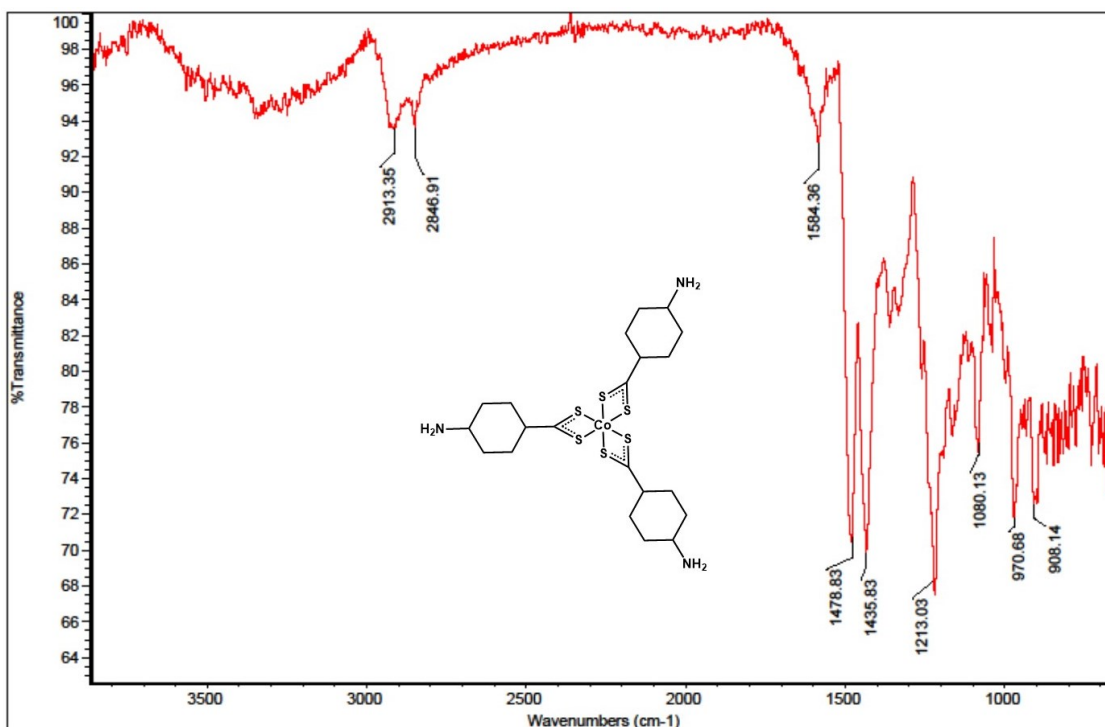


Figure B.10 IR spectrum of 2.Co.

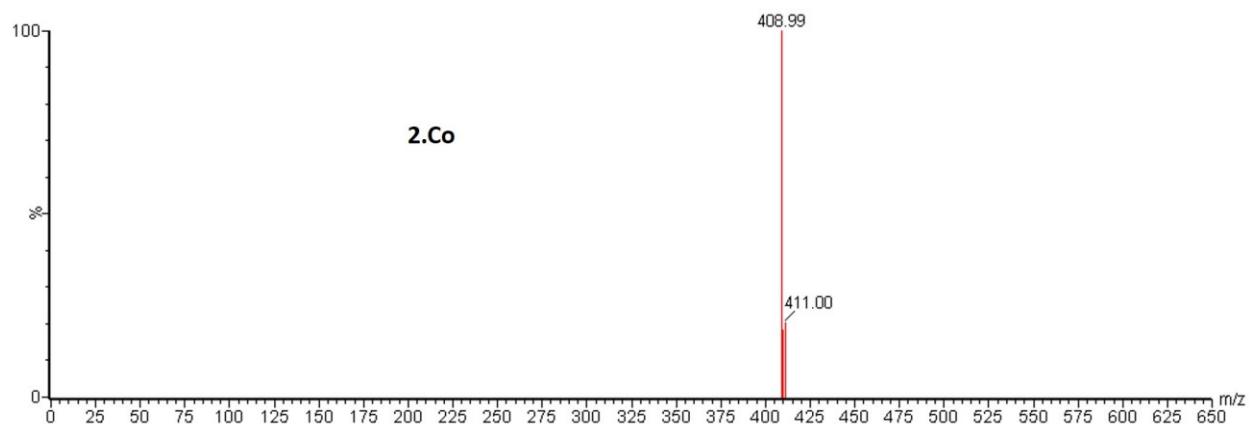


Figure B. 11 Mass spectrum of **2.Co**

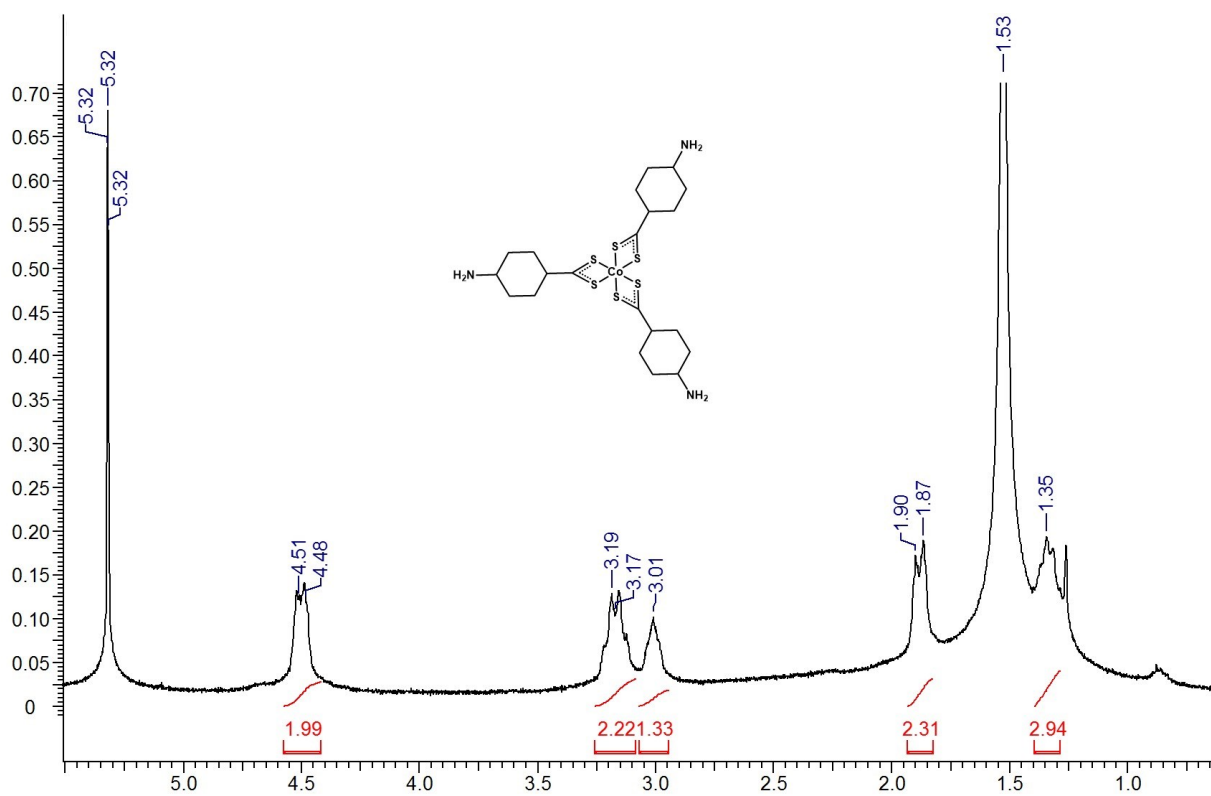


Figure B.12 ¹H NMR spectrum of **2.Co**.

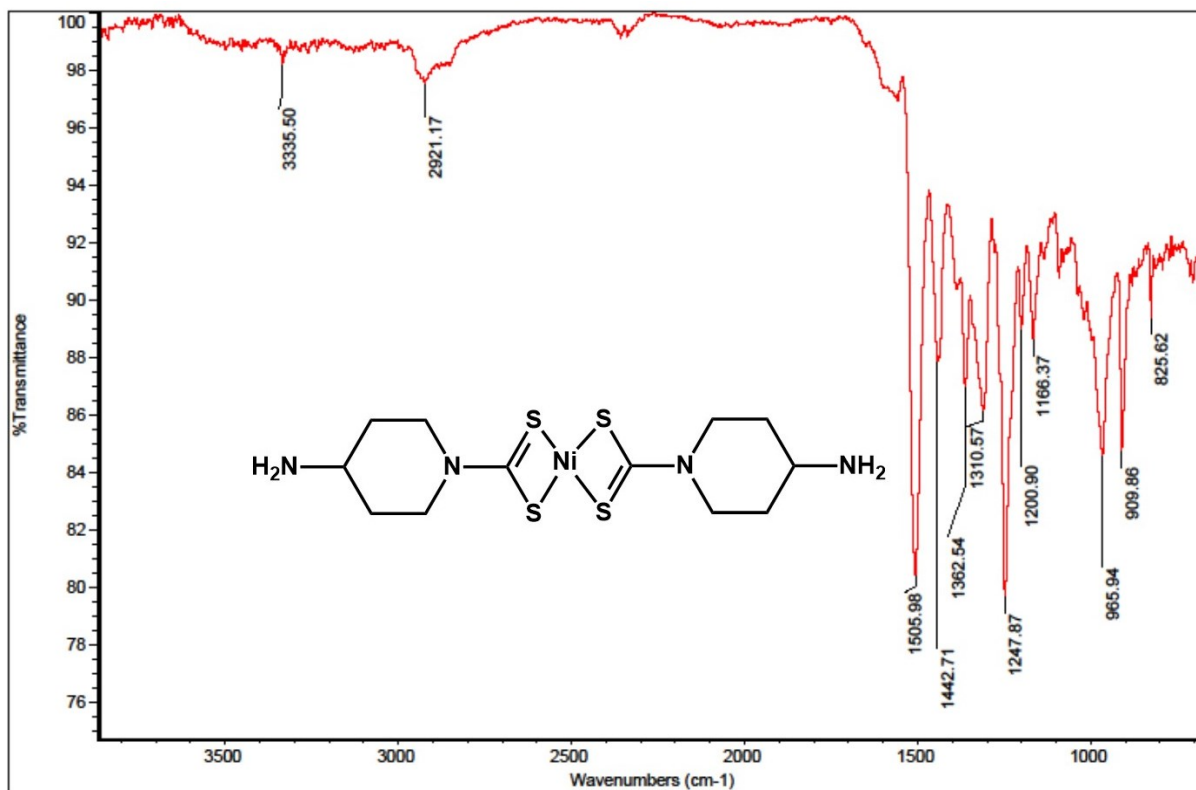


Figure B.13 IR spectrum of 2.Ni.

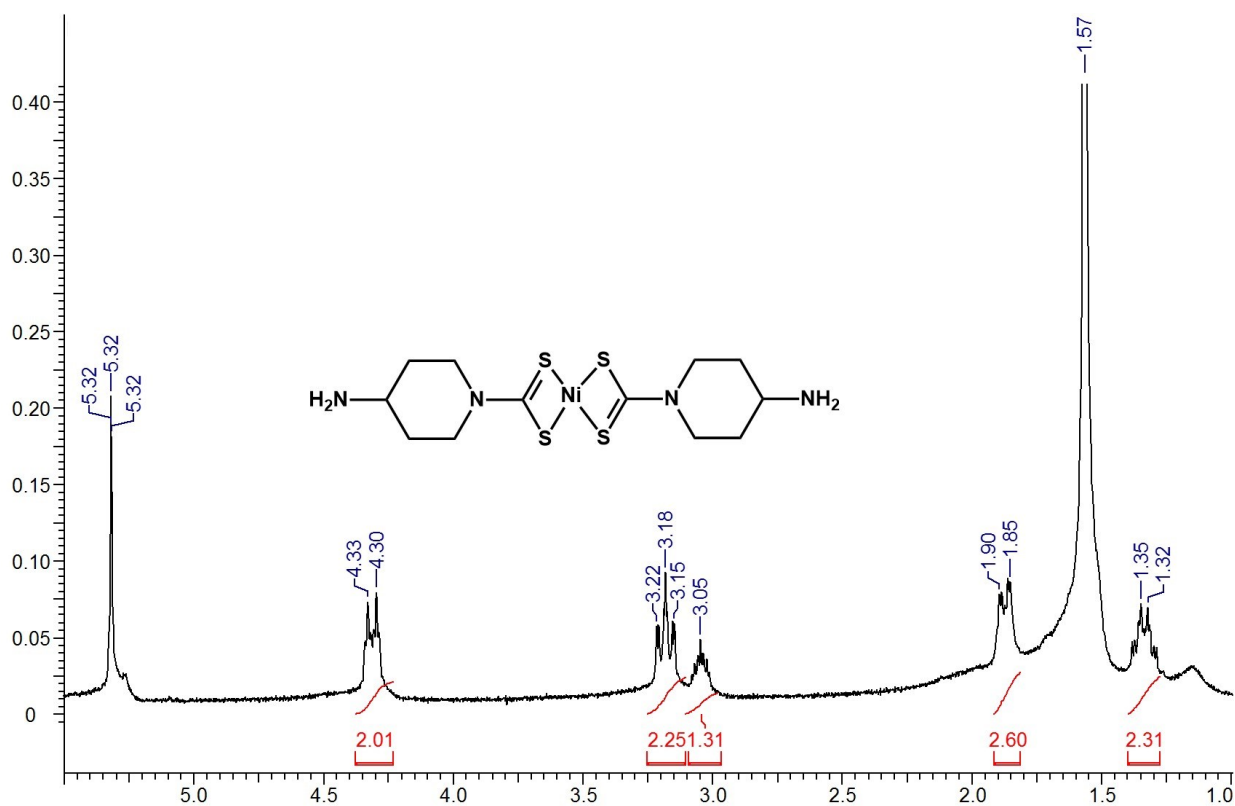


Figure B.14 ¹H NMR spectrum of 2.Ni.

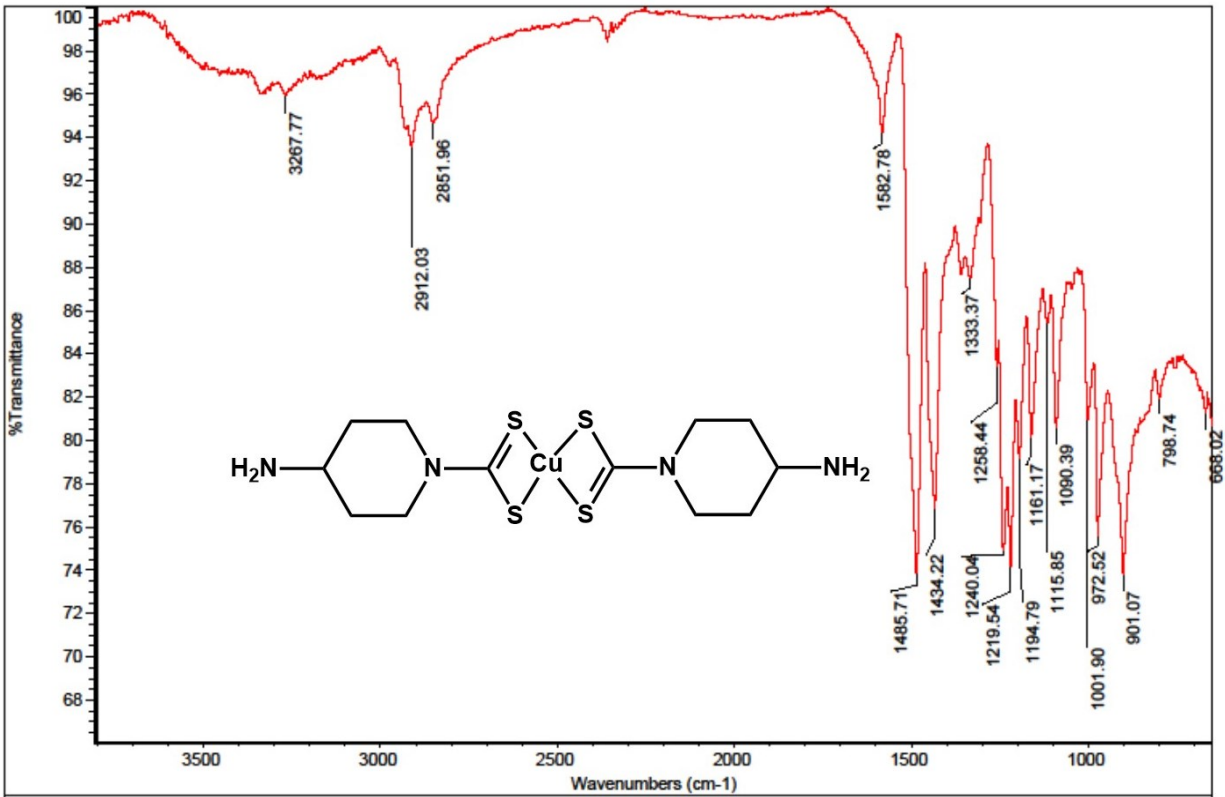


Figure B.15 IR spectrum of 2.Cu.

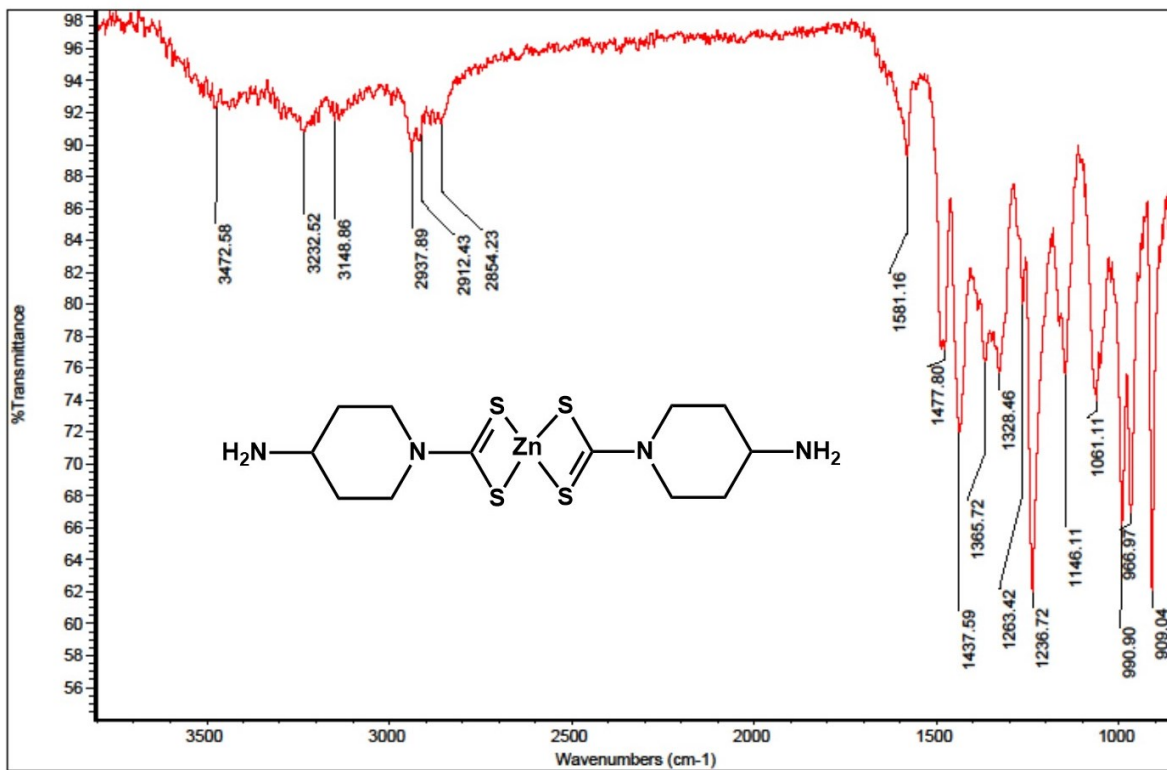


Figure B.16 IR spectrum of 2.Zn.

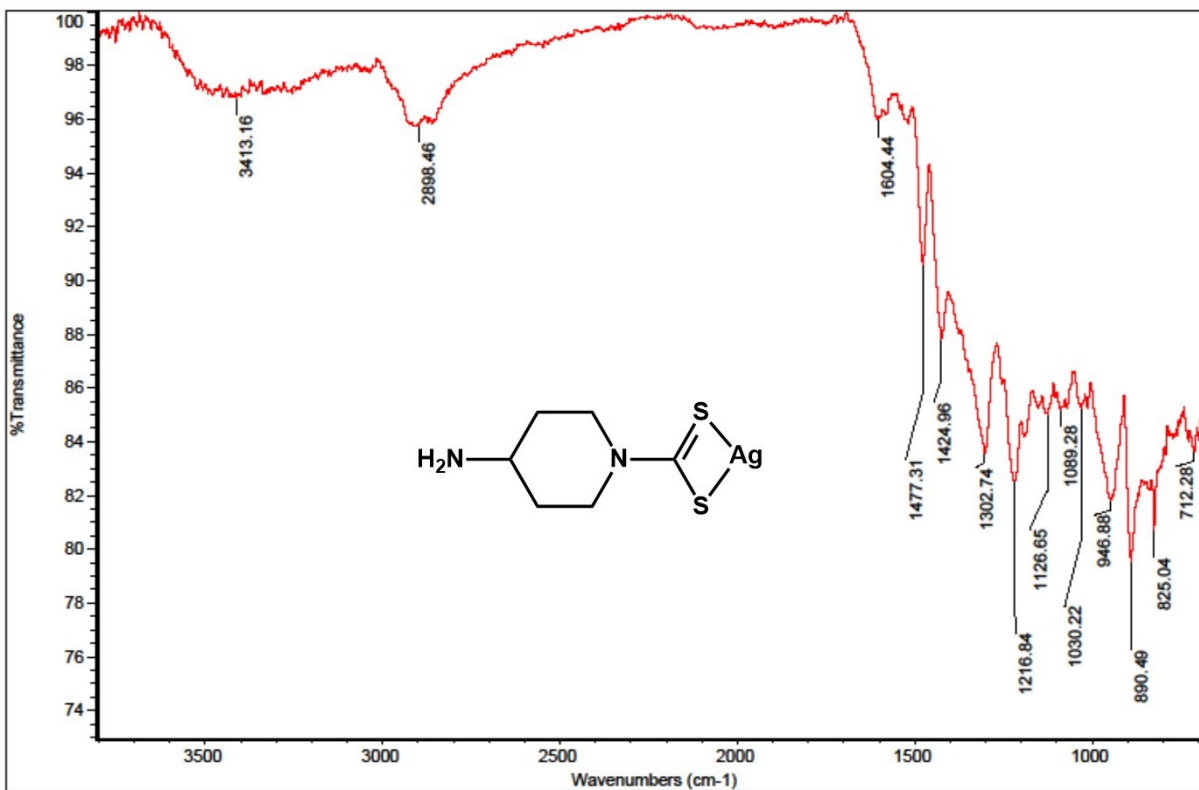


Figure B.17 IR spectrum of 2.Ag.

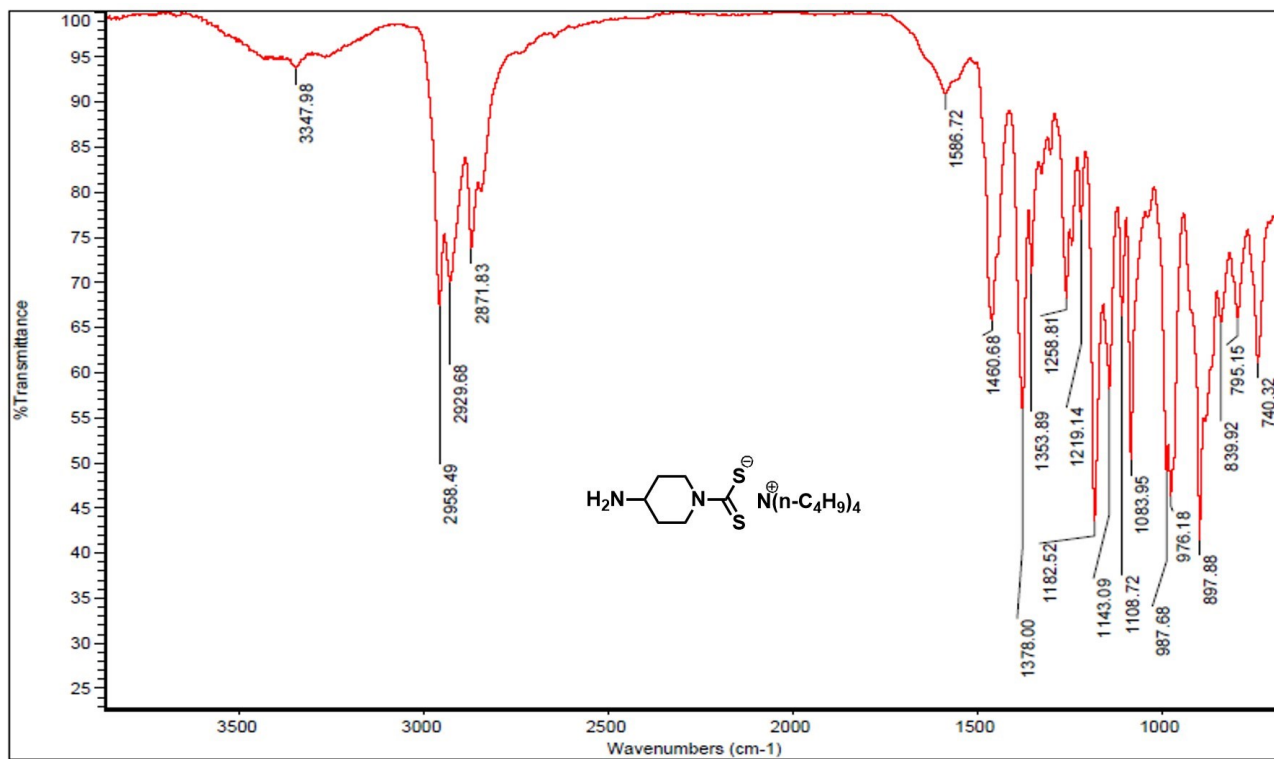


Figure B.18 IR spectrum of 3.

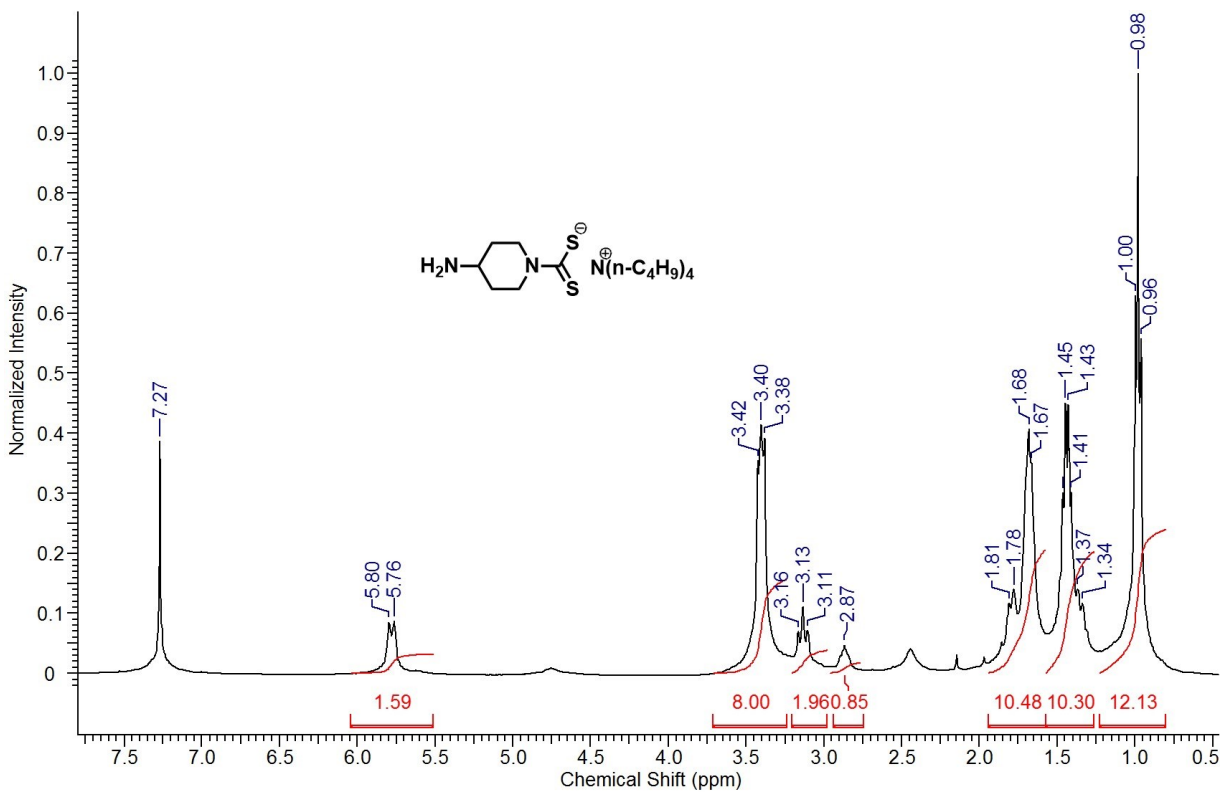


Figure B.19 ^1H NMR spectrum of 3.

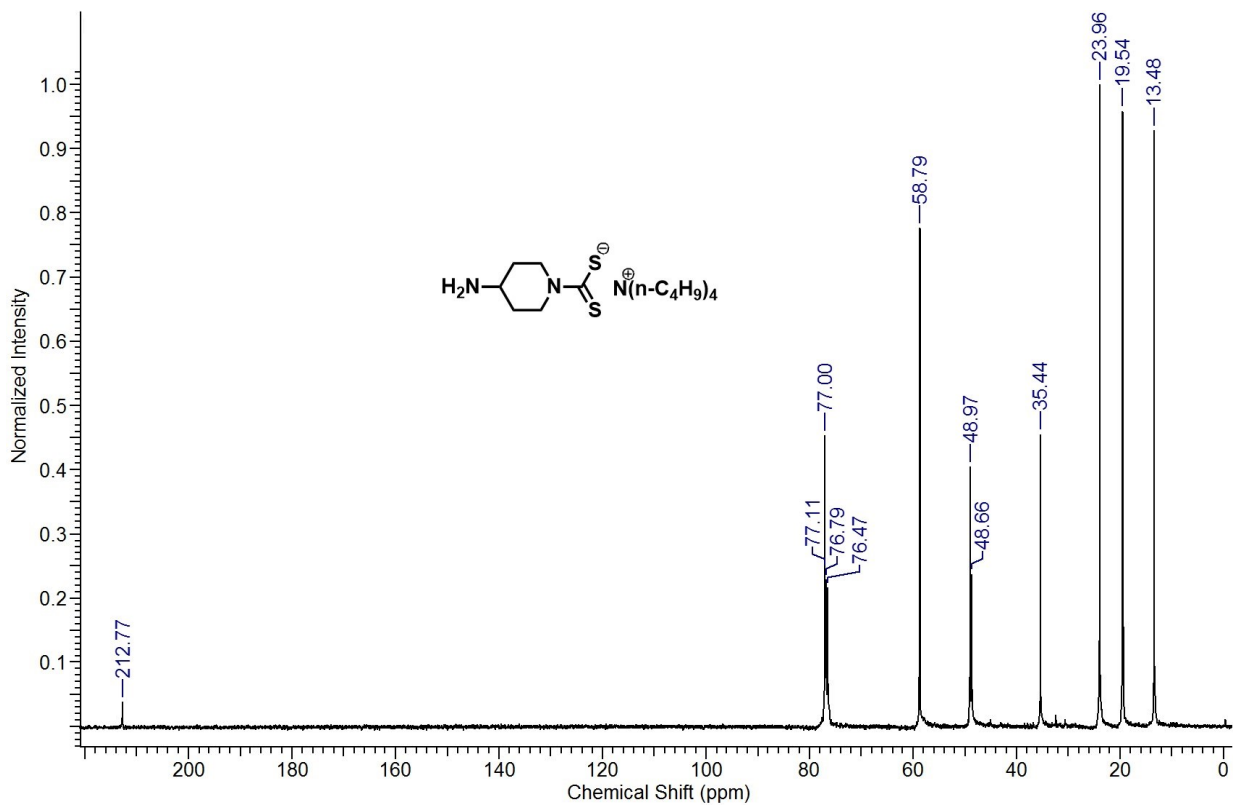


Figure B.20 ^{13}C NMR spectrum of 3.

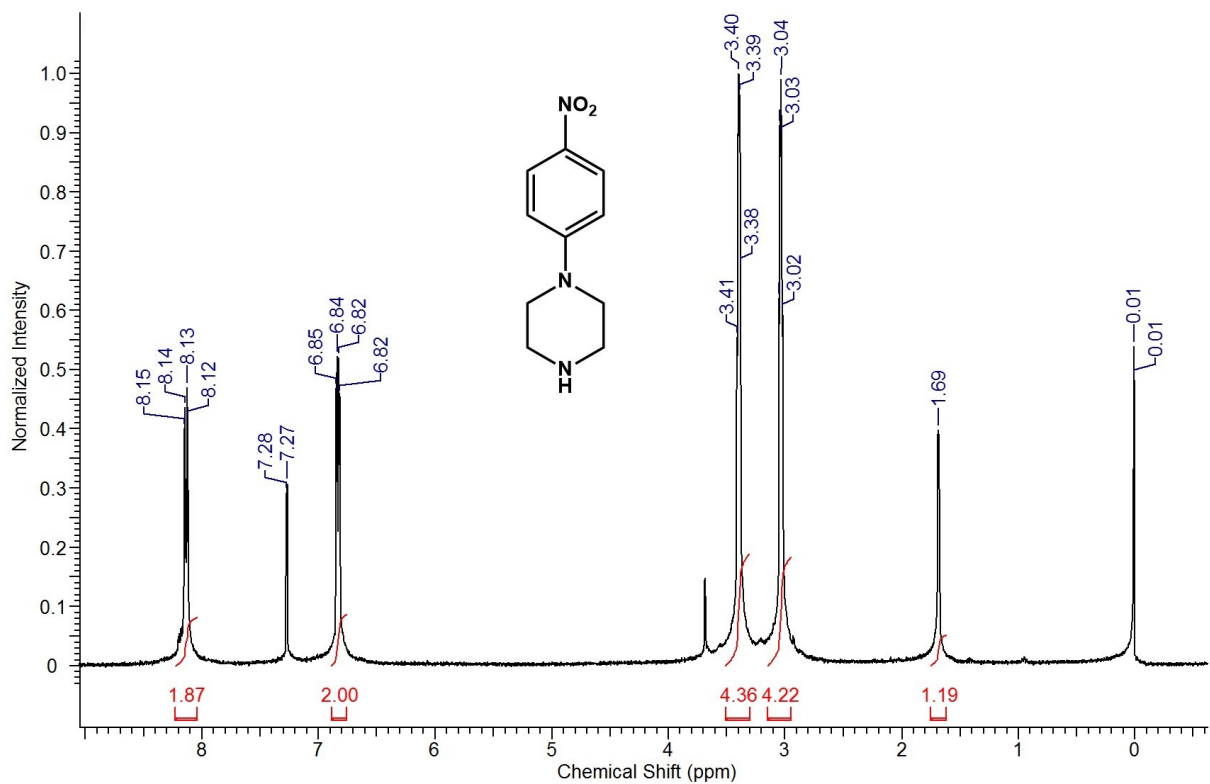


Figure B.21 ^1H NMR spectrum of 4.

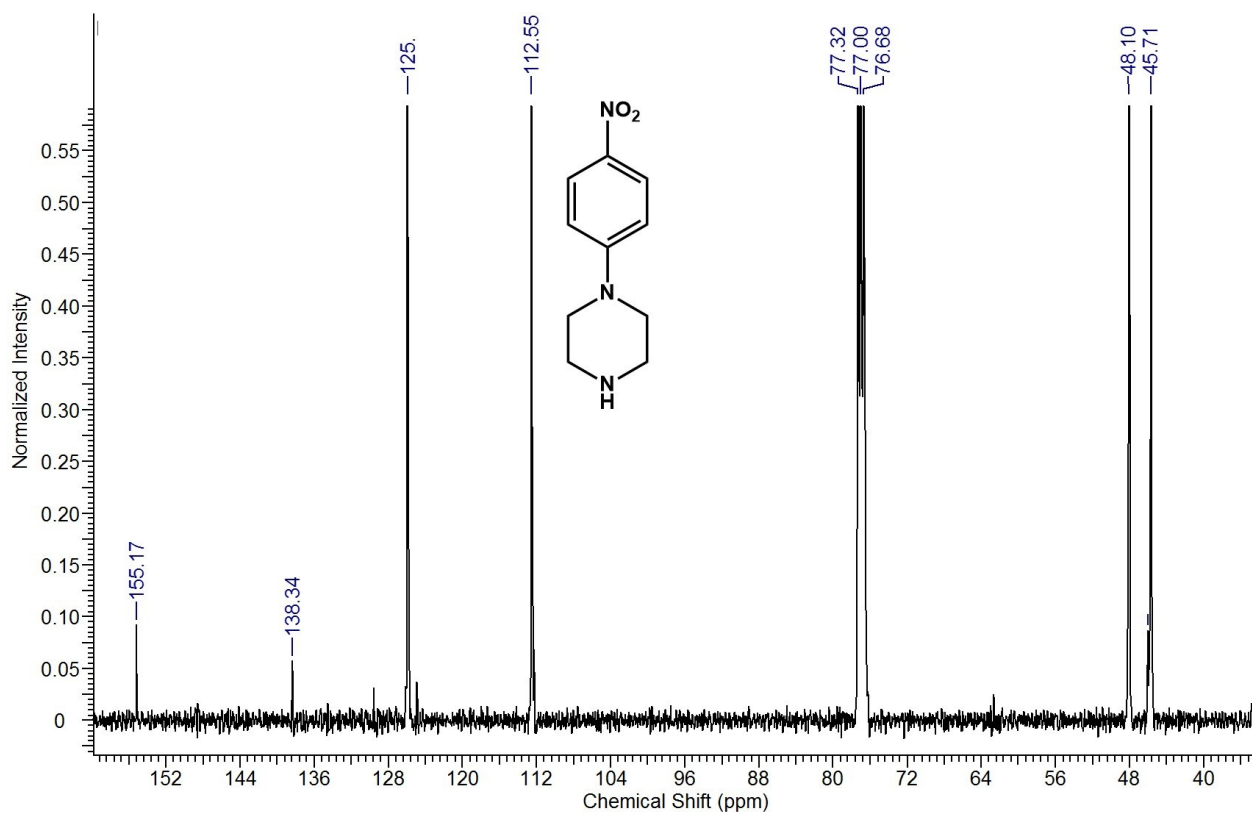


Figure B.22 ^{13}C NMR spectrum of 4.

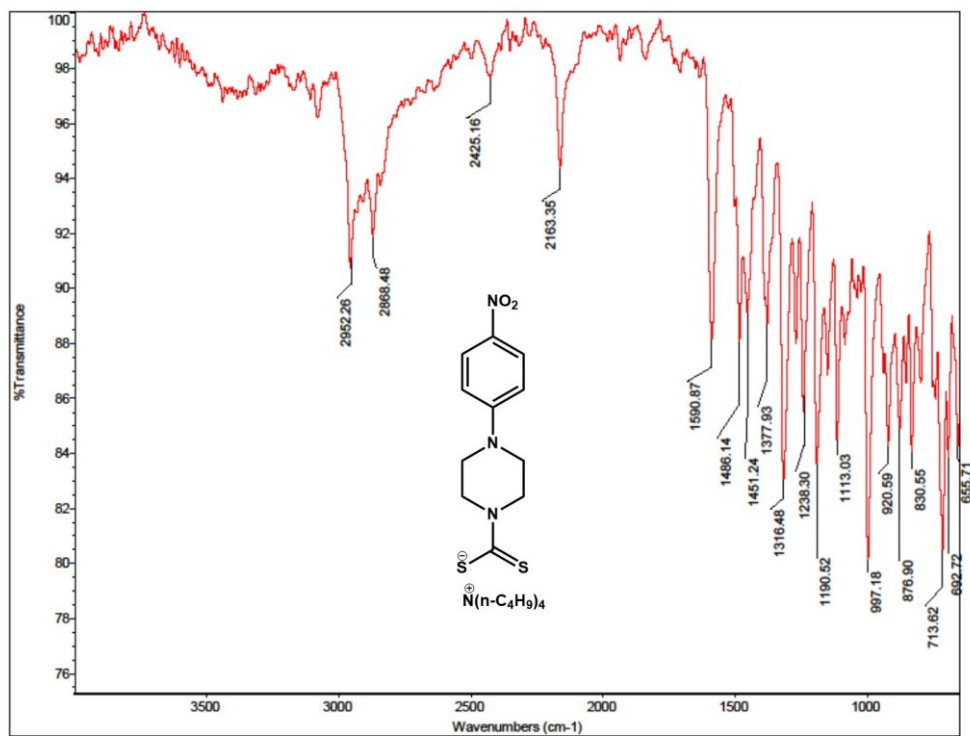


Figure B.23 IR spectrum of 5.

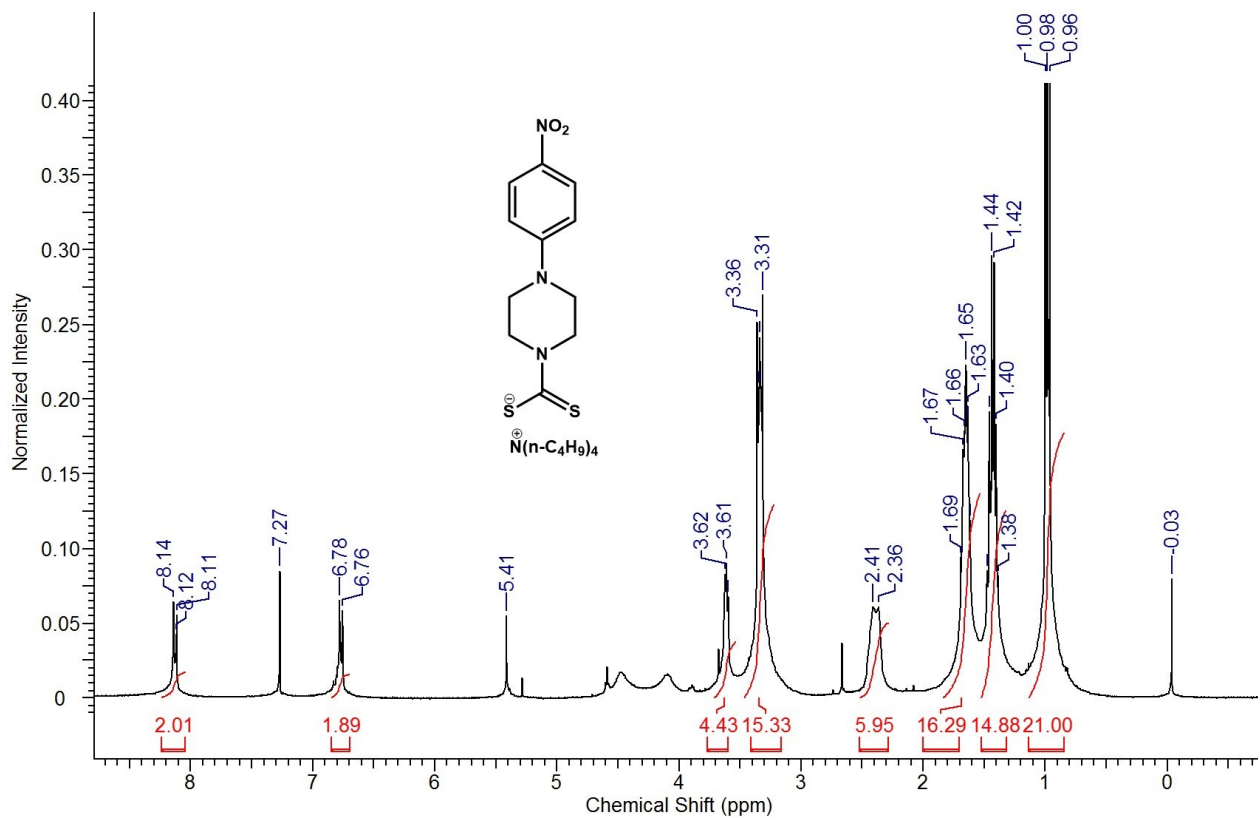


Figure B.24 ^1H NMR spectrum of 5.

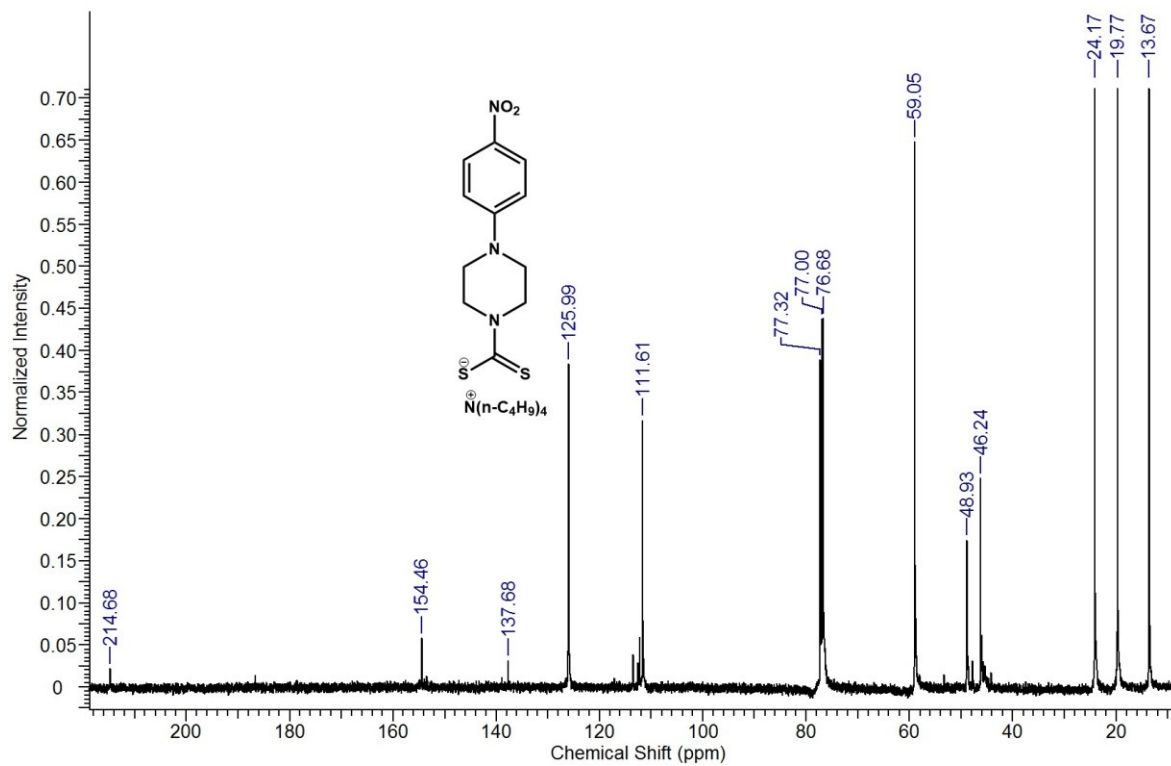


Figure B.25 ^{13}C NMR spectrum of **5**.

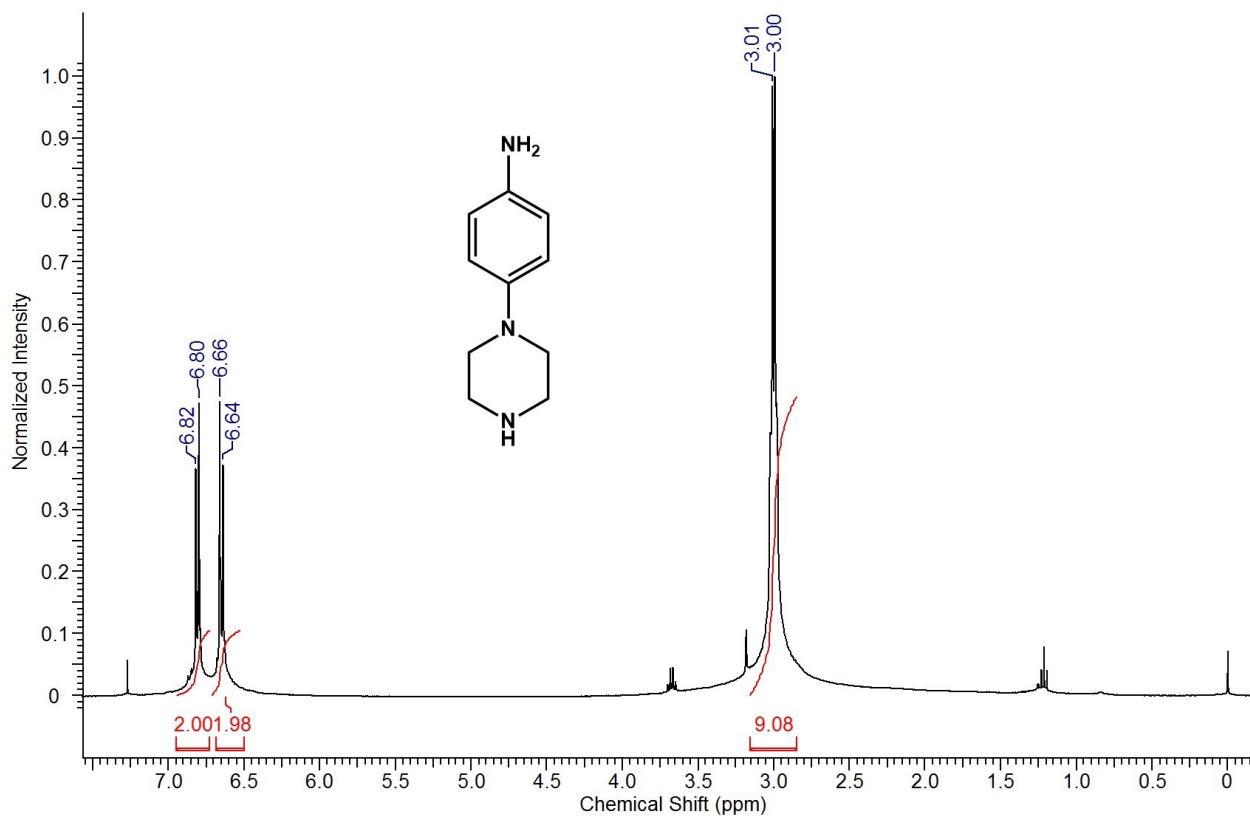


Figure B.26 ^1H NMR spectrum of **6** in CDCl_3 .

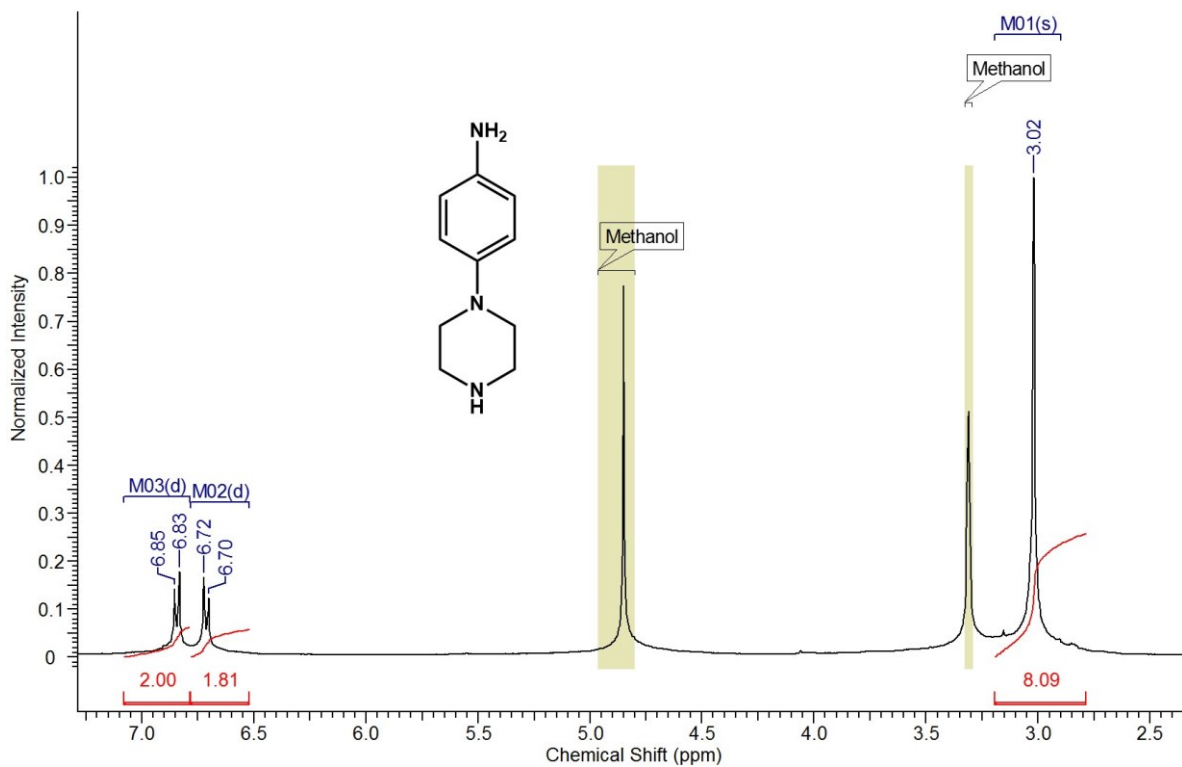


Figure B.27 ^1H NMR spectrum of **6** in CD_3OD .

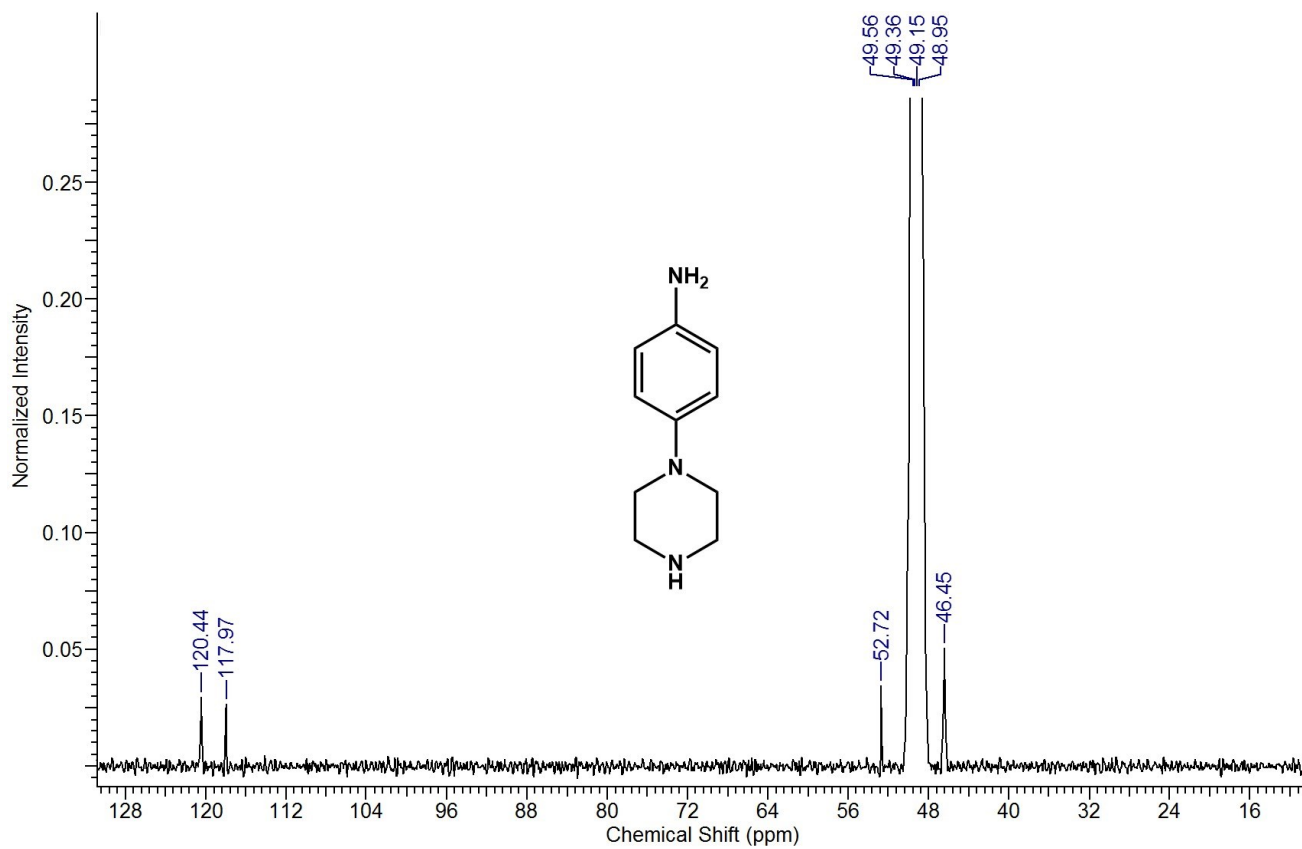


Figure B.28 ^{13}C NMR spectrum of **6** in CD_3OD .

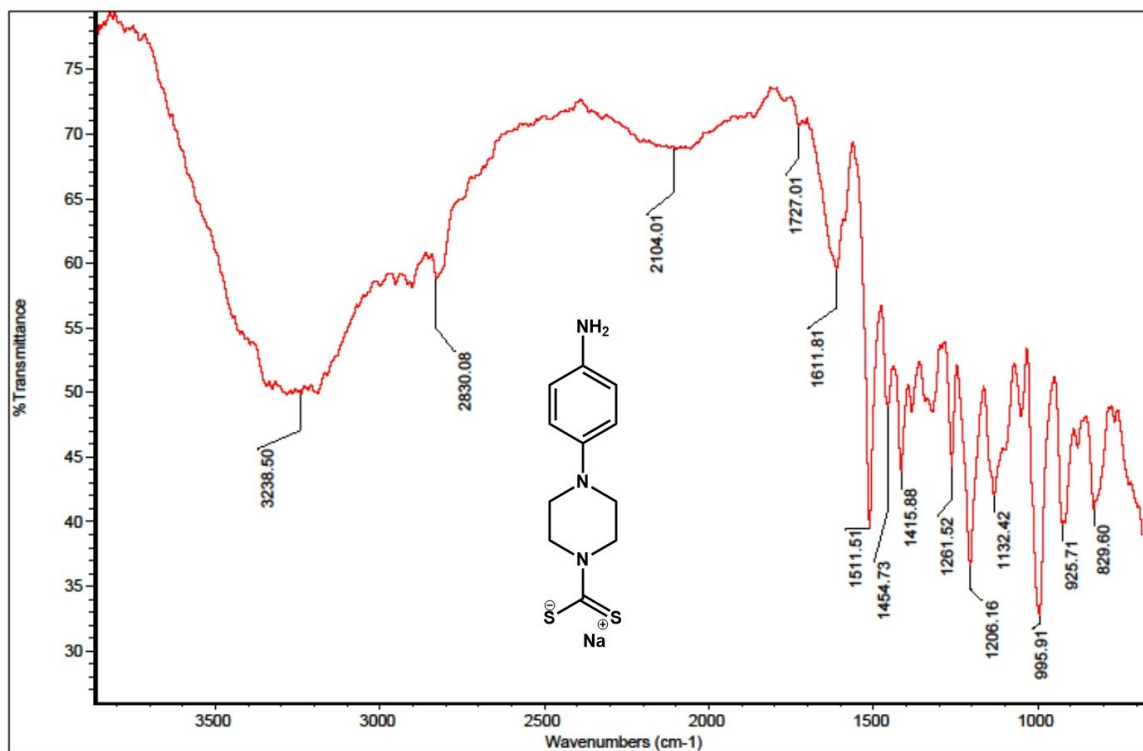


Figure B.29 IR spectrum of 7.

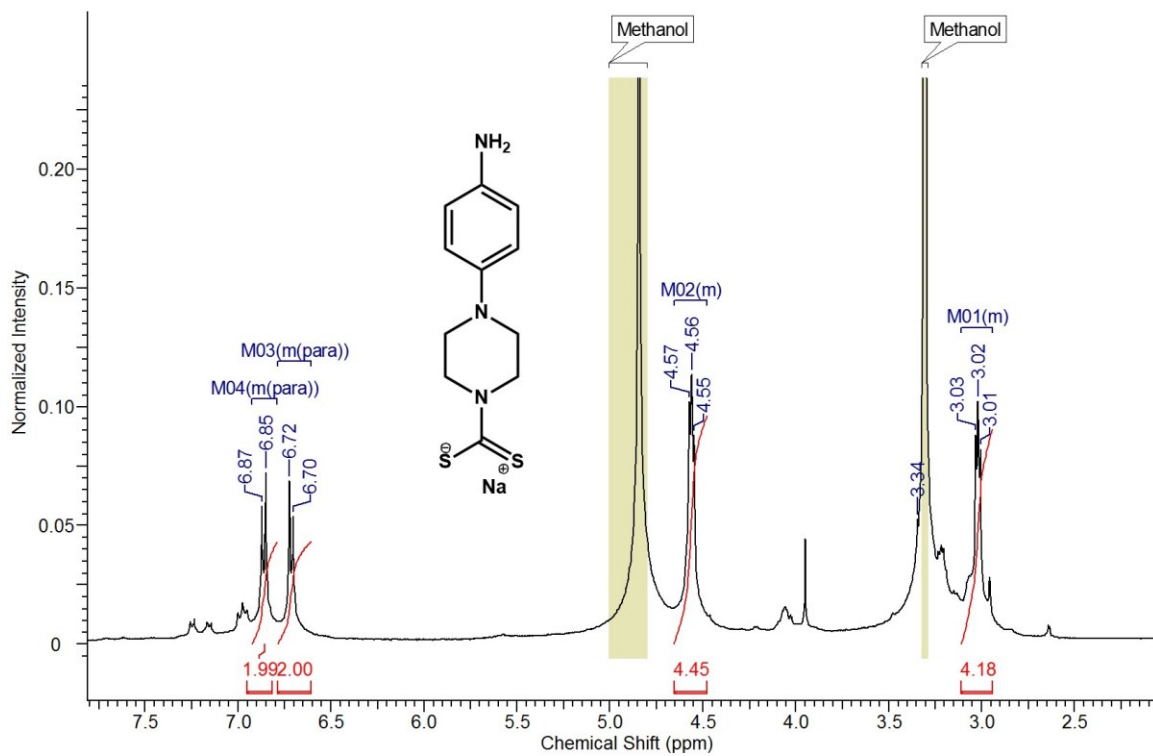


Figure B.30 ¹H NMR spectrum of 7.

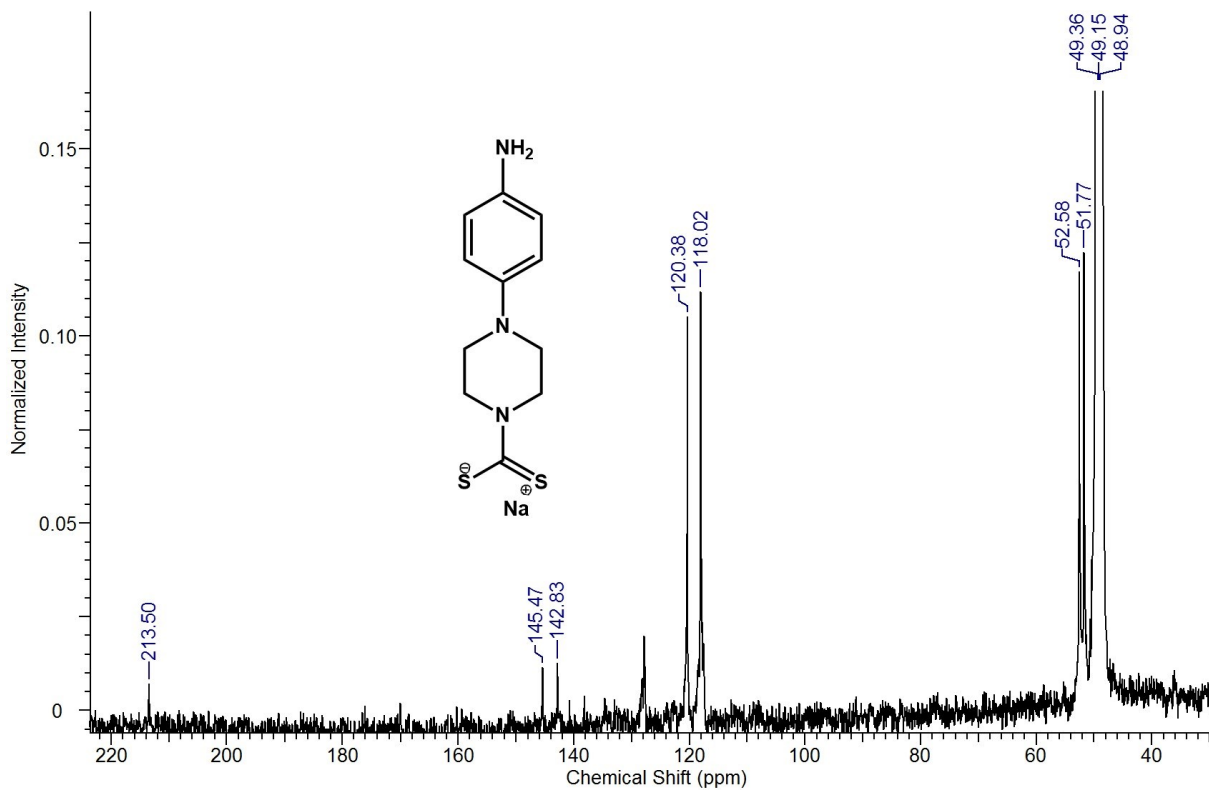


Figure B.31 ^{13}C NMR spectrum of 7.

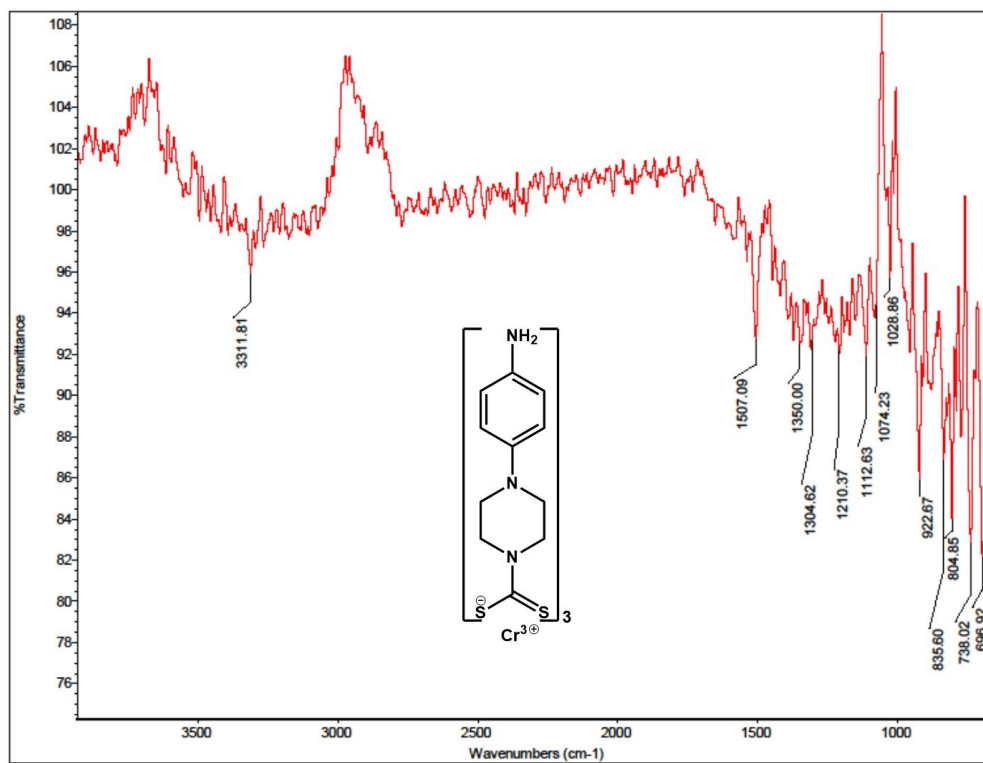


Figure B.32 IR spectrum of 7.Cr.

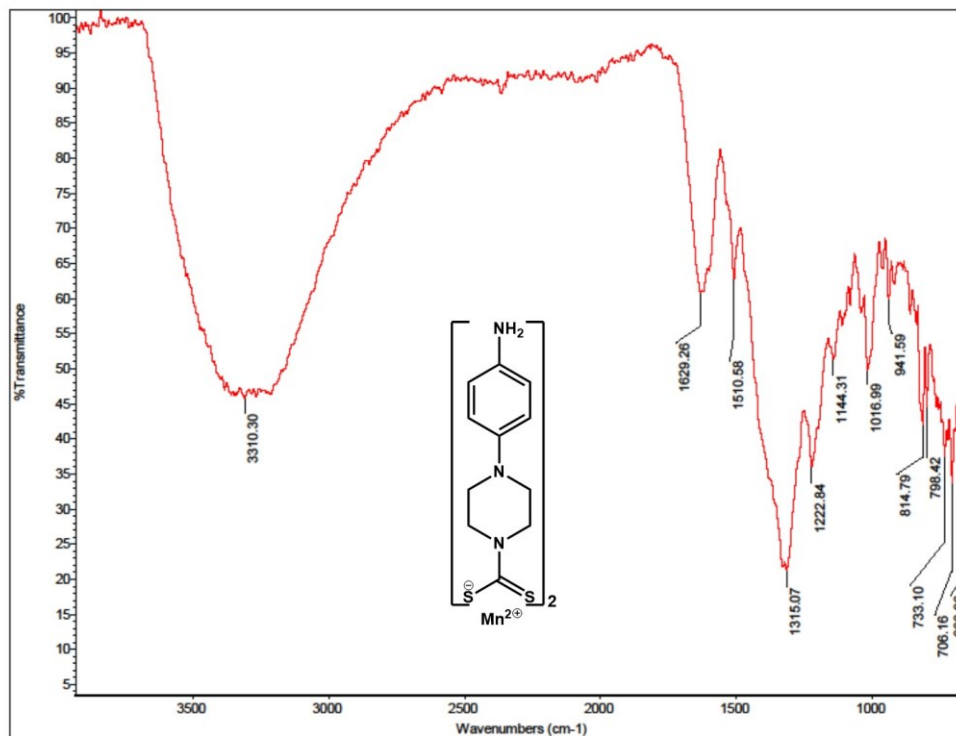


Figure B.33 IR spectrum of 7.Mn.

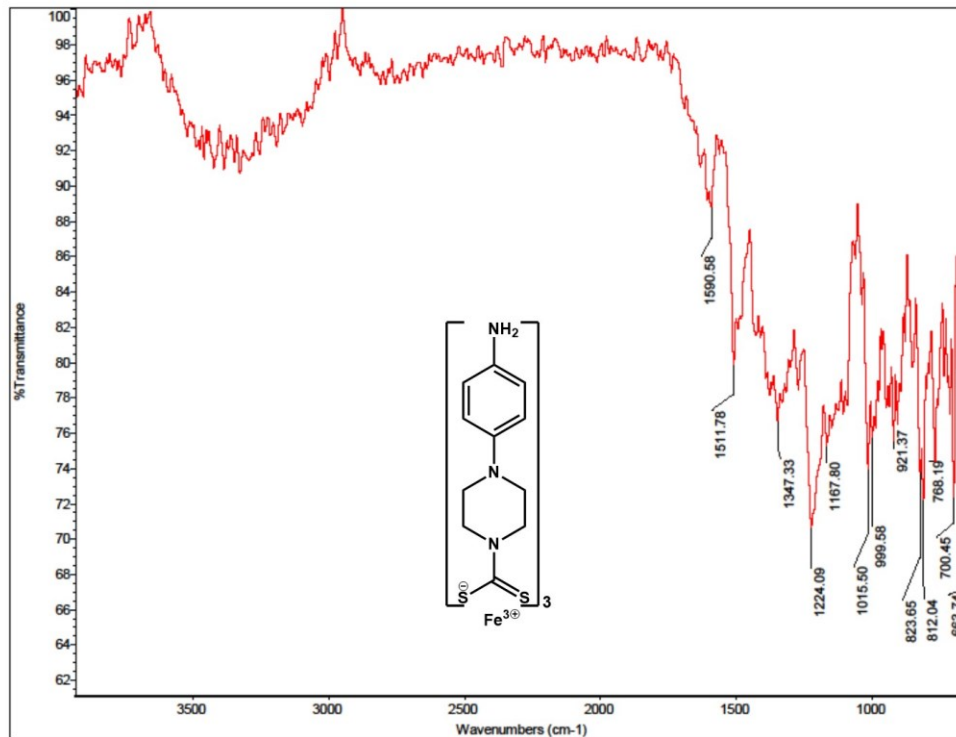


Figure B.34 IR spectrum of 7.Fe.

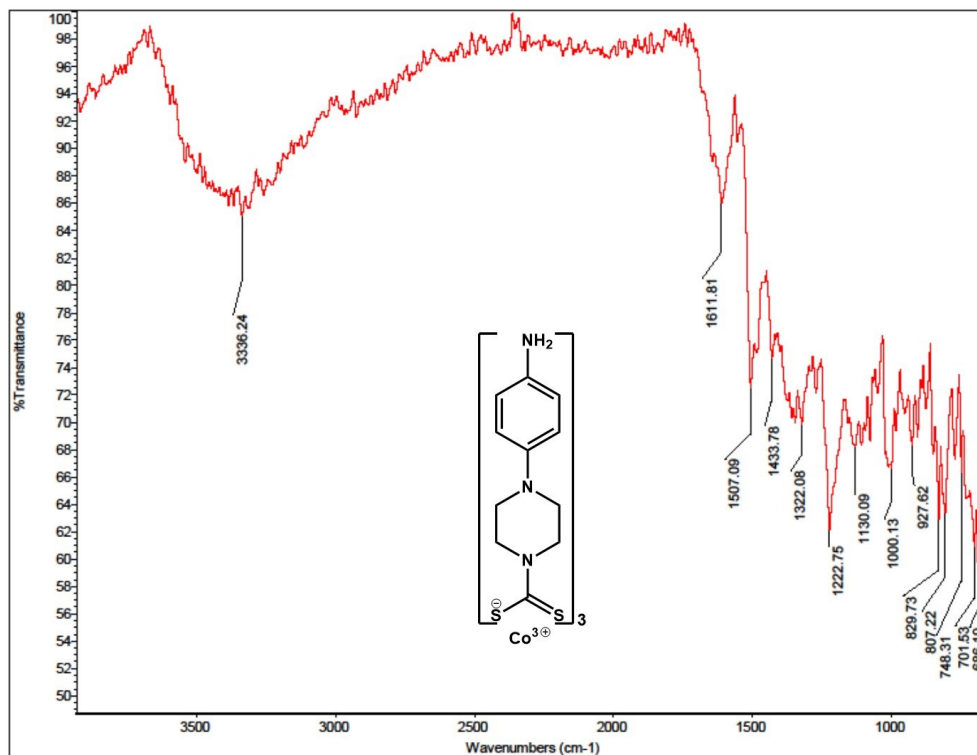


Figure B.35 IR spectrum of 7.Co.

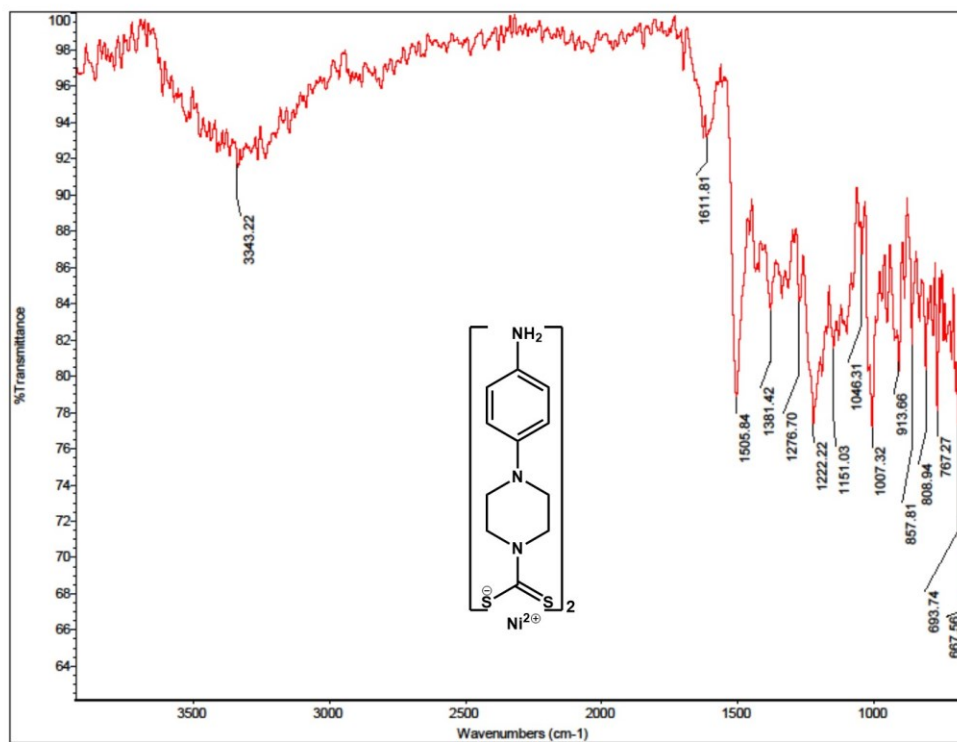


Figure B.36 IR spectrum of 7.Ni.

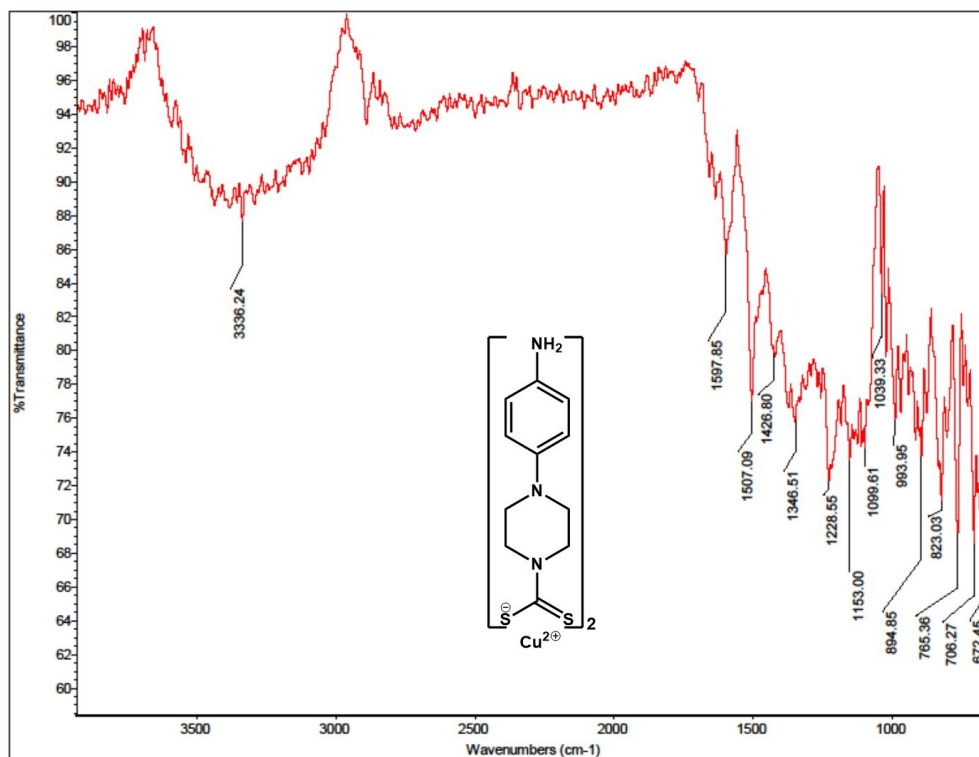


Figure B.37 IR spectrum of 7.Cu.

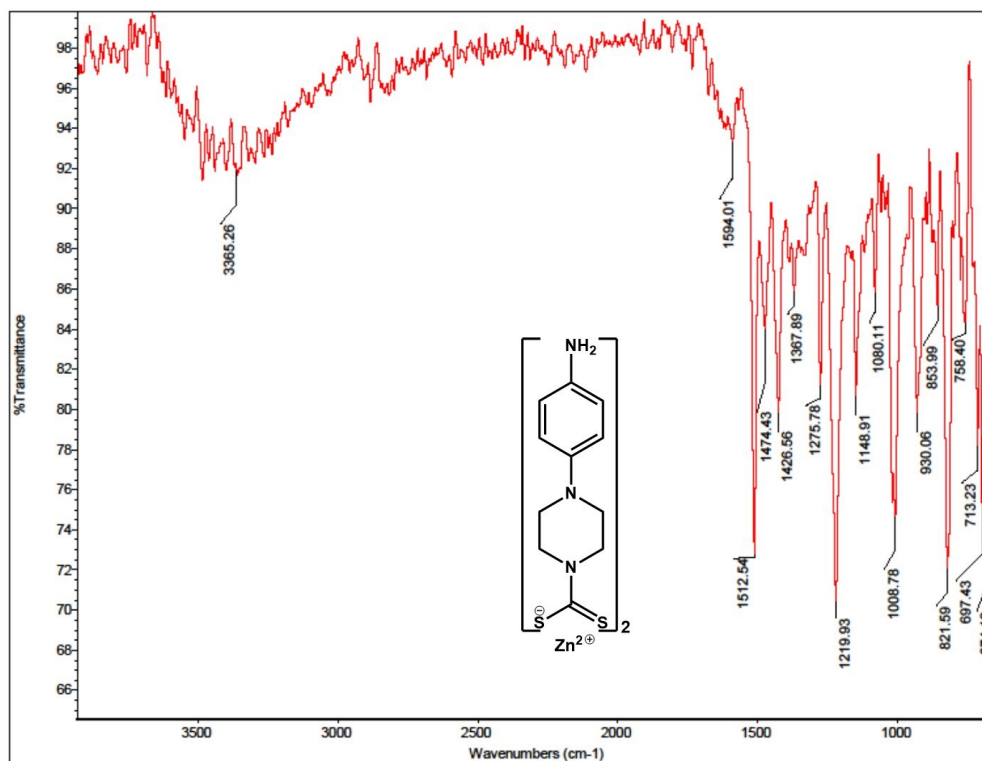


Figure B.38 IR spectrum of 7.Zn.

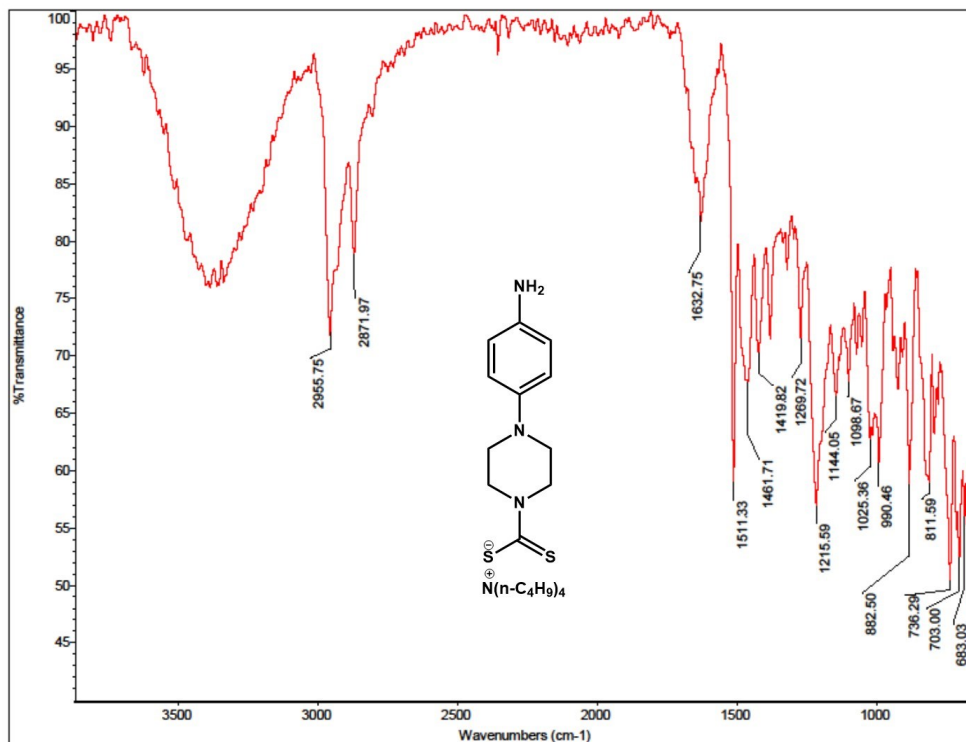


Figure B.39 IR spectrum of 8.

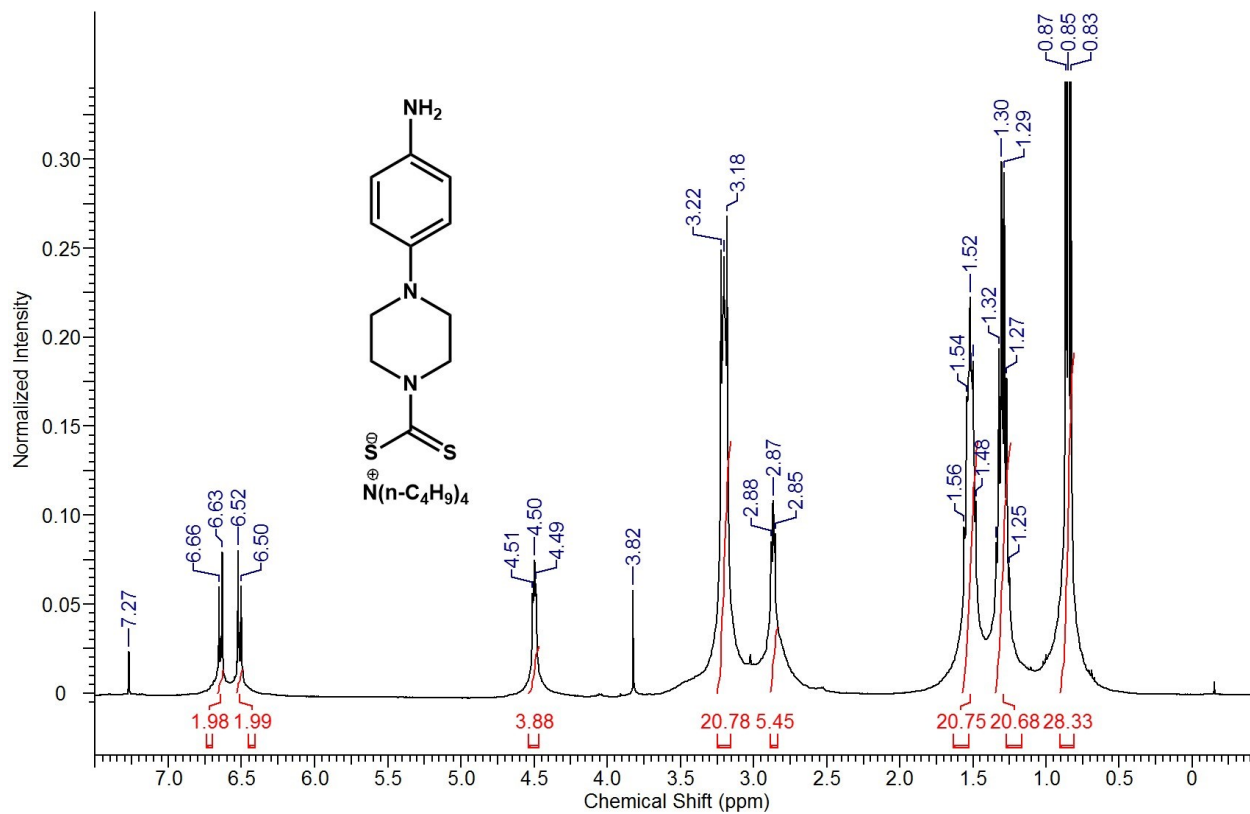


Figure B.40 ¹H NMR spectrum of 8.

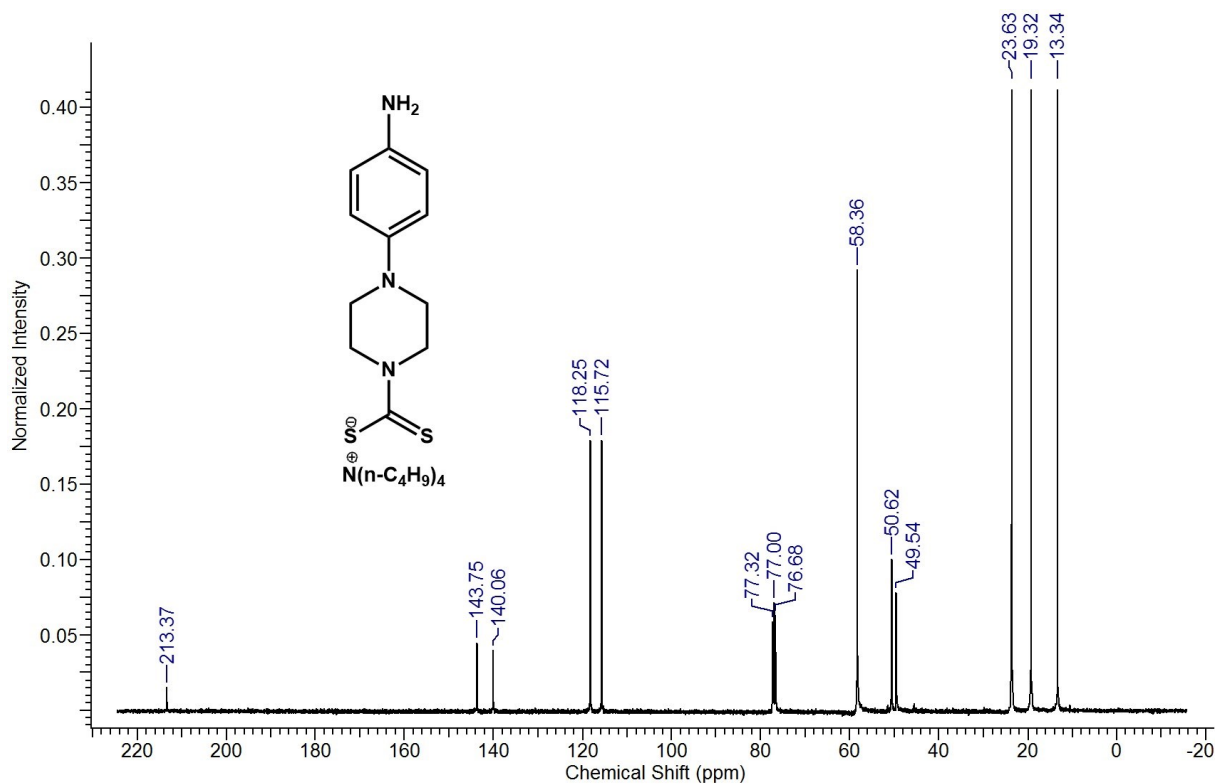


Figure B.41 ^{13}C NMR spectrum of **8**.

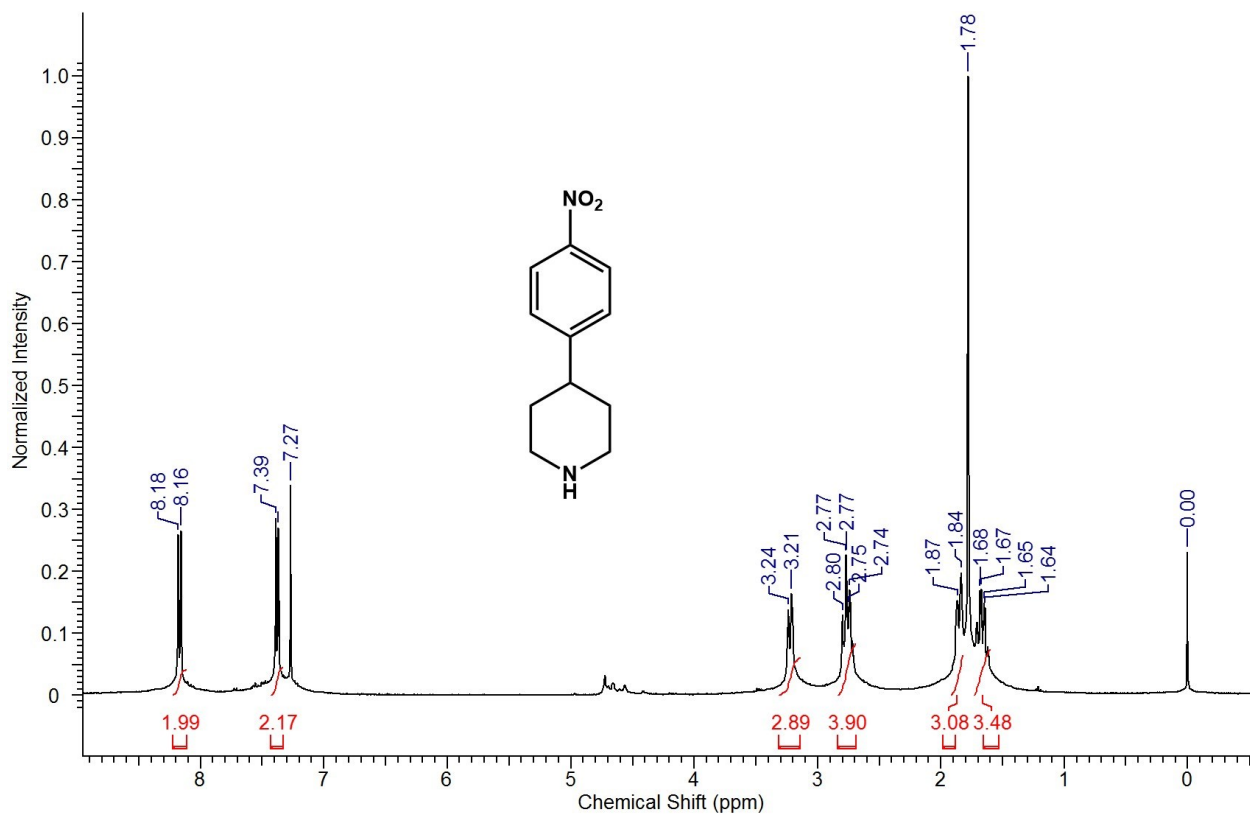


Figure B.42 ^1H NMR spectrum of **9**.

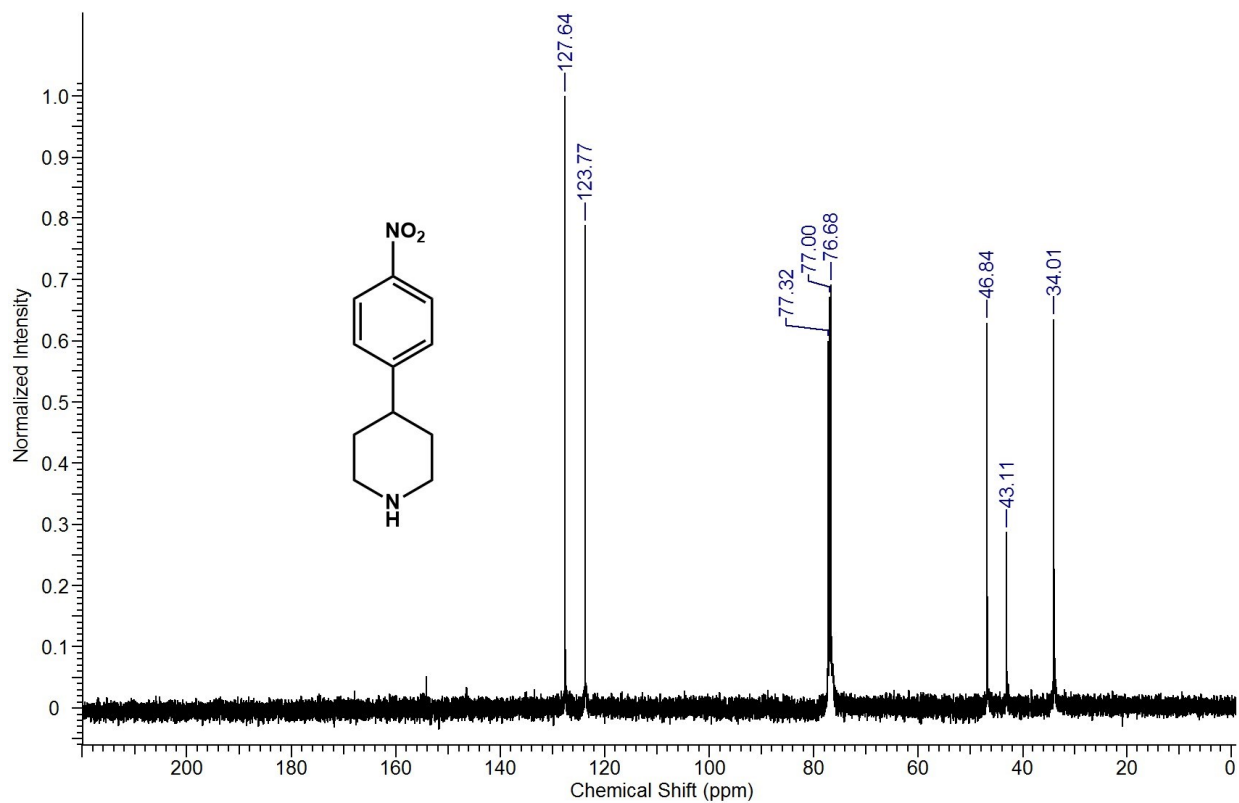


Figure B.43 ^{13}C NMR spectrum of **9**.

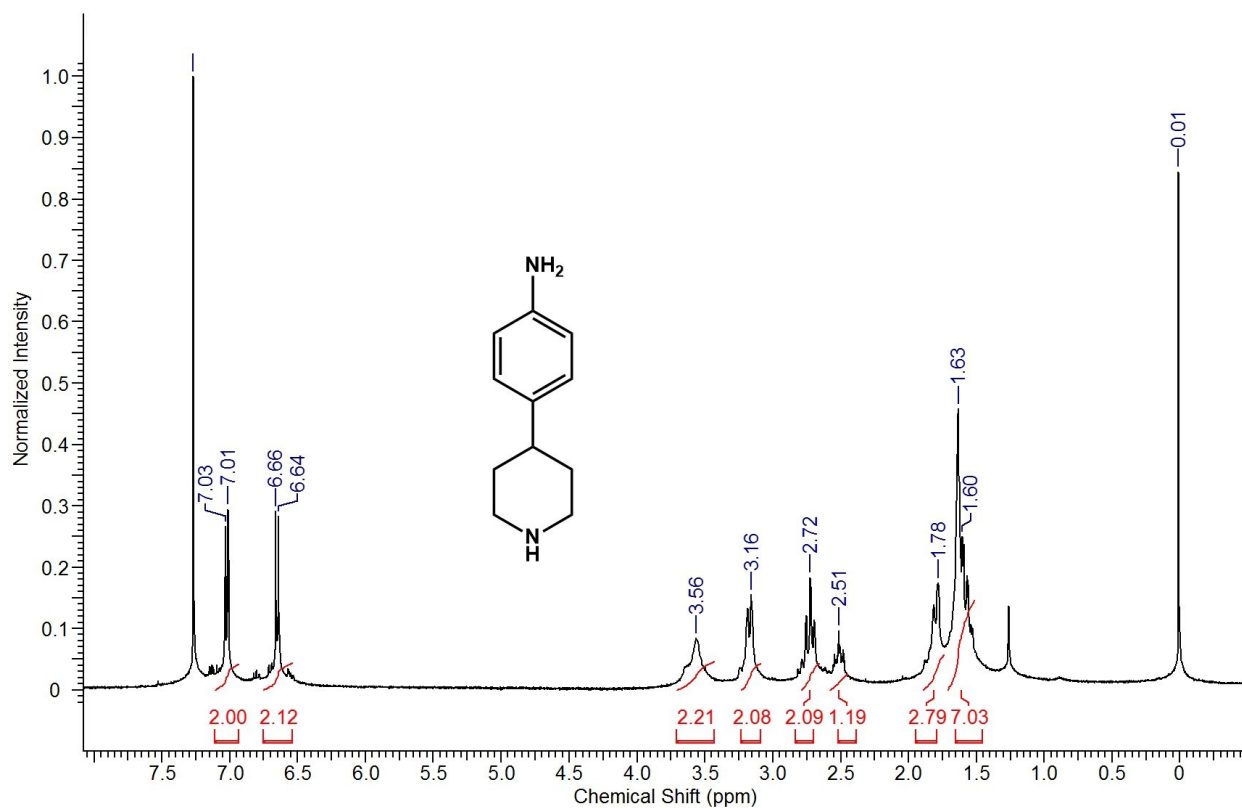


Figure B.44 ^1H NMR spectrum of **10** in CDCl_3 .

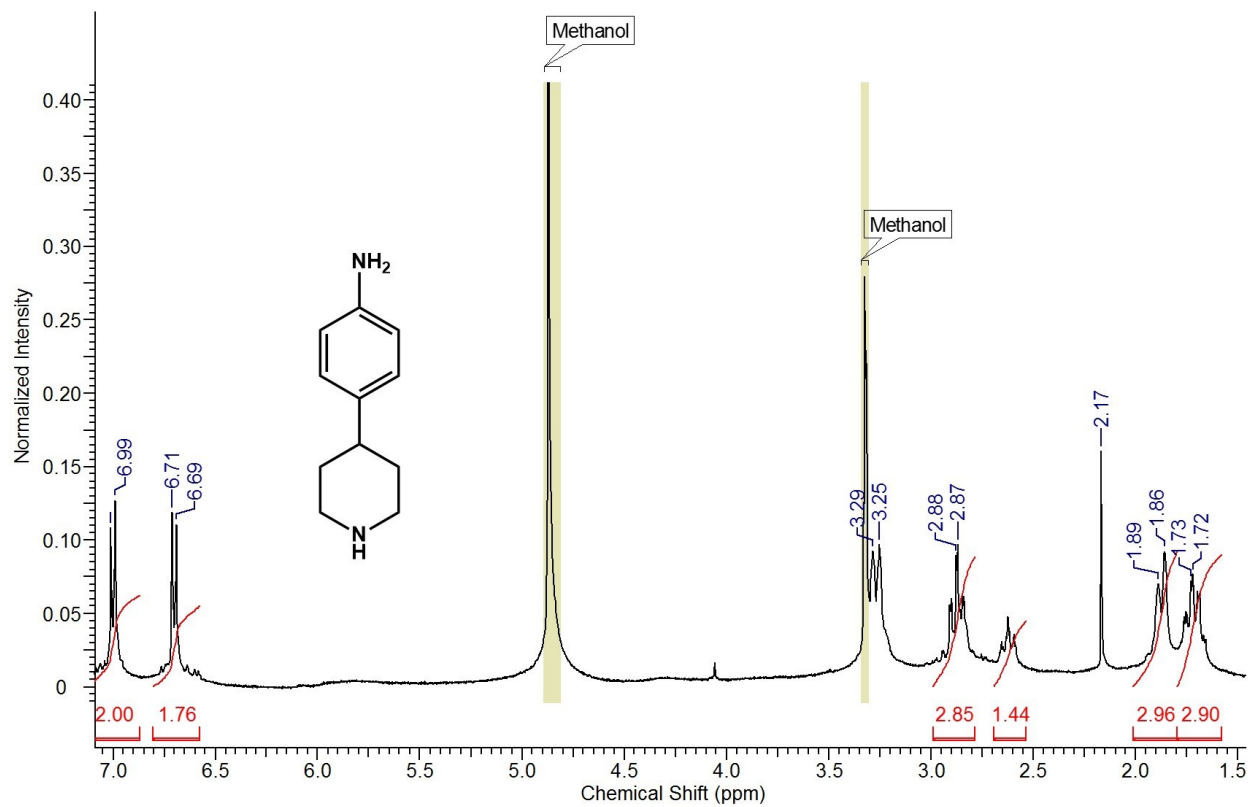


Figure B.45 ^1H NMR spectrum of **10** in CD_3OD .



Figure B.46 ^{13}C NMR spectrum of **10**.

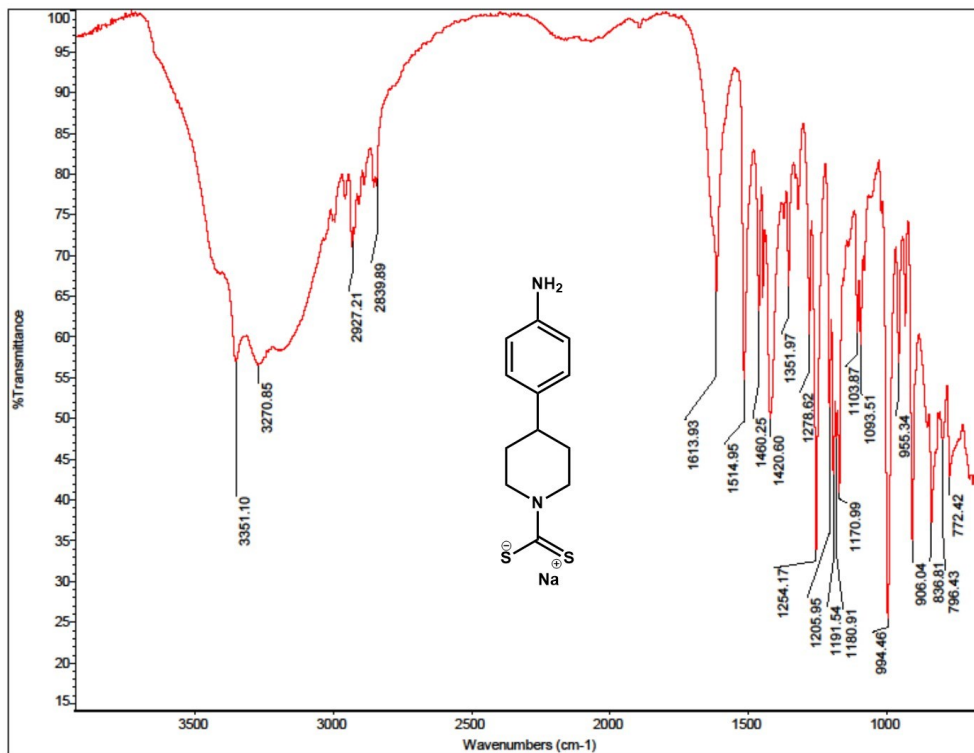


Figure B.47 IR spectrum of 11.

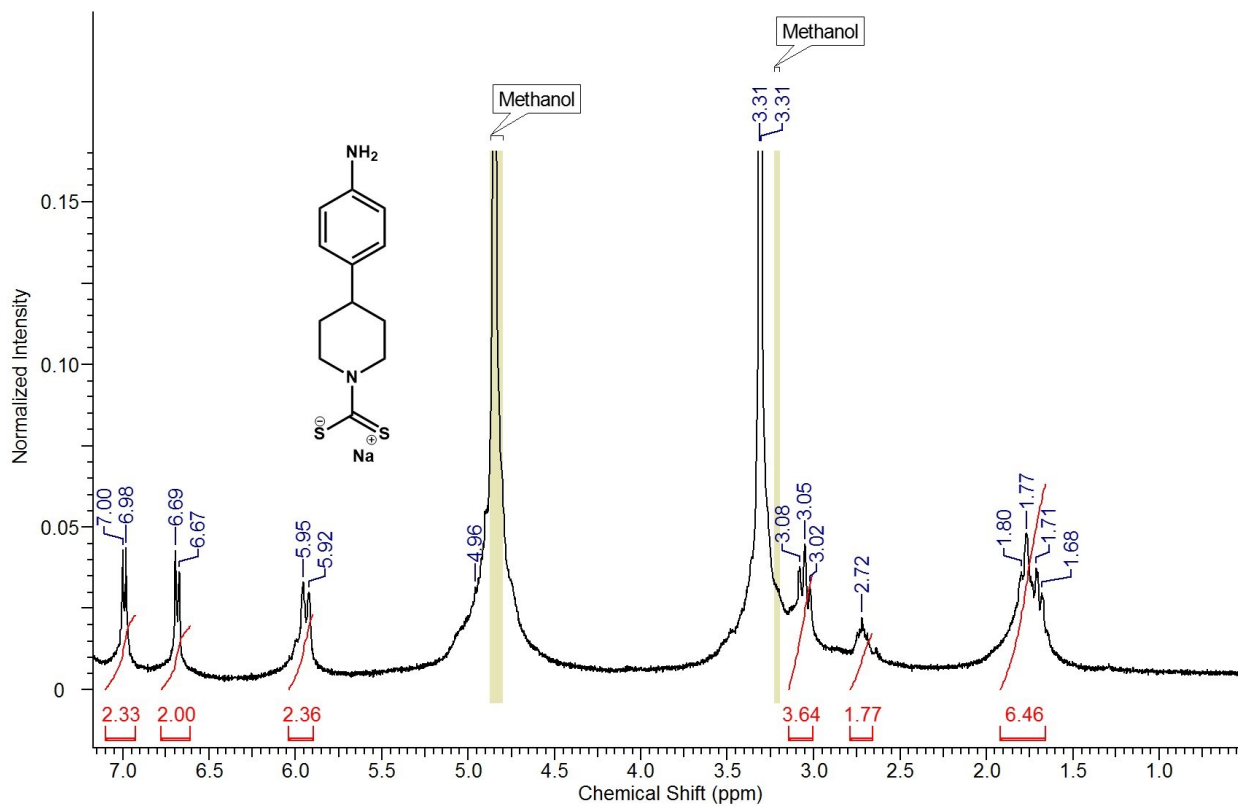


Figure B.48 ¹H NMR spectrum of 11 in CD₃OD.

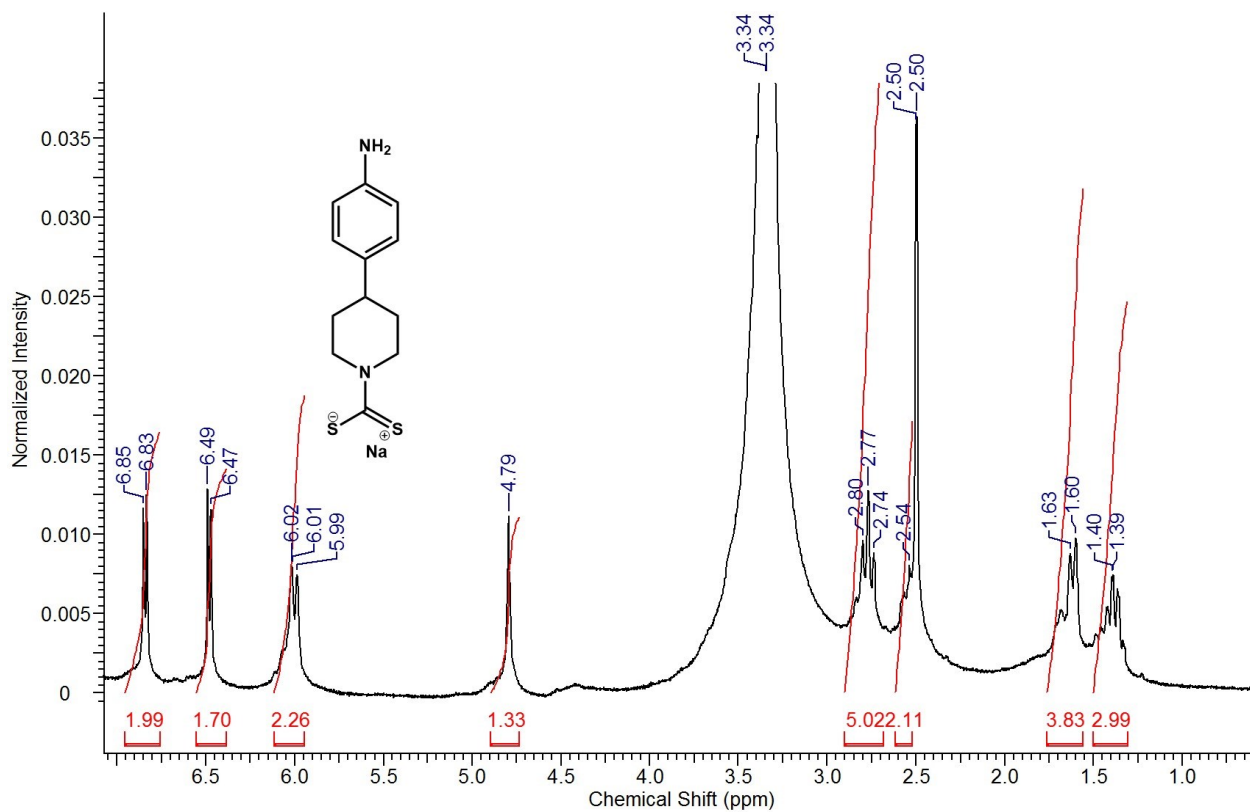


Figure B.49 ^1H NMR spectrum of **11** in DMSO.

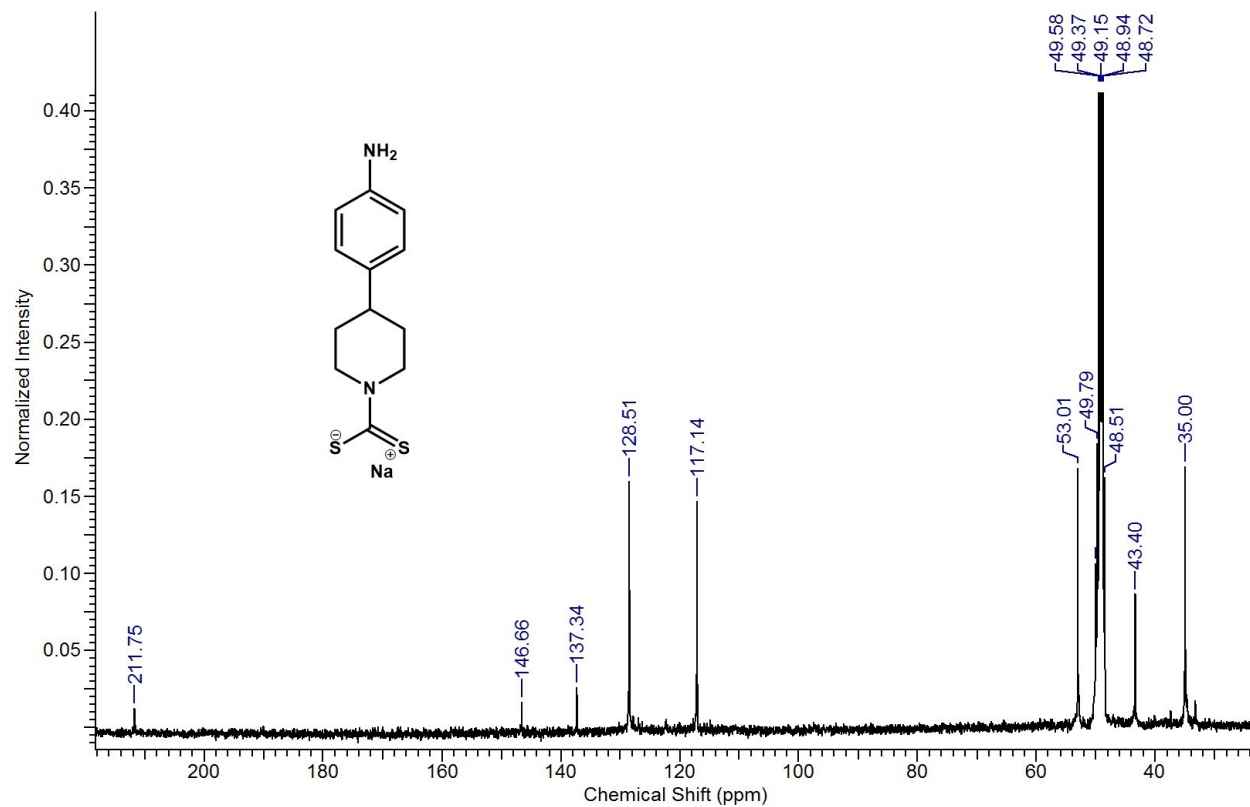


Figure B.50 ^{13}C NMR spectrum of **11**.

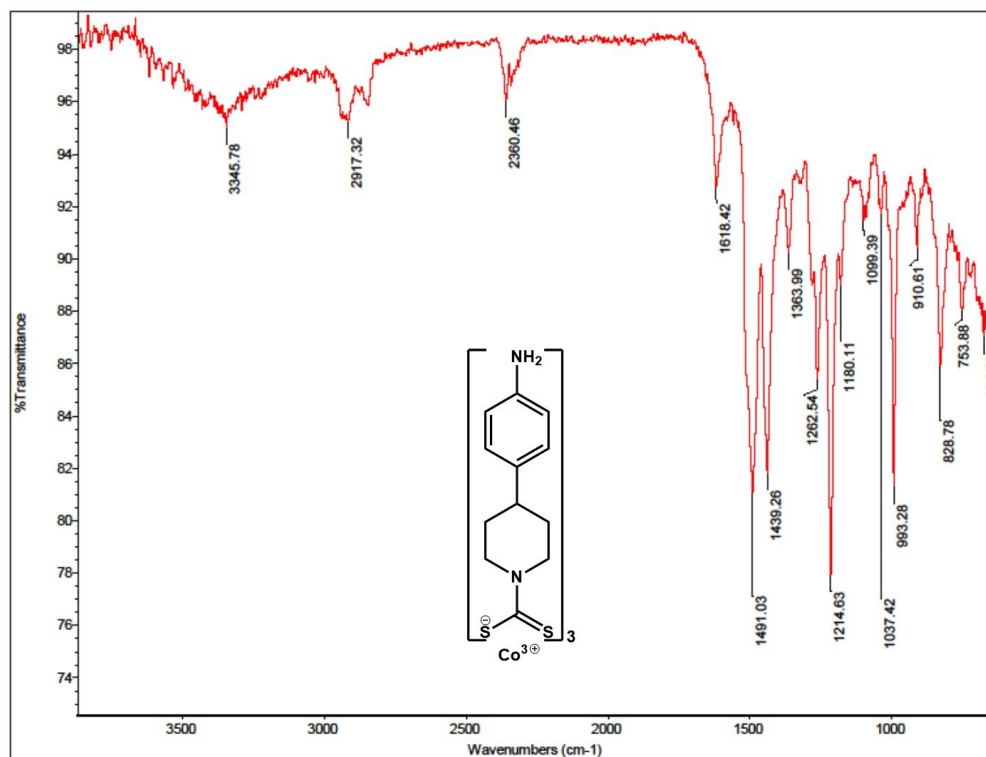


Figure B.51 IR spectrum of 11.Co.

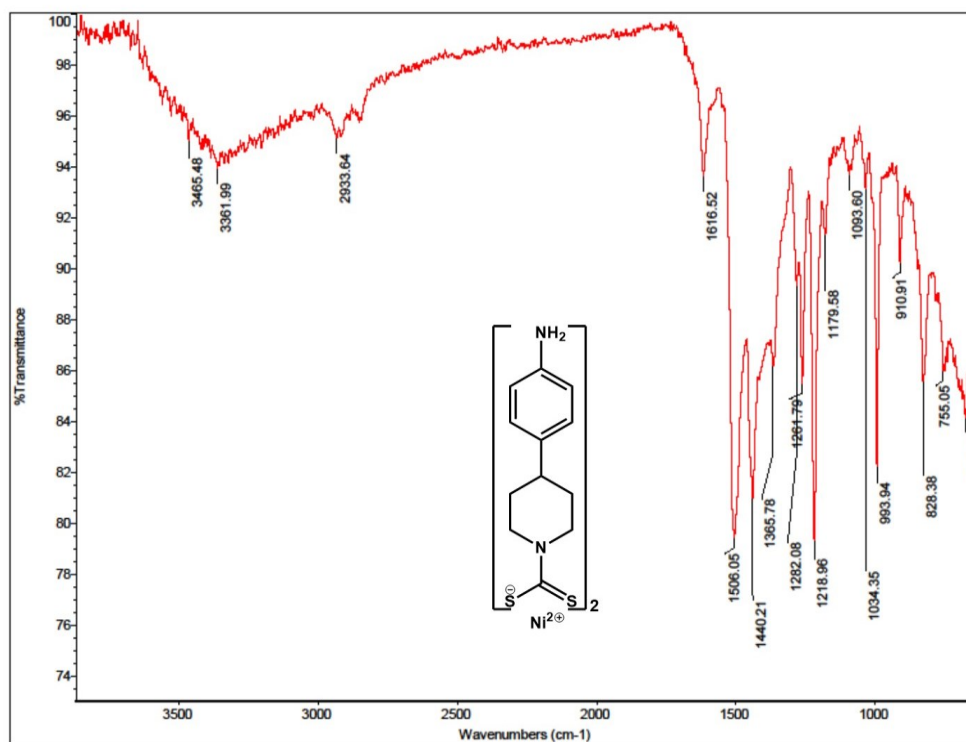


Figure B.52 IR spectrum of 11.Ni.

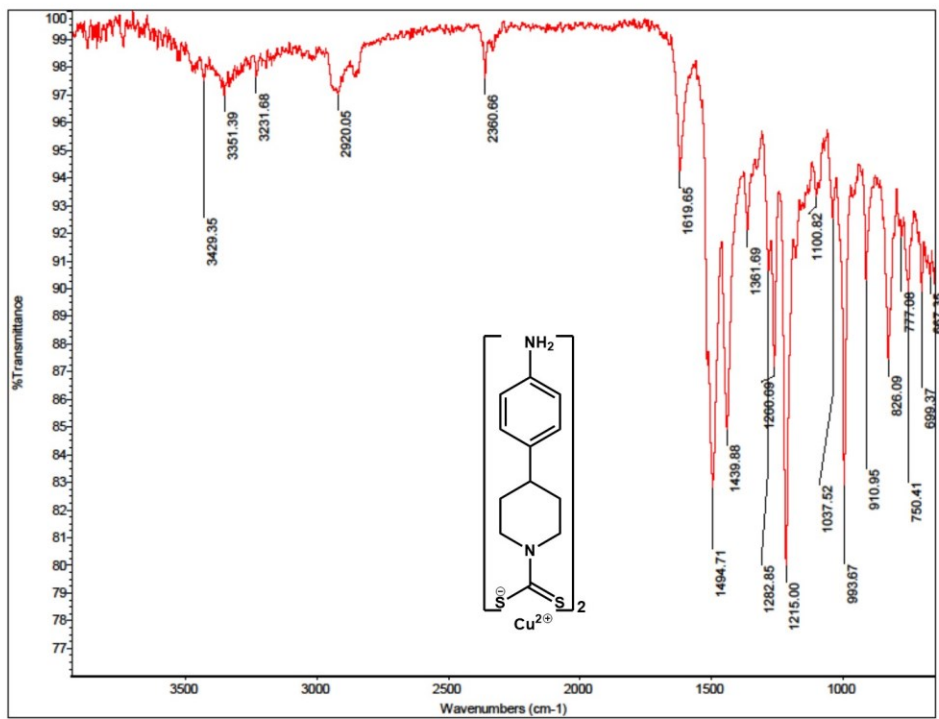


Figure B.53 IR spectrum of 11.Cu.

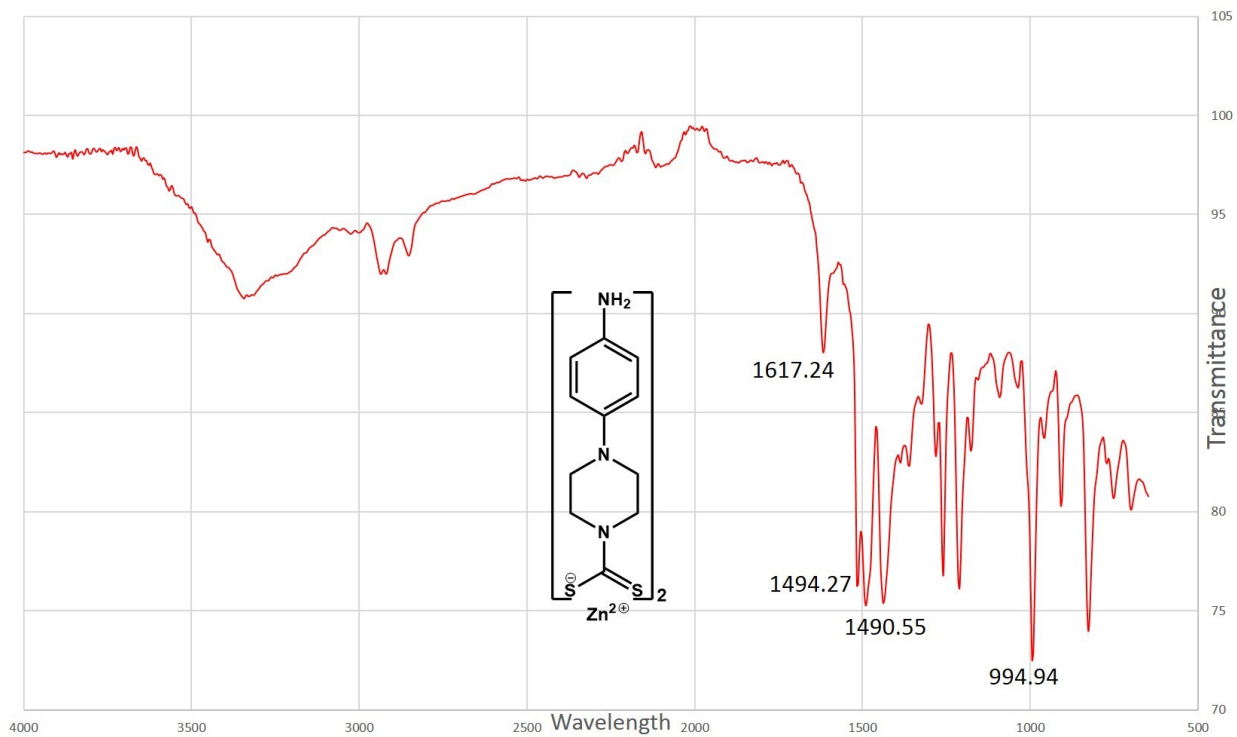


Figure B.54 IR spectrum of 11.Zn.

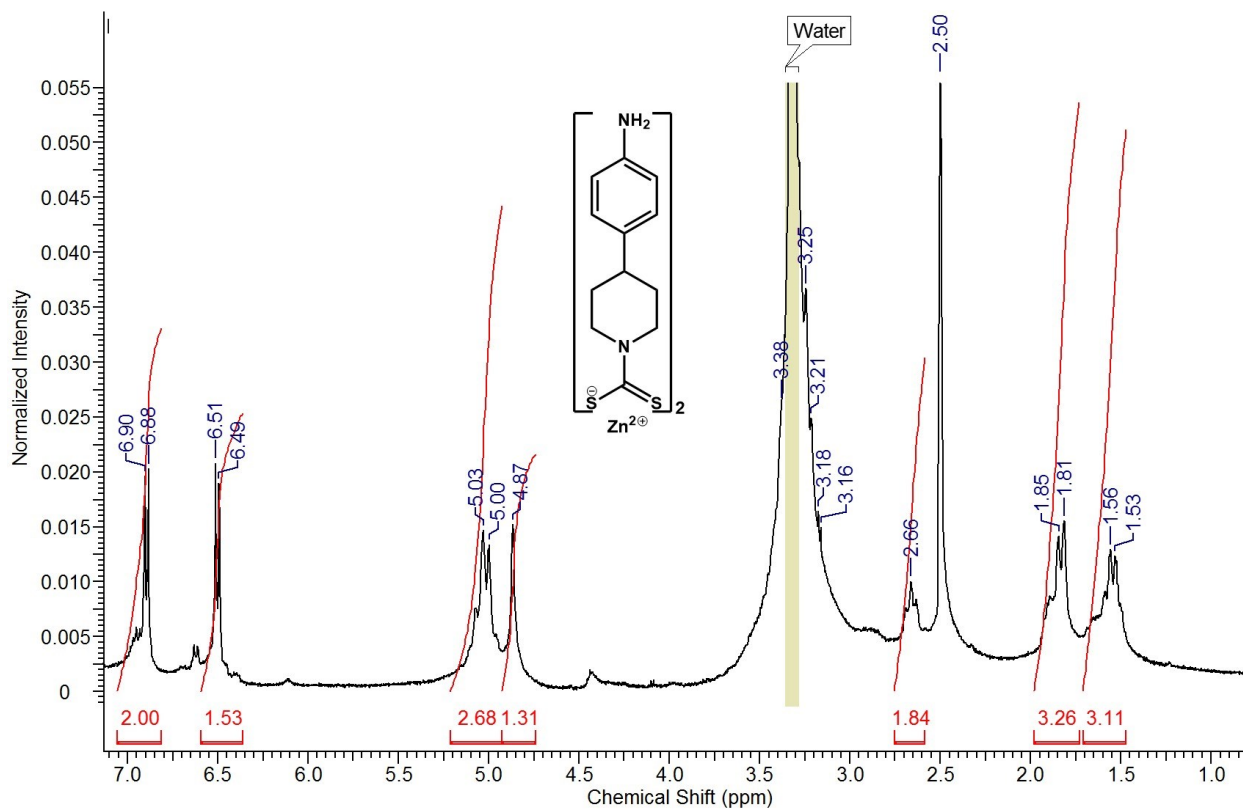


Figure B.55 ^1H NMR spectrum of **11.Zn**.

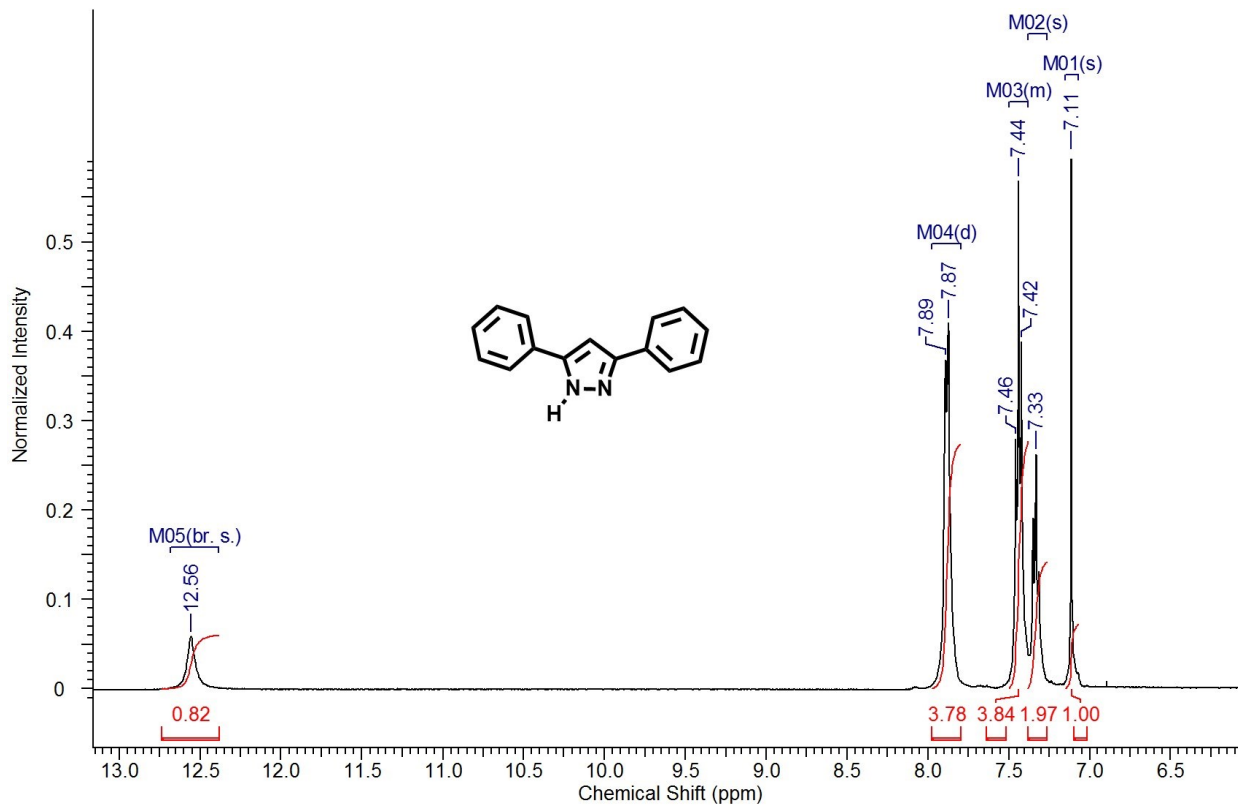


Figure B.56 ^1H NMR spectrum of **12**.

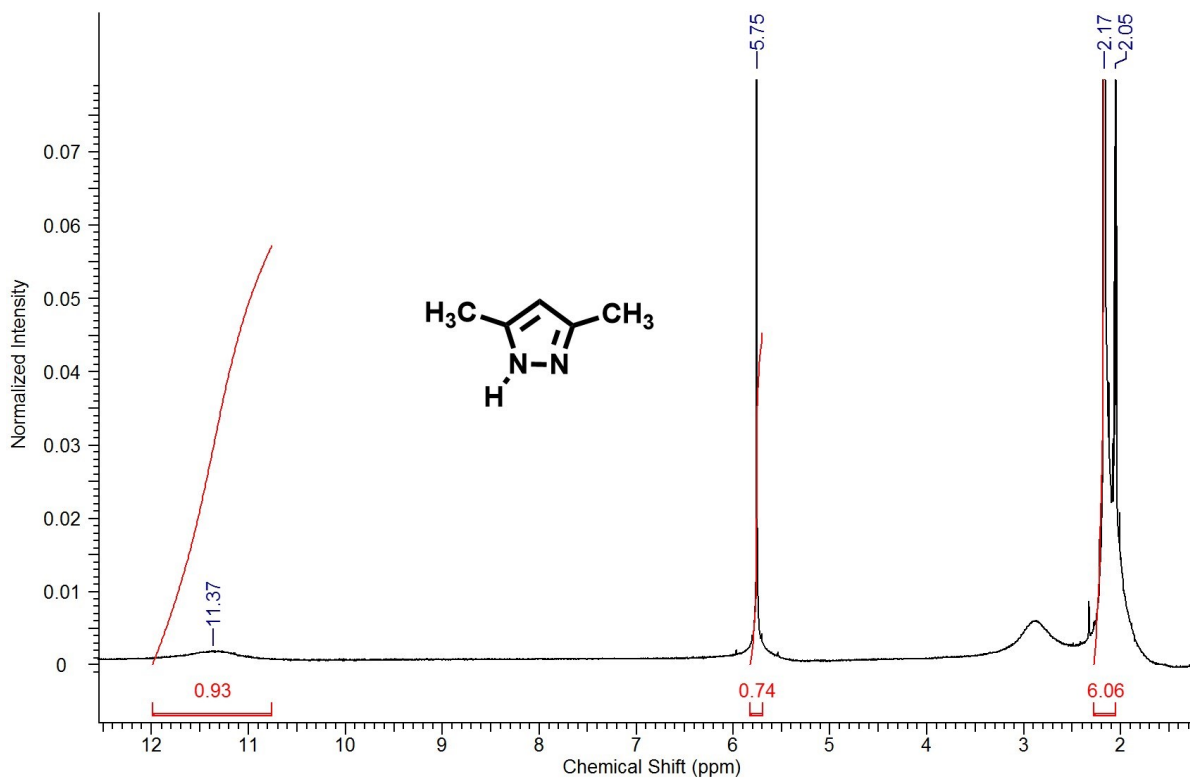


Figure B.57 ^1H NMR spectrum of 3,5-dimethylpyrazole.

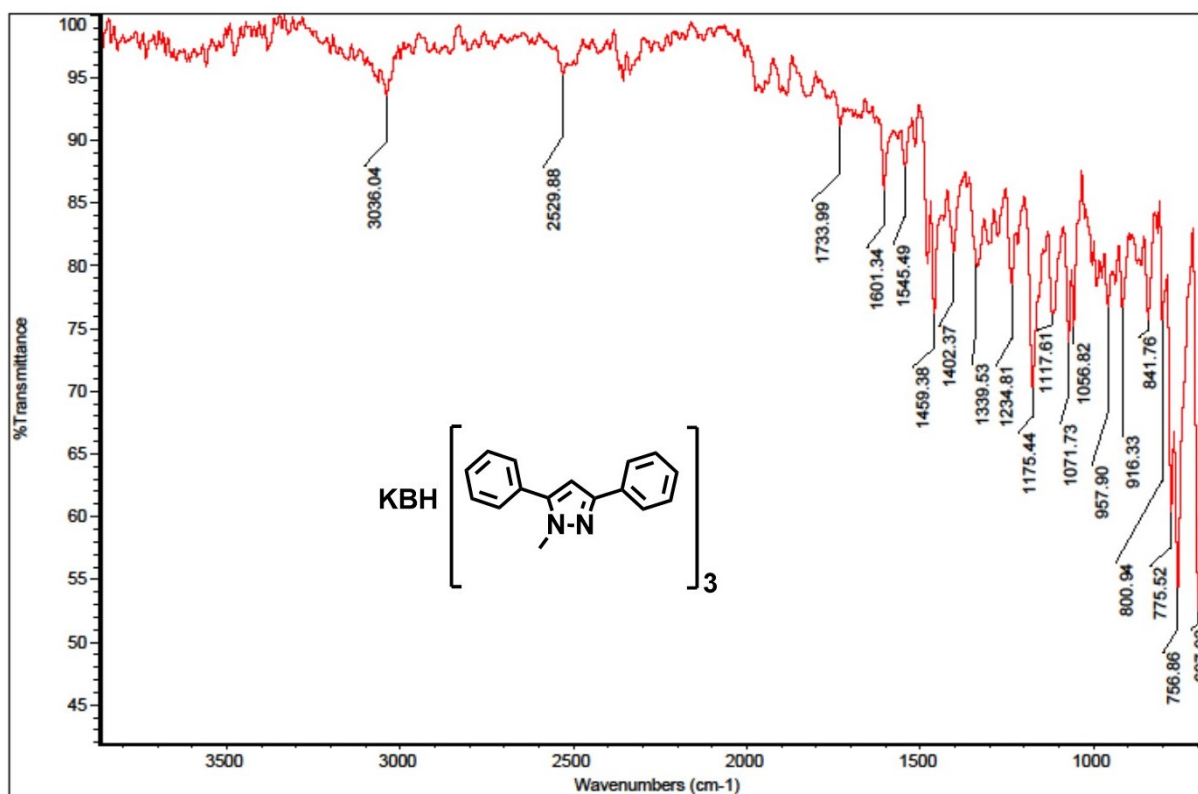


Figure B.58 IR spectrum of 13.

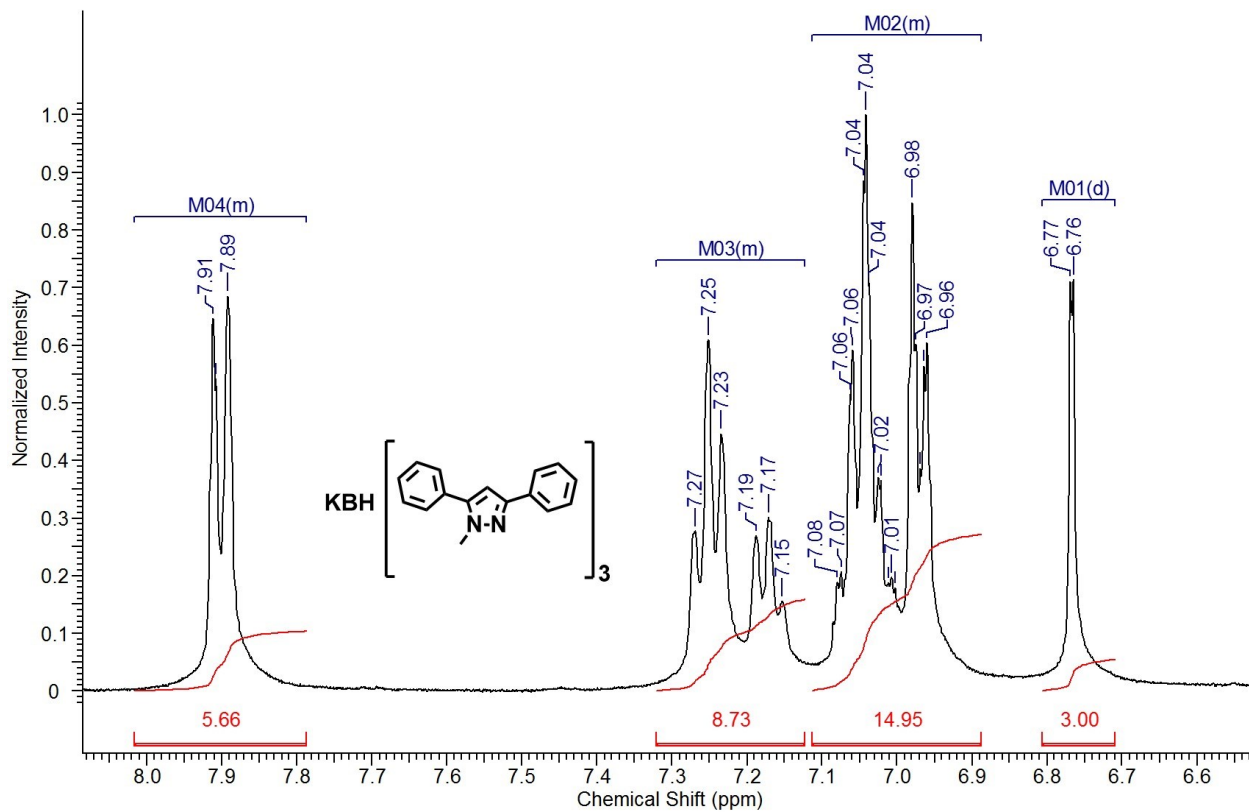


Figure B.59 ^1H NMR spectrum of 13.

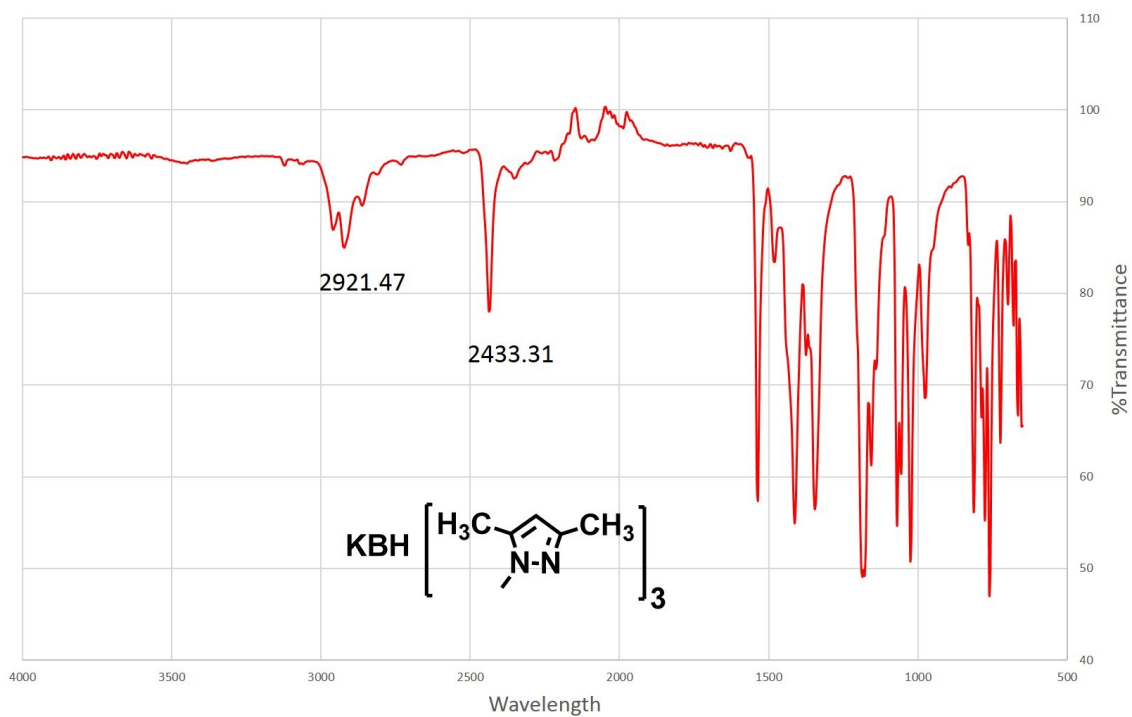


Figure B.60 IR spectrum of 14.

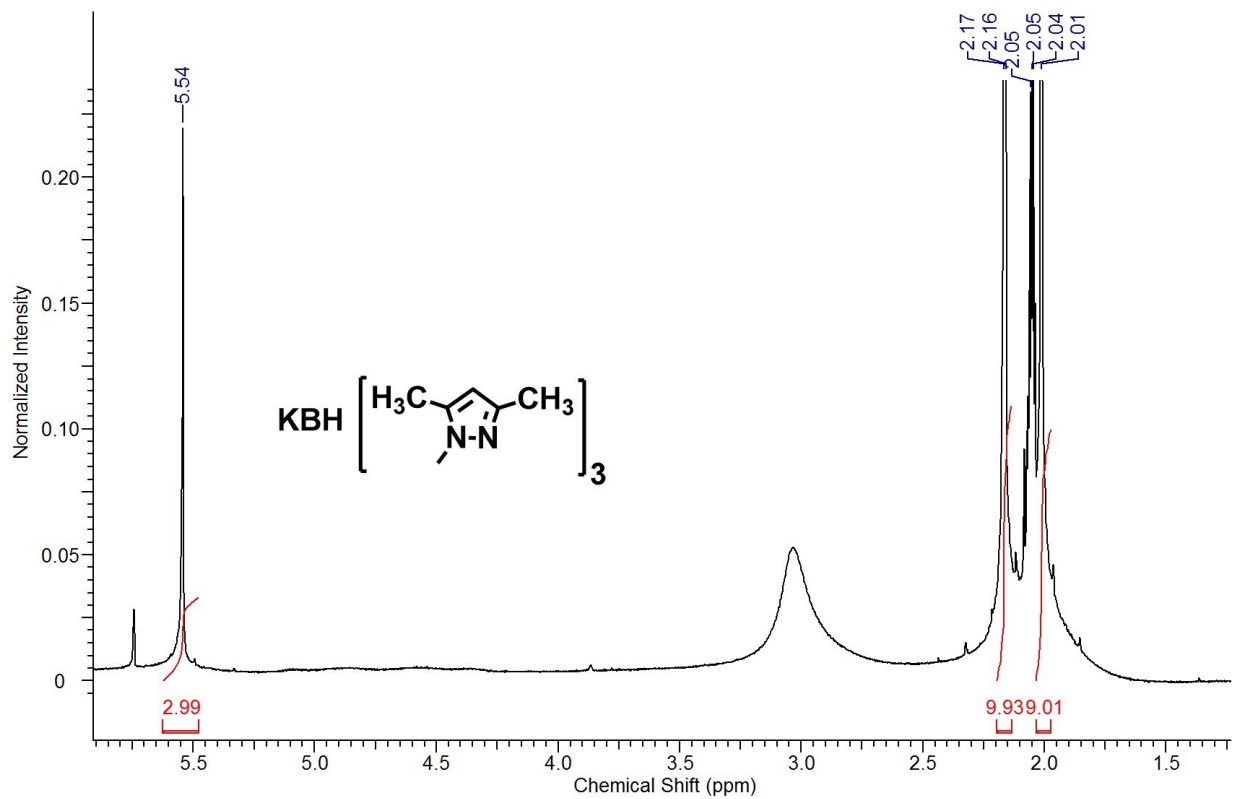


Figure B.61 ^1H NMR spectrum of 14.

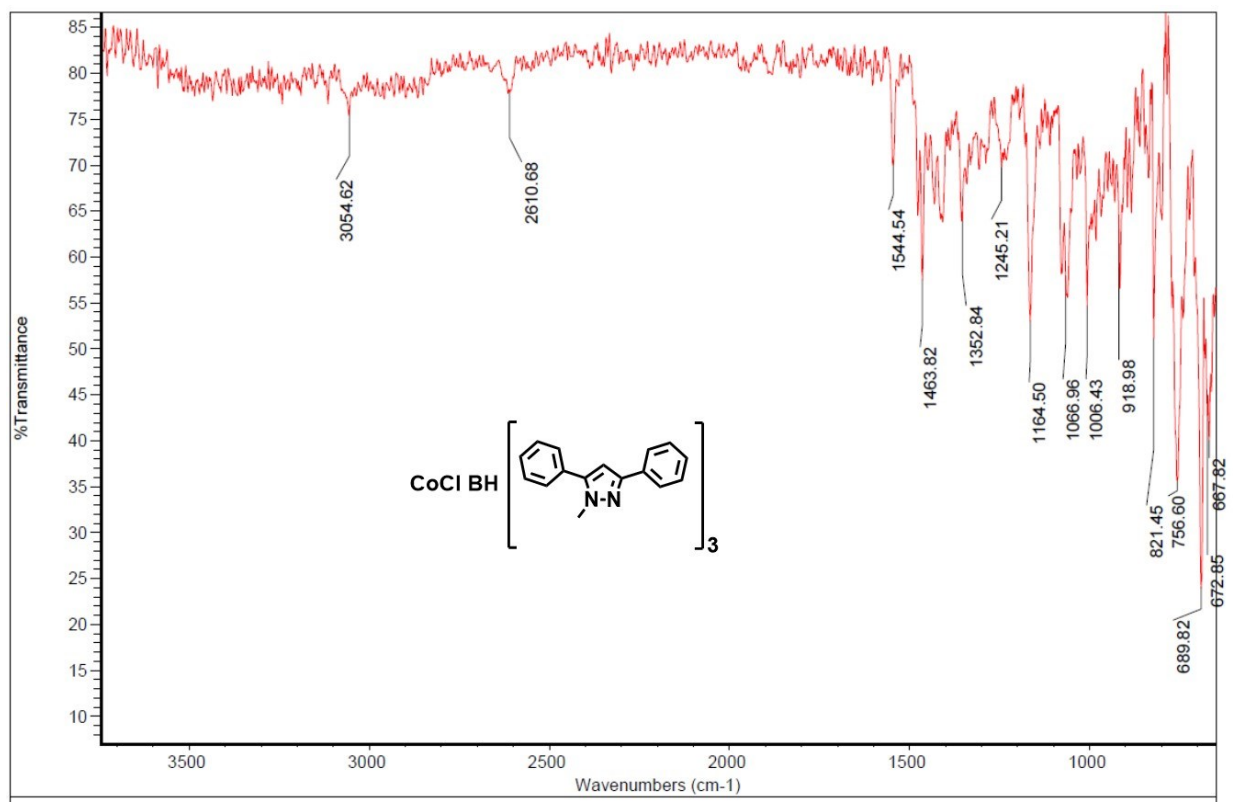


Figure B.62 IR spectrum of 15.

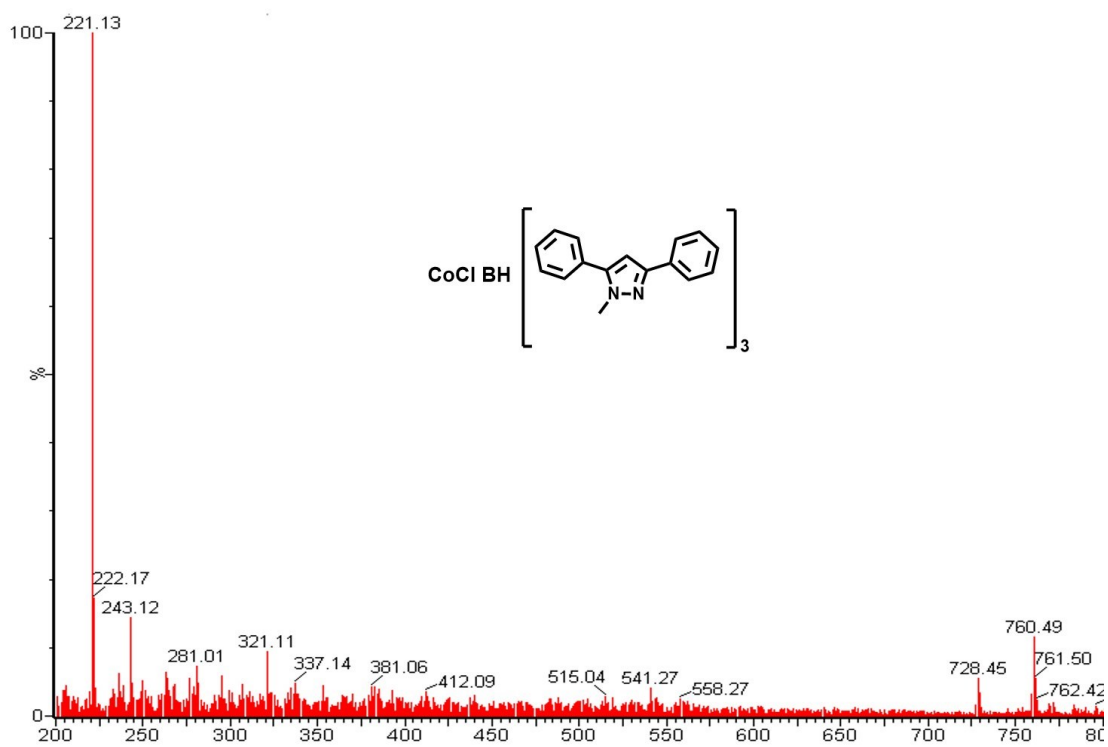


Figure B.63 ESI-MS spectrum of 15.

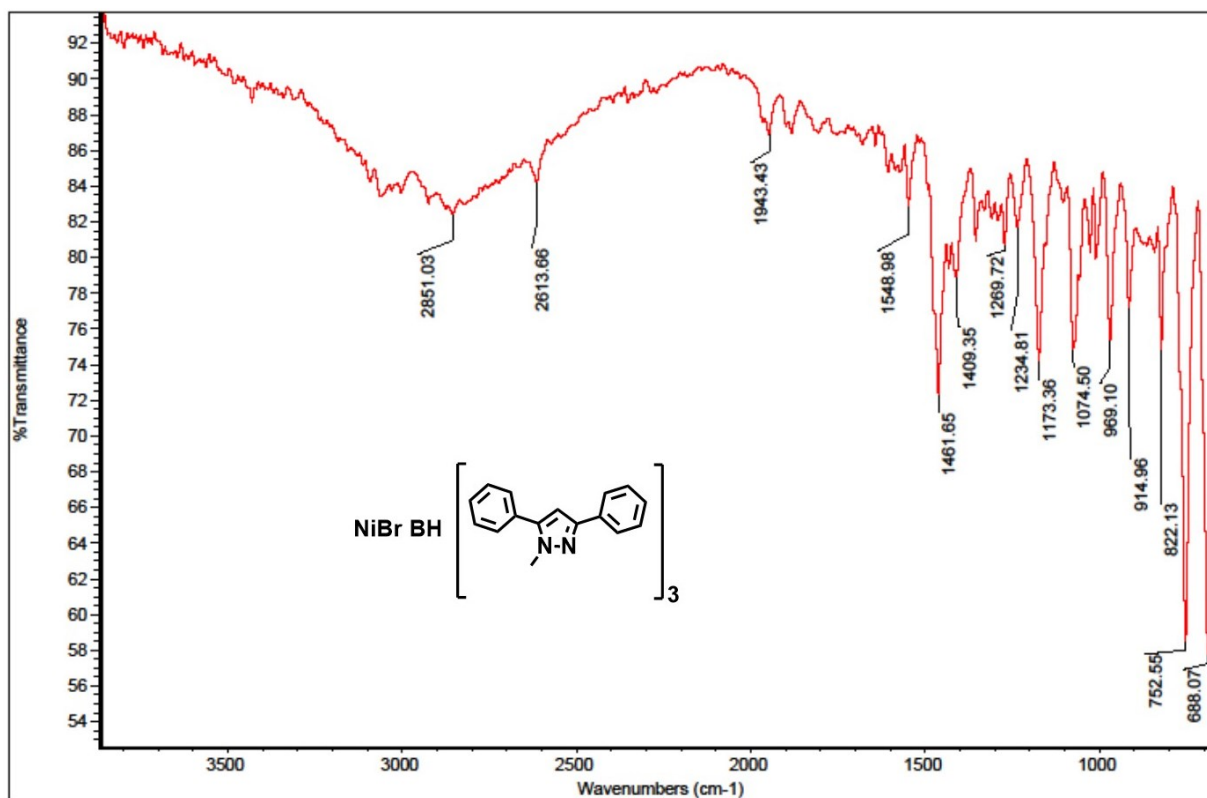


Figure B.64 IR spectrum of 16.

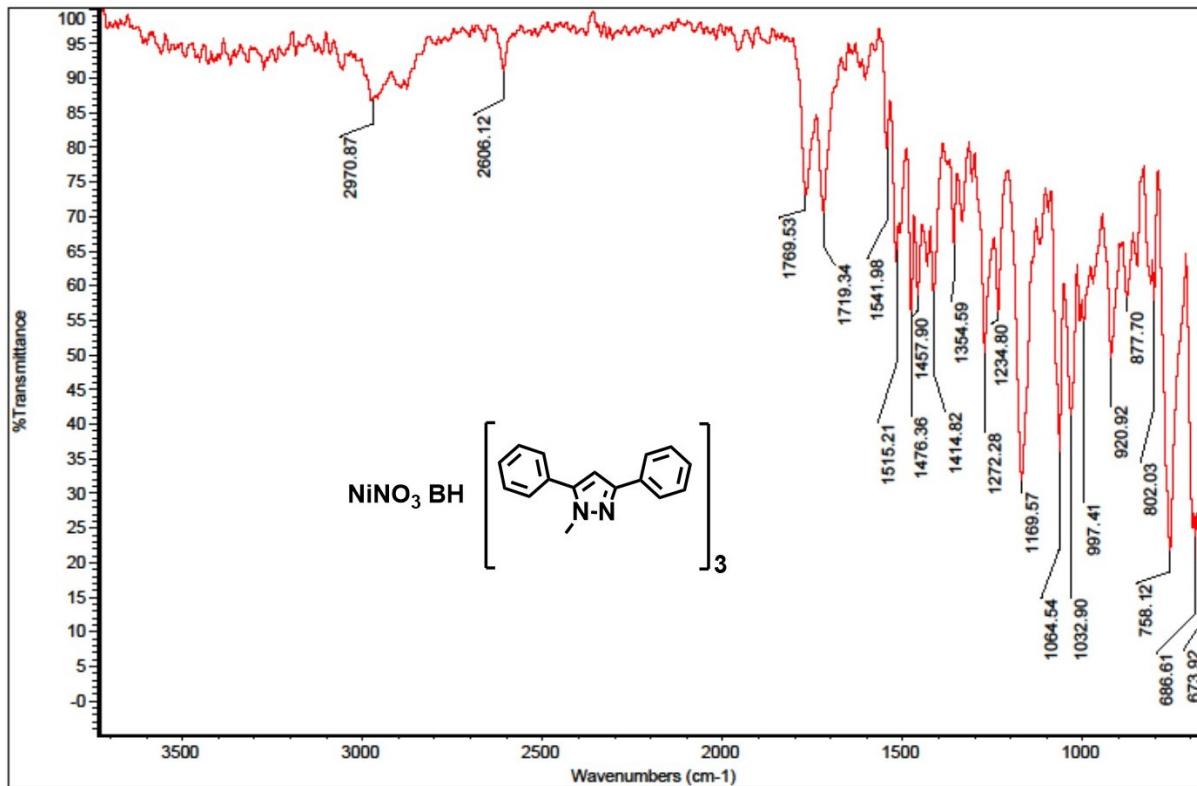


Figure B.65 IR spectrum of 17.

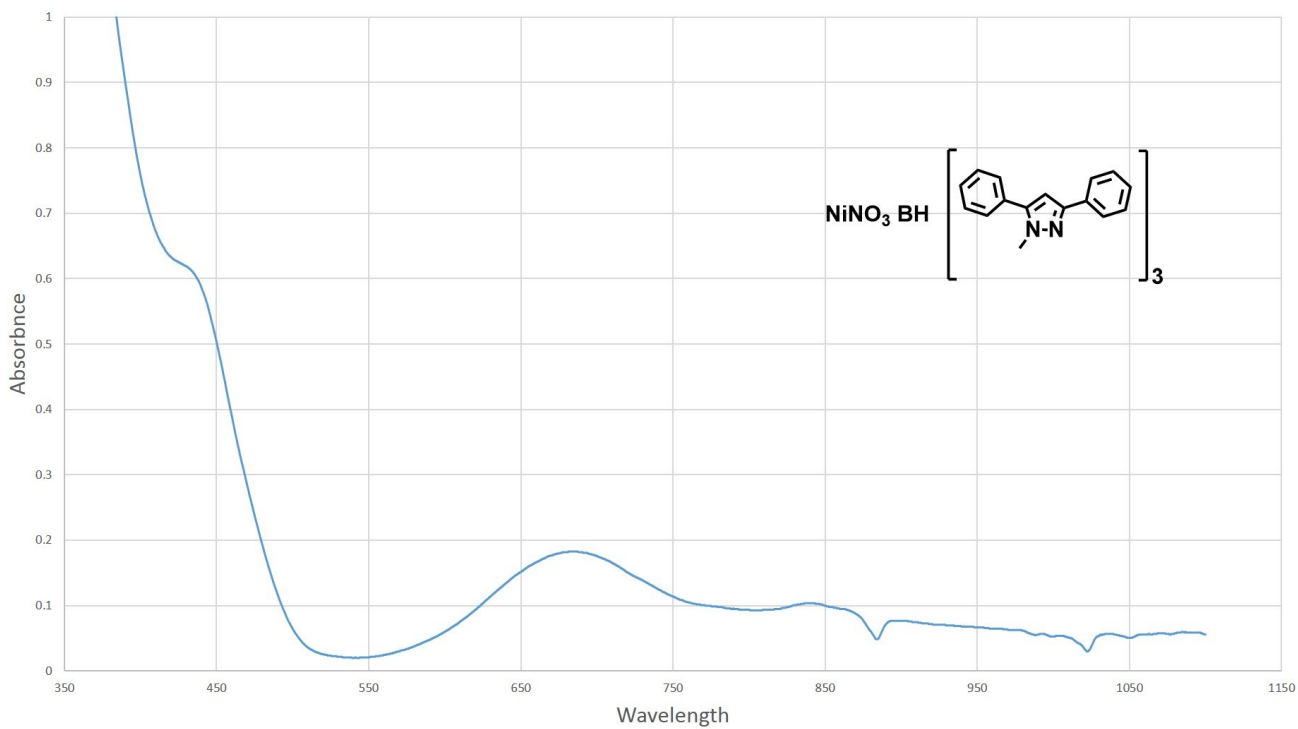


Figure B.66 UV-Visible spectrum of 17.

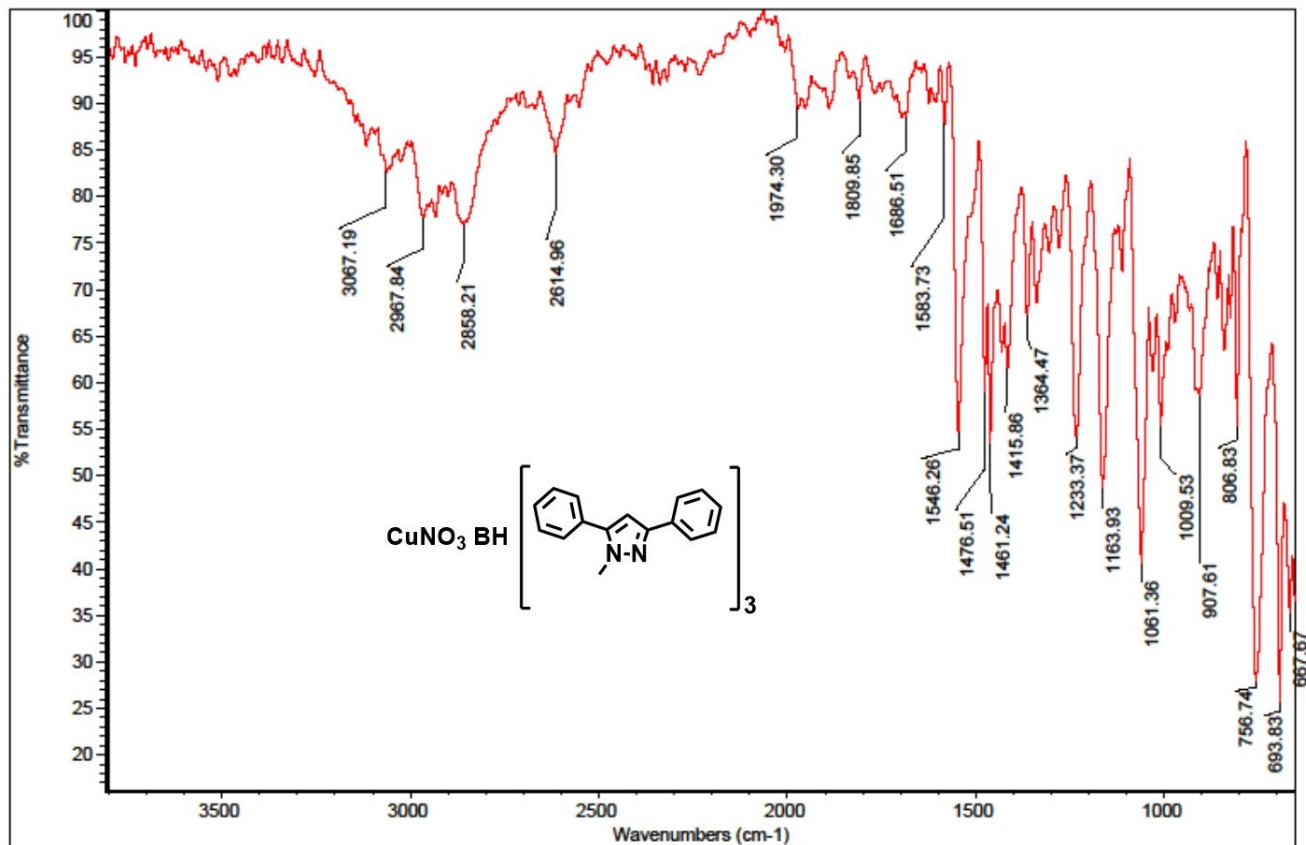


Figure B.67 IR spectrum of 18.

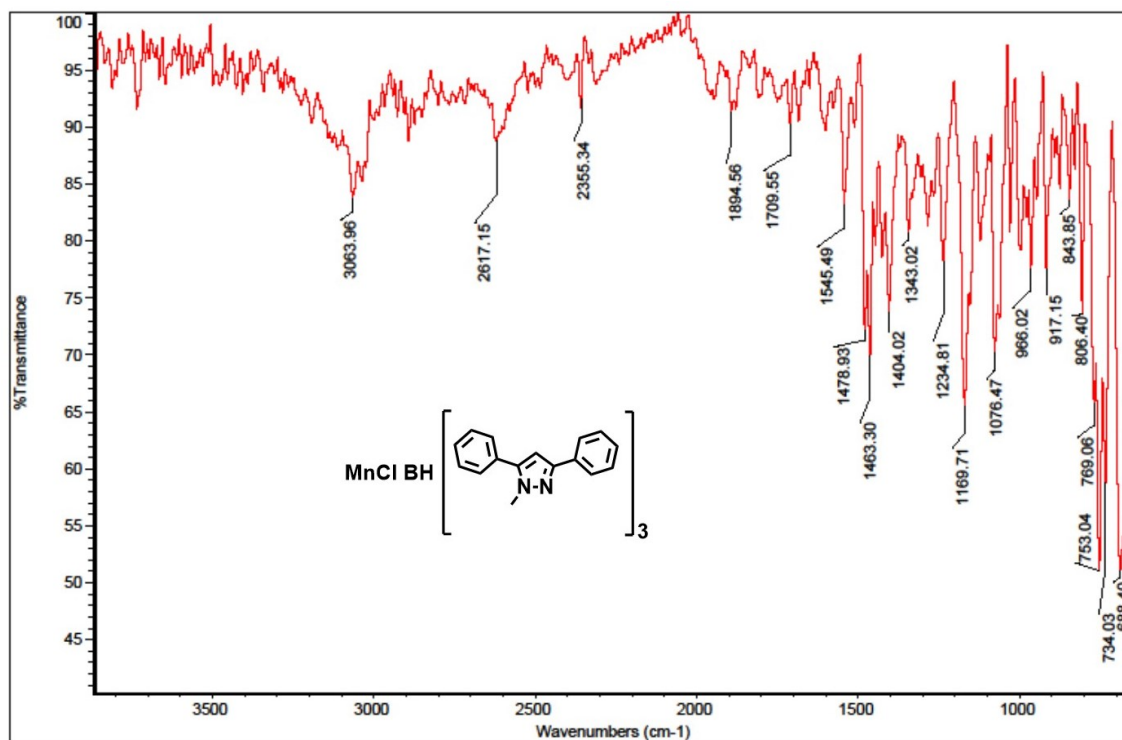


Figure B.68 IR spectrum of 19.

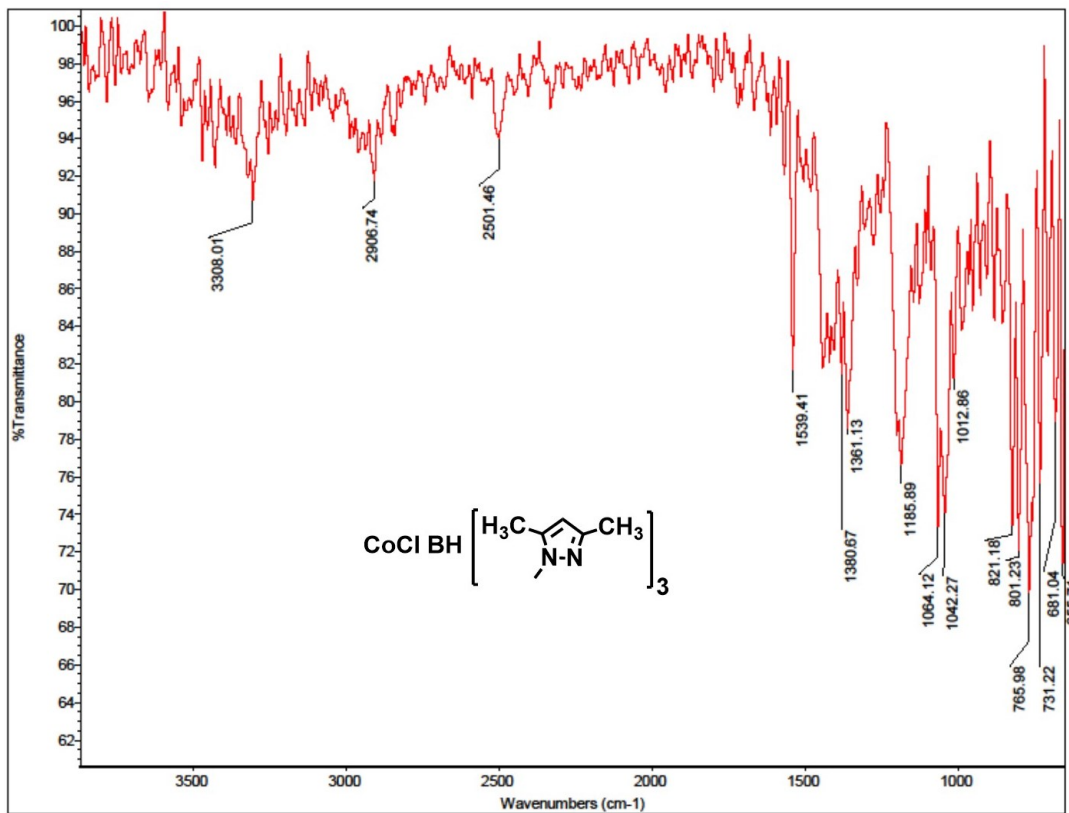


Figure B.69 IR spectrum of 20.

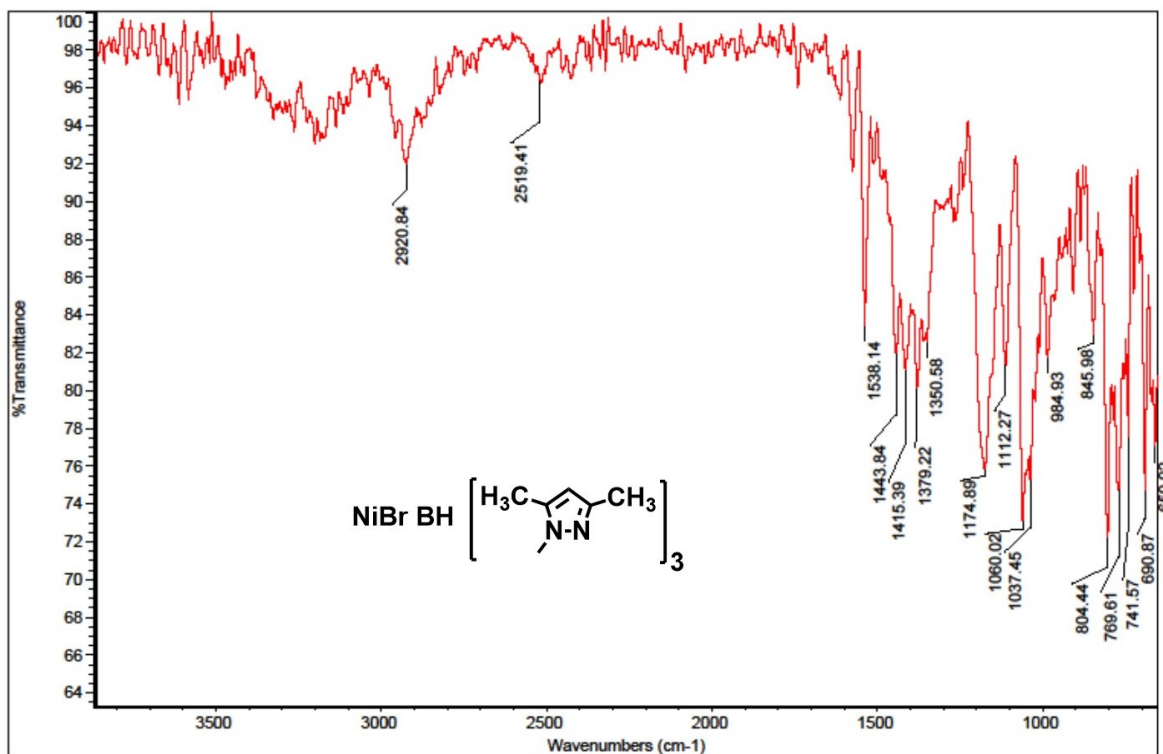


Figure B.70 IR spectrum of 21.

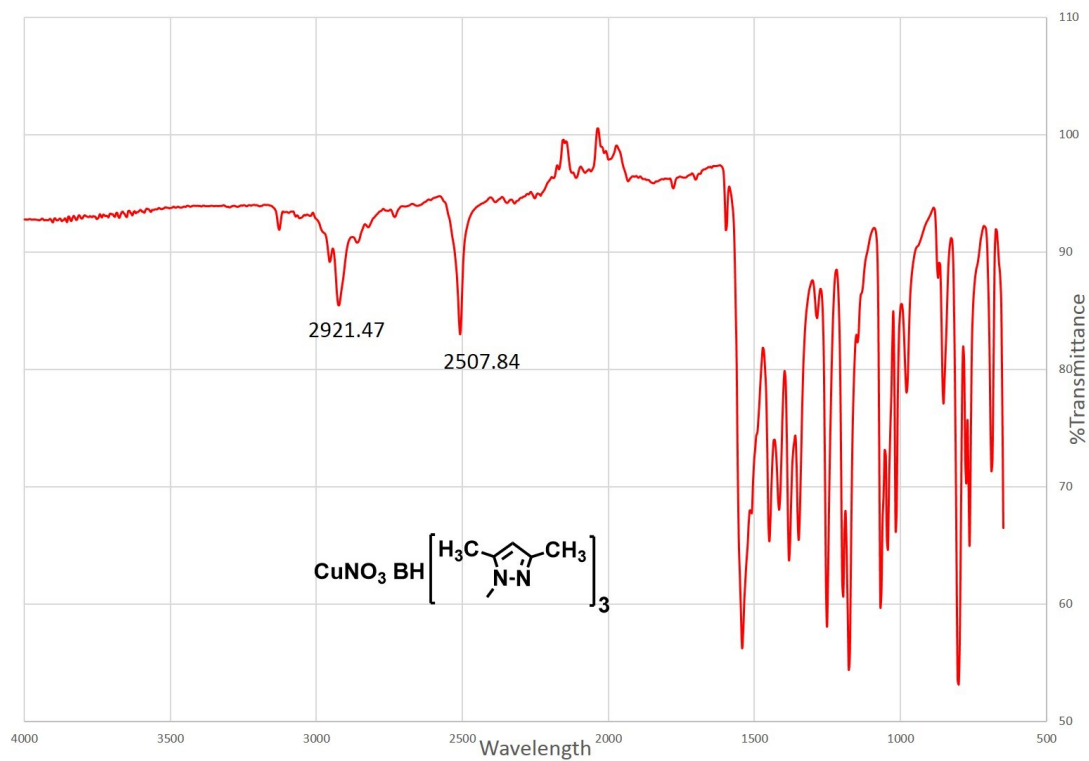


Figure B.71 IR spectrum of 22.

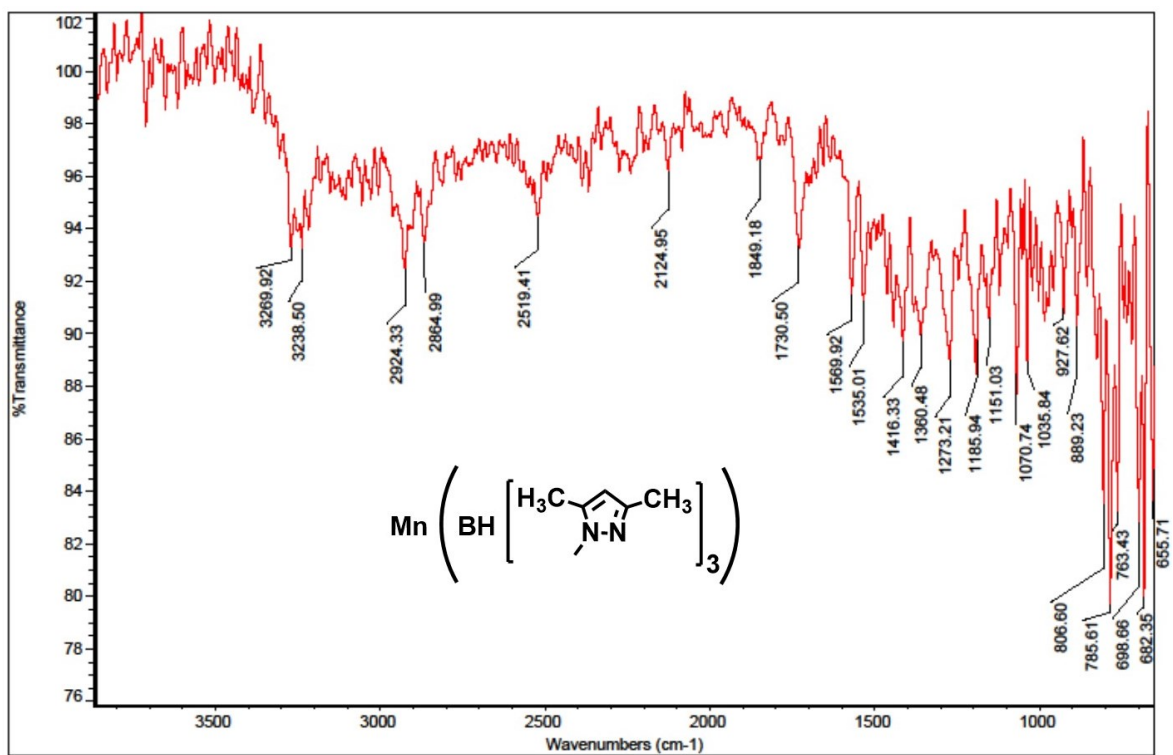


Figure B.72 IR spectrum of 23.

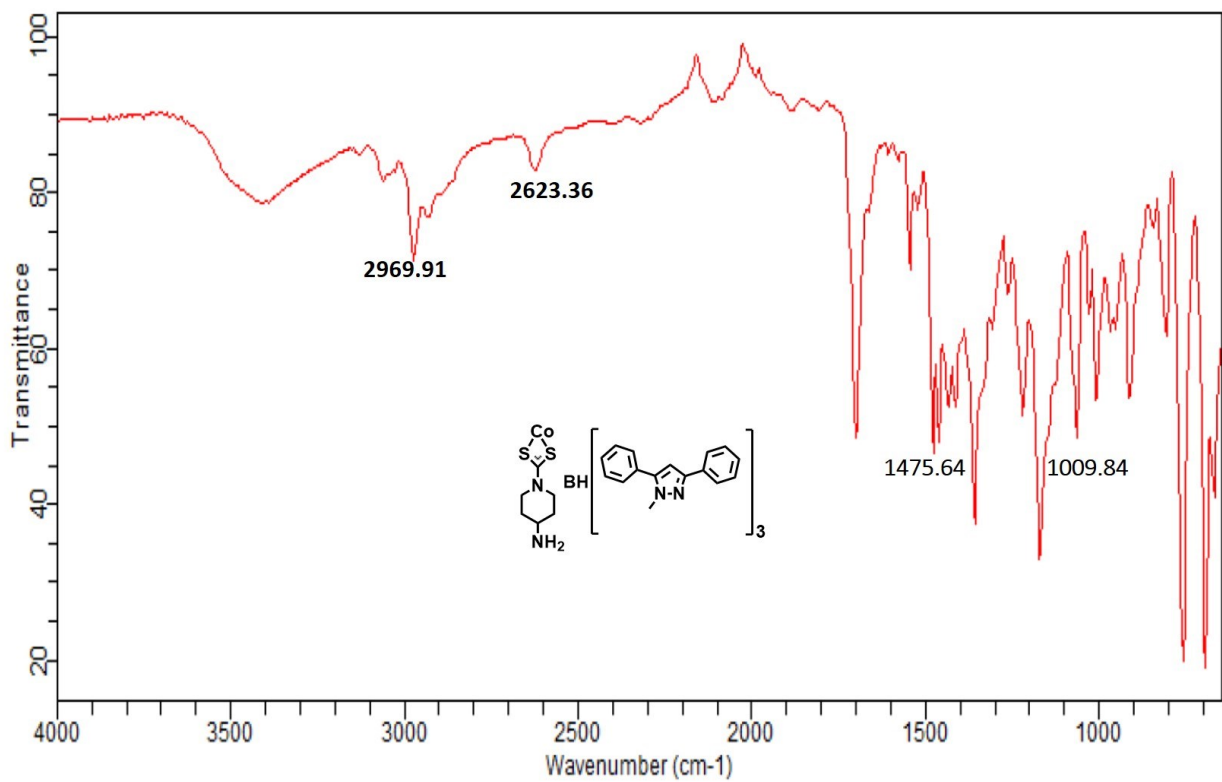


Figure B.73 IR spectrum of 24.

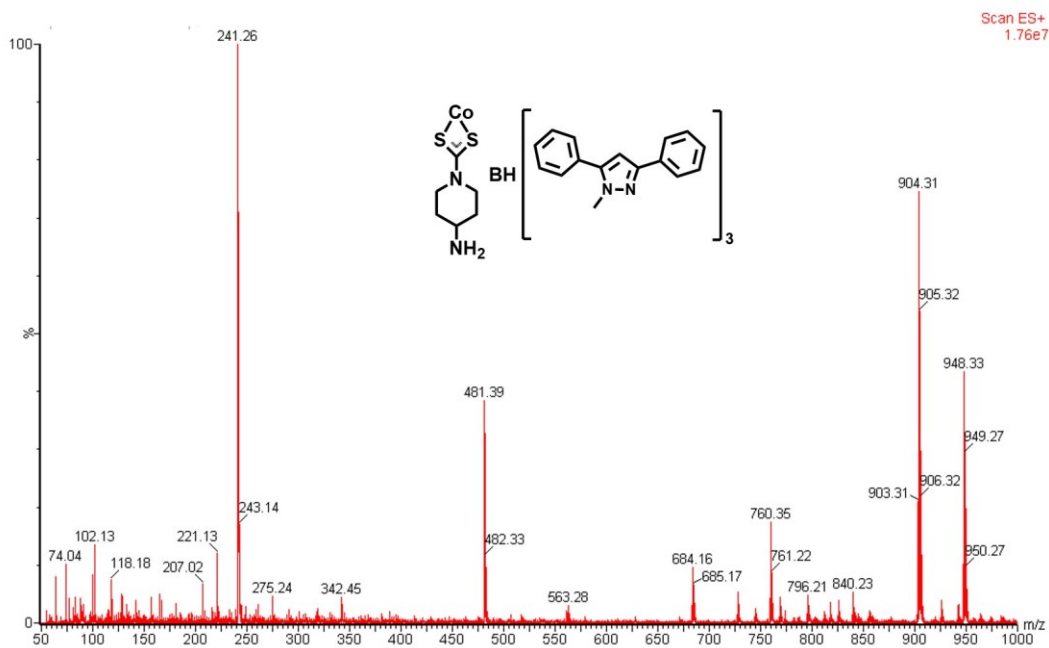


Figure B.74 ESI-MS spectrum of 24.

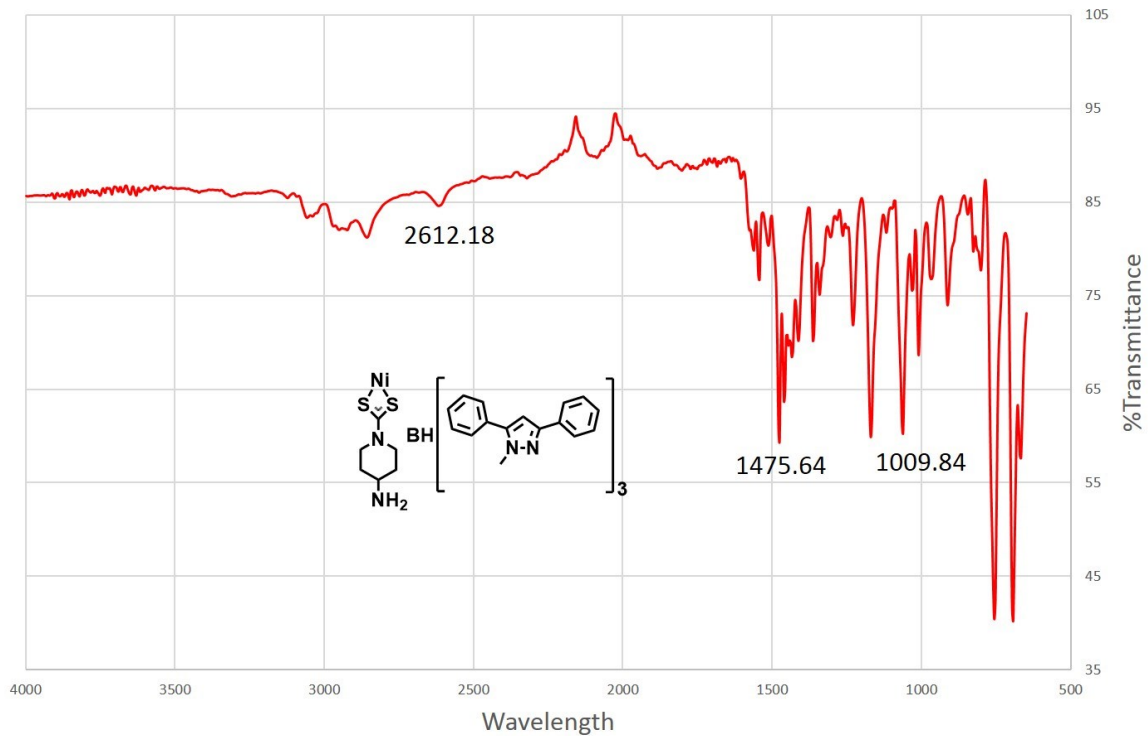


Figure B.75 IR spectrum of 25.

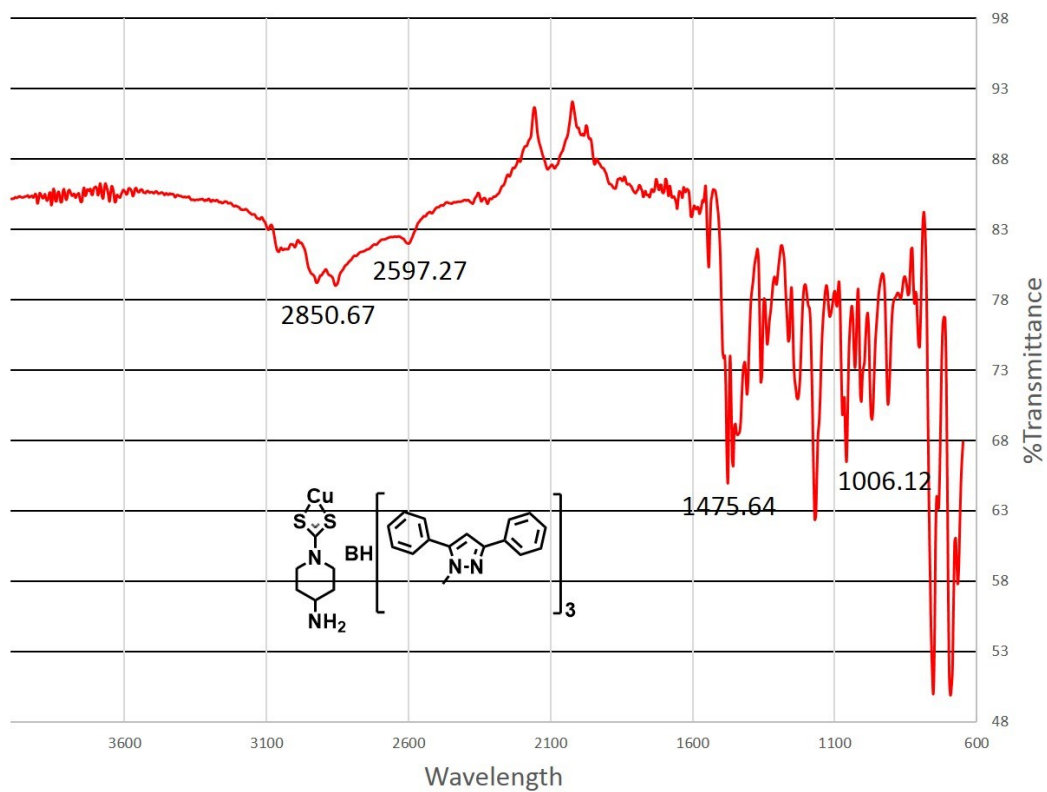


Figure B.76 IR spectrum of 26.

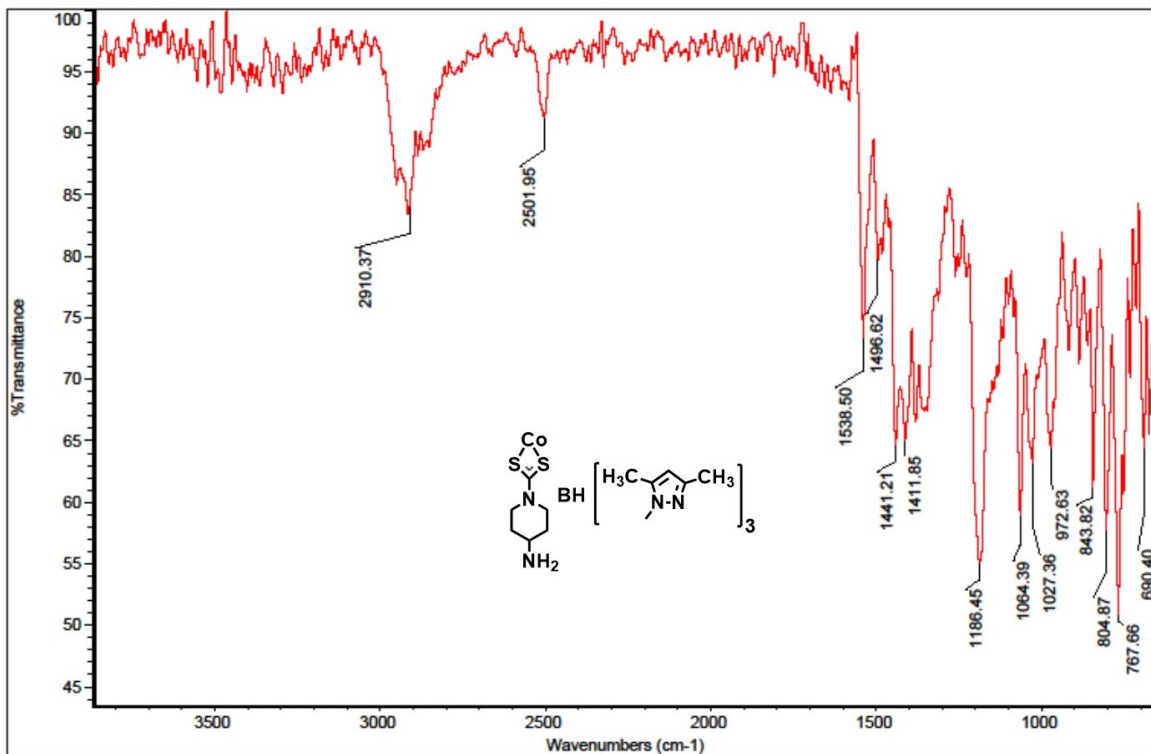


Figure B.77 IR spectrum of 27.

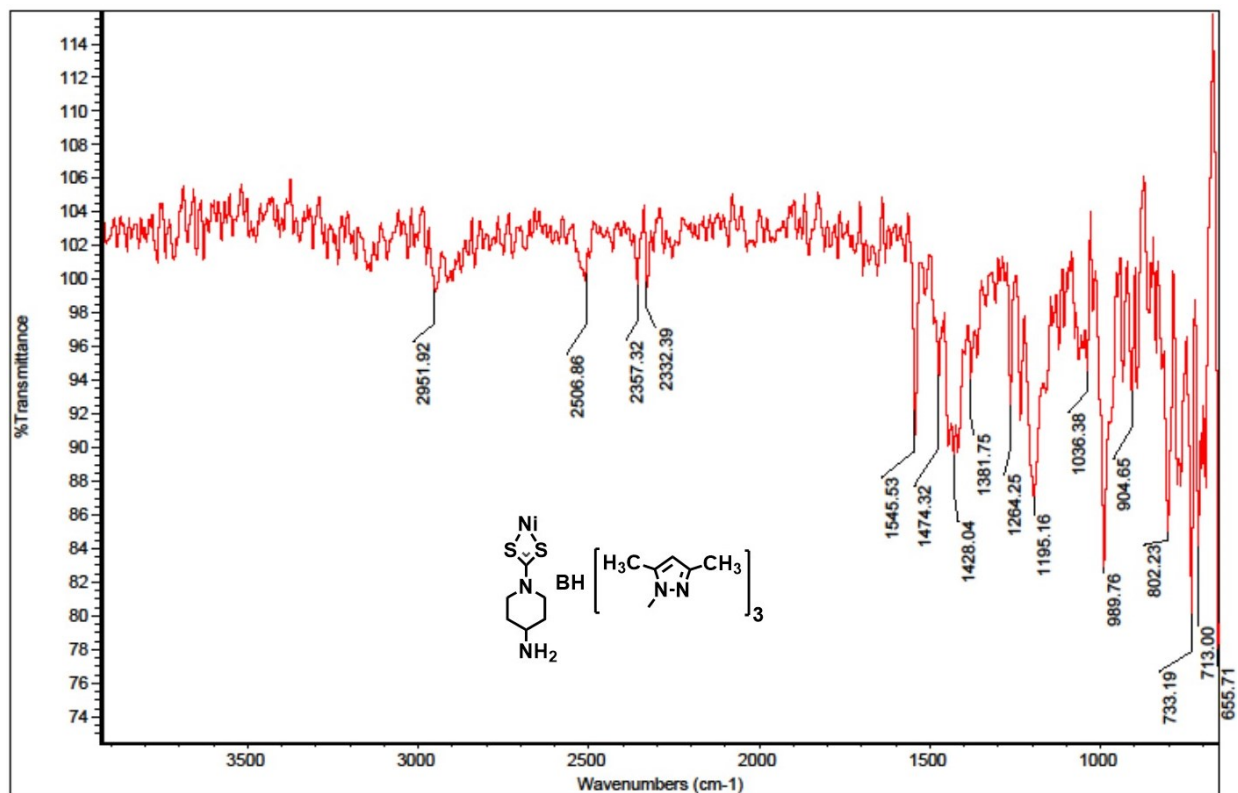


Figure B.78 IR spectrum of 28.

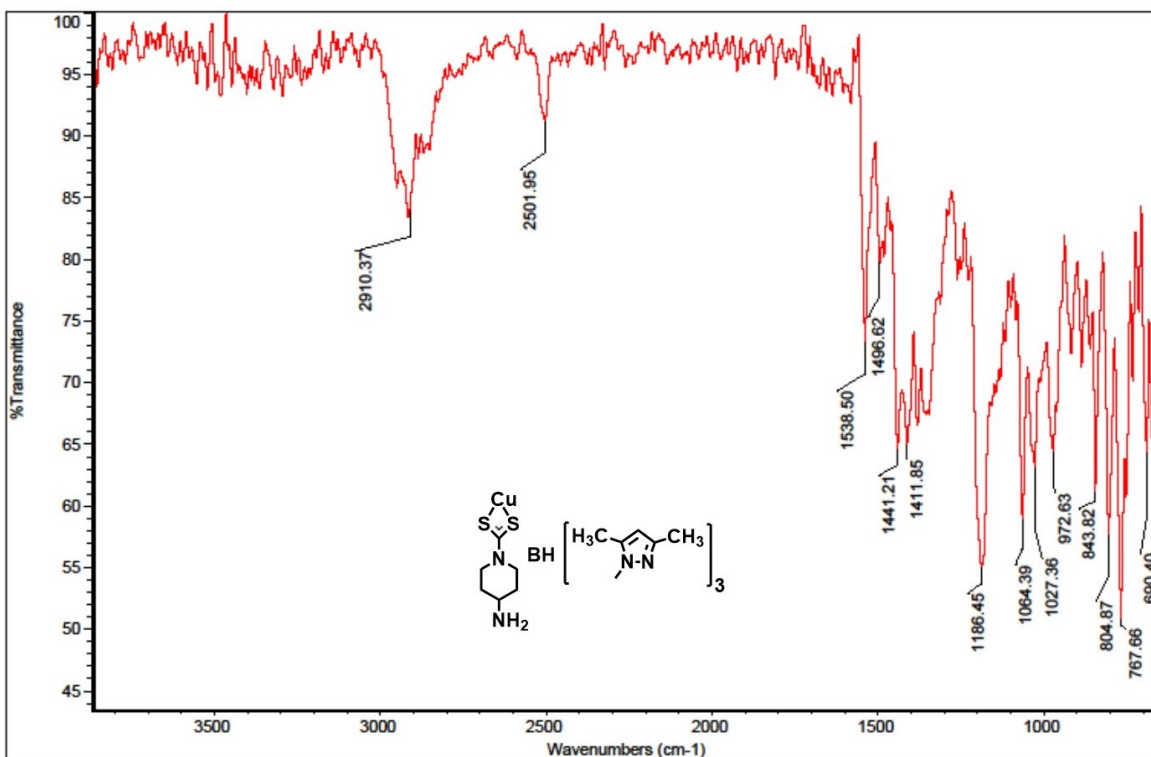


Figure B.79 IR spectrum of 29.

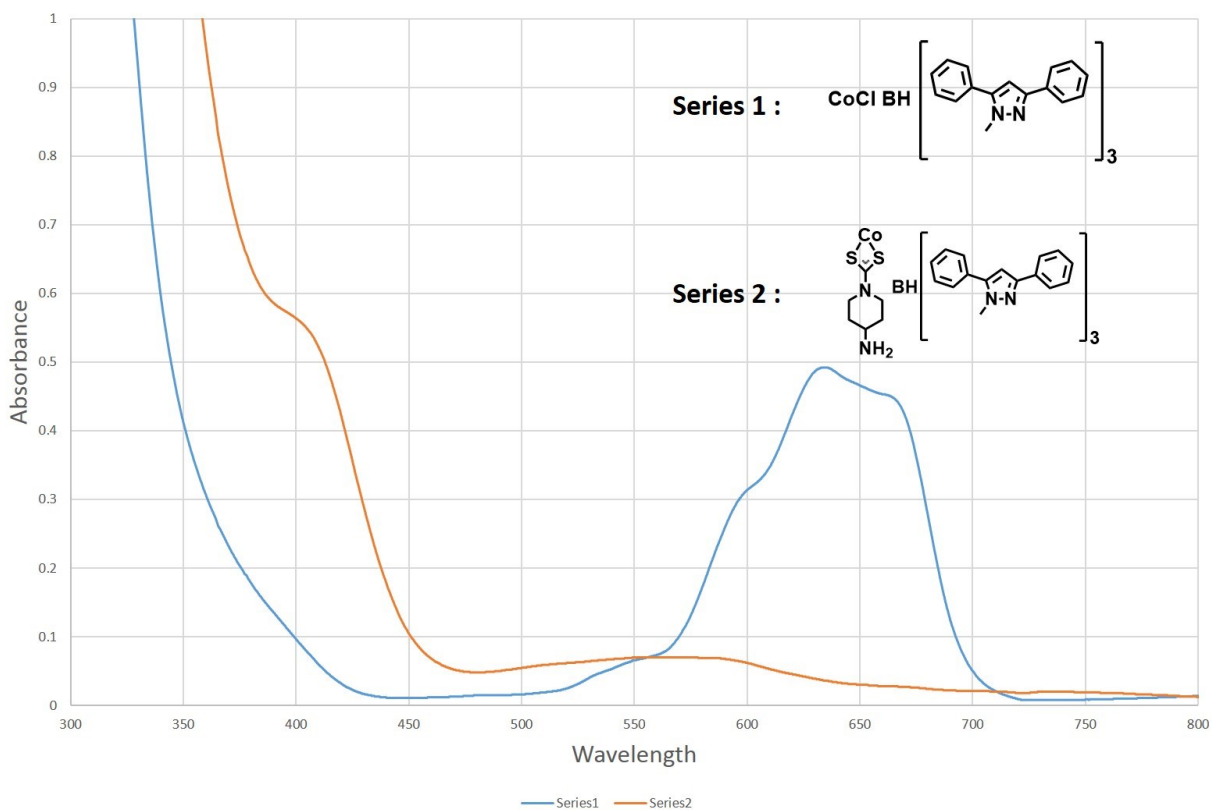


Figure B.80 UV-Visible spectrum of 15 and 24.

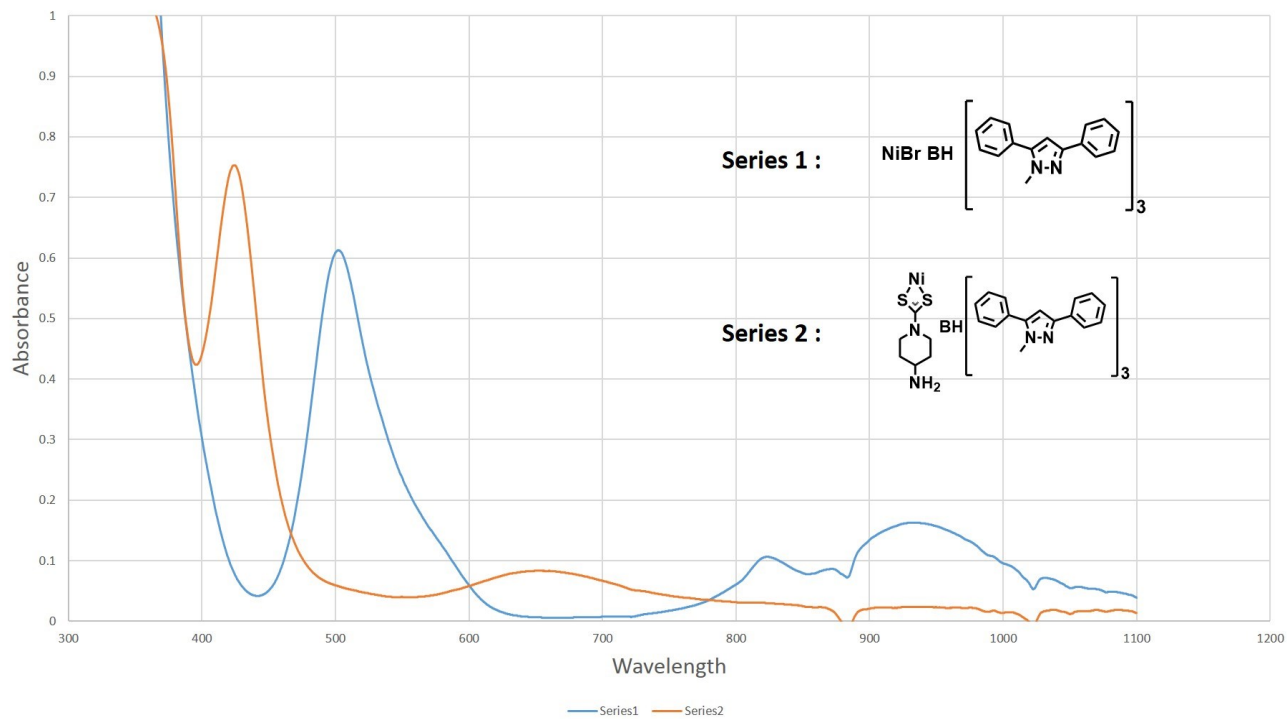


Figure B.81 UV-Visible spectrum of **16** and **25**.

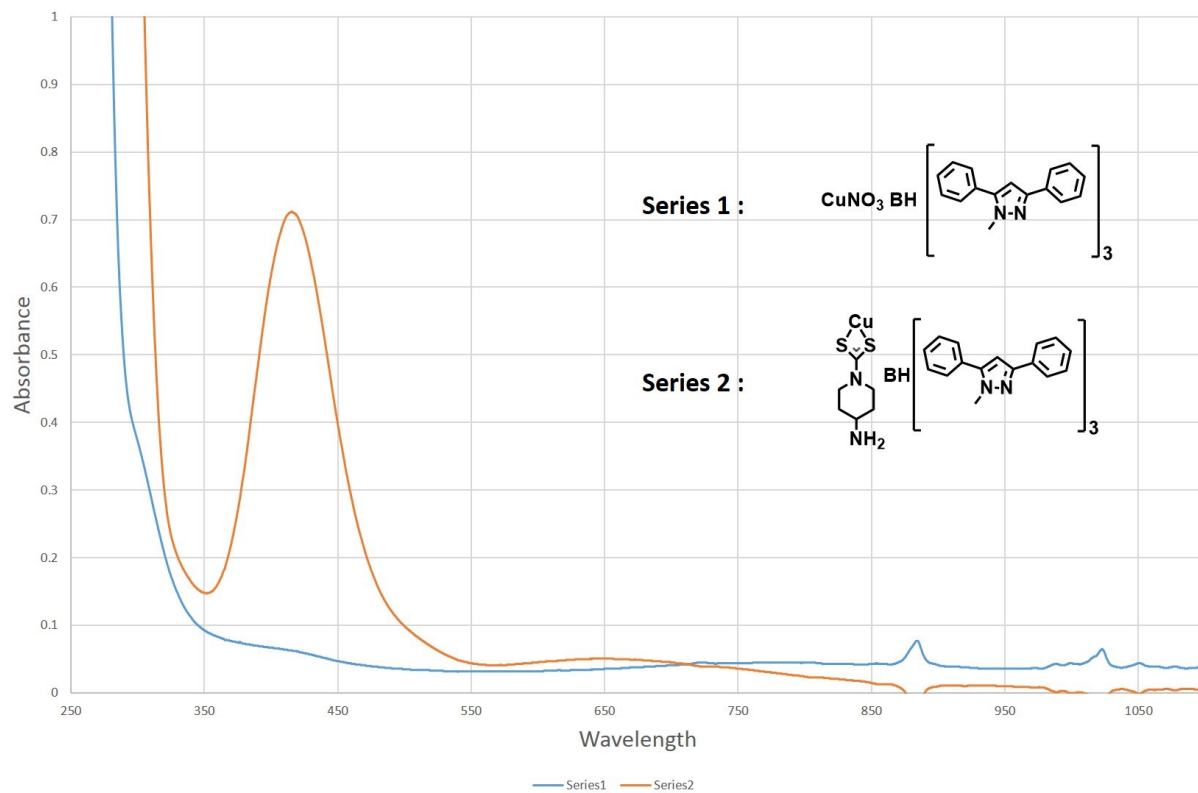


Figure B.82 UV-Visible spectrum of **18** and **26**.

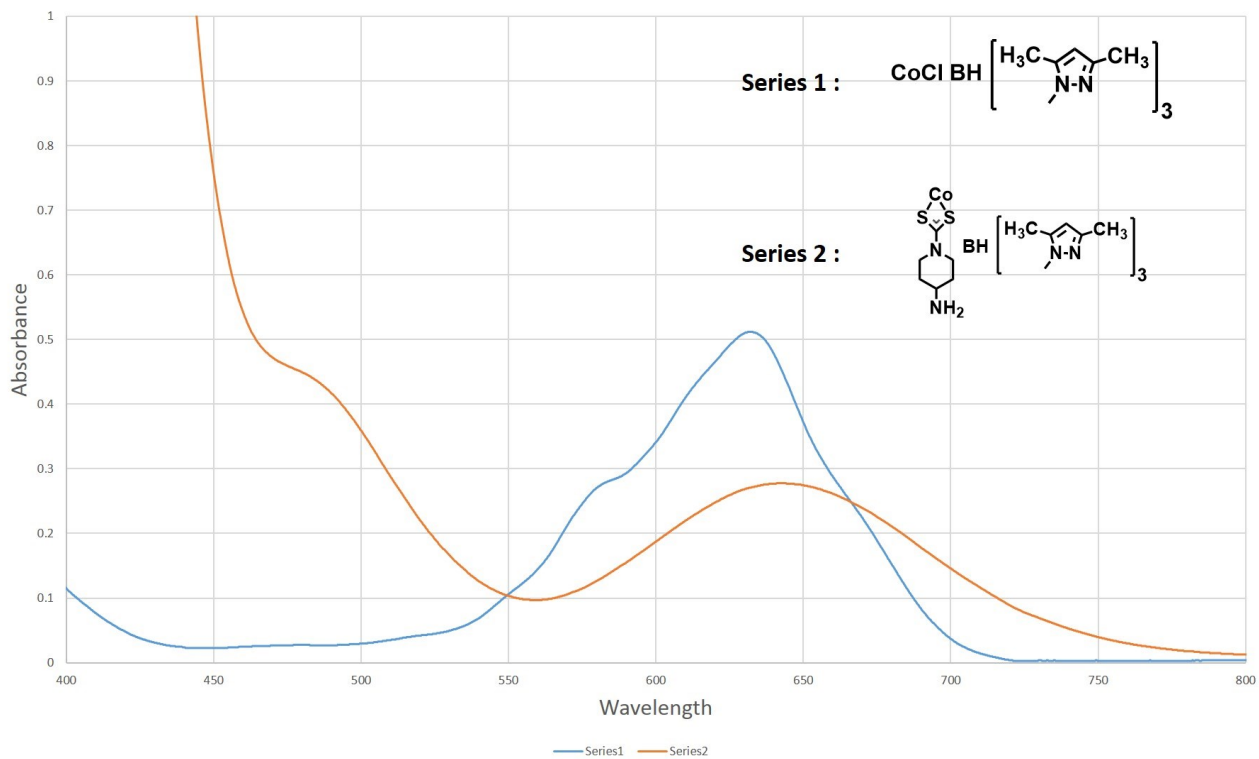


Figure B.83 UV-Visible spectrum of **20** and **27**.

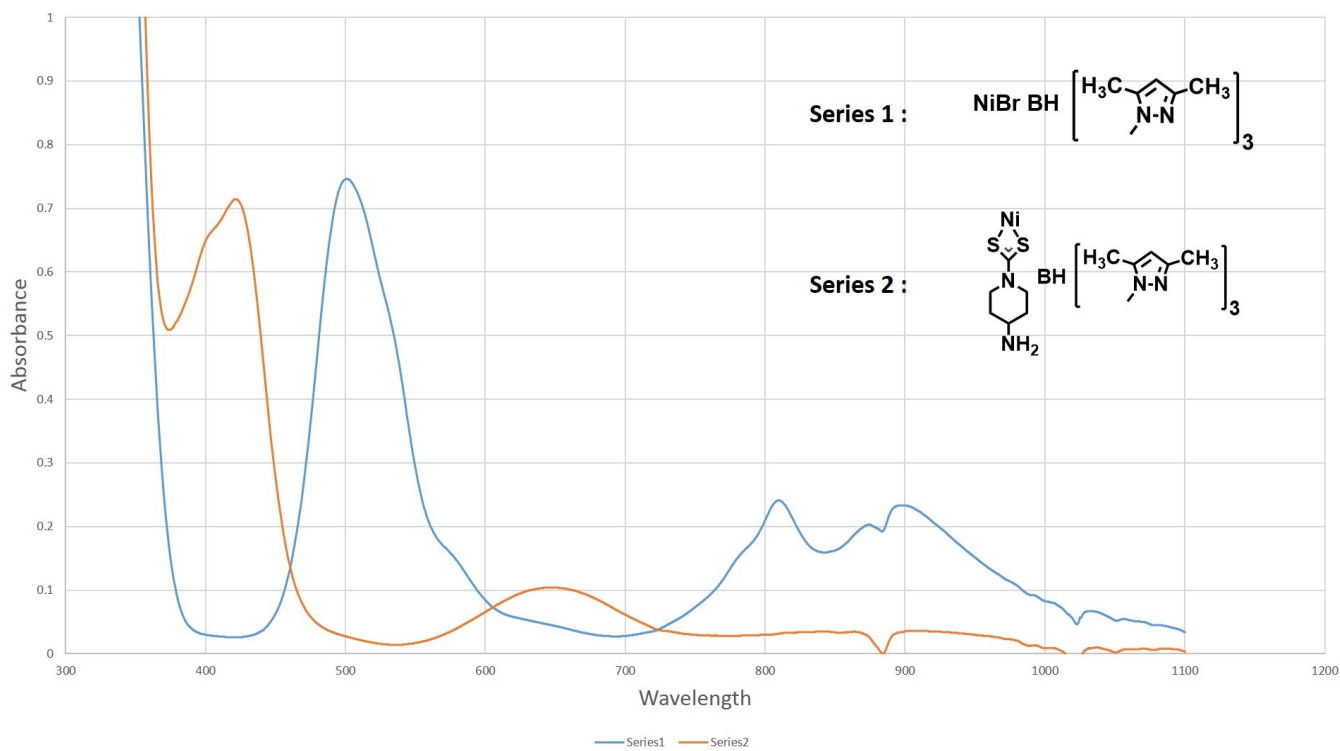


Figure B.84 UV-Visible spectrum of **21** and **28**.

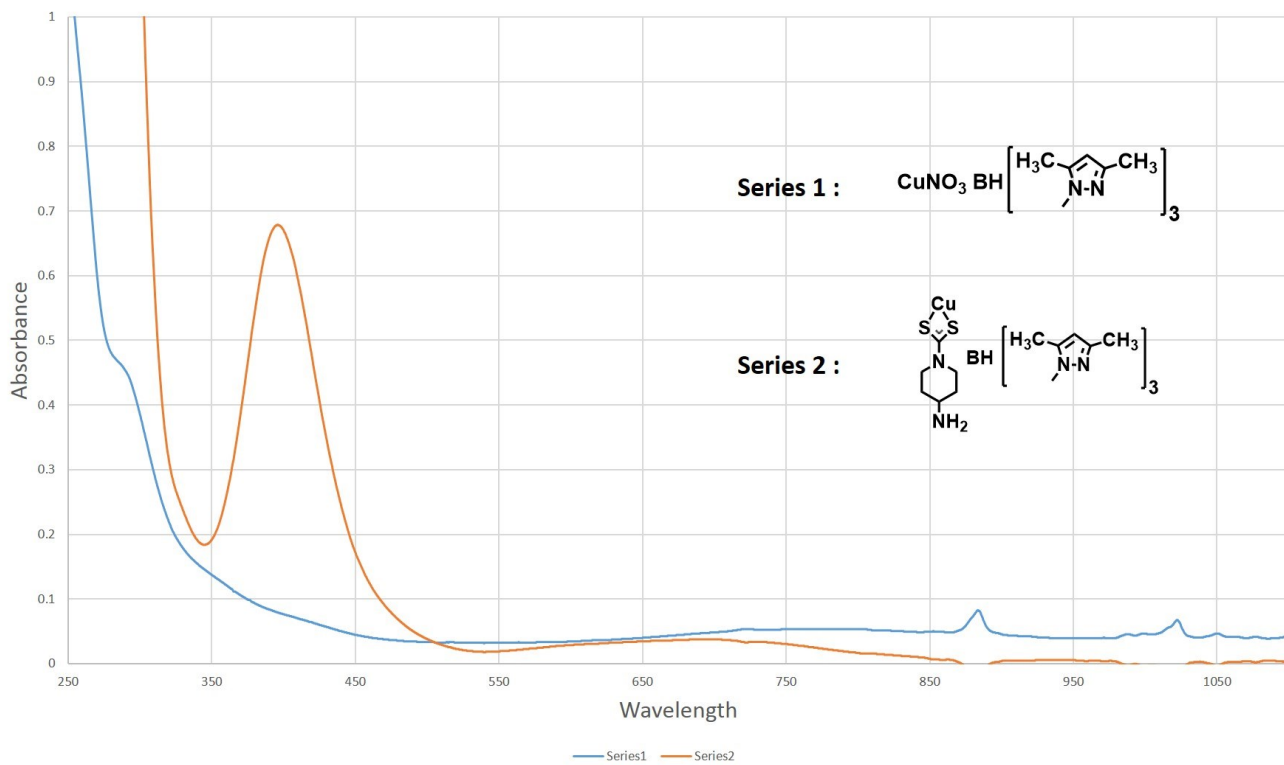


Figure B.85 UV-Visible spectrum of 22 and 29.

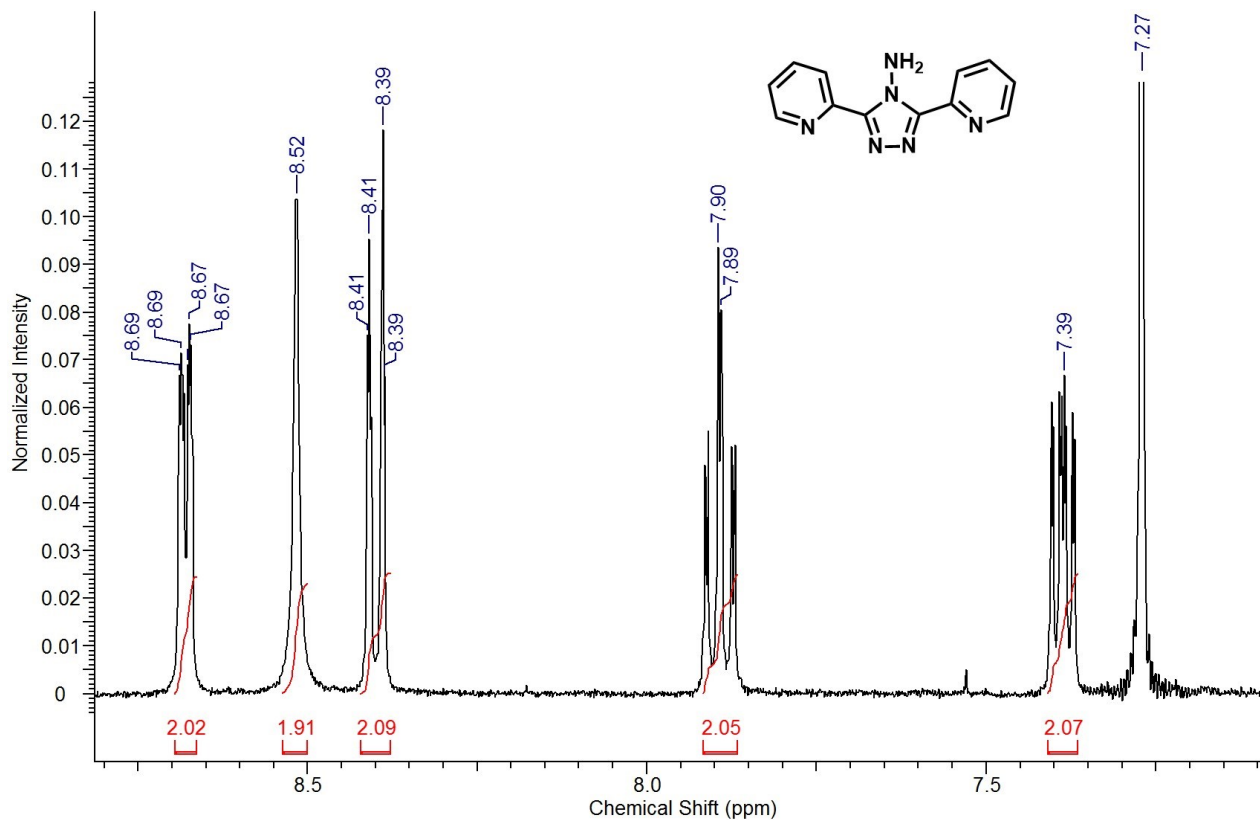


Figure B.86 ^1H NMR spectrum of 30.

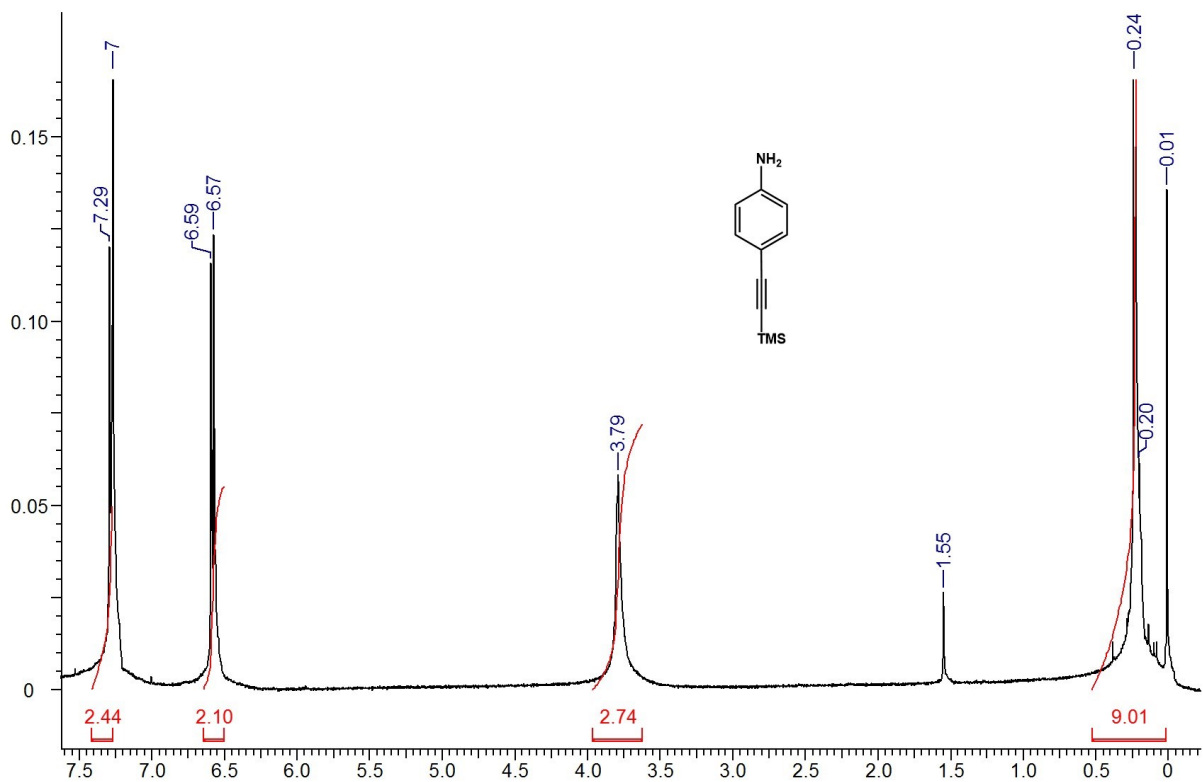


Figure B.87 ^1H NMR spectrum of **31**.

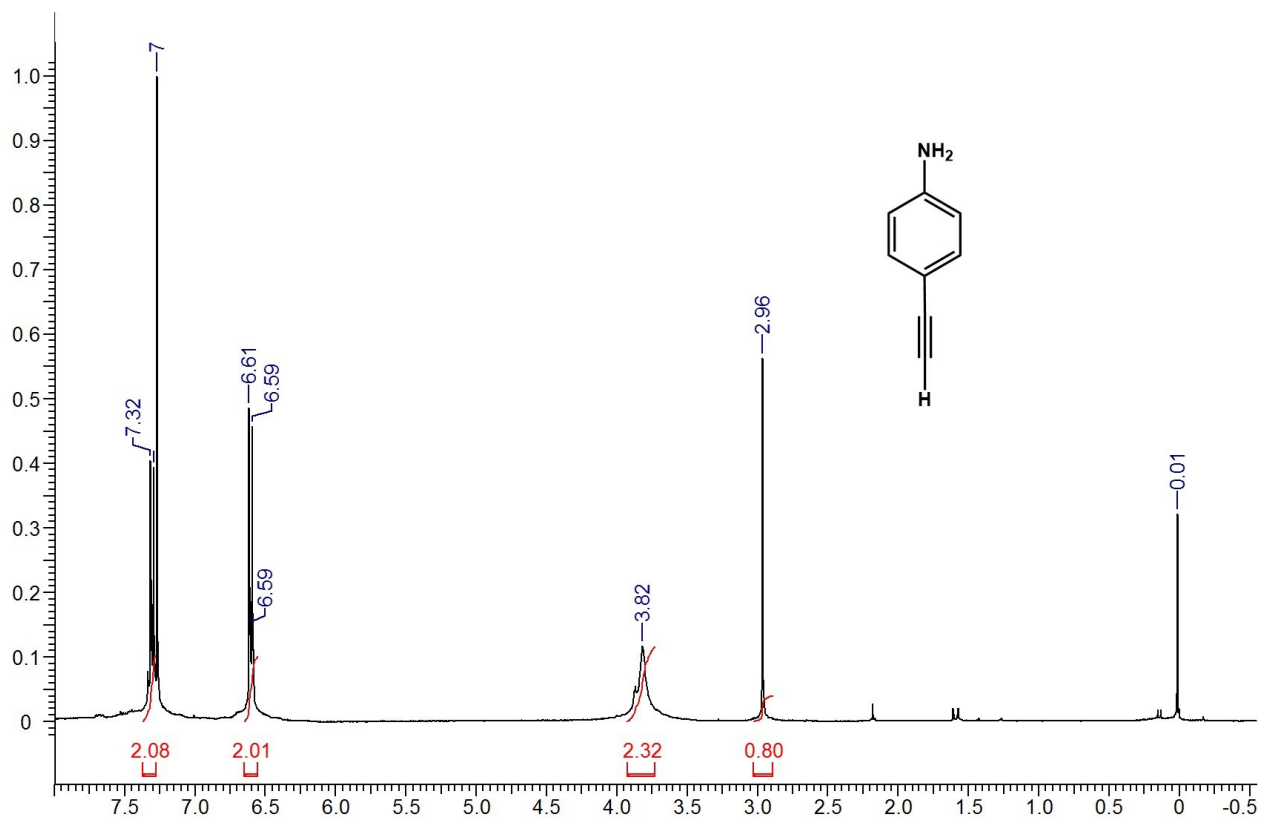


Figure B.88 ^1H NMR spectrum of **32**.

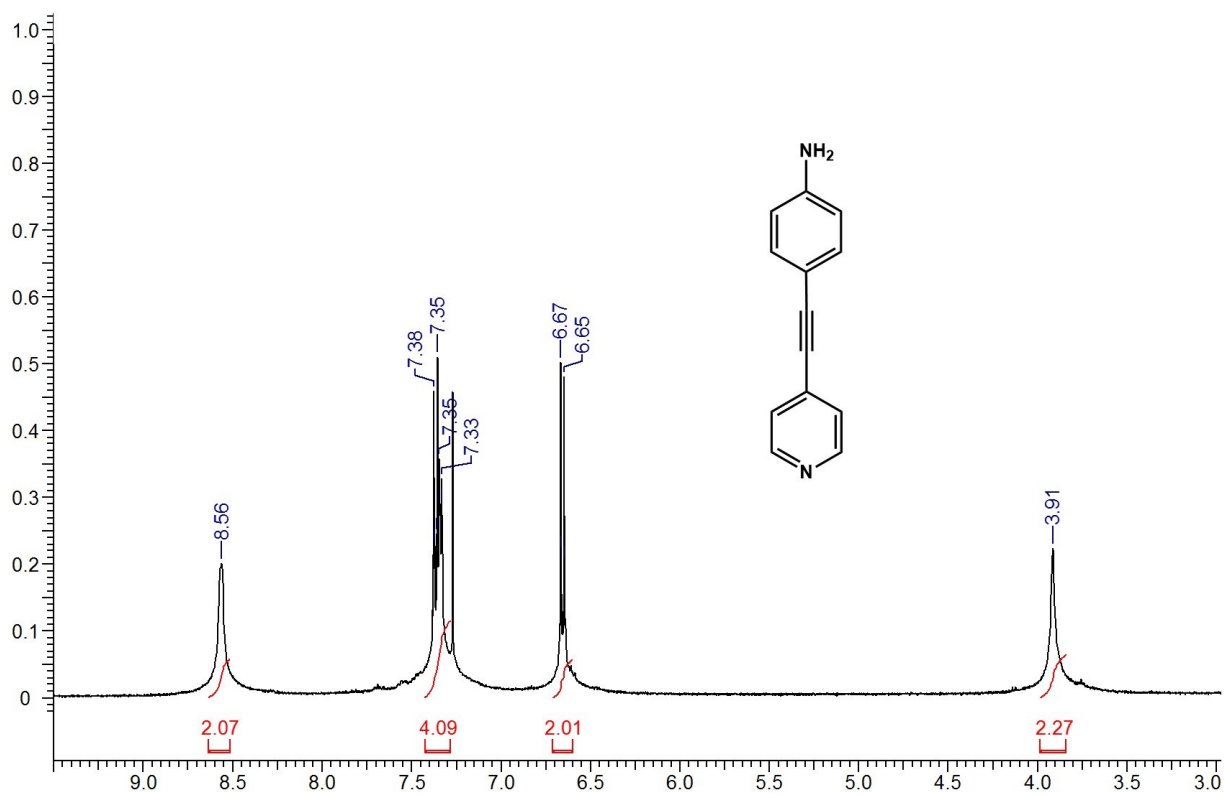


Figure B.89 ^1H NMR spectrum of **33** in CDCl_3 .

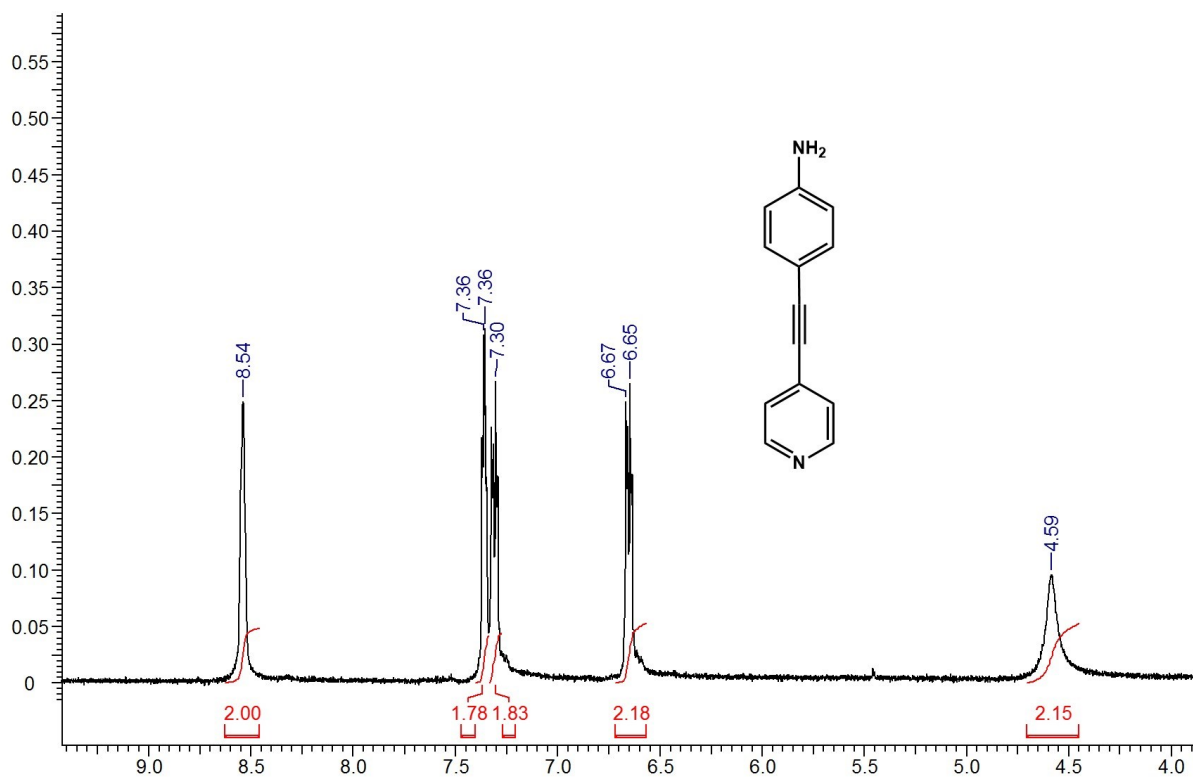
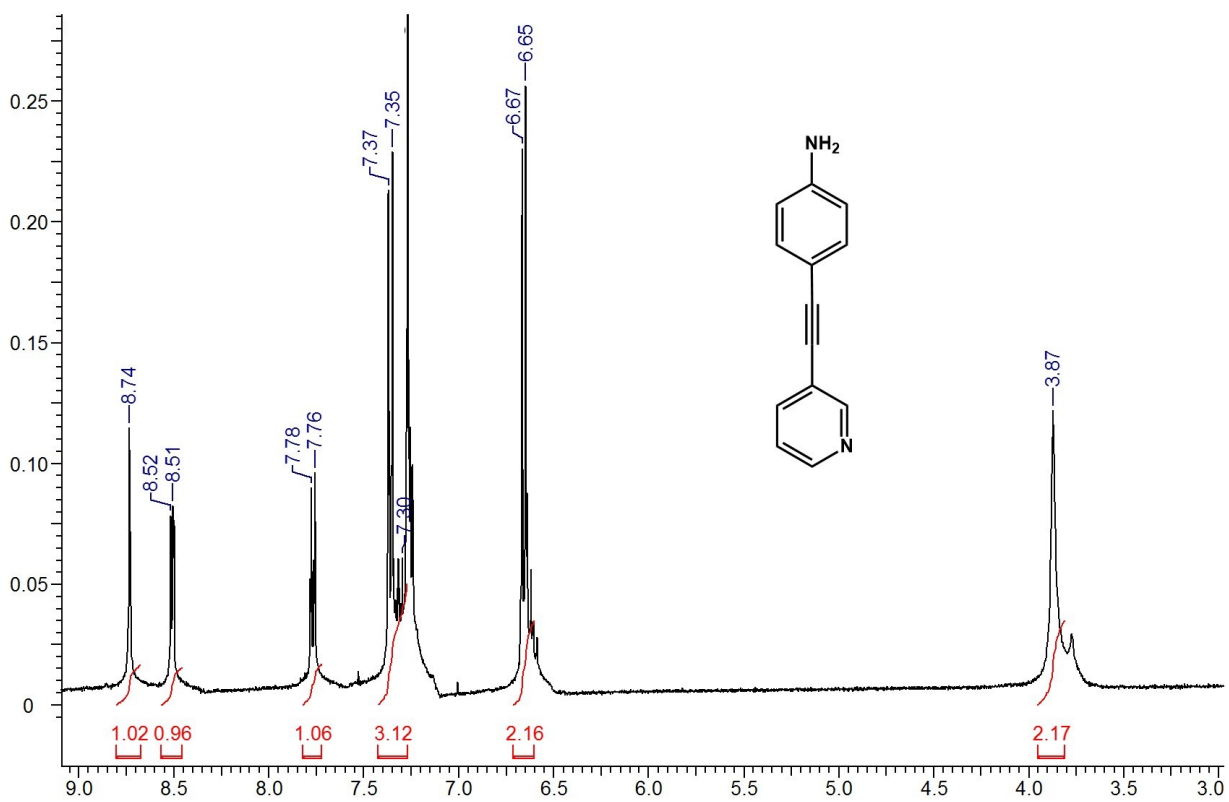
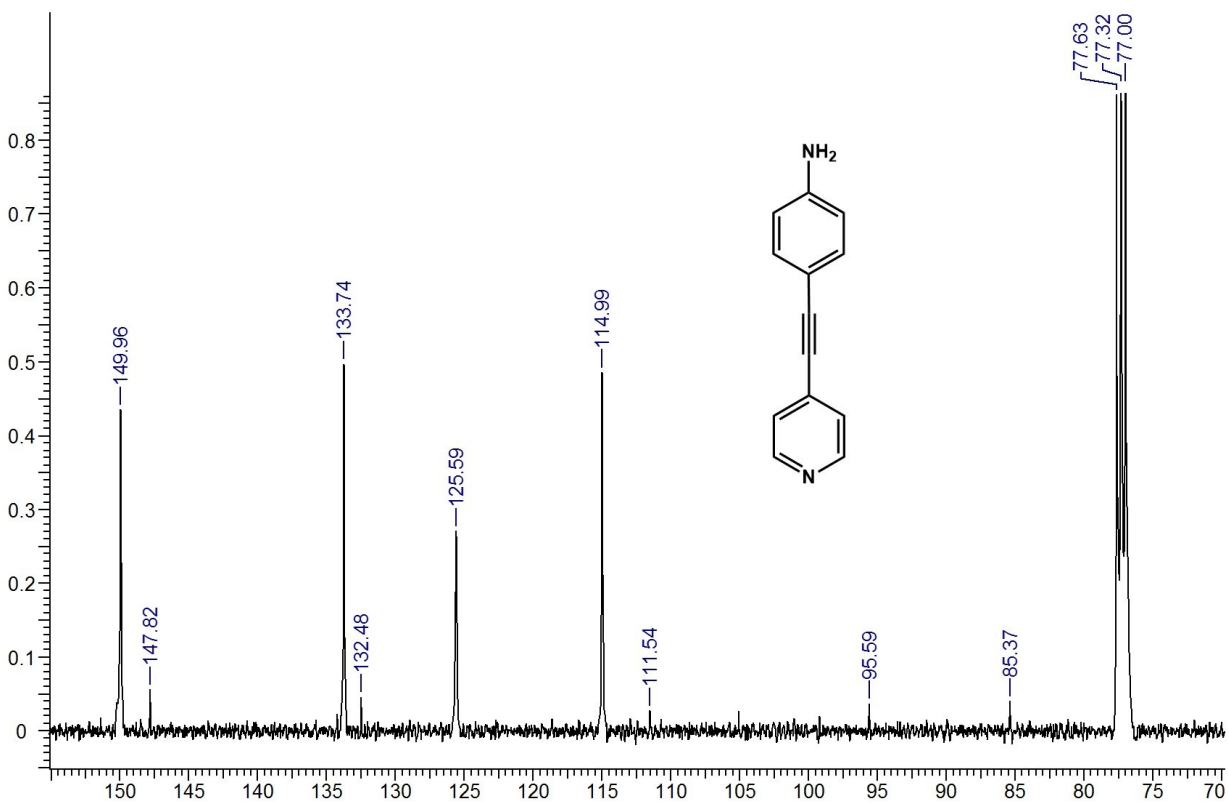


Figure B.90 ^1H NMR spectrum of **33** in CD_3CN .



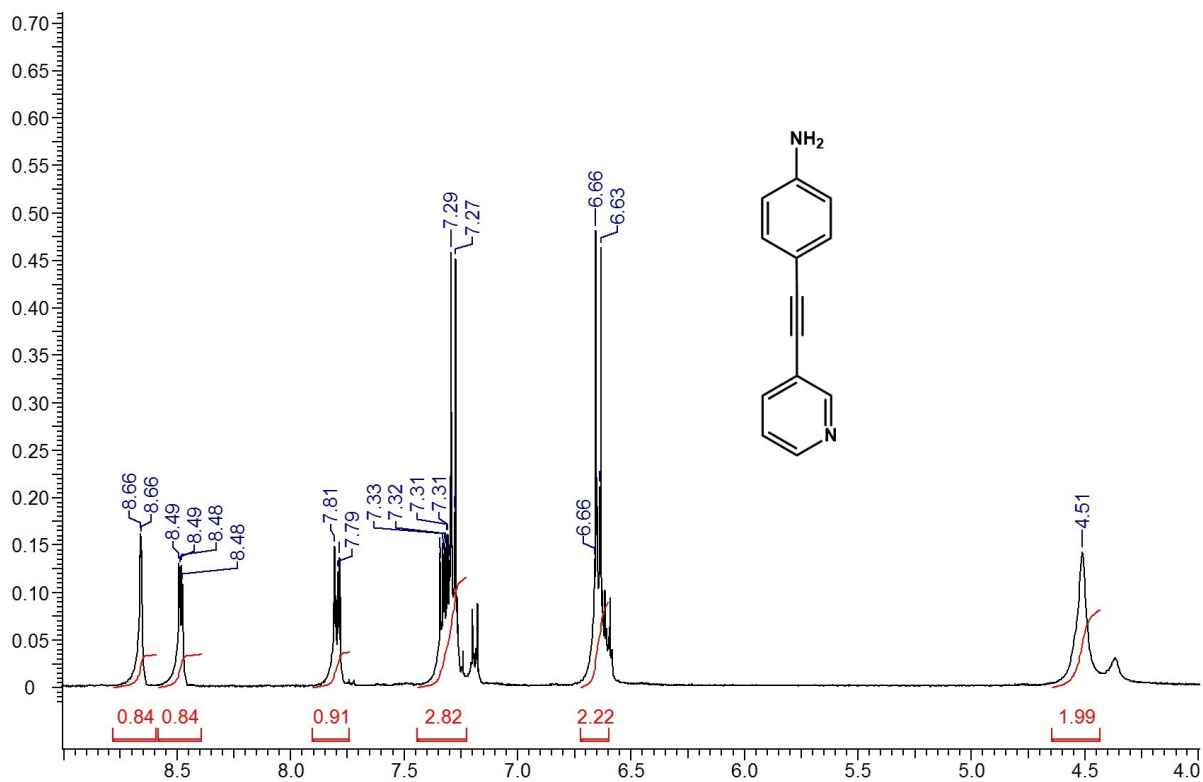


Figure B.93 ^1H NMR spectrum of **34** in CD_3CN .

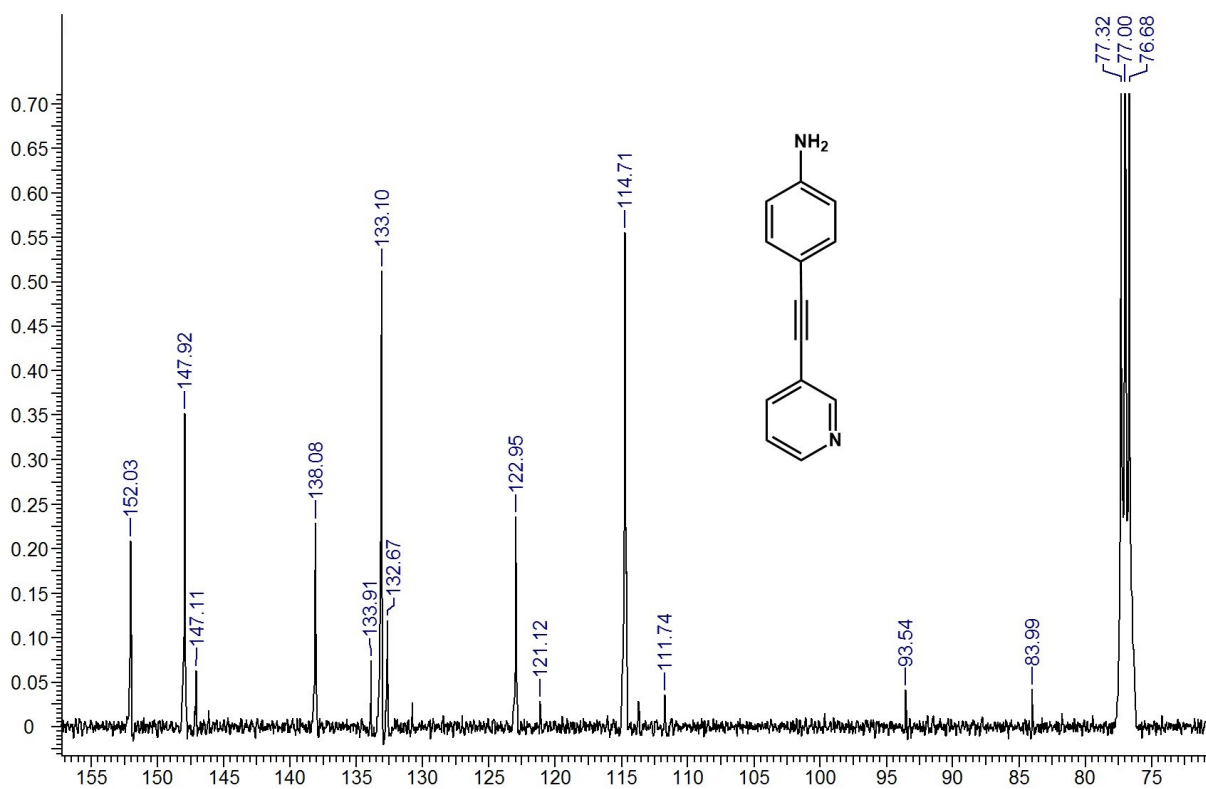


Figure B.94 ^{13}C NMR spectrum of **34** in CDCl_3 .

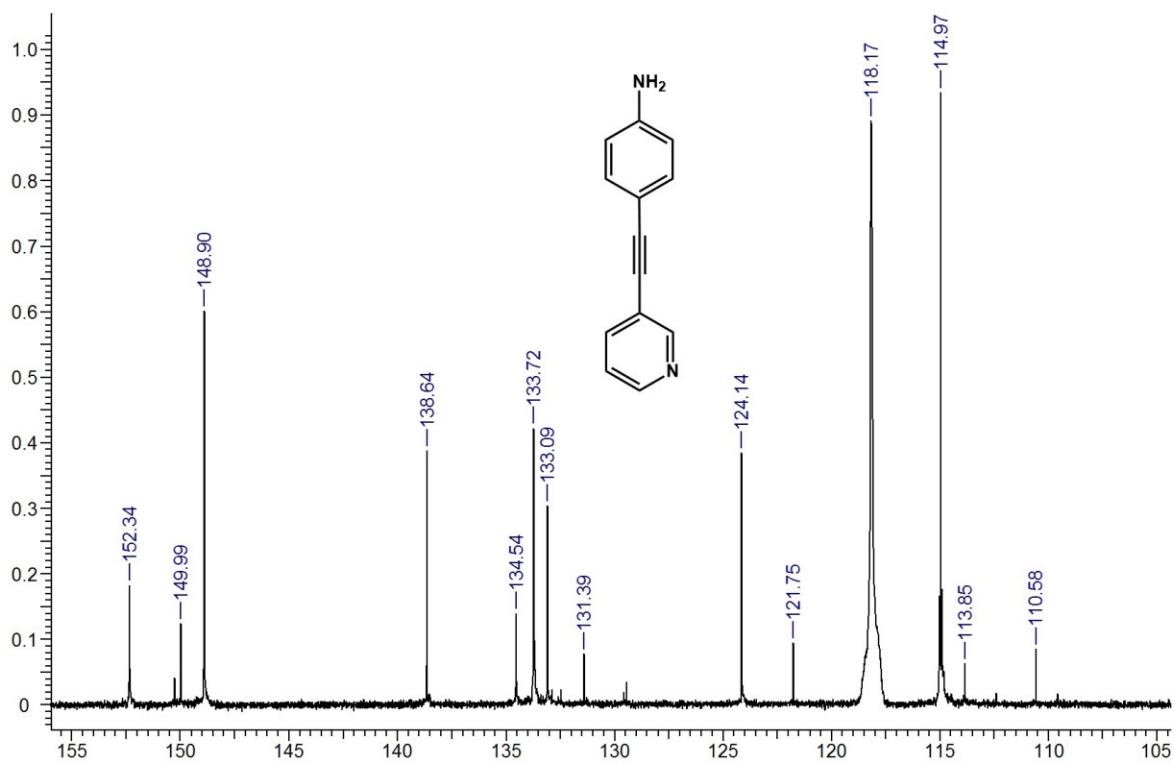


Figure B.95 ^{13}C NMR spectrum of **34** in CD_3CN .

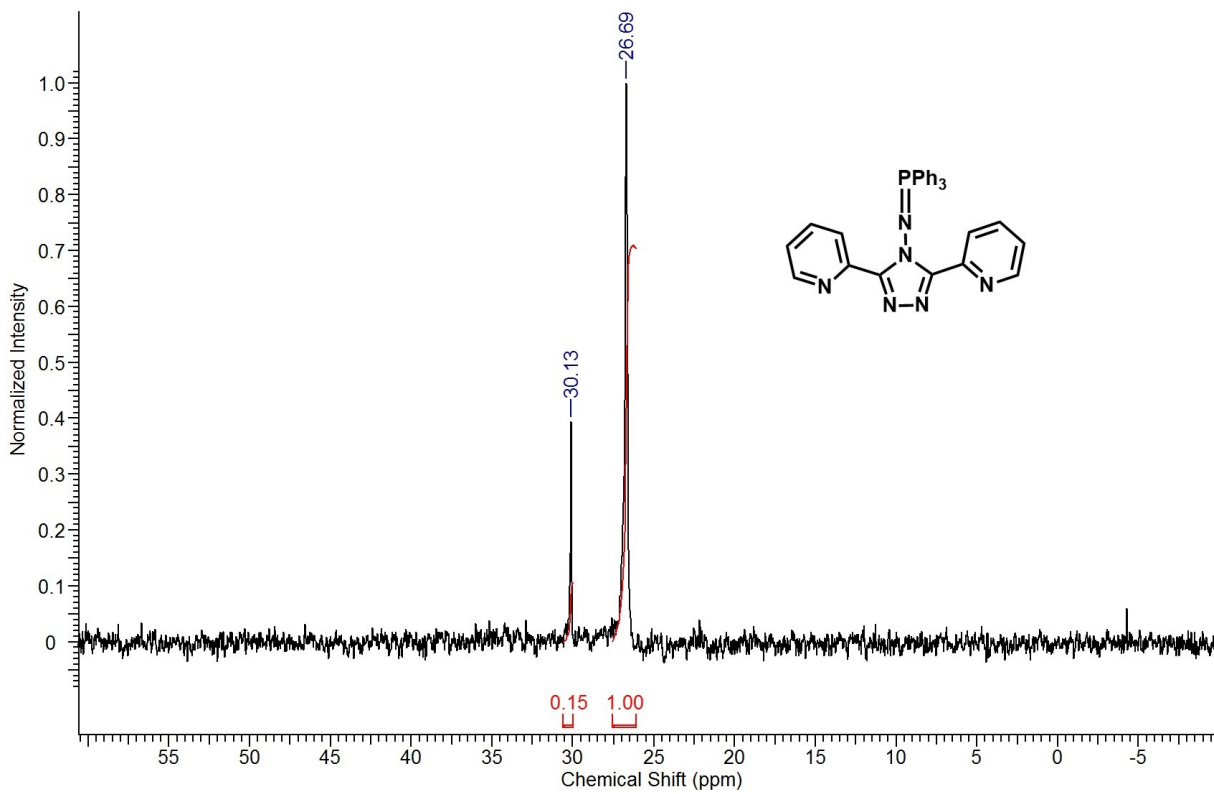


Figure B.96 ^{31}P NMR spectrum of **35**.

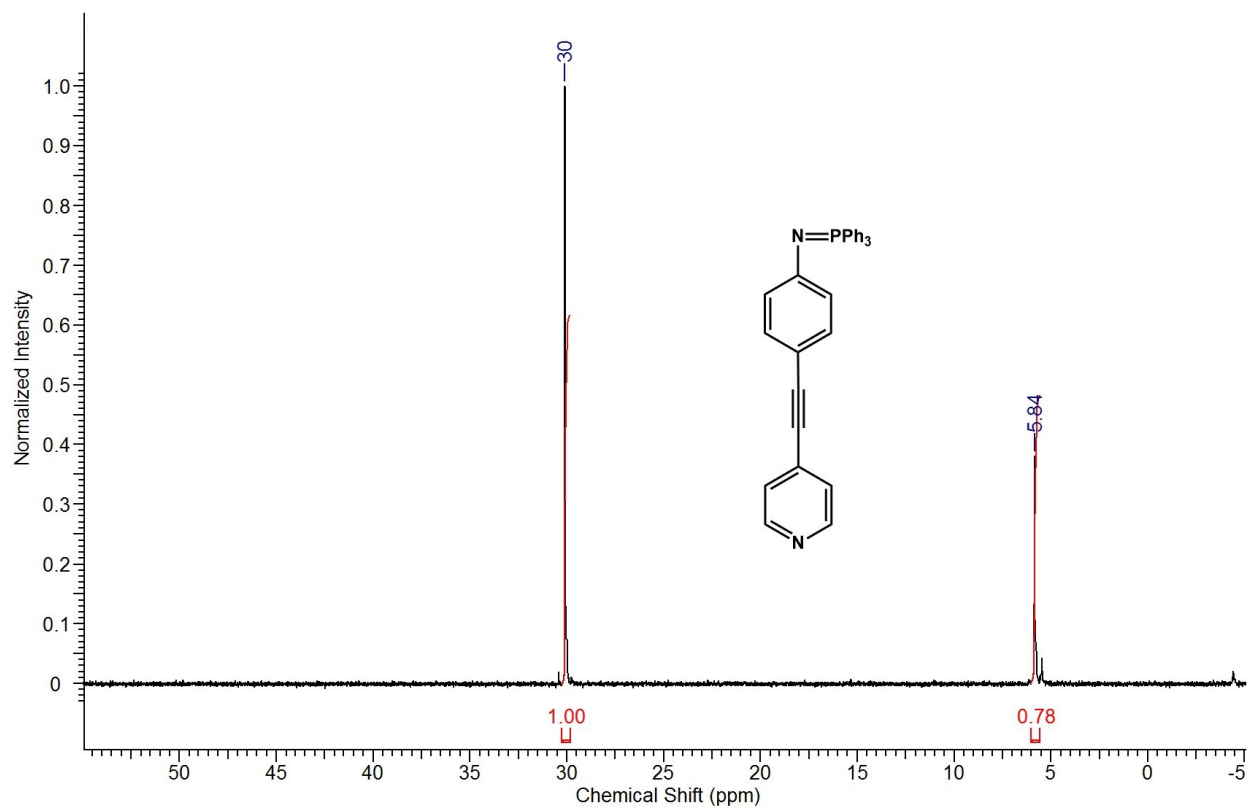


Figure B.97 ^{31}P NMR spectrum of **36**.

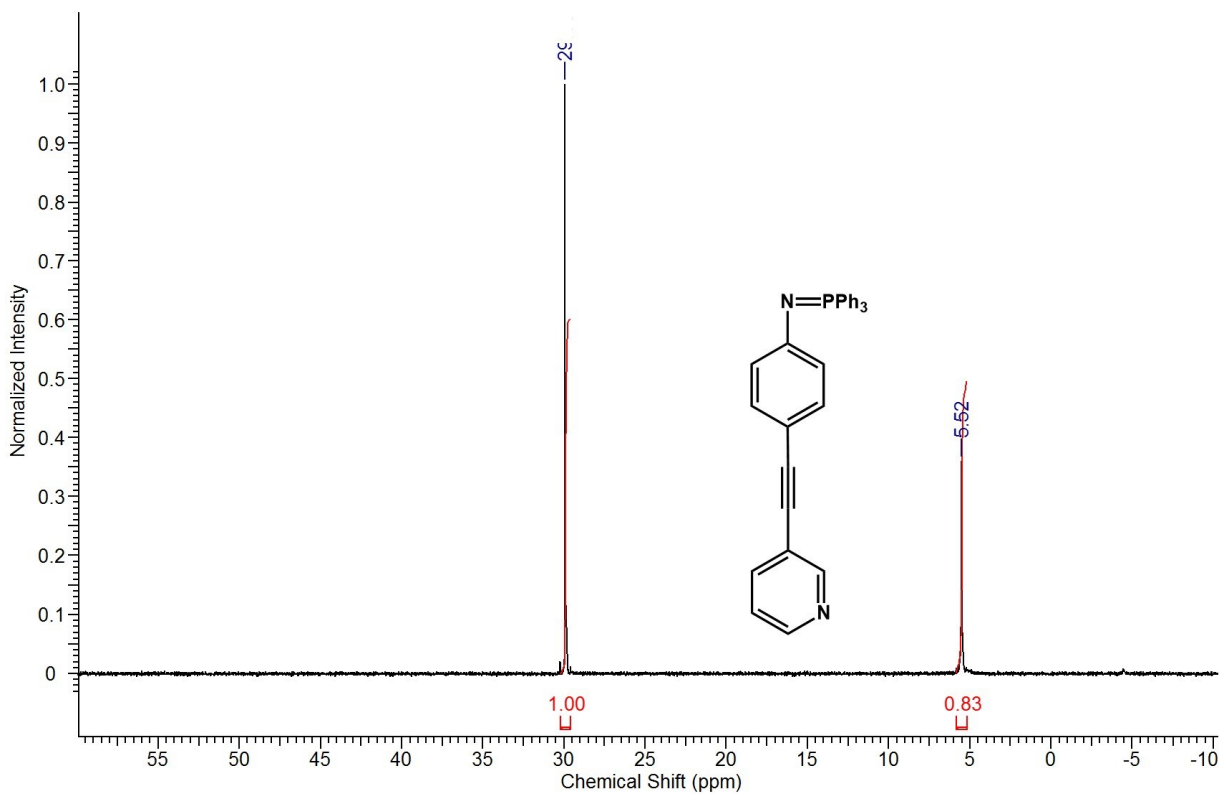


Figure B.98 ^{31}P NMR spectrum of **37**.

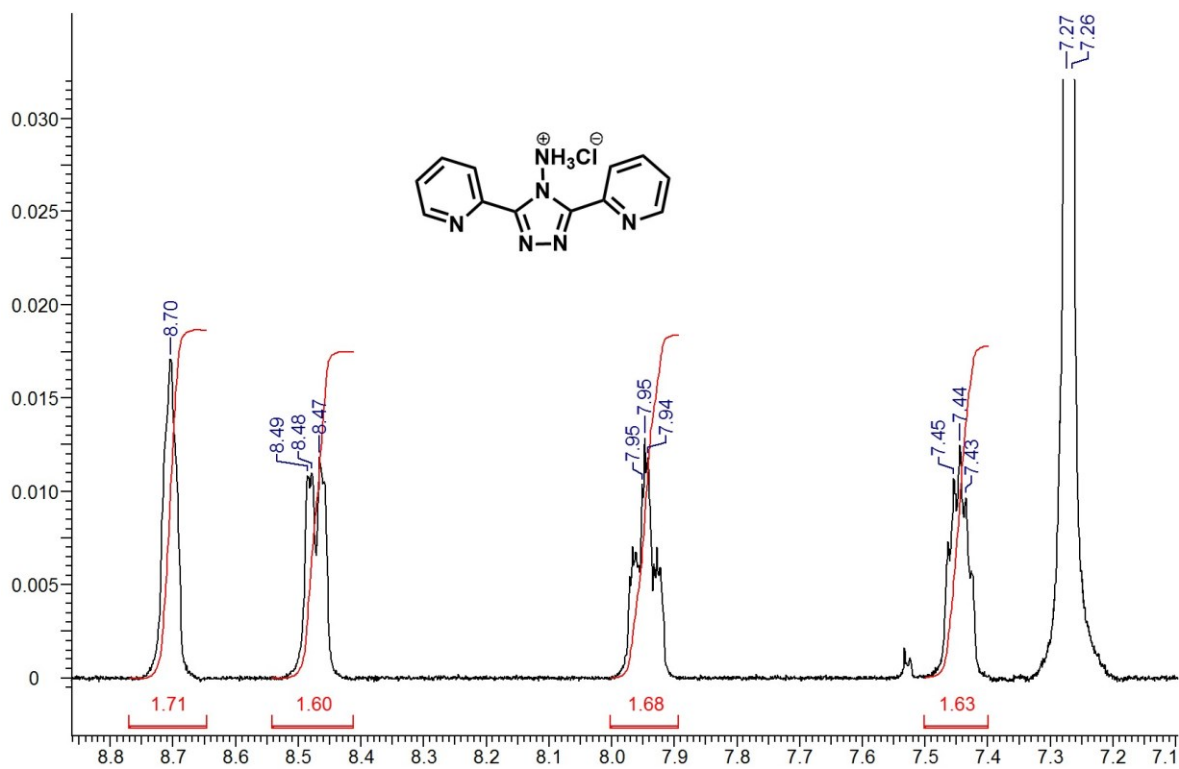


Figure B.99 ^1H NMR spectrum of 38.

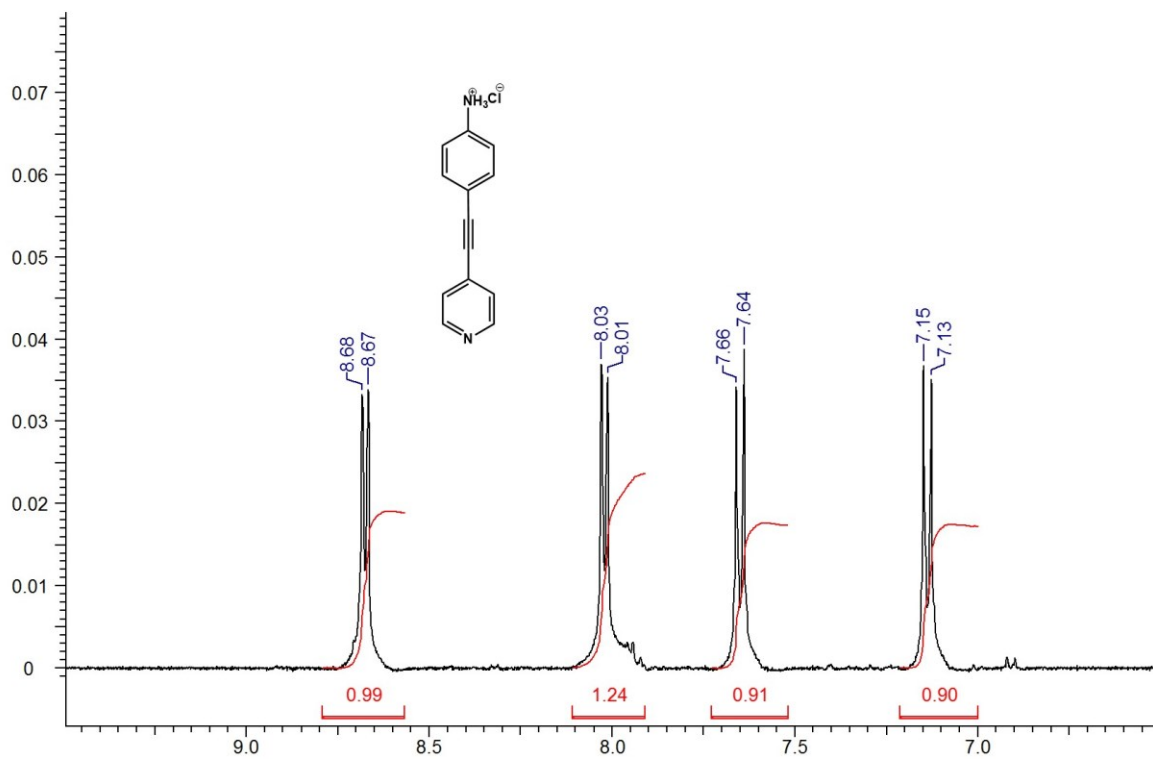


Figure B.100 ^1H NMR spectrum of 39.

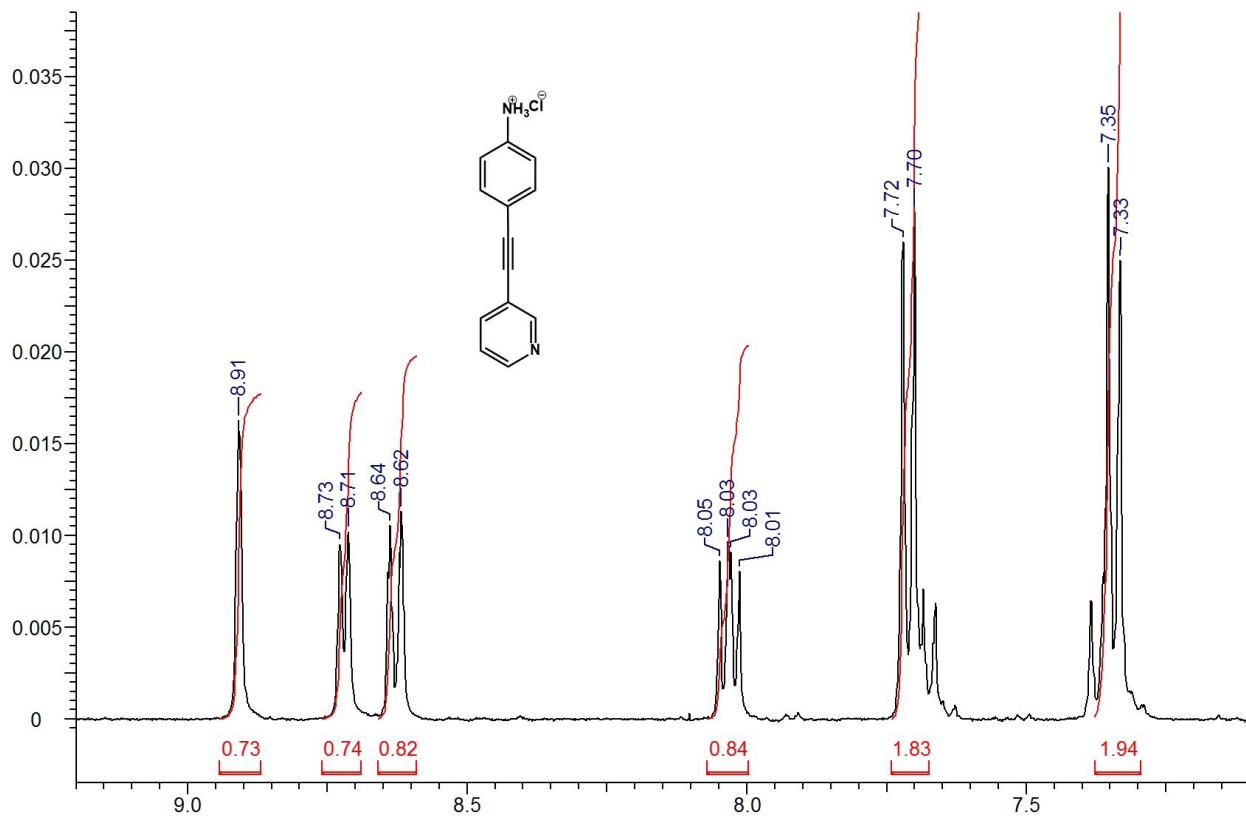


Figure B.101 ^1H NMR spectrum of 40.

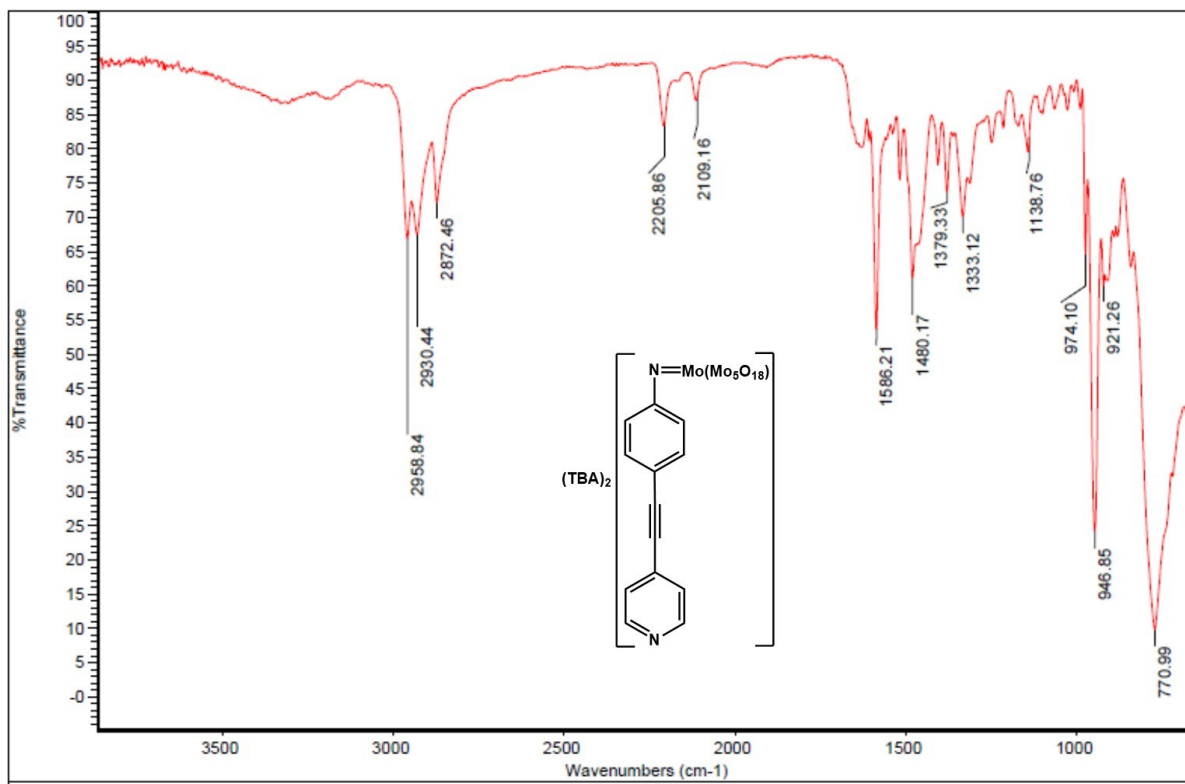


Figure B.102 IR spectrum of 41.

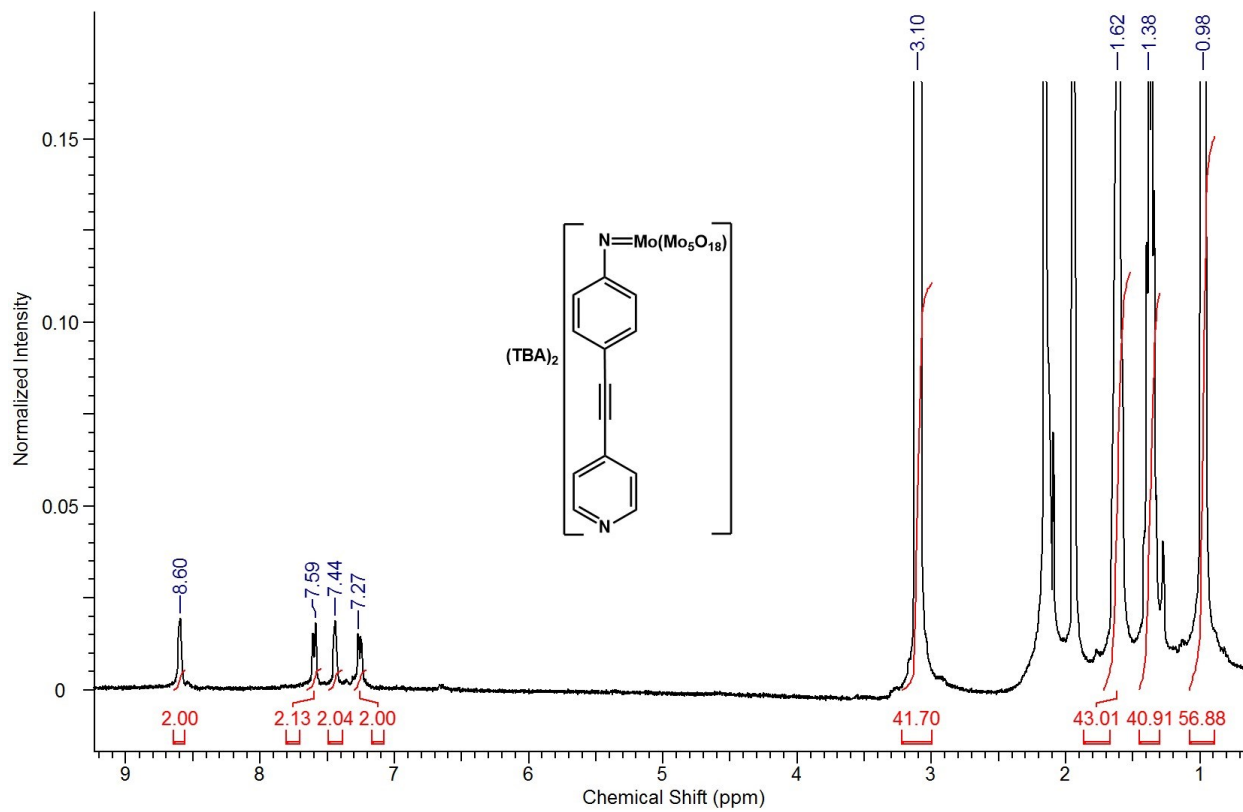


Figure B.103 ^1H NMR spectrum of 41.

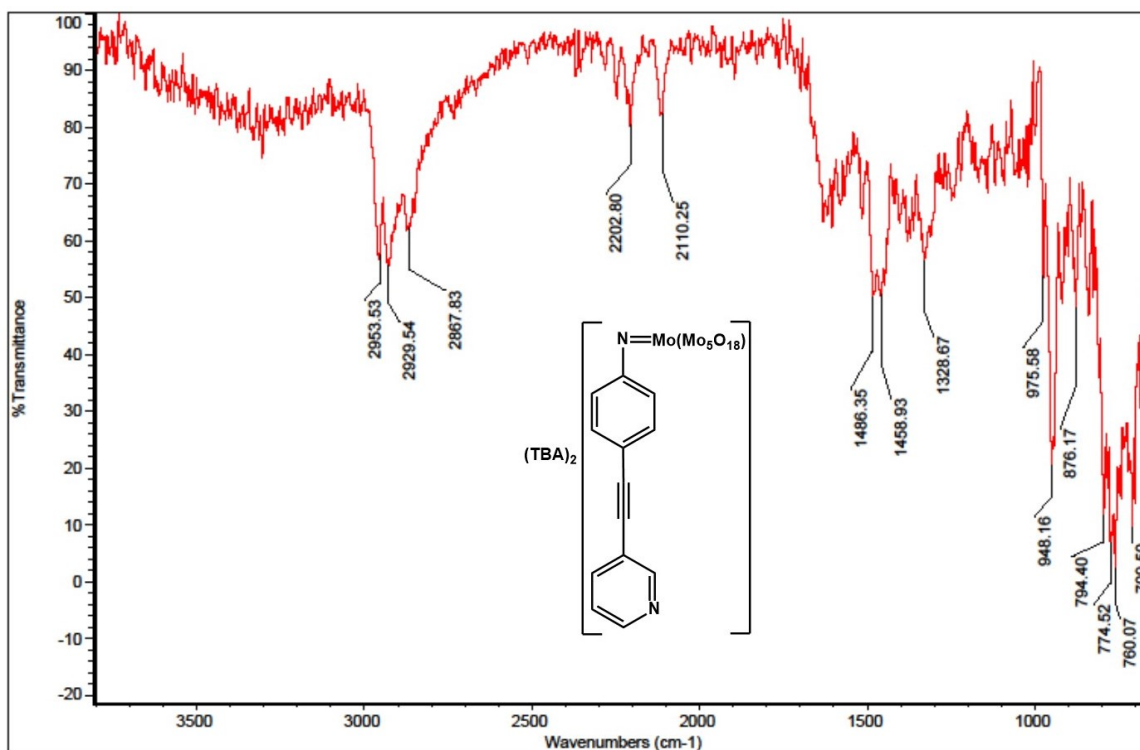


Figure B.104 IR spectrum of 42.

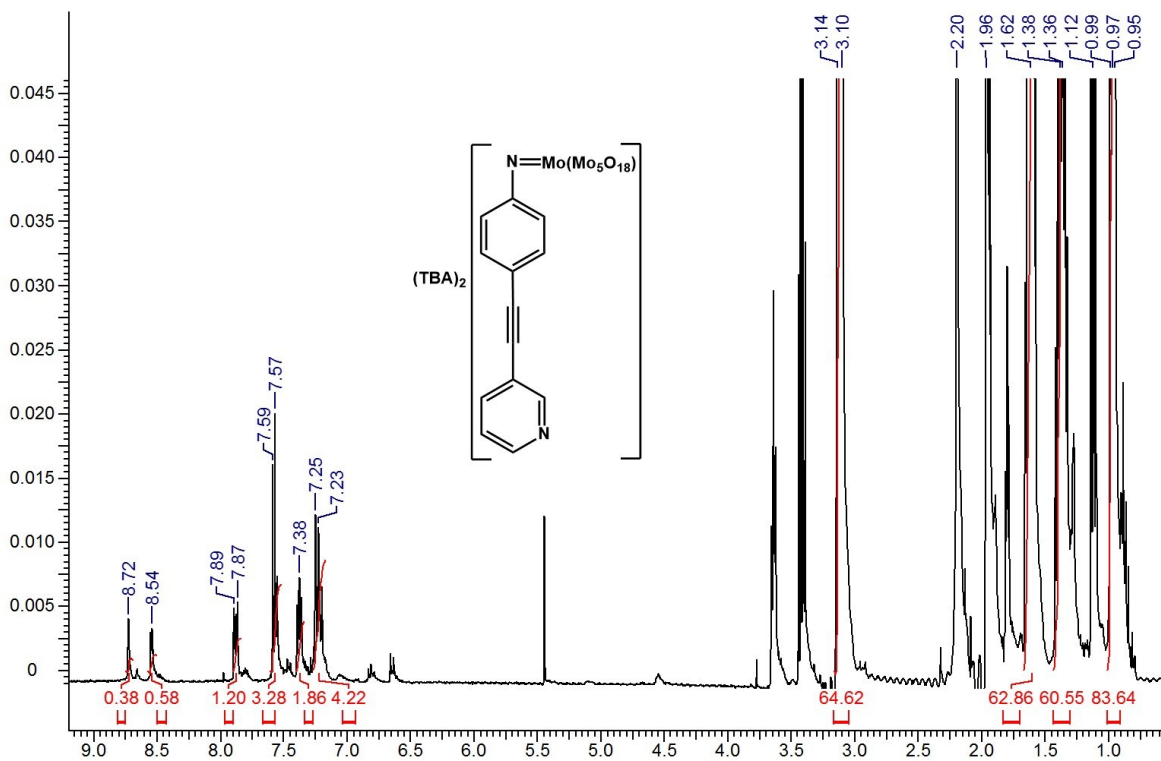


Figure B.105 ¹H NMR spectrum of 42.

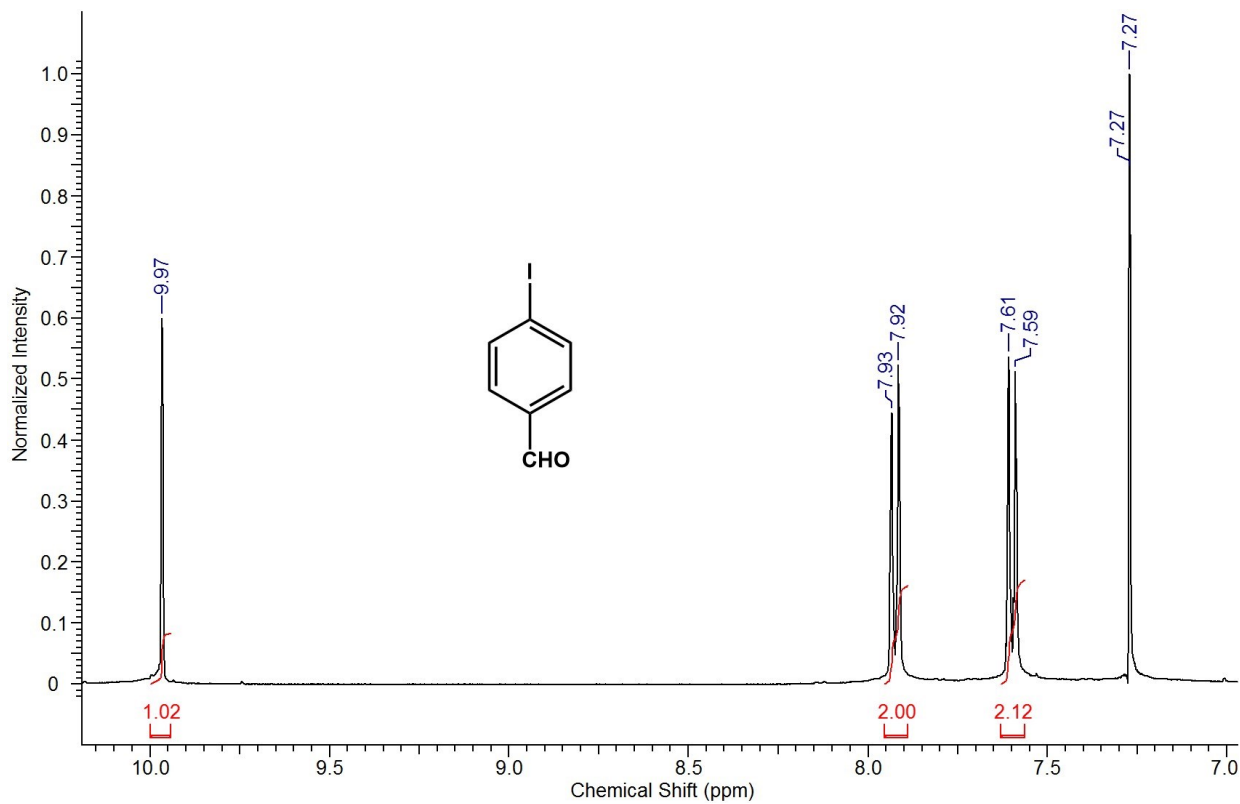


Figure B.106 ¹H NMR spectrum of 43.

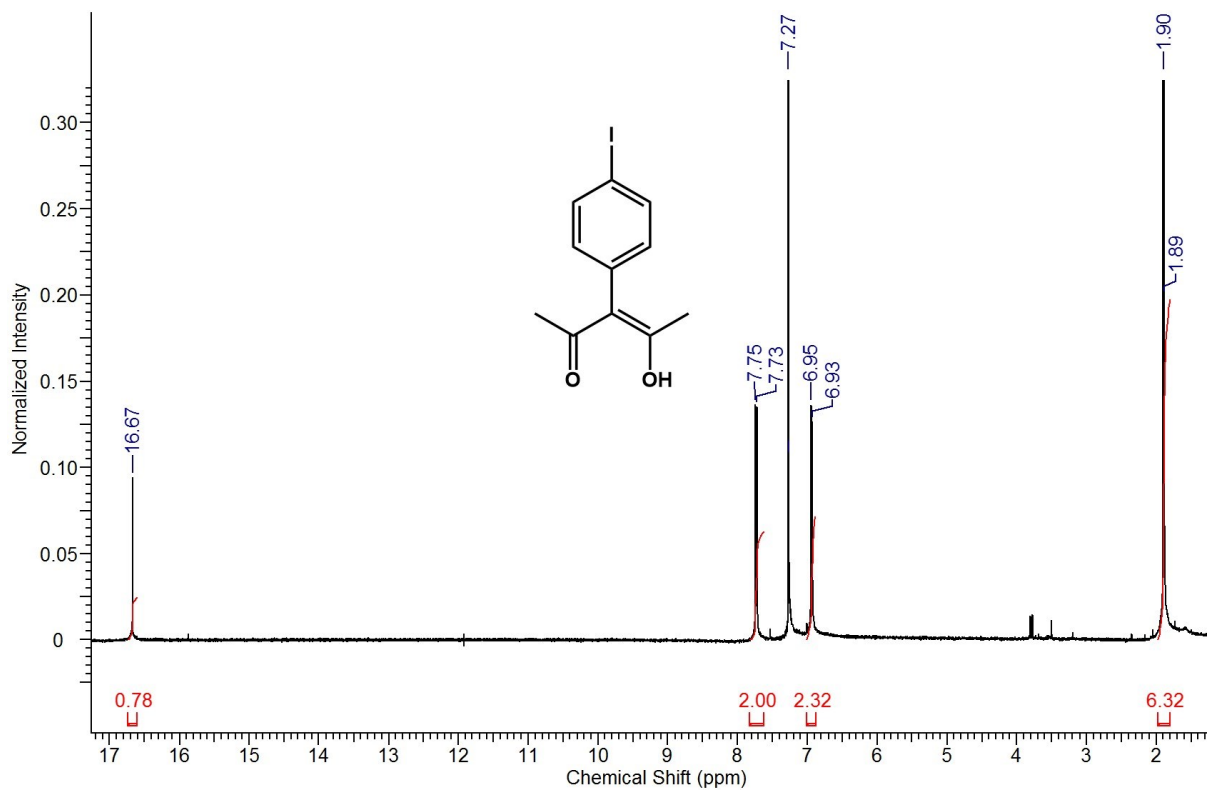


Figure B.107 ^1H NMR spectrum of 45.

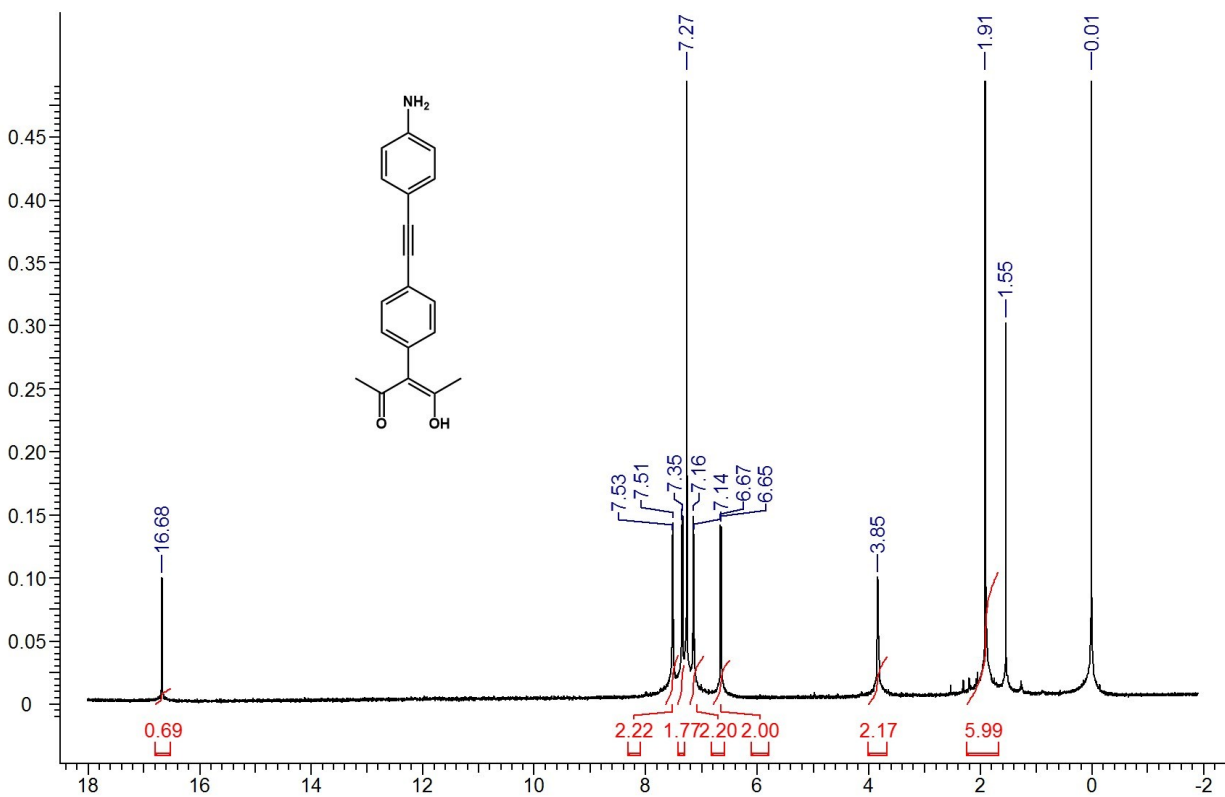


Figure B.108 ^1H NMR spectrum of 46.

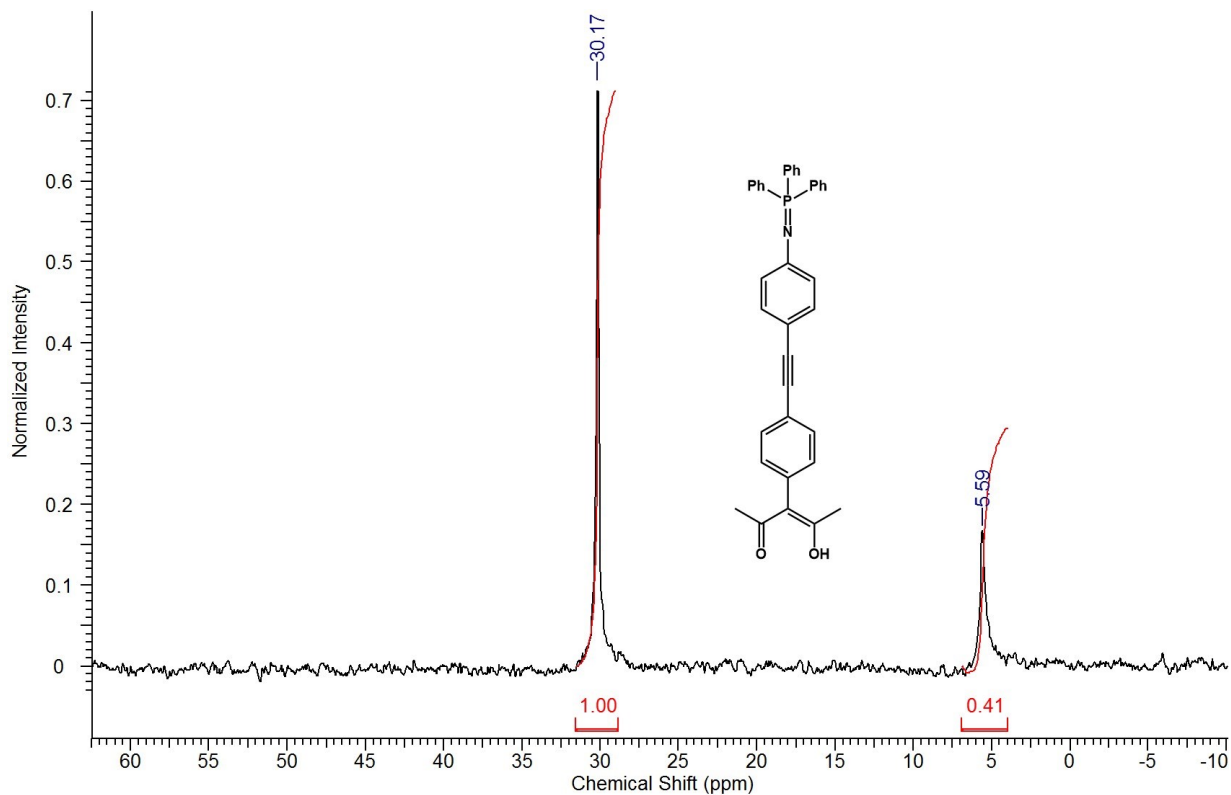


Figure B.109 ^{31}P NMR spectrum of 47.

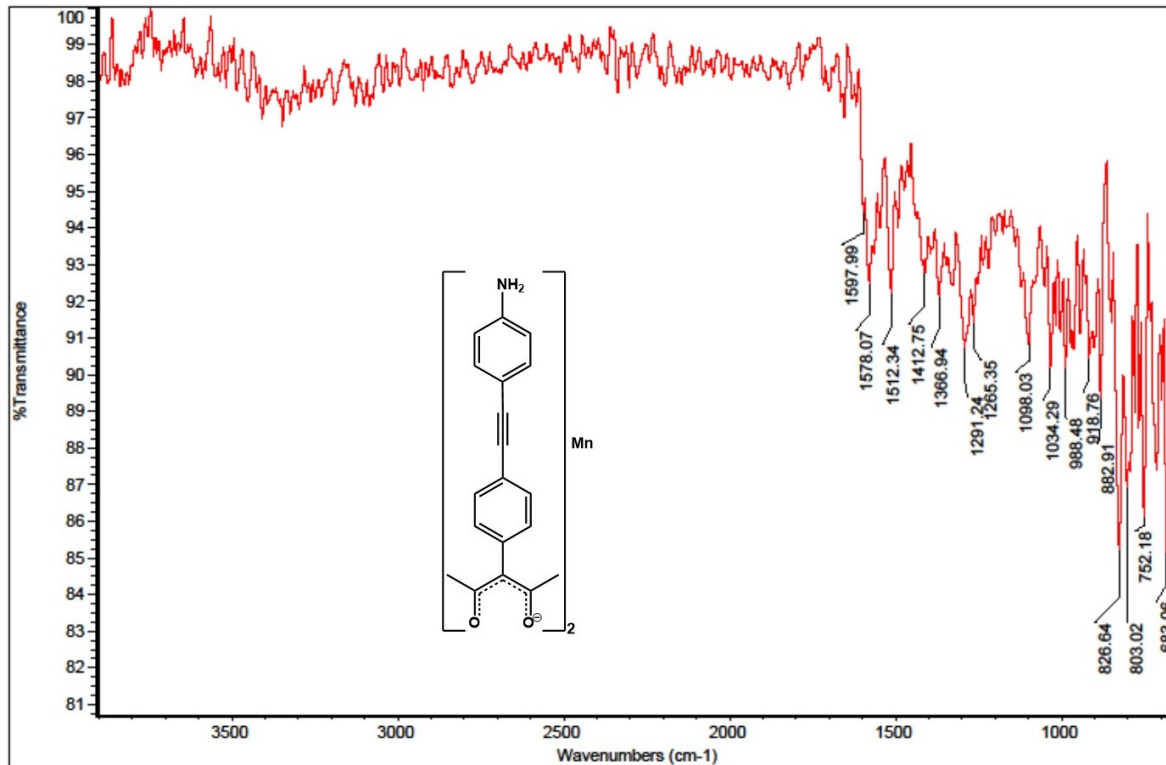


Figure B.110 IR spectrum of 46.Mn.

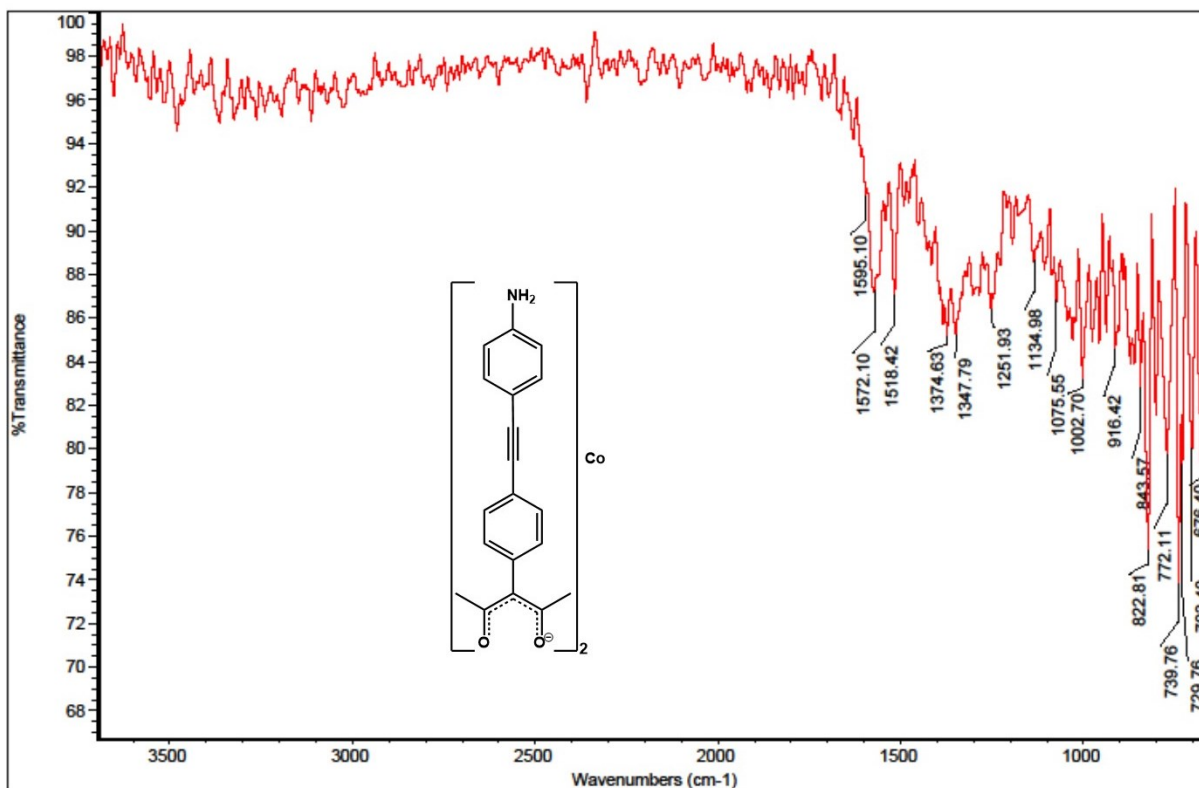


Figure B.111 IR spectrum of 46.Co.

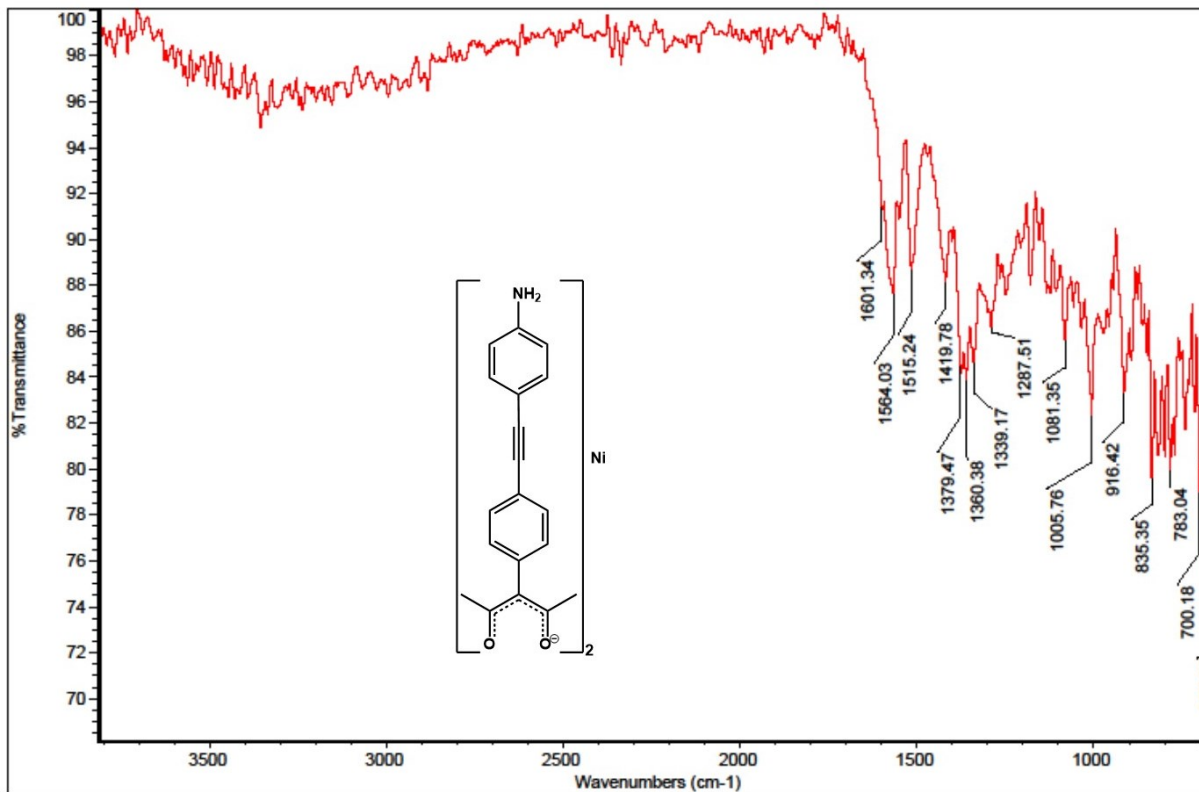


Figure B.112 IR spectrum of 46.Ni.

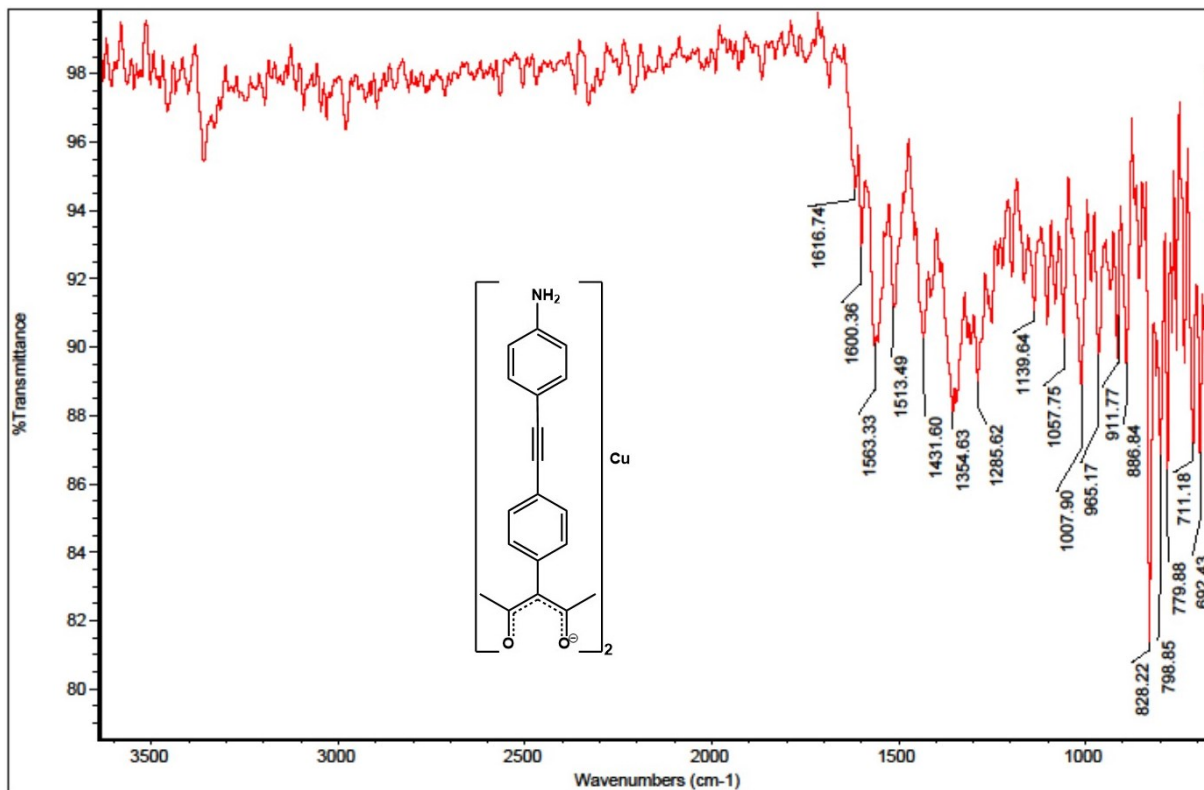


Figure B.113 IR spectrum of 46.Cu.

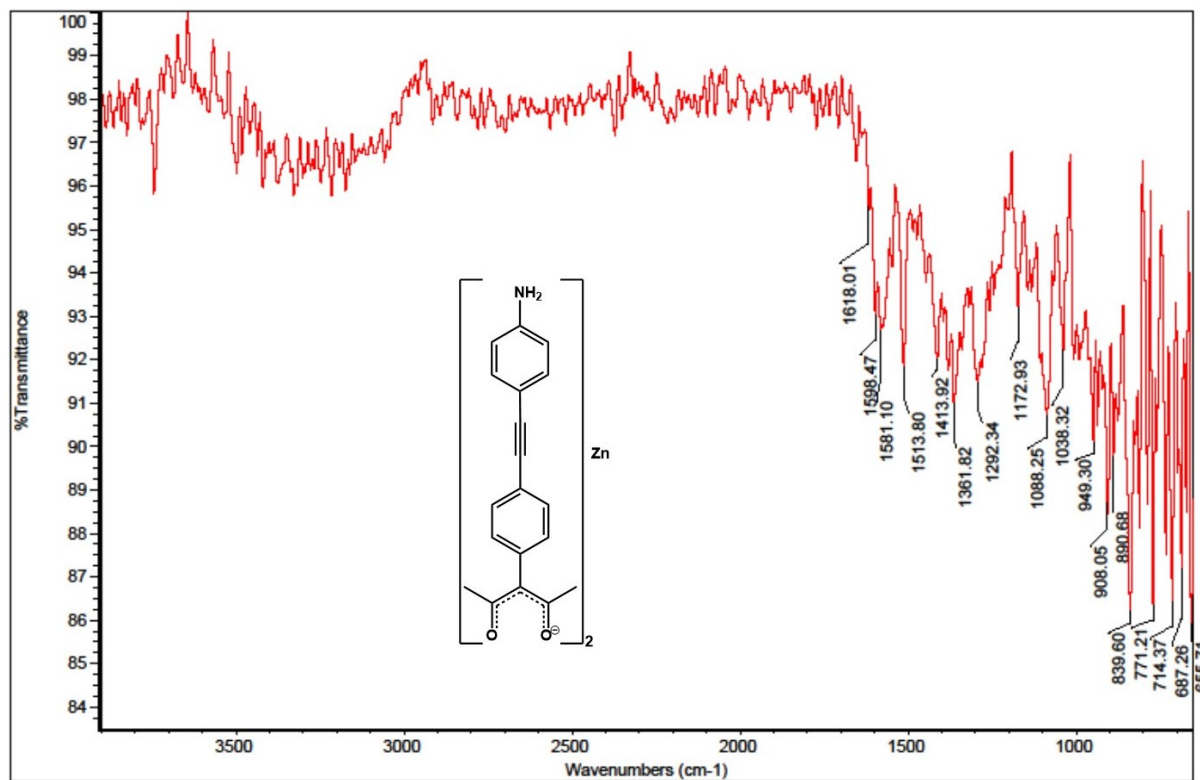


Figure B.114 IR spectrum of 46.Zn.

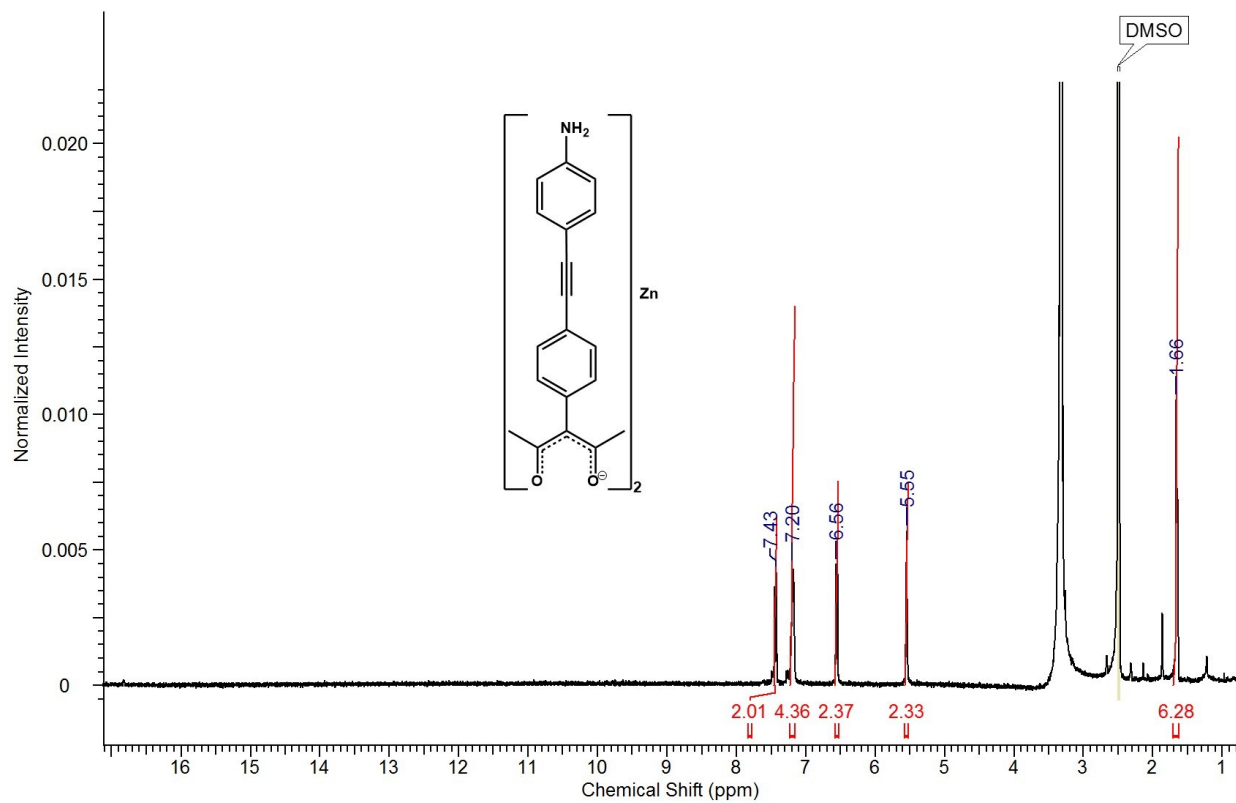


Figure B.115 ^1H NMR spectrum of 46.Zn.

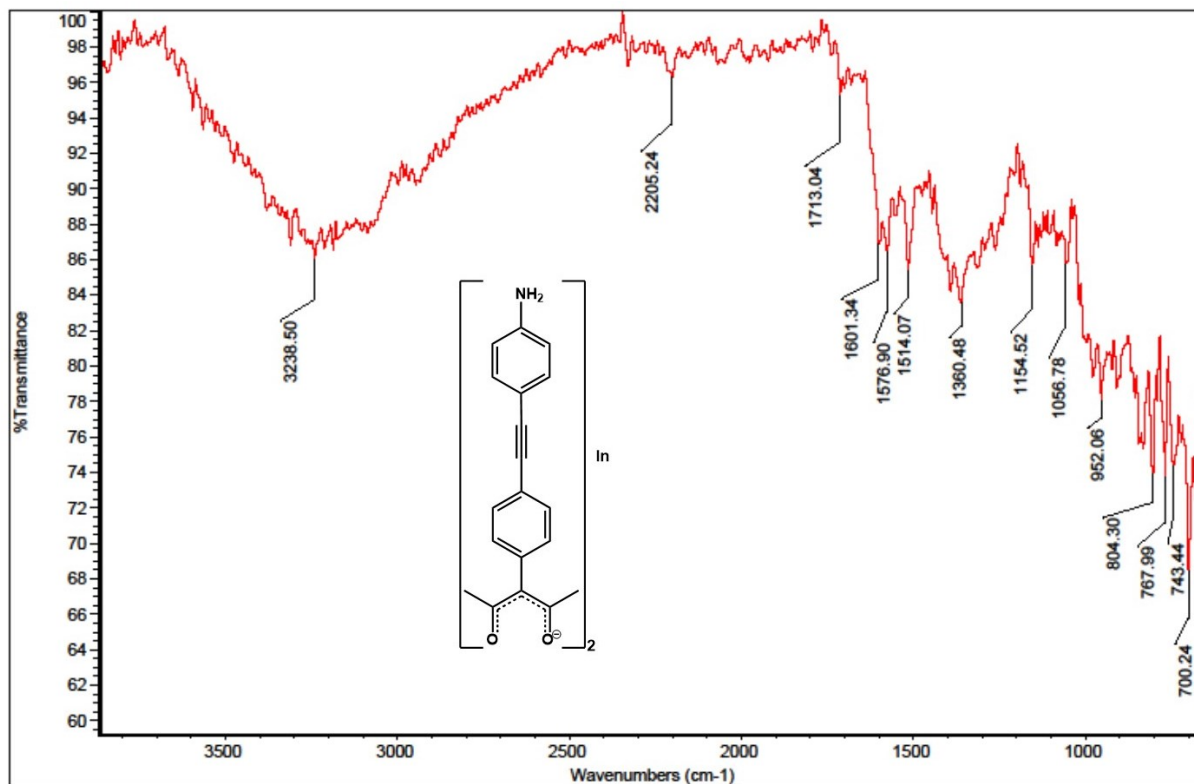


Figure B.116 IR spectrum of 46.In.

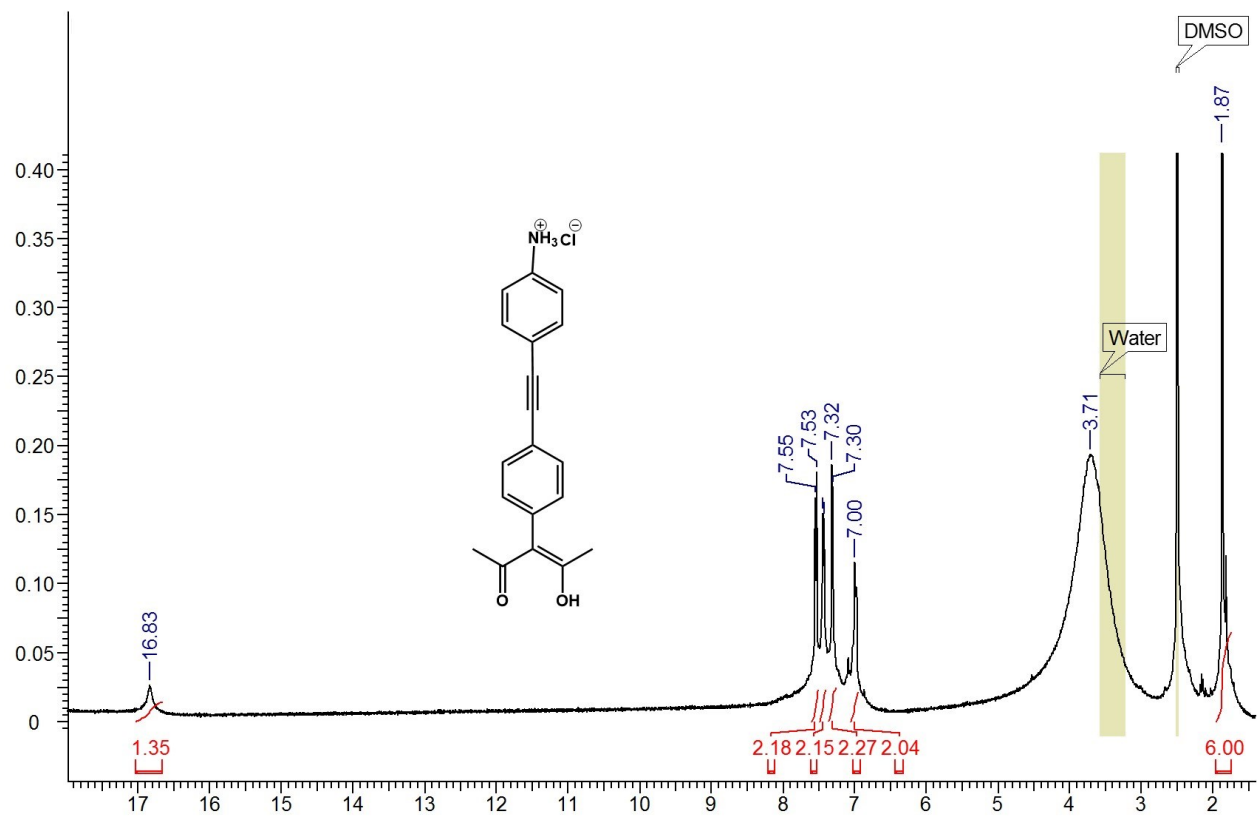


Figure B.117 ^1H NMR spectrum of **48**.

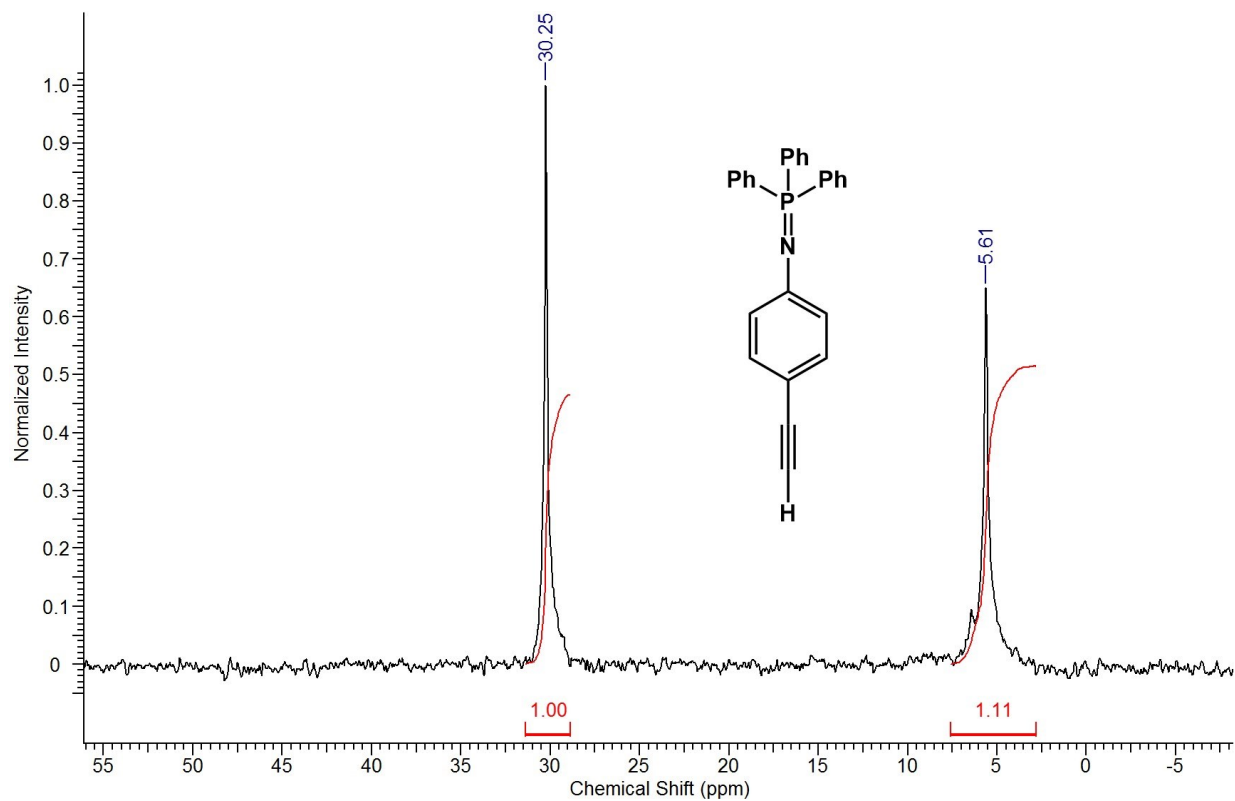


Figure B.118 ^{31}P NMR spectrum of **49**.